University of Dundee

DOCTOR OF PHILOSOPHY

The Role of the Mammalian Target of Rapamycin (mTOR) in Cytotoxic T Lymphocytes

Hukelmann, Jens Ludger

Award date:
2014

Awarding institution:
University of Dundee

Link to publication

The Role of the Mammalian Target of Rapamycin (mTOR) in Cytotoxic T Lymphocytes

Jens Ludger Hukelmann

This thesis is submitted

for the degree of

Doctor of Philosophy (Ph.D.)

to the University of Dundee

September 2014

Contents

List of figures

Abbreviations

Abbreviations	
4EBP1	eukaryotic translation initiation factor 4E-binding protein 1
AGC	family of PKA, PKG and PKC related kinases
Akti	Akt inhibitor VII
AMP	adenosine-5'-monophosphate
AMPK	AMP activated protein kinase
APC	antigen presenting cell
APS	ammonium persulfate
ATP	adenosine-5'-triphosphate
βME	beta mercapto ethanol
BSA	bovine serum albumin
CD	cluster of differentiation
CTL	cytotoxic T lymphocyte
Da	Dalton
DAVID	Database for annotation, visualization and integrated discovery
DC	dendritic cell
DNA	deoxyribonucleic acid
DTT	dithiothreitol
ECAR	extracellular acidification rate
ECL	enhanced chemiluminescence
EDTA	ethylenediaminetetraacetic acid
EGTA	Ethylene glucol tetraacetic acid
ELISA	enzyme-linked immunosorbent assay
ER	endoplamatic reticulum
ERK	extracellular sigal regulated kinase
ESI	electrospray ionisation
ETC	electron transport chain
FA	formic acid
FBS	fetal bovine serum
FDR	false discovery rate
FITC	fluorescine isocyanate
Foxo	forkhead domain transcription factor
FSC	forward scatter
GAPDH	glyceraldhyde-3-phosphate dehydrogenase
GDP	guanosine-5'-diphosphate
GEF	guanosine exchange factor
GO	gene ontology
GSK3α/β	glycogen synthase kinase 3α/β
GTP	guanosine-5'-triphosphate
HEPES	4-(2-hydroxyethyl)-1-piperazineethanesulfonic acid
HRP	horseradish peroxidase
HT	high throughput
IFN	interferon
IAA	iodoacetamide
IL	interleukin
IRS1/2	Insulin receptor substrate 1/2

kDa	kilodalton
KEGG	Kyoto encyclopaedia of genes and genomes
Klf2	krüppel-like factor 2
LCMV	lymphocytic choriomeningitis virus
LDH	lactate dehydrogenase
LFQ	labelfree quantification
LTQ	linear trap quadrupole
MALDI	matrix assisted laser desorption/ionisation
MAPK	mitogen activated protein kinase
MEK	mitogen activated ERK kinase
MHC	major histocompatibility complex
mRNA	messenger RNA
mTOR	mammalian/mechanistic target of rapamycin
mTORC1/2	mTOR complex 1/2
m/z	mass over charge
NEM	N-ethylmaleimide
NP40	nonidet P40
OCR	oxygen consumption rate
OxPhos	oxidative phsophorylation
p-	phospho-
PAGE	polyacrylamide gel electrophoresis
PBS	phosphate buffered saline
PBST	phosphate buffered saline plus 0.05% (w/v) Tween 20
PDK1	3-phosphoinositide-dependent protein kinase-1
PE	phycoerythrin
PFK	phosphofructokinase
PH	pleckstrin homology
PIP_2	phosphatidylinositol-4,5-bisphosphate
PIP_3	phosphatidylinositol-3,4,5-trisphosphate
PI3K	phosphatidylinositol-3-kinase
PKA	protein kinase A
PKB	protein kinase B (Akt)
PKC	protein kinase C
PKD	protein kinase D
PKM1/2	pyruvate kinase, muscle isoform 1/2
ppm	parts per million
PPP	pentose phosphate pathway
PRAS40	proline rich Akt substrate 40
PTEN	phosphatase and tensin homologue deleted on chromosome 10
Ref	reference
RIPA	radioimmunoprecipitation assay buffer
RNA	ribonucleic acid
rpm	revolution per minute
RPMI	Roswell Park memorial Institute-1640
RSK	p90 ribosomal S6 kinase
S / Ser	serine
S1PR1	sphingosine-1-phosphate receptor 1
S6	ribosomal protein S6

S6K	p70 ribosomal S6 kinase
SAX	strong anion exchange chromatography
SDS	sodium dodecyl sulphate
SEC	size exclusion chromatography
SHIP	Src homology 2-containing inositol 5-phosphatase
SILAC	stable labelling with amino acids in cell culture
SSC	side scatter
STAT	signal transducer and activator of transcription
T / Thr	threonine
TCA	trichloro acetic acid
TCEP	tris(2-carboxyethyl)phosphine
TCR	T cell receptor
TEMED	tetramethylethylenediamine
TFA	trifluoroacetic acid
Tris	tris(hydroxymethyl)aminomethane
WT	wild type
Y / Tyr	tyrosine

Acknowledgements

First of all, I would like to thank my supervisor Doreen Cantrell for taking me into the lab despite falling asleep in the first meeting with her. Without her constant support and encouragement, guidance and inspiration, enthusiasm and optimism, "DAC-attacks" and challenges I would not have been able to finish this project and I do not think I could have worked in a better environment than I did. Thank you.

A big thank you to all members of the DAC lab, especially to

'Princesa' Maria, who constantly had to endure, educate and quiet me,

Liz, for BBQs and Huskies,

George & Kasia, for constant entertainment and Freudian slips,

Dave F., for taking care of me in the first months and leaving me with litres of beer,

but also Aneesa (for geography lessons) Arlene, Carmen, Christina, Dave W., Gavin, Julia, Lana, Linda, Mahima, Marouan, Rosie, Sarah, Stephen, Xingping and everybody else form the lab and division that I have forgotten.

Thank you also to members of the Lamond lab, particularly Mark, Sara, Tony and Yasmeen who helped me tremendously with all MS related questions (and paintballs).

I would also like to thank my family for their support and Emily for sticking to me as well as all the other unforgettable people I have met in the last couple of years: Daniel for luring me to Dundee in the first place, Ashwath for constant curries and a trips to Iceland and India, Alistair for doing stupid things in the highlands.

Declaration

Candidate:

The candidate is the author of the thesis: that, unless otherwise stated, all references cited have been consulted by the candidate; that the work of which the thesis is a record has been done by the candidate and that it has not been previously accepted for a higher degree. Provided that if the thesis is based upon joint research, the nature and extent of the candidate's individual contribution shall be defined.

……………………………………………………

Jens Ludger Hukelmann

Supervisor:

I certify that the conditions of the relevant Ordinance and Regulations have been fulfilled.

……………………………………………………

Professor Doreen A. Cantrell

Abstract

The serine-threonine kinase mammalian target of rapamycin (mTOR) is an important integrator of nutrient, cytokine and growth factor sensing in T cells and controls transcriptional programs that determine CD8$^+$ cytotoxic T cell fate and trafficking. mTORC1 is inhibited by the drug rapamycin which is a powerful immunosuppressant used in the clinic in the context of organ transplantation. However, not much is known about the full extent of the role of mTOR signalling in CTL.

We thus utilised high resolution quantitative mass spectrometry to define the mTOR regulated CTL proteome and map the abundance and isoform expression of more than 6700 proteins in CTL. The data provide unbiased analysis of how mTORC1 reprograms the transcriptional and proteome landscape of T cells. The results show that mTORC1 controls expression of approximately 700 proteins with equal numbers of up and down regulated proteins. This illustrates that mTORC1 inhibition does not lead to a general decreases in protein levels but initiates a diverse reprogramming in gene expression and in particular drives selective decreases and increases in the expression of key metabolic regulators, effector molecules, adhesion molecules and adapter proteins. The proteomic approach also allowed us to detect effects caused by mTORC1 inhibition that were not caused by changes in the corresponding transcripts but solely due to posttranscriptional mechanisms.

One striking result was the dominance of mTORC1 negative feedback control of the serine/threonine kinase PKB. This prompted detailed analysis of the role of mTOR in the regulation of the phosphatidylinositol (3,4,5)-trisphosphate (PIP$_3$) signalling effector PKB in CTL. A striking observation was that mTOR inhibitors allow T cells to accumulate very high levels of PIP$_3$ and cause T cells to hyperactivate the serine/threonine kinase PKB and moreover reprogram PKB activation. PKB activity

was thus uncoupled from mTORC2 activity and explained the similar phenotype of selective mTORC1 vs combined mTORC1/2 inhibition.

Collectively these experiments highlight the power of high resolution analysis of proteomes to uncover critical signalling checkpoints that control T cell differentiation and give new insights about how mTORC1 inhibitors control T cell function.

1. Introduction

1.1. An introduction to the immune system

Every living being is constantly confronted with a multitude of pathogens – viruses, bacteria, fungi and other uni- and multicellular parasites – and thus requires a complex network of cells and molecules to defend the body from these threats.

Skin, cornea and mucosal membranes represent the first line of defence to keep pathogens at bay. However, breaches in these protective layers are inevitable and thus further mechanisms are required to deal with inevitable infections. Pathogens entering the body are usually initially detected in the body by the innate immune system. The innate immune system is also known as the unspecific immune system as it uses generic, but rapid responses to deal with pathogens. An important strategy of the innate response is the employment of pattern recognition receptors that detect molecules that are characteristic of pathogens but not of the host like lipopolysaccharides derived from gram-negative bacteria or double stranded RNA derived from viruses. Once these molecules have been detected the innate immune response is triggered which leads to the recruitment of immune cells to the site of infection via cytokine release, the activation of the complement system and the removal of foreign substances and cell debris by specialised white blood cells. The innate immune response also leads to the activation of the adaptive immune system via a process known as antigen presentation. In contrast to the unspecific and generic response of the innate immune system, the purpose of the adaptive immune system is to develop a specific and long-lasting response to particular pathogens when these are encountered for a second time. This specific response comes at a price, as the adaptive immune response takes several days to develop and is thus not able to react as quickly to infection as the rapid response of the innate system. Humoral components like antibodies (which are made and released

by B cells) as well as cell-mediated components (with T cells playing a central role)
contribute to the adaptive immune response. Pluripotent hematopoietic stem cells in the
bone marrow (BM) are the source for cells constituting the innate and the adaptive
immune system. The stem cells in the BM give rise to two kinds of progenitor cells,
common myeloid and common lymphoid progenitors. Macrophages, dendritic cells,
granulocytes and mast cells are all derived from the myeloid progenitor, whereas B
cells, T cell and natural killer all derived from the common lymphoid progenitor. "B"
and "T" cell indicate the different fates of these cells: B cells mature in the bone
marrow, whereas T cell progenitors migrate into the thymus, where they undergo further
differentiation into different $CD4^+$ and $CD8^+$ T cells. Initially, these naïve B and T cells
are small, quiescent cells which circulate through the body via the blood and the
lymphatic which they enter and exit several times a day. However, if a suitable antigen
is presented to the lymphocytes by a specialised antigen presenting cell, lymphocytes
are activated and thus exit their quiescent state. This activation is accompanied by a
massive surge in anabolic activity to enable a rapid proliferative burst that leads to a
dramatic increase in cell numbers and the differentiation into effector cells. These
effector cells then migrate to the site of infection and attempt to eliminate the pathogen
or pathogen infected cell. Most effector lymphocytes collapse and die once the infection
is cleared. But a few long-lived cells remain which subsequently form the memory of
the immune system. These memory cells then form the basis for a faster and increased
immune response if a pathogen carrying the same antigen is encountered again.

1.2. T cell development in the thymus

As mentioned before, all lymphocytes are generated from a common lymphoid
progenitor in the bone marrow. T cell progenitors then migrate to the thymus where

they undergo further development. One of the most important aspects of T cell development is the generation of a functioning T cell receptor (TCR) on a cell that expresses either a CD4 or CD8 co-receptor. The diversity of TCR expressed by T cells is one of the foundations of the adaptive immune system as the TCR is responsible for the detection of specific antigens presented to them by major histocompatibility complexes (MHC). Two major classes of TCR expressing cells can be distinguished: T cells expressing an αβ-TCR, which make up the vast majority of T cells in the human body, or T cells expressing a γδ-TCR. Several other invariant proteins are associated with the αβ or γδ subunits and collectively form the T cell receptor complex: Two TCRζ subunits (linked to each other via disulphide bonds) as well as the CD3 complex, which consists of CD3γ, CD3δ and two CD3ε subunits. The αβ-TCR is restricted to the recognition of antigens presented to it by either a MHC class I (if the CD8 co-receptor is expressed) or MHC class II (if the CD4 co-receptor is expressed). In contrast to that, the γδ TCR is not MHC restricted. The T cell progenitors which enter the thymus are so-called double-negative (DN) thymocytes as they express neither the CD4 nor the CD8 co-receptor. Through various intermediate steps these cells then enter a double positive (DP, positive for both CD4 and CD8) stage. Successful rearrangement of the TCRβ chain orchestrated by RAG proteins[1] and subsequent expression of a pre-TCR complex is crucial for development to the DP stage as the pre-TCR is required for survival signalling that prevents the thymocytes from entering apoptosis. CD4/CD8 DP cells then perform rearrangement and maturation of the TCRα chain and the successful outcome of this process leads to the formation of a functional TCR. The nascent TCR, together with the CD4 or CD8 co-receptor will then interact with MHC Class I and II molecules loaded with host derived self-peptides which are expressed by epithelial cells in the thymus. The strength and duration of the interaction of this TCR-MHC interaction will determine whether the T cells pass the positive selection process and

commit to the CD4 or CD8 lineage[2]. Furthermore, TCR which bind too strongly to the MHC complexes in the thymus will initiate apoptotic signalling which ensures the removal of T cells with potential autoimmune properties (negative selection)[2]. The result of this stringent maturation process is the generation of either CD4 or CD8 positive cells which will leave the thymus and populate the periphery.

1.3. T cell receptor signalling

As mentioned earlier, the T cell receptor (TCR) is an octomeric transmembrane complex consisting of a TCRα and a TCRβ chain linked to each other by a disulphide bond which is joined by three dimeric molecules: a CD3γ/ε and a CD3δ/ε heterodimer as well as a TCRζ/ζ (CD247) homodimer. The TCRα and β chains only contain a short cytoplasmic tail without any significant domains whereas CD3γ, δ and ε contain one and TCR3ζ three immunoreceptor-tyrosine-based activation motif (ITAM) domains. ITAM motifs contain a characteristic $YxxI/Lx_{(6-8)}YxxI/L$ sequence motif[3] whose tyrosine residues can be phosphorylated upon ligand binding of the TCR by tyrosine kinases of the Src family, Lck and Fyn[4,5,6,7]. It has been demonstrated that the ITAM motifs are sequestered in the cell membrane in the absence of TCR ligand and that this mechanism is involved in the regulation of ITAM phosphorylation[8]. However, further studies contradicted the importance of this mechanism[9] and the role of this sequestration mechanism in regulating ITAM phosphorylation remains disputed. TCR binding to ligands leads to the juxtaposition of the TCR with the CD4/8 co-receptors. This leads to the recruitment of the tyrosine kinase Lck to the TCR/CD3 complex. The activity of Lck is regulated by two tyrosine-phosphorylation sites: Tyr394, which can be phosphorylated by either trans-autophosphorylation or by Fyn, lies within the catalytic domain activation loop and needs to be phosphorylated for Lck activity. The

phosphorylation of Lck on Tyr505 by Csk on the other hand locks Lck in an auto-inhibitory state via binding to its Src homology (SH) 2 domain[10] and needs to be relieved by CD45 in order to enable phosphorylation of Tyr394[11]. However, high CD45 or other tyrosine phosphatase activity can also negatively regulate Lck activity by dephosphorylating Tyr394[11,12]. Activated Src kinases are able to phosphorylate the Tyrosine residues on the ITAM motifs which leads to the recruitment Zeta-chain-associated protein kinase 70 (ZAP70)[13,14] via its tandem SH domains[15], however, ZAP70 also needs to be phosphorylated on Tyr493 by Lck to enable binding to ITAMs[16]. Active ZAP70 is then able to phosphorylate linker for T cell activation (LAT) on tyrosine residues 127, 132, 171, 191 and 226[17] and Src homology 2 domain containing-containing leukocyte phosphoprotein 76 (SLP-76). Additional adaptor proteins of the GRB2 family including GRB2, GADS and GRAP contain SH2 domains and can bind to phosphorylated tyrosine residues of LAT[18]. GADS can also associate with SLP-76 and thus links SLP-76 and LAT[19]. LAT, SLP-76 and the GRB2 family member do not show catalytic activity themselves but are scaffolding proteins whose assembly triggers multiple biochemical pathways.
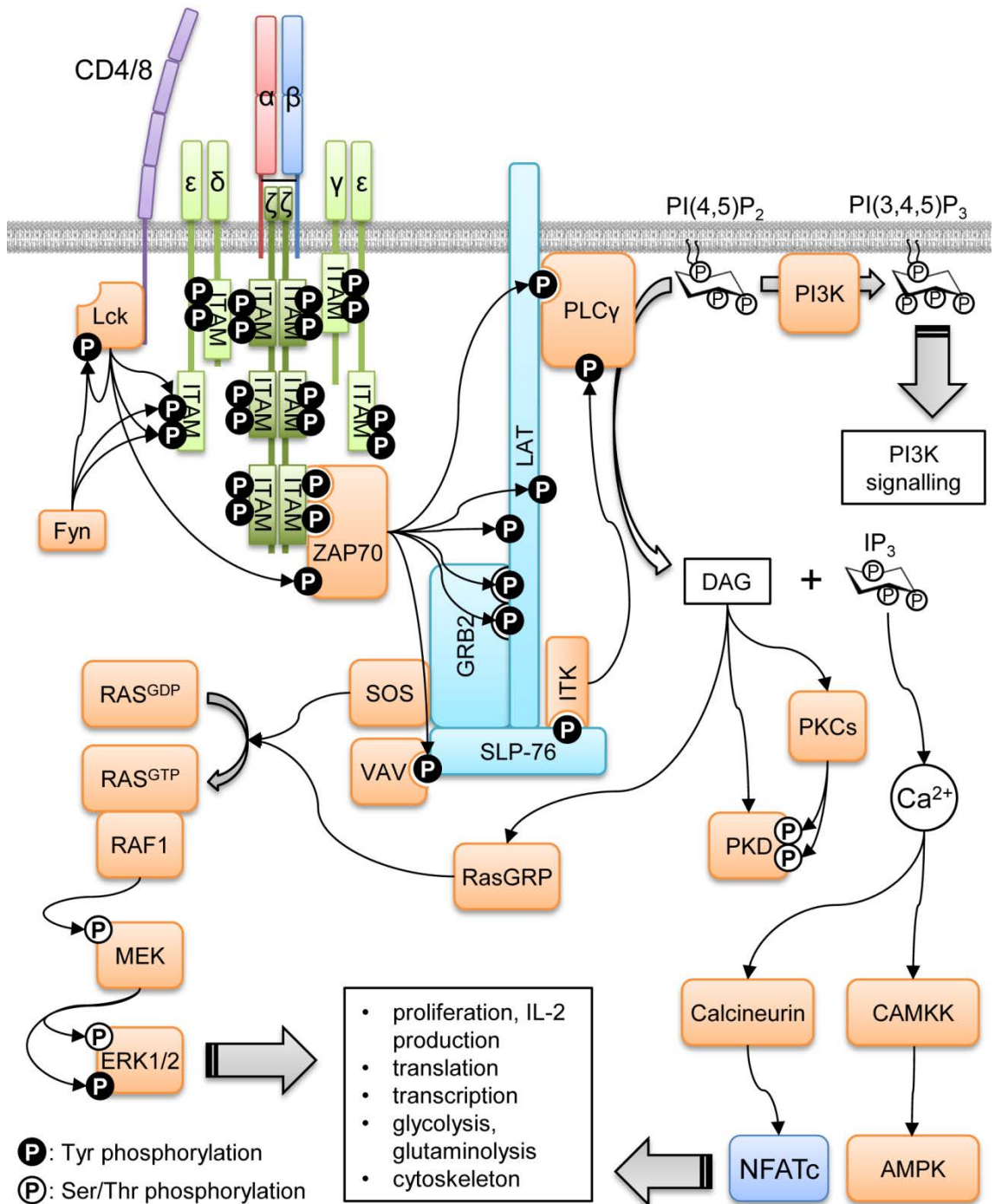
Figure 1.1: T cell antigen receptor signalling.
ITAM motifs of αβTCR and CD subunits protrude into the cytoplasm and can be tyrosine-phosphorylated by Lck to provide docking sites for ZAP70 via SH2 domains. ZAP70 activates several scaffolding proteins including LAT, Gads and SLP-76. Phosphorylation of these proteins leads to further recruitment of PLCγ, VAV, ITK and other signalling molecules. Upon signalling, membrane bound (DAG, PIP_3) and soluble (IP_3, Ca^{2+}) second messengers are formed which transduce the ligand binding by the TCR.

Phospolipase C (PLC)γ1 contains a SH2 domain and can bind to phosphorylated Tyr132 on LAT[17,20] which is critical for PLCγ1 activity. However, binding of PLCγ1 to

LAT is not sufficient to fully activate PLCγ1 as it also needs to be phosphorylated on Tyr783 by IL-2–inducible T cell kinase ITK[21]. ITK and PLCγ1 are also both able to bind to SLP-76 via their SH2 domains and the binding is required for the activity of both enzymes[22,23].

PLCγ1 is a key signalling initiator as it catalyses the generation of the second messengers inositol 1,4,5-trisphosphate (IP_3) and diacylglycerol (DAG) from phosphatidylinositol 4,5-bisphosphate (PIP_2)[24]. IP_3 is released from the membrane and can bind to its receptor on the surface of the endoplasmatic reticulum (ER) which is linked to a ligand-gated Ca^{2+} channel. The IP_3 binding to its receptor activates the channel leading to the release of Ca^{2+} from the ER lumen into the cytoplasm[25]. The rapid decrease of Ca^{2+} levels in the ER also leads to the accumulation of stromal interacting molecule 1 (STIM1) in the membrane of the ER which in turn can interact with Orai1 Ca^{2+} channels on the plasma membrane which increase Ca^{2+} levels even further[26]. The combined effects of Ca^{2+} release from the ER and influx from the extracellular space lead to a drastic increase of intracellular Ca^{2+} levels from 10-100 nM in the resting state to 500-1000 nM in stimulated cells[27]. The increase in Ca^{2+} levels then leads to the activation of Calcineurin, a protein-phosphatase, and calmodulin-dependent kinase (CAMKK). Calcineurin is an important regulator of T cell activation as it controls the phosphorylation of nuclear factor of activated T cell, cytoplasmic (NFATc)[28]. NFATc dephosphorylation leads to the translocation of the transcription factor into the nucleus where initiates the transcription of genes like IL-2, TNF-α and IFN-γ. The importance of this pathway is further illustrated by the effcts of calcineurin inhibitors like cyclosporin which have been used as immunosuppressants in the context of organ transplantation for more than 30 years[29]. An important substrate of TCR activated CaMKK is the serine/threonine kinase adenosine monophosphate-activated kinase (AMPK)[30], an important regulator of the energy balance in the cell[31].

PLCγ1 activity also leads to the formation of another second messenger, DAG. In contrast to IP_3 which is hydrophilic and thus freely diffuses into the cytoplasm upon PIP_2 hydrolysis, DAG remains anchored in the plasma membrane and thus leads to the recruitment of proteins to the membrane. Proteins shown to bind to DAG are members of the protein kinase C and D families (PKC and PKD) of which several are expressed in T cells[32] but also RASGRP1 which is a GTP exchange factor that activates downstream effectors like RAS[33] and thus mitogen-activated protein kinase (MAPK) signalling. The activation and recruitment of protein of the PKC family, particularly PKCθ, forms the basis for the formation of the immunological synapse (IS), the interface between T cell and antigen presenting cells (APC)[34,35]. DAG generated by TCR activation only accumulates in close proximity to the contact area of the T cell with the APC and the sharp DAG gradient thus enables the localised accumulation of PKC and PKD members[36]. This accumulation of PKC at the plasma membrane is considered to be the rate limiting step of PKC activation, as other regulatory mechanisms of PKC, like the phosphorylation of the T loop residues by phosphoinositide-dependent kinase 1 (PDK1)[37], also occur in the absence of TCR triggering. PKC isoforms control a wide range of T cell functions involved in cytotoxic activity of CTL by PKCδ[38], activation of NF-κB signalling via CARMA1[39] and cell motility[40,41]. Another substrate of PKC proteins are PKD family members like the highly expressed PKD2. As mentioned before, these proteins are also recruited to the plasma membrane by DAG[42]. However, unlike PKC members which are constitutively phosphorylated by PDK1 on their T loop activation sites and which are activated by the DAG recruitment, sustained association of PKD2 with DAG is not required for their catalytic function[43]. Once bound to DAG, PKD2 can be phosphorylated by PKC on Ser707 and Ser711 within the activation loop of the kinase domain of PKD2 which in turn stabilises the active conformation of the kinase. This allows PKD2 to dissociate

from the membrane into the cytoplasm while retaining its catalytic activity[44]. PKD2 thus provides a link of the membrane bound TCR signalling to the cytosol. The importance of PKD2 signalling in T cells has been demonstrated by PKD2 variants with mutated T loop residues which cannot be phosphorylated by PKC. These cells are not able to transduce TCR signalling and fail to produce pro-inflammatory cytokines like IFN-γ and IL-2[45,46].

MAPK signalling is also initiated by the generation of DAG as DAG activates the aforementioned GTP exchange factor (GEF) RASGRP. RASGRP associates with and activates the small G-protein RAS by exchanging RAS-bound GDP for GTP. RAS can also be activated by another GEF, Son of Sevenless (SOS)[47], which is associated with the LAT-GRB2 adaptor complex. RAS[GTP] then subsequently activates the serine-threonine kinase RAF1 by binding to its RAS-binding domain which relieves the auto-inhibition of RAF-1[48]. RAF-1 is a MAPKKK and as such phosphorylates its down-stream substrate MEK which in turn phosphorylates the MAPK extracellular signal-regulated kinase (ERK) 1 and 2. The MAPKK are dual-specificity kinases and are able to phosphorylate threonine and tyrosine residues within a TxY motif in their substrates and thus lead to their activation. ERK1 and 2 on the other hand are serine-threonine kinases. One of the down-stream targets of ERK is ELK1 which is an activator of the activator protein (AP)-1 complex, which is a heterodimeric complex consisting of JUN and FOS. AP-1 is a key transcription factor which regulates processes like differentiation, proliferation and apoptosis in lymphocytes[49].

TCR triggering also recruits class I phosphoinositide 3-kinases (PI3K) to the plasma membrane where they can phosphorylate phosphatidylinositol-4,5-bisphosphate (PI(4,5)P$_2$) at the 3' position to generate phosphatidylinositol-3,4,5-trisphosphate (PIP$_3$). PIP$_3$ levels are tightly controlled by the activity of two lipid phosphatases: phosphatase

and tensin homolog (PTEN) dephosphorylates PIP_3 at the 3' position to revert it back to $PI(4,5)P_2$, while another lipid phosphatase, SH2-domain containing inositol polyphosphate 5-phosphatase (SHIP) 1/2, dephosphorylates PIP_3 at the 5' position to generate $PI(3,4)P_2$. Increased PIP_3 can be detected within seconds of TCR triggering[50,51,52,53]. Elevated PIP_3 levels can be maintained for hours, however, PI3K activity is required for maintaining these high levels as inhibition of activated PI3K with PI3K inhibitors like LY294002 rapidly decreases PIP_3 levels. PI3K is a heterodimer consisting of a p110 catalytic subunit and a p85 regulatory subunit. The p110δ isoform has been shown to be the major p110 subunit in lymphocytes[54]. However, the exact mechanism by which PI3K is activated upon TCR triggering is not known. Early studies proposed a mechanism by which p85 is recruited directly to phosphorylated LAT via its SH2 domains[55] while later studies showed that p85 can also bind to SLP-76 on phosphorylated tyrosine residues 113 or 128[56]. Moreover, PIP_3 generation through the CD28 co-stimulator was not abrogated when p110δ was not able to bind to the phospho-tyrosine binding motif of CD28[52]. PI3K activation via Ras is another potential mechanism by which PIP_3 levels can be controlled in T cells[57,58].

1.4. T cell subpopulations

As all experiments in this thesis have been performed in $CD8^+$ cytotoxic T lymphocytes (CTL), the following chapter will focus on the description of this particular T cell subset. However, several other subsets with specific roles exist in the immune system. Most of these cells express an αβ-TCR and either the CD4 or the CD8 co-receptor and can thus be divided into $CD4^+$ and $CD8^+$ T cells and their respective subsets.

1.4.1. CD4^{+} T cells

In contrast to CTL which are the effector T cells in the body and deliver the lethal blow to infected cells, CD4 cells do not actively perform effector function but assist CTL as well as B cell formation and function and are thus termed T helper (T_H) cells[59] which can be further classified into T_H1, T_H2[60,61] and T_H17 cells. T_H1 cells secrete pro-inflammatory cytokines like IFN-γ, IL-2, TNFα and lymphotoxins and thus support macrophages, CTL and IgG B cells. Intracellular pathogens like bacteria and viruses trigger a T_H1 response while extracellular parasites and helminths trigger a T_H2 response. T_H2 cells secrete IL-4, IL-5, IL-6 and IL-13 and enhance B-cell mediated humoral immune responses. T_H17 cells represent a third subset[62] and are characterised by the expression of IL-17 and IL-22 which helps the immune system battle fungal infections[63,64].

An emerging theme of helper T cell biology is the fact that fate decisions of CD4 cells are not definite and that these cells are not necessarily terminally differentiated. The tacit assumption was that helper T cells express a single master transcriptional regulator which controls a transcriptional program leading to the differentiation into a specific subset. However, it became clear that many 'signature' cytokines which were thought to be uniquely expressed by certain subsets can actually be expressed by a wide range of immune cell subsets. For example, IL-10 was initially considered to be exclusively expressed by T_H2 cells but was later discovered to be expressed by T_H1, Tregs and a variety of other innate immune cells as well (reviewed in[65]). Furthermore, elegant studies using fate markers showed that T cells can change their phenotype[66]. Following the fate of cells expressing IL-17, the hallmark cytokine of T_H17 cells, revealed that these cells are able to stop expressing this cytokine and adapt a phenotype similar to T_H1 cells characterised by expressing IFN-γ[66]. It became clear that CD4^{+} T cells are actually able to express several master transcription factors simultaneously and thus

drive different transcriptional programs depending on the transcription cytokine milieu, master regulator and other transcription factors (reviewed in[67]).

A critical population are CD4^{+} T regulatory cells (Treg). These are cells that generally suppress the immune response by down regulating the induction and proliferation of effector T cells in order to prevent excessive immune reactions[68]. They are characterised by high expression of CD4, the IL-2 receptor α-chain (CD25) as well as FoxP3, an unique transcriptional regulator of Treg function[69,70,71]. The importance of Tregs is illustrated by so-called 'scurfy' mice with non-functional FoxP3: These mice suffer from over-proliferation of CD4+ cells, multi-organ infiltration and excessive levels of several cytokines and die within 16-25 days after birth[69]. Human immune dysregulation, polyendocrinopathy, enteropathy, X-linked syndrome (IPEX) is the equivalent of the scurfy phenotype in humans[72]. The exact mechanisms by which Tregs exert their immune-regulatory effects are not known yet. However, several mechanisms have been proposed: Depriving effector T cells of IL-2 due to high expression of IL-2R on Tregs[73], involvement of the negative regulator of T cell activation, CTLA-4[74] as well as the secretion of cytokines and growth factors including IL-10, IL-35, granzyme B, IL-9 and TGF-β (reviewed in [75,76]).

1.4.2. CD8^{+} cytotoxic T lymphocytes

If an infection occurs in the body, CD8^{+} T cells will be primed by APC expressing a suitable MHC class I-antigen complex in lymph nodes or other secondary lymphoid organs. However, the TCR-MHC interaction is not enough and CD8^{+} T cells require further signals triggered by co-stimulatory molecules. The successful activation of the naïve T cells will then induce dramatic changes in the metabolism of CTL as characterised by the drastic up regulation of amino acid, glucose and iron transporters[77].

This is also necessary as the T cell will thereafter initiate a massive clonal expansion; studies have estimated that a single T cell may undergo up to 19 cell divisions (equivalent to a 500,000 fold increase in numbers)[78] and might undergo cell divisions within 4-6 hours[van 79] or even as little as two hours[80]. The metabolic reprogramming is characterised by a switch from a metabolic state that mainly relies on the oxidative phosphorylation of fatty acids to a state where the cells predominantly use aerobic glycolysis and glutaminolysis to fuel their growth[81]. Even though this metabolic switch or "Warburg effect"[82] is not as efficient in terms of molecules ATP gained per molecule of glucose (2 mol ATP per mol glucose for anaerobic glycolysis vs 34-36 mol ATP per glucose mol for the complete oxidation of glucose) it does however enable the cell to utilise intermediates of the glycolytic pathway for the synthesis of nucleotides, phospholipids and other macromolecules[81] and thus to satisfy their anabolic demands. The transcription factor Myc has been shown to be crucial for the induction of the transcriptional changes underlying the activation induced metabolic switch, as deletion of Myc in T cells blocked activation induced growth and proliferation due to reduced overall metabolic activity[83]. The high metabolic rates of clonally expanding CTL are maintained by high activity of MAPK[84] and PDK1-mTOR-Hif1α[85] signalling. In contrast to other cell systems, the activity of PKB is not required for CTL proliferation and metabolic activity[86]. This work will be discussed later in the thesis.

If TCR signalling is activated in a fully differentiated T cell it will prompt the T cell to trigger its effector, i.e. cytotoxic function. This second TCR triggering occurs if the CTL recognises MHC class I molecules loaded with non-self-antigens usually derived from cells infected with either viruses or intracellular bacteria or tumourigenic cells. Virus infections caused by lymphocytic choriomeningitis virus (LCMV), cytopathic vaccinia virus, influenza virus[87], hepatitis B virus, or human immunodeficiency virus[88] have been shown to be effectively cleared by CTL, while intracellular bacterial

infections with *salmonella enterica* Typhi[89], *chlamydia trachomatis*[90] *mycobacterium tuberculosis*, and *listeria monocytogenes* have also shown to be resolved by CTL. TCR triggering stops CTL migration and leads to the formation of the immunological synapse (IS) at the interface of CTL and target cell. This highly organised structure forms within minutes of dramatic rearrangements of the cell membranes and the microtubule organising centre (MTOC) and consists of three concentric regions, known as the central, peripheral and distal supramolecular activation complexes (c, p or dSMAC, respectively)[91]. As the cSMAC is enriched in proteins involved in TCR signalling like TCRζ, Lck, ZAP-70 and PKCθ, it was initially assumed this site was where the actual TCR signalling occurred, however, later studies indicated that TCR signalling originates in fact in the dSMAC and then migrates to the cSMAC, which is where the TCR is ultimately internalised and signalling is degraded[92]. The pSMAC on the other hand is an actin- and integrin rich region which has been proposed to act as an 'O-ring' and thus seal the IS to prevent leakage of effector molecules[93]. PLCγ activation due to TCR signalling leads to the association of the MTOC with the IS[94,36] and subsequently to a migration of cytolytic vesicles to the MTOC and thus an accumulation of vesicles at the IS within the cSMAC. The vesicles then release their contents into the intercellular space: Effector molecules include perforin, granzymes, cathepsins and hexaminidases and trans-membrane receptors like Fas ligand. How do these molecules then kill the target cells? Perforin contains a lytic membrane-inserting MACPF domain and it was initially suggested that perforin forms pores in the target cell's membrane through which other effector proteins might enter[95]. Later studies[96] then showed that the delivery of granzymes by perforin involves a two-step process that initially leads to the formation of transient pores in the cell membrane of the target cells. These pores then trigger endocytosis by the target cell in an attempt to repair the damaged cell membrane. Perforin then facilitates pore formation within the endosomal membrane which

ultimately delivers the granzymes into the target cell's cytosol. The best characterised

granzyme is granzyme B which is a serine protease that cleaves after aspartic residues[97],

a unique specificity among eukaryotic serine proteases which is only shared with

caspases and lead to discovery of an caspase-3 activating mechanism responsible for

CTL mediated killing[98]. Later studies revealed cytotoxic activity of granzyme by cell

death via the mitochondrial pathway as well[99]. Cathepsin B on the other hand is a

protease that is able to cleave perforin and is thought to be a mechanism by which CTL

protect themselves from their own cytolytic granules[100]. However, Cathepsin B

deficient CTL do not show high rates of 'self-destruction'[101] indicating that other

protective mechanisms must be active as well. Fas ligand (FasL or CD95L), another

effector molecule within cytolytic vesicles[102], kills target cells by a different

mechanism. Membrane-bound FasL is the ligand for the Fas receptor (CD95), a death

receptor whose oligomerisation leads to the formation of the death-inducing signalling

complex (DISC) after binding FasL. The formation of DISC ultimately leads to the

activation of caspase-8 and thus to the triggering of apoptosis in the target cell[103].

Mechanisms to prevent autotoxicity via FasL include the inactivation of FasL activity

by shedding its extracellular domain[104], which actively blocks the induction of

apoptosis[105]. A third mechanism of CTL mediated killing utilises tumour necrosis factor

α (TNFα). TNFα is primarily produced as a membrane bound homotrimer[106], but can be

cleaved by the metalloprotease TACE/ADAM17 to produce a soluble homotrimer[107].

Both forms of TNFα are biologically active and have distinct and overlapping

properties[108]. However, killing via TNFα is thought to be relatively insignificant as it

takes several hours to induce apoptosis in the target cell and thus Fas and perforin

mediated mechanism are considered to be the major mediators of CTL killing[109,110,111].

More recent studies suggest that TNFα mediated killing may play a critical role in the

killing of virus-infected cells with down-regulated or absent MHC I expression via

endothelial cell cross-presentation[112]. In addition to that, TNFα is also thought to recruit neutrophils and eosinophils to infected sites[113,114] and to increase the expression of epithelial adhesion molecules to enhance the entry of lymphocytes into peripheral tissues[115]. In addition to TNFα, CTL release other pro-inflammatory cytokines as well. Particularly IL-2 and IFN-γ are noteworthy as they possess various important functions in the immune system. IFN-γ is an important activator of macrophage function and also enhances the expression of MHC class II as well as Fas[116,117].

1.4.3. CD8^{+} memory T cells

The activation of naïve CD8 T cells leads to a proliferative burst and the generation of large number of CTL. Most of these CTL die by a process called activation induced cell death (AICD) or because they are deprived of the cytokines necessary for survival. This massive onset of apoptosis leads to a decrease in cell numbers to 5-10% of the cells at the height of the response. The surviving cells will differentiate into long-living memory cells which form the key element of the adaptive immune response. Upon re-encounter with their antigen they will rapidly activate resulting in a faster and stronger immune response than in their first encounter[118]. The exact mechanisms and signals that decide whether an effector T cell differentiates into a memory cell are not known. Initially the selection was thought to be random[119], whereas recent studies proposed different models of T cell diversification like the asymmetric cell fate model or decreasing potential model. The different models are discussed extensively elsewhere[120,121,118].

1.5. Cytokine signalling

1.5.1. IL-2 (and other γ_c-cytokines)

Interleukin-2 (IL-2) is a cytokine with diverse function that is produced after antigen activation and plays a key role in the immune response. It was discovered 35 years ago as a biological agent found in the supernatant that was sufficient to promote growth of lymphocytes *in vitro*[122,123]. IL-2 is a four α-helix bundle type I cytokine[124] and played a fundamental role as a general model for cytokine signalling as it was the first class I cytokine to be cloned[125] and the first class I cytokine for which the receptor was cloned[126,127]. The high-affinity IL-2 receptor ($K_d = 10^{-11}$ M) is a heterotrimer which consists of IL-2Rα (CD25), IL-2Rβ (CD122) and the common gamma chain (γ_c or CD132). The IL-2Rα contributes to this high affinity with a high association rate ($k = 10^7$/M/s) while the βγ-complex contributes a slow dissociation rate ($k^{\grave{}} = 10^{-4}$/s)[128,129]. The β-chain is also shared with the IL-15 receptor while γ_c is shared with the receptors for IL-4, IL-7, IL-9, IL-15 and IL-21. The importance of γ_c as a subunit of so many receptors is illustrated by humans with defects in this subunit: patients suffering severe combined immunodeficiency (SCID) have virtually no T cells and are extremely vulnerable to infectious diseases[130]. Apart from the high-affinity IL-2 receptor, alternative receptor combinations can also occur as IL-2Rβ and γ_c are able to form a dimeric receptor with an intermediate affinity ($K_d = 10^{-9}$ M) and IL-2Rα is able to bind IL-2 without any other subunit, albeit at low affinity ($K_d = 10^{-8}$ M). The IL-4, IL-7, IL-9 and IL-21 receptors are all heterodimers consisting of the γ_c and their respective unique α-chains. IL-15 shares the IL-2Rβ and γ_c but possesses a unique IL-15Rα subunit. Interestingly, this subunit signals *in trans*, i.e. with βγ subunits on neighbouring cells but not βγ complexes on the same cell. IL-2 and IL-15 are similar mitogens but differences in the signal strength of these two cytokines ultimately leads to different effects on cell size and growth of IL-2 and IL-15 maintained CD T cells[131].

How do cytokine receptors like the IL-2 receptor signal upon ligand binding? The γ_c receptors are similar to the TCR in that their cytoplasmic domains do not show any catalytic activity but serve as scaffold and adaptor proteins to kinases. Binding of IL-2 leads to the dimerization of the IL-2Rβ and γ_c chain which leads to a conformational change in their cytoplasmic tails which activates the Janus family tyrosine kinases JAK1 and JAK3. JAK1 associates with IL-2Rβ whereas JAK3 is bound to γ_c[132,133]. The JAK kinases will then phosphorylate and activate each and also phosphorylate key tyrosine residue on IL-2Rβ. One of this sites, Tyr341 (Tyr338 in humans) serves as a binding motif for the SH2 domain of Src homology 2 containing transforming protein 1 (SHC1)[134]. Further recruitment of other adaptor molecules including GRB and SOS leads to the activation of RAS-MAPK and PIP$_3$ signalling and thus promoting cell growth and metabolism. Other sites (Tyr395 and Tyr498 in mice, Tyr392 and Tyr510 in humans) lead to the recruitment of STAT transcription factors, particularly STAT5a/b[134] but also to a lesser extent STAT3 or STAT1 via their respective SH2 domains.

Binding of the STAT transcription factors to IL-2Rβ leads to their phosphorylation by JAKs, dimerization and release from IL-2Rβ and translocation into the nucleus where they initiate a transcriptional programme required for effector function, cell growth[134], and differentiation[135,136]. Recent studies also revealed higher order structures for STAT5[137]. STAT5-tetramers control the transcription of a subset of genes which is not regulated by STAT5 dimers, including IL-2Rα.

STAT signalling is a critical mediator of the transcriptional program induced by IL-2 and other γ_c cytokines. This is illustrated by mice lacking STAT5a and STAT5b which show a 99% perinatal lethality rate and the few mice that survived showed abnormal lymphoid development with atrophic thymuses and few remaining thymocytes similar to SCID[138]. T cell specific knockouts of STAT5 showed relatively modest effects on

thymocytes numbers but drastic defects on peripheral T cells, particularly CD8^{+} T cells[138]. IL-2 dependent Treg cells were also virtually absent[138]. Thus STAT5a/b play an important role not only T cell development but also in the homeostasis of mature T cells.

One the other hand, mice lacking only one isoform showed less pronounced phenotypes: STAT5a deletion leads to mice with defects in IL-2 induced proliferation[139] due to decreased expression of the IL-2Rα chain. However, maximal proliferation could still be achieved at IL-2 levels high enough to signal through the intermediate affinity βγ receptor complex. However, despite the role of STAT5 in mediating IL-7 signalling, there was no major defect in the lymphoid development and splenocytes numbers were only modestly decreased[139]. The STAT5b deficient mice show a similar phenotype to STAT5a deficient mice regarding the IL-2 induced proliferation of splenocytes, however, as STAT5b is important for the expression of the IL2-Rαas well as the IL-2Rβ chain, high levels of IL-2 are not able to overcome the proliferative defects[140]. STAT5b deficient mice also show a marked defect in IL-15 mediated proliferation of T cells as well as defects in IL-15 mediated proliferation and function of NK cells[140]. On the other hand, T cell development was only slightly affected by STAT5b deletion.

Another signalling pathway which is regulated by the IL-2 receptor is the phosphatidylinositol-4,5-bisphosphate 3-kinase (PI3K) pathway[141]. PI3K is a heterodimer consisting of a catalytic (p110, in lymphocytes particularly the p110δ isoform[142]) and a regulatory subunit (p85) and is readily activated upon IL-2 binding. How is PI3K activity regulated upon IL-2R triggering? One possibility is that IL-2Rβ is phosphorylated on Tyr338 and bound by SHC via its phosphotyrosine-binding-domain (PTB)[143] and the binding subsequently leads to the phosphorylation of tyrosine residues of SHC. The SH2 domain on GRB2 is able to bind to these residues and proline rich

motifs within GRB2 are bound by SH3 domains on GAB2 which leads to tyrosine phosphorylation of GAB2. The PI3K subunit is then able to bind to this phosphorylated GRB2/GAB complex via its SH2 domains[144,145]. PI3K is a lipid kinase and its activity leads to the generation of phosphatidylinositol-3,4,5-trisphosphate (PIP_3) by phosphorylation of phosphatidylinositol-4,5-bisphosphate. The reverse reaction is facilitated by phosphatase and tensin homolog (PTEN) whereas another lipid phosphatase, SH2 containing inositol phosphatase (SHIP), hydrolyses PIP_3 to phosphatidylinositol-3,4-bisphosphate and thus also controls PIP_3 levels. PIP_3 serves as a second messenger for proteins containing a pleckstrin homology (PH) domain and recruits these proteins to the plasma membrane. One of the best studied proteins which is activated by PIP_3 is protein kinase B (PKB), a serine/threonine kinase of the AGC protein kinase family[146]. Binding of PKB to PIP_3 via its PH domain leads to a rate-limiting conformational change[147] which allows PKB to be phosphorylated on Thr308 within its T-loop by phosphoinositide-dependent kinase-1 (PDK1). Once activated, PKB can dissociate from the membrane and remain active to phosphorylate substrates distal to the membrane. Co-localisation of PKB and PDK1 is facilitated via two different mechanisms: The first one is dependent on high levels of PIP_3 to which PDK1 can bind via its PH domain. While this PH-domain depending binding to PIP_3 does not affect the activity of PDK1 as it is constitutively active[148], it does allow for the co-localisation with PKB and subsequent phosphorylation of Thr308. The second mechanism relies on the phosphorylation of Ser473 at the C-terminal hydrophobic motif of PKB by mTORC2[149]. PDK1 contains a so-called PIF-binding pocket which can bind to phosphorylated PKB Ser473 and thus facilitate binding. Interestingly, most of the AGC protein kinases members which are phosphorylated by PDK1 contain recognition motifs for this PIF pocket but PKB is the only kinase that can be phosphorylated by PDK1 via the PIP_3 dependent mechanism[146]. mTORC2 not only phosphorylates Ser473

on PKB but also the equivalent hydrophobic motif sites on several other AGC kinases like protein kinase C (PKC) and serum- and glucocorticoid-induced kinase 1 (SGK)[146]. The upstream signals which regulate mTORC2 activity are not known but PKB Ser473 phosphorylation is sensitive to PI3K inhibitors indicating that PI3K activity is important for mTORC2 function. The PIF-pocket and the PIP$_3$-dependent mechanism of PKB activation are able to compensate for each other if one mechanism is inactive. Mice expressing a PDK1 mutant which is not able to bind PIP$_3$ still show residual PKB phosphorylation at Thr308[150] and cells lacking the mTORC2 subunit Rictor and thus mTORC2 activity also still show low levels of PKB Thr308 phosphorylation[149].

What is the role of PKB in transducing IL-2 signalling? PKB activity controls the subcellular localisation and transcriptional activity of the FoxO1/3 transcription factors: Phosphorylation of FoxOs by PKB on several residues leads to their exclusion from the nucleus, binding to 14-3-3 protein and thus termination of transcriptional activity[151,152]. FoxO target genes include several cytokines, cytokine receptor and other transcription factors. For example, the expression of the α-chain of the receptor for IL-7, an important cytokine in T homeostasis is regulated by FoxO[153]. Krüppel-like factor 2 (KLF2) is another protein controlled by FoxO transcription factors. KLF2 controls the expression of CD62L, the chemokine receptor CCR7[153] and S1P$_1$[154] all of which are important for the normal trafficking program of T cells. The exclusion of FoxOs from the nucleus due to PKB activity leads to the loss of KLF2 and consequently to changes in the trafficking behaviour of T cells[153,155]. PKB also controls effector function and differentiation in CTL: Expression of several granzymes, FasL, perforin and IFN-γ in CTL is sustained by PKB[86]. PKB also regulates the expression of several cytokine receptors. It is a positive regulator of the IL-12Rβ1 subunit but represses the expression of the IL-6 receptor and the CD27 co-receptor[86,156]. How does PKB act as a transcriptional activator or repressor? Both effects can be explained by the control of FoxO localisation by PKB:

FoxOs act as transcriptional activators for the *Klf2* and *Il7r* genes but act as repressors of *Ifng*. However, PKB does not control metabolism and protein biosynthesis in T cells as suggested by several studies[149,157,131] but is restricted to control the transcriptional program controlling T cell differentiation and function[86]. PKB activity is furthermore not required for proliferation or survival of CTL which is inconsistent with the idea that PKB is involved in the regulation of CTL metabolism[86].

A simplified illustration of IL-2 signalling is shown in Figure 1.2.

At this point it is important to mention that TCR triggered CD8$^+$ T cells can be maintained *in vitro* in the presence of IL-2. In fact, these primed and treated cells will maintain rapid proliferation rates for several days and differentiate into effector CTL[131,158,159]. Constant replenishment of fresh IL-2 is necessary as the cells will otherwise stop proliferation and enter apoptosis[160].
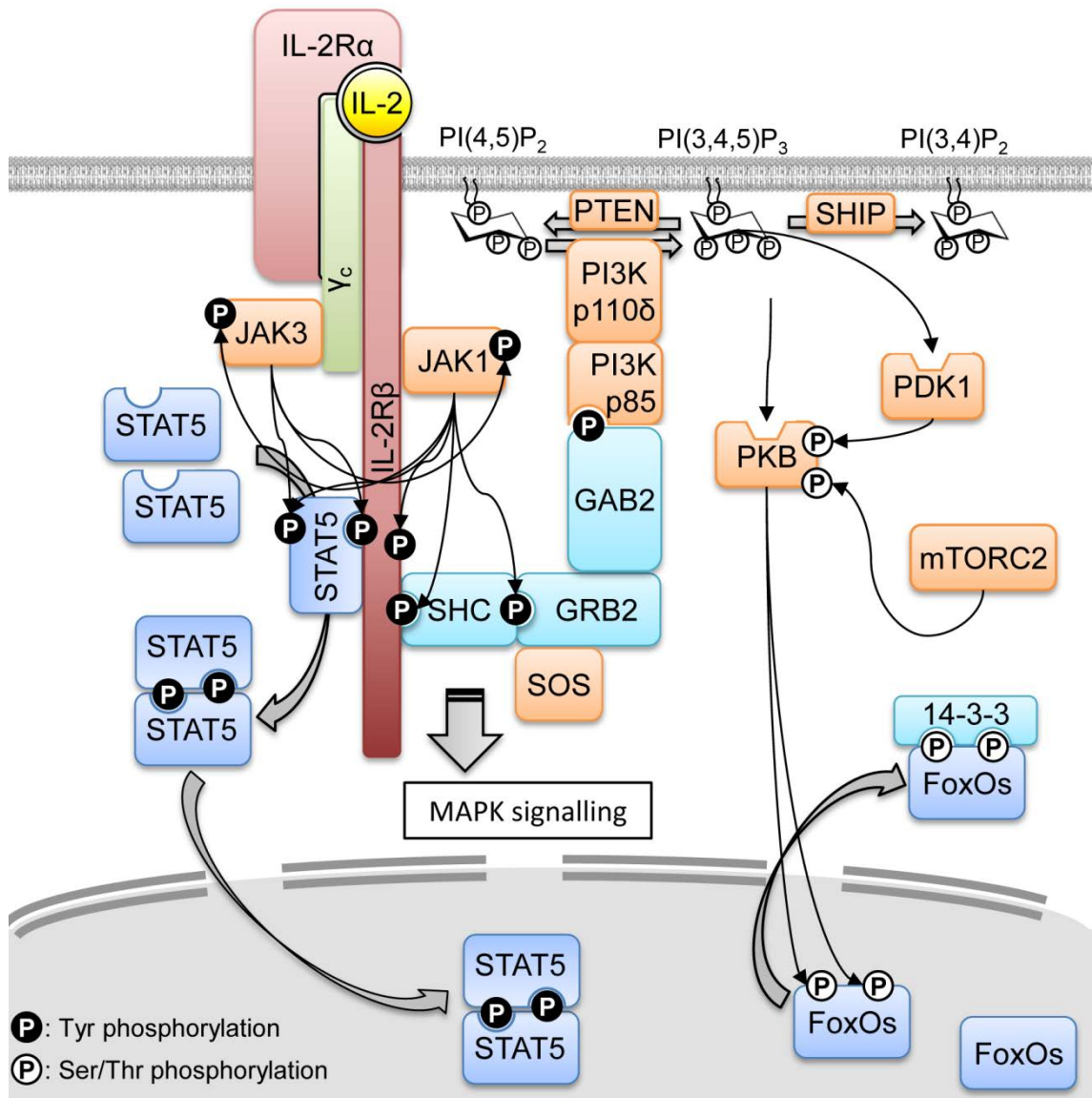
Figure 1.2: IL-2 signalling.
The high affinity IL-2 receptor consists of the IL-2Rα, IL-2Rβ and the common gamma chain (γc) subunits. JAK1/3 are constitutively associated with IL-2Rβ and the γc, respectively and activated upon cytokine induced receptor dimerization. Activation leads to the trans-autophosphorylation of the JAKs and phosphorylation of the cytolic domains of the receptors which then serve as docking domains for STAT5. Bound STAT5 is phosphorylated, dimerises with a second p-STAT5 molecule and translocates into the nucleus. SHC is also recruited to the receptor and phosphorylated by the JAKs. Recruitment of further adaptor molecules then triggers MAPK signalling. IL-2 also induce PI3K signalling leading to the translocation of FoxO transcription from the nucleus into the cytoplasm effectively stopping their transcriptional activity.

1.5.2. IL-12

The following description of IL-12 cytokine family members will mostly focus on IL-12 itself, as it was used along IL-2 for the *in vitro* generation of cytotoxic T-lymphocytes throughout the PhD project.

Unlike IL-2 described before, the IL-12 cytokine family does not bind to receptors of the common gamma chain family. IL-12 is rather the founding member of a family of four known interleukins, apart from IL-12 these are IL-23, IL27 and IL-35. IL-12 cytokines show a unique structure, as they are the only heterodimeric cytokines and several members of the family share their subunits: IL-12 and IL-23 both contain a p40 subunit apart from another specific subunit (p19 for IL-23, p35 for IL-12), while IL-27 and IL-35 share the Ebi3 subunit, and while IL-27 contains a unique p28 subunit, IL-35 shares the p35 subunit together with IL-12. The corresponding receptors also show this chain sharing theme[161,162]: IL-12 signals via the IL-12Rβ1 and IL-12Rβ2 chains[163], IL-23 via IL-12Rβ1 and IL-23R[164], IL-27 via gp130 and IL-27R[165] and IL-36 signals via IL-12Rβ2 and gp130, but can also signal via gp130-gp130 and IL-12Rβ2-IL-12Rβ2 homodimers[166]. All receptors signal via the JAK-STAT pathway[167], in a similar way as described previously for IL-2. IL-12 transduces its signalling via STAT4, IL-23 via STAT3 and STAT4, IL-27 via STAT1 and STAT3 and IL-35 via STAT1 and STAT4. Figure 1.3 illustrates the relationship between the different IL-12 cytokines, their receptors and major down-stream signalling components.
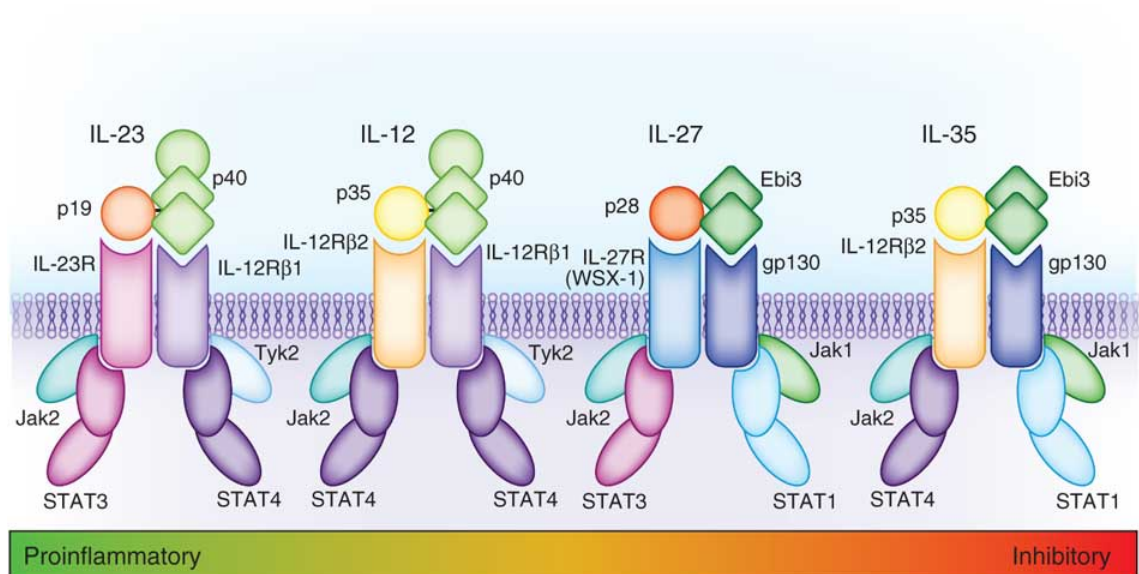
Figure 1.3: Cytokine receptors of the IL-12 family.

Members of the IL-12 of cytokines and their corresponding receptor and JAK-STAT signalling components are shown.
Figure adapted from[168]

IL-12 is produced by macrophages, dendritic cells and B cells as a response to microbial pathogens[169]. The importance of IL-12 family signalling has been shown in human patients with IL-12Rβ1 deficiency and thus impaired pro-inflammatory signalling via IL-12 and IL-23. These patients showed an increased susceptibility to otherwise harmless pathogens like mycobacteria and salmonella[170]. The effects of IL-12Rβ2 deletion on the other hand seem to be dominated by signalling defects in the IL-35 pathway. The development of autoimmunity, lymphoproliferation and B cell tumours indicates that IL-35 signalling plays an important role in controlling B-cell activation[171]. The importance of the IL-12Rβ1-p40 signalling in battling microbial infections is further illustrating by mice lacking the IL-12 p40 subunit which were more susceptible to bacterial infections, showed decreased IFN-γ expression and generally a higher mortality rate[172]. Mice lacking the p35 subunit were still able to moderately control bacterial infections and survived longer after infection[172]. This indicates that IL-23 plays a more important role in protective responses against microbial infection[172].

Interestingly, IL-12 triggers a positive feedback loop in which IL-12 increases the expression of IFN-γ which in turn stimulates additional antigen-presenting cells to produce even more IL-12. Early studies showed that even though TCR triggering and co-receptor stimuli were sufficient to generate effector CTL, addition of IL-12 led to increased CTL numbers *in vitro*[173] and later studies showed the importance of IL-12 signalling in the context of *listeria monocytogenes* infection *in vivo* as well[174]. Further studies then showed that IL-12 signalling together with IFN-γ leads to the up regulation of CD25 and thus augments IL-2 receptor signalling in CTL leading to increased proliferation but not survival[175]. It was also shown that IL-12 signalling is able to

increase IFN-γ production in CD8$^+$ T cells and the differentiation of KLRG1$^+$ effector subpopulation in the context of *Toxoplasma gondii* infections[176]. Studies in OT-I TCR transgenic CD8$^+$ T cells proposed that IL-12 enhances mTORC1 activity and thus regulates the effector versus memory fate[177].

1.6. mTOR and the integration of nutrient signalling

1.6.1. Overview

The aim of the thesis was determine the full impact of the immunosuppressant rapamycin on CTL. Rapamycin is a macrolide produced by *Streptomyces hygroscopicus* and was identified in 1975 as an antifungal agent[178], however, later studies suggested the use of rapamycin as an immunosuppressant[179]. Why is rapamycin an immunosuppressant? Early studies used T cell models like CTLL or Kit-225 cells, both of which are absolutely depending on IL-2[123,180], to describe the effects of rapamycin. Rapamycin treatment led to decreased proliferation rates in these cells which led to the assumption that rapamycin inhibition was interfering with IL-2 signalling and thus leading to a cell cycle block[181]. However, later studies then showed that rapamycin selectively inhibited IL-2 induced S6K activity[182] but did not interfere with IL-2 induced MAPK signalling and the expression of transcription factors like MYC and FOS[183] or the phosphorylation of STAT5[184]. Further studies then showed that the proliferation of primary T cells was in fact not abrogated upon rapamycin treatment[185] and thus rapamycin must exert its immunosuppressive effects by other mechanisms which are still not fully understood.

The yeast model played an important role in the identification of the molecular basis of rapamycin as the target of rapamycin (TOR) was initially identified in yeast in 1991[186]. Four different groups then independently identified RAFT1[187]/FRAP[188]/RAPT[189]/

mTOR[190,190] as the homolog to yeast TOR and thus the mammalian target of rapamycin (mTOR). mTOR is a 289 kDa protein of the family of the phosphatidylinositol 3-kinase-releated kinase family[191] and is the catalytic component of two complexes, mTORC1 and mTORC2 which are defined by their respective subunits. As it was the case with TOR itself, the existence of two distinct TOR signalling complexes was initially shown in yeast[192] and later documented in mammals as well[149]. Apart from mTOR itself, mTORC1 contains the scaffolding protein regulatory-associated protein of mTOR (Raptor), mammalian lethal with Sec13 protein 8 (mLST8), the inhibitory protein proline-rich Akt substrate 40 kDa (PRAS40), and the DEP-containing mTOR-interacting protein (Deptor)[193]. mTORC2 shares some components with mTORC1 like mTOR and mLST8 but furthermore contains unique subunits like the scaffolding protein rapamycin-insensitive companion of mammalian TOR (Rictor), protein observed with rictor (Protor) and several isoforms of MAPKAP1 (mSIN1). Rapamycin selectively inhibits mTORC1 by initially binding to the protein FKBP12[187] in the cell and the resulting FKBP12-rapamycin complex is then able to bind to and inhibit mTORC1. A detailed crystal structure of mTORC1 has been recently published[194] which showed that rapamycin-FKBP12 inhibits mTORC1 by binding to the so-called FRB domain within the mTOR subunit, which is an important substrate binding site for mTOR. However, it is not known why rapamycin only directly inhibits mTORC1 but not mTORC2. On the other hand, chronic exposure to rapamycin has shown to be able to affect mTORC2 as well, as it leads to the sequestration of the mTOR-raptor complex and reduces the pool of freely available mTOR in the cell leading to disturbed mTORC2 assembly and function[195]. The magnitude of this effect is thought to be dependent on the relative levels of mTOR, Raptor and Rictor within the cells and thus varies for different cell types[149,195]. Catalytic inhibitors of mTOR itself have been developed[196] which inhibit both mTORC1 and mTORC2 and are currently tested in several clinical trials

due to their potential anti-tumour properties[197]. Rapamycin is currently used as an immunosuppressant to prevent organ – particularly kidney – rejection[198] and as coronary stent coating[199].

The exact mechanism by which rapamycin promotes immunosuppression is not known. Some studies showed that rapamycin negatively affects CD8 effector T cell differentiation while promoting CD8 memory formation via its control of the transcription factor T-bet and Eomesodermin[200,177,201]. Rapamycin is also thought to affect the immune response by promoting the formation of CD4$^+$FoxP3$^+$ T regulatory cells[202].

mTORC1 is also a sensor for nutrient signalling and thus links metabolism and immune function of T cells. Environmental cues like growth factors, cytokines, nutrients like glucose and amino acids are integrated by mTORC1 and control the cell's metabolic profile[203,204,205].

1.6.2. Signalling up-stream of mTOR

Given the importance of mTOR signalling, what signals control the activity of mTOR? mTORC1 is a central integrator of nutrient and cytokine signalling (positive regulators of mTORC1 activity) and negative inputs like hypoxia, ER stress and low energy levels. Recent studies have shown that all these signals are integrated at the focal point of mTORC1 activation, the lysosome[206,207], and most of them signal through the tuberous sclerosis complex (TSC), an upstream inhibitor complex of mTORC1 that consists of TSC1, TSC2[208] and TBC1D7[209]. TSC inhibits mTORC1 activity by acting as a GTPase-activating protein (GAP) for the Rheb GTPase, the immediate upstream regulator of mTORC1[210,211,212,213]. High TSC activity thus correlates with low mTORC1 activity while low TSC activity or TSC knockout lead to hyperactivation of mTORC1. TSC

integrates several upstream signals that control mTORC1 activity. TSC2 can be phosphorylated by PKB on several sites[214,215], some of which (Ser939 and Thr1462) are highly conserved and also found in *Drosophila* TSC2. Recent studies[216,217] have shown how these phosphorylations affect the ability of TSC to inhibit mTORC1 signalling: Unphosphorylated TSC is located to the lysosome and thus in close proximity to Rheb, where it can exert its GAP activity and down regulate mTORC1 signalling. Phosphorylation of TSC2 by PKB on several sites leads to the dissociation of TSC from the lysosome resulting in mTORC1 activation. Phosphorylated residues on TSC2 have also been proposed to facilitate binding to 14-3-3 proteins and thus further sequestering TSC away from lysosomally bound Rheb[218]. MAPK signalling via ERK1/2 has also been proposed to inhibit TSC function and thus increases mTORC1 activity[219]. However, residues phosphorylated by ERK (Ser660 and Ser540) are different from the sites phosphorylated by PKB and also effect TSC function differently: Phosphorylation on TSC Ser660 by ERK leads to disintegration of the TSC complex[219] whereas PKB mediated phosphorylation maintained TSC integrity and preserved GAP-activity of TSC[216,217]. PKB has also been shown to phosphorylate and inactivate PRAS40, a negative regulator of mTORC1 signalling[220,221,222]. AMPK is also able to phosphorylate TSC2 on Ser1388[215] and in contrast to the aforementioned phosphorylations by PKB and ERK, phosphorylation of TSC2 by AMPK leads to increased TSC activity and thus reduced mTORC1 signalling[215]. However, the exact mechanism by which phosphorylation of TSC2 by AMPK controls TSC activity is not known.

In addition to the inputs mentioned above, it has long been appreciated that amino acids are also crucial for mTORC1 signalling, particularly L-leucine and L-glutamine. However, mouse embryonic fibroblasts derived from TSC2 deficient mice were still sensitive to changes in amino acid availability, indicating that amino acids are sensed via a TSC independent pathway[223,224].So how do L-leucine and other amino acids like

L-glutamine activate mTORC1 signalling? Amino acid levels within a cell are sensed by a still unknown mechanism at the lysosome which is dependent on RAG GTPases[206,207]. Active heterodimers of RagA/B and RagC/D (RagA/B^{GTP}-RagC/D^{GDP}) are formed in the presence of amino acids by the GEF activity of the so-called Ragulator complex[225] and recruit mTORC1 via its Raptor subunit to the lysosome[206,226]. Once at the lysosome, mTORC1 is activated by Rheb, which is constitutively present at the lysosome.[225,213].

What is known about the components of mTORC1 signalling in T cells? Many of the aforementioned pathways which regulate mTORC1 activity depending on the nutrient availability are also active in T cells[227,228,229]. Interestingly, naïve T cells only show low mTORC1 activity accompanied with low rates of metabolic activity. However, the demands of an activated T cells are not to be understated and in fact it has become clear now that the reprogramming of metabolism is crucial for the activation, differentiation and function of T cells[230]. TCR activation leads to the activation of MAPK signalling and thus ERK1/2 which in turn control the expression of the transcription factor c-Myc which initiates a metabolic shift[84,231,83]. TCR signalling via the calcium-calcineurin pathway also leads to the up regulation of the large amino acid transporter Slc7a5 which facilitates L-leucine transport into activated T cells[227]. Leucine is known to be an important regulator for mTORC1 activity[232] and does not only enable high protein biosynthesis rates due its role as a building block for proteins but also as a positive regulator for mTORC1 activity. Interestingly, the deletion of Slc7a5 did not lead to defects in T cell development or the homeostasis of the naïve T cell pool[227]. However, Slc7a5 deficient naïve T cells were not able to differentiate or proliferate as they were not able to perform the metabolic switch required to sustain the high metabolic demand of activated T cells. This could be explained by the fact that Slc7a5 deficient T cells failed to up-regulate the transcription factor c-Myc, which is known to be crucial for the

metabolic reprogramming of T cells upon TCR triggering[83]. The glucose transporter Glut1 is among the genes controlled by c-Myc expression. Thus, T cells derived from Slc7a5 deficient mice showed a drastic decrease in both L-leucine and glucose uptake, explaining why these cells were not able to activate mTORC1 signalling upon TCR triggering and failed to perform the metabolic switch required for proliferation and differentiation of effector T cells[227]. The TCR thus 'hijacked' the evolutionary conserved mechanism by which amino acid uptake regulates mTORC1 activity, a strategy which is further complemented by the TCR-controlled expression of the L-glutamine transporter ASCT2 and thus glutamine flux into the cell[229].

T cells express AMPK-α1[30] which is a crucial sensor for glucose levels in activated T cells and restricts mTORC1 activity to cells which do not meet the metabolic rates to enable their energy demanding effector function[233]. The expression of glucose transporters is mandatory for T cells as they are otherwise not able to sustain glucose levels sufficient to maintain high ATP/AMP levels in order to restrict AMPK-α1 activity and thus maintain high Rheb activity. Effector T cells require low levels of AMPK-α1 activity to sustain high mTORC1 activity and in fact, AMPK-α1 is dispensable for the generation, proliferation and function of CTL[233]. However, these cells need to down-regulate mTORC1 activity and thus T cell metabolism to perform the transition from effector into memory T cells. AMPK-α1 deficient CD8^{+} T cell showed striking defects in this transition, indicating that AMPK-α1 might be important in the down regulation of the metabolic program that underlies the effector-to-memory transition[233,200].

Most models of lymphocyte signalling postulate a linear PI3K-PKB-mTORC1 pathway, assuming that phosphorylation and thus inactivation of TSC and PRAS40 by PKB is crucial for mTORC1 activity[234,235]. Unfortunately, many experiments used the

unspecific yet popular PI3K inhibitor LY294002 which is in fact also a potent mTORC1 inhibitor and thus leads to a misinterpretation of the results gained from these studies[236]. The idea of a linear PI3K-PKB-TSC-mTORC1 pathway was further supported by the fact that TSC deficient T cells show increased mTORC1 activity upon TCR stimulation leading to disturbed immune homeostasis[237]. However, there is no direct biochemical evidence that PKB phosphorylation of TSC2 does indeed lead to a relocalisation or decrease in the GAP activity of TSC in T cells. Thus TSC2 phosphorylation by PKB and mTORC1 activity are often only correlating in T cells. We have also shown that specific PI3K and PKB inhibitors do not abolish mTORC1 activity[85] whereas the deletion of PDK1 in T cells completely abolished mTORC1 activity[86]. PDK1 and not PKB is thus a major regulator of mTORC1 activity in T cells.

1.6.3. Substrates down-stream of mTOR

Ribosomal protein S6 kinase (S6K) and the eukaryotic initiation factor 4E binding protein1 (4EBP1) are mTORC1 substrates which have been studied in great detail. S6K has been proposed to be involved in the transcription of ribosomal RNA (rRNA) and ribosomal mRNA as well as cap dependent translation and ribosomal biogenesis in general[238]. Phosphorylation of 4EBP1 by mTORC1 leads to its dissociation and thus activation of eIF4E which has been demonstrated to play a crucial role in the translation of mRNA containing a so-called 5'-terminal oligopyrimidine (TOP) motif[239]. The TOP motif is a common motif of mRNA coding for ribosomes and proteins belonging to the eukaryotic initiation factor 2 and 3 family and thus expression of these proteins is significantly affected by mTOR inhibition[239]. High protein synthesis rates require mechanisms to deal with the cellular stress caused by high levels of unfolded proteins. mTORC1 has been shown to be a regulator of global proteasomal degradation rates by

controlling the expression of subunits of the 26S proteasome[240] and thus coupling protein biosynthesis and quality control mechanisms. mTORC1 activity has also been shown to promote lipid biosynthesis by regulating the expression of many lipogenic genes. Key transcription factors which regulate the expression of these genes are sterol-regulatory-element-binding proteins (SREBPs) whose maturation has been shown to be controlled by mTORC1[241]. Studies showed that mTORC1 regulates the processing and nuclear accumulation of these transcription factors via S6K, however, the exact mechanism is still not known[241]. Autophagy processes have also been shown to be controlled by mTORC1. Autophagy describes the basic catabolic mechanism by which a cell degrades dysfunctional or unnecessary proteins and other cellular components via lysosomes and serves as a major mechanism to promote cell survival and to maintain cellular energy levels[242]. mTORC1 signalling has been shown to inhibit autophagy while mTORC1 inhibition leads to a stimulation of this process in order to maintain intracellular amino acid levels even in poor environmental conditions[243,244]. ULK1 and ATG13 have been shown to be the major down-stream substrates of mTORC1 whose phosphorylation by mTORC1 leads to their inactivation and thus inhibition of autophagy[245]. mTOR has furthermore been linked to control STAT signalling in the innate immune response[246]. This study showed that rapamycin inhibited Tyr phosphorylation on STAT3 and thus repressed its transcriptional activity. Interestingly, this STAT3 dephosphorylation led to decreased expression of the anti-inflammatory cytokine IL-10 but led to increased expression of pro-inflammatory cytokines via NF-κB signalling and thus mTORC1 inhibition led to the promotion of an overall pro-inflammatory phenotype rather than immune-suppression. As mentioned before, many models propose a linear PI3K-PKB-mTOR signalling pathway by which mTORC1 activity is controlled by PI3K activity. However, mTORC1 has also been shown to affect PI3K signalling via an S6K-depending feedback mechanism[247]. According to this

model, mTORC1 controls the protein levels of the insulin receptor substrate (IRS) 1/2 which serves as an adaptor molecule for the PI3K p85 subunit. Inhibition of mTORC1 and thus S6K leads to decreased phosphorylation of IRS1/2 and reduced targeting to the 26S proteasome which in turn increases IRS levels and thus PI3K activity. Furthermore, global phospho-proteomic studies have proposed a second feedback mechanism by which mTORC1 controls PI3K activity[248,249]. According to this model, mTORC1 phosphorylates and thus sustains high levels of the adaptor protein GRB10 which is a negative regulator of receptor tyrosine kinase (RTK) activity. Inhibition of mTORC1 activity thus leads to decreased levels of GRB10 and relieves the RTK block. However, it is not known whether the IRS1/2 or the GRB10 mediated feedback mechanism are relevant for T cell biology.

Many mechanisms and ideas regarding mTOR biology are derived from studies in transformed cell lines and are thus not necessary valid for lymphocyte biology. The rather minor role for PKB in controlling mTORC1 activity in lymphocytes is an example for this dilemma, as it illustrates that ideas and models derived from other cell systems are not automatically transferable to other systems.

An overview illustrating mTORC1 signalling in T cells is shown in Figure 1.4.
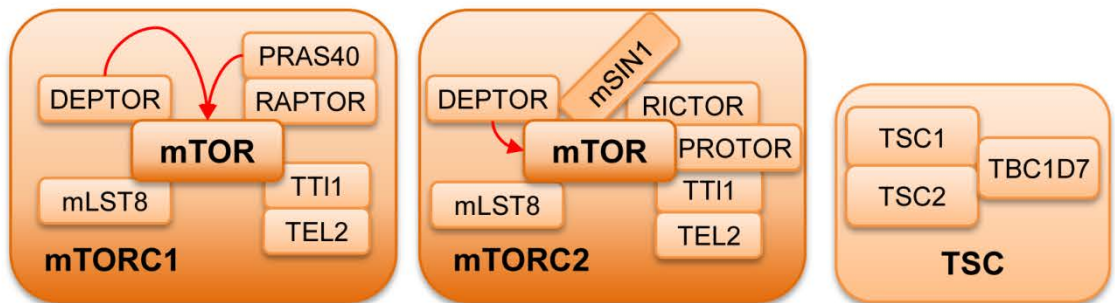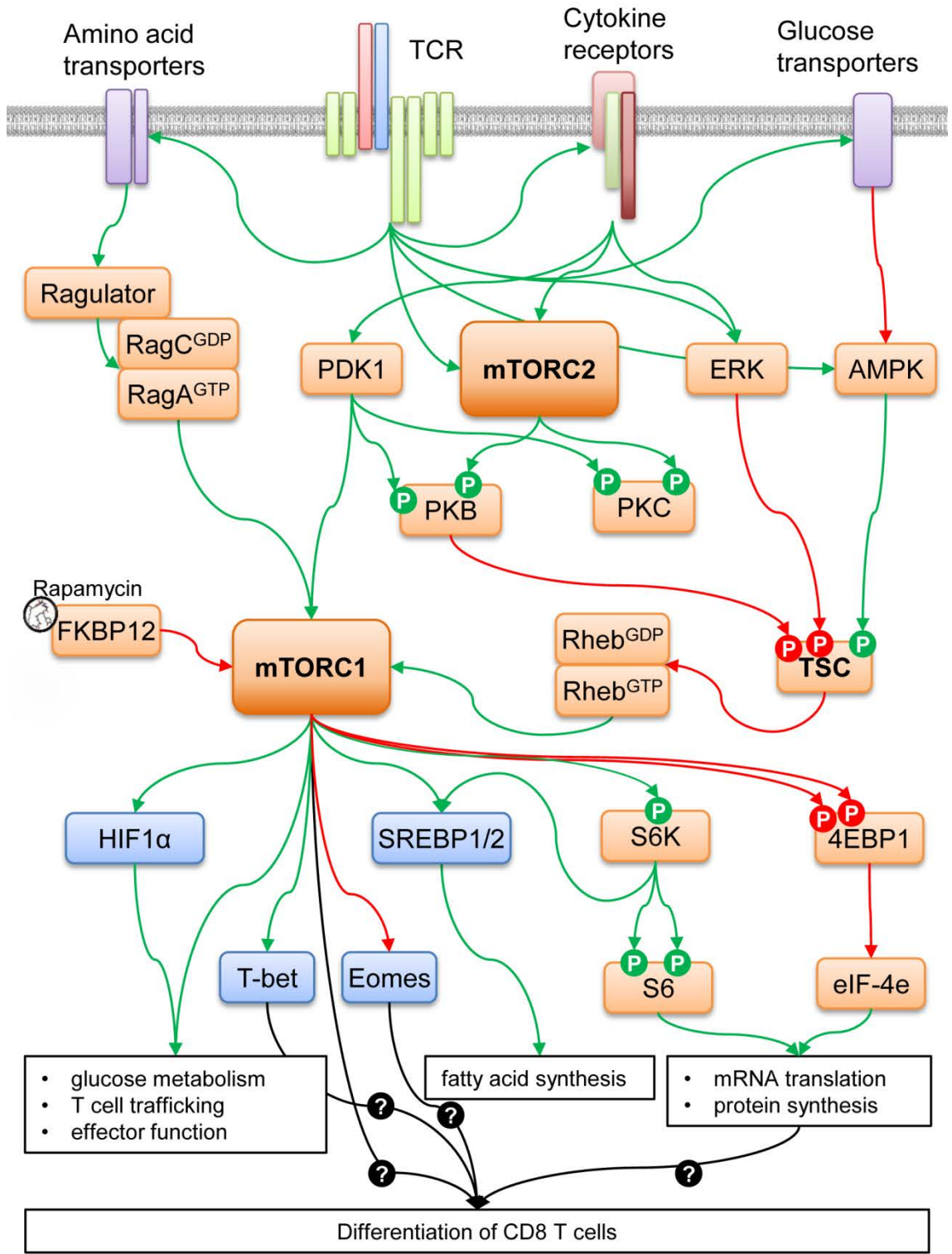
Figure 1.4: mTOR signalling in CD8 T cells.
TCR triggering leads to increased expression of amino acid, glucose and cytokine receptors. Amino acid levels are detected at the lysosome and lead to the formation of the $RagA^{GTP}/C^{GDP}$-complex via the Ragulator complex. $RagA^{GTP}/RagC^{GDP}$ tethers mTORC1 to the lysosome. Glucose signalling (via AMPK) and cytokine signalling (via PIP_3 and MAPK) are integrated at the TSC complex. TSC is the GAP for Rheb, the direct up-stream activator of mTORC1 at the lysosome. Active mTORC1 controls T cell metabolism, trafficking and effector partially via Hif1α. Expression and maturation of SREBP1/2 via mTORC1 controls fatty acid biosynthesis. mRNA translation and protein biosynthesis are controlled by the direct mTORC1 substrates S6k and 4EBP1. mTORC1 also controls the balance of the transcription factors T-bet and Eomesodermin and thus affects CD8 T cell differentiation. The contribution of T-bet/Eomesodermin independent pathways to CD8 T cell differentiation is not clear. mTORC2 activation is less well understand but dependent PIP_3 signalling. Important substrates of mTORC2 are PKB and PKC, PKB has also been shown to be a positive regulator of mTORC1.

1.6.4. mTOR control of CD8^{+} effector function and trafficking

As mentioned before, deletion of the negative regulator of mTORC1, TSC, in T cells leads to mTORC1 hyperactivation and hyperactive responses to TCR triggering as shown by increased levels of CD25 and expression of nutrient transporters[237]. However, hyperactivated mTORC1 signalling in these cells also led to increased apoptosis and disturbed immune homeostasis in general. Other studies showed that the transcription factor T-bet plays an important role in the effector function CTL and that mTORC1 controls the expression of T-bet[177]. Inhibition of mTORC1 thus led to suppression of T-bet expression but on the other hand increased levels of another transcription factor, Eomesodermin which drives the transcriptional program for a memory phenotype. mTORC1 thus controls the effector vs memory fate in CD8 T cells by controlling these two crucial transcription factors and inhibition of mTOR skews the balance towards the generation of memory T cells[200,250]. Araki *et al.*[200] illustrated in a lymphocytic choriomeningitis virus (LCMV) model that rapamycin treatment led to an increases of virus specific memory T cells. This increase was mainly caused by reduced levels of apoptotic cell death rather than increasing the proliferation of memory T cell precursors.

Furthermore, inhibition of mTORC1 during the contraction phase of CD8 T cells also lead to memory cells of higher quality as mTORC1 inhibition accelerated the memory T-cell differentiation programme. The findings of this study were confirmed by the results by He *et al.*[250], who also used a LCMV model but used cells generated and treated with rapamycin *in vitro* and then adoptively transferred them into mice. Furthermore, rapamycin treated cells in this study showed higher tolerance to nutrient and growth factor withdrawal.

mTORC1 has also been shown to control T cell trafficking. The adhesion molecule CD62L (L-selectin) is required for the tethering and rolling of naïve T cells along blood vessel walls[251] which is followed by the binding of endothelial chemokines like CCL19 and CCL21 to their receptor, CCR7, which is expressed on naive lymphocytes[252,253]. Subsequent activation of integrins expressed on T cells and their interaction with intercellular interaction molecules (ICAM) will eventually lead to a firm adhesion of cells to and transmigration through the high endothelial venules (HEV) and thus will cause the T cells to enter lymph nodes. Unless naïve T cells encounter an APC presenting a suitable MHC-antigen complex, they will migrate out of the lymph node back into the blood vasculature. The process is regulated by the sphingosine-1-phosphate receptor (S1PR1) and the concentration gradient of its ligand, $S1P_1$, directs the egress of T cells out of the lymph. T cells down regulate the expression of CD62L and CCR7 as part of the differentiation into effector T cells but up regulate other receptors that control homing to inflamed tissue, including inflammatory cytokine receptors like CXCR3 and CCR5[254]. Studies showed that the down regulation of CD62L and CCR7 during effector T cell differentiation is mediated by mTORC[155]. High mTOR activity causes down regulation of Krueppel-like factor 2 (KLF2) which is a key transcription factor for CCR7 and CD62L. However, the exact mechanism by which mTORC1 signalling controls the expression of KLF2 is not known.

1.7. Thesis aims

In order to reveal the role of mTOR signalling pathways in CTL we decided to use quantitative mass spectrometry based proteomics approaches to describe the mTOR regulated proteome in CTL. More specifically we want to use a label-free quantification (LFQ) approach to

- define the total proteome of CTL and map abundance and isoform specificity of proteins expressed by T cells and to
- define the mTOR regulated proteome.

We furthermore want to benchmark our label-free quantification approach with established strategies of quantitative proteomics like SILAC in order to see whether universally applicable approaches like LFQ are suitable for quantitative mass spectrometry studies in lymphocytes.

We will also compare the effects of mTOR inhibition on the proteome with the effects on the mTOR controlled transcriptome to gain deeper insight into the mechanisms by which mTOR controls gene expression.

Catalytic inhibitors of mTOR like KU-0063794 not only inhibit mTORC1 but also mTORC2. We will thus compare the effects of mTORC1 inhibition by rapamycin with the effects of combined mTORC1/mTORC2 inhibition to describe the role of mTORC2 signalling in CTL.

1.8. Mass spectrometry

A substantial part of the experiments performed during the PhD project utilised quantitative mass spectrometry. Thus it is important to understand principles of mass spectrometry and analysis of data generated by these approaches. We therefore summarised the basic knowledge in the field of proteomics on the following pages.

1.8.1. Introduction to mass spectrometry

A mass spectrometer can be a considered a (very accurate) balance which is able to determine the mass/charge (m/z) ratio of any kind of ions. The basics of mass spectrometry go back to the late 19th century when researchers observed rays in gas discharges that travelled either from cathode to anode or vice versa. It was later discovered that strong magnetic field could change the direction of travel of these rays according to their mass-to-charge ratio. Even though early mass spectrometers were already used in the Manhattan Project during World War II to separate uranium atoms[255] it was not until 1958 when the first peptide ions were analysed.

A mass spectrometer consists of three main components

- an ion source which acts as an entry point for the sample into the mass spectrometer and ionises the sample and transfers it into the gas phase
- one (or more) mass analyser that separates the different ions within the sample by their mass-to-charge by applying a magnetic field and thus enables the analysis of more than one ion within the sample
- a detector that records a mass spectrum by analysing the abundance of the ions

Macromolecules like proteins or peptides are easily fragmented when ionised and thus prevented mass spectrometry based approaches from a wide spread use in biology. Only

since the advent of softer ionisation methods like matrix assisted laser desorption/ionisation (MALDI)[256] and electrospray ionisation (ESI)[257] mass spectrometers are being used more frequently in life sciences. ESI is now the preferred method of sample ionisation in MS based proteomics and its discovery and development for the analysis of biomolecules by John Fenn was awarded with the Nobel Prize in Chemistry in 2002[258].

ESI works by solubilising the sample in a suitable liquid which is then being charged. Subsequent evaporation of the carrier liquid will result in the charge to remain on the peptides themselves (Figure 1.5). The sample is injected into a chromatography column and a high electric potential is applied at the fine tip of the column. Due to the accumulation of the same charge the liquid then disperses into several small droplets whose size further decrease due to the evaporation of the liquid in the evaporation chamber. Eventually the coulombic charges will lead to a bursting of the droplets as the decrease in droplet size increases the charge concentration in the liquids. Eventually all liquid will evaporate leaving multiple charged ions which are typical for ESI as compared to MALDI which preferable generates singly charged ions[259].
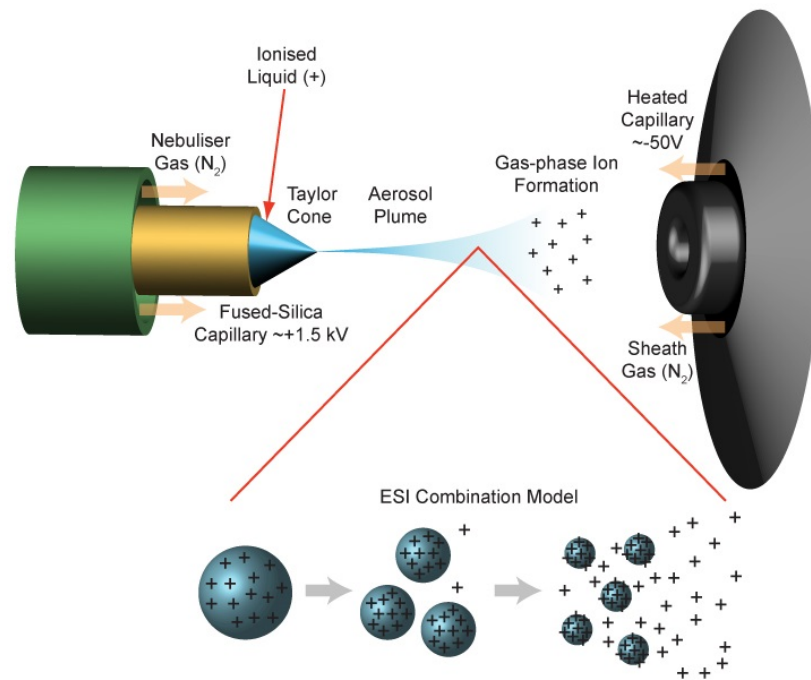
Figure 1.5: electrospray ionisation
A sample consisting of concentrated peptides is injected into a chromatography column.
At the end of the capillary the sample is ionised and enters the mass spectrometer.
The image was reproduced from:
http://www.lamondlab.com/MSResource/LCMS/MassSpectrometry/electrosprayIonisati
on.php

The mass spectrometer used for the experiments in this thesis was a LTQ Orbitrap

Velos (Thermo)[260] which is depicted in Figure 1.6. The sample is ionised using the nano

ESI and passes into the mass spectrometer via the S lens. The S lens serves as a ring

guide which focusses the sample into the mass spectrometer. The lens consists of two

stacks of metal rings which are charged and thus focus the ion beam of the sample. The

electrostatic field of the S lens also ensures that only charged particles are focused and

enter the mass spectrometer which is advantageous as the mass spectrometer is only

able to detect charged ions. The S lens also transfers the sample from atmospheric

pressures into the low pressure environment within the mass spectrometer.
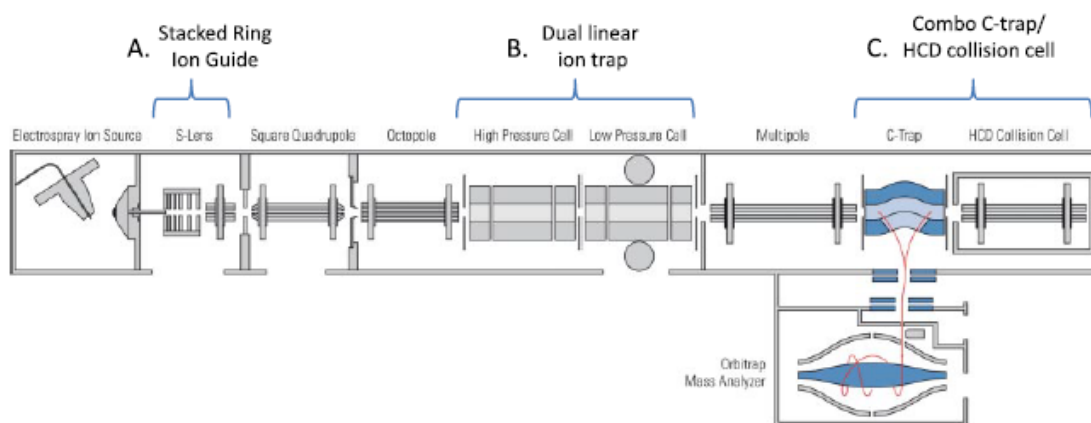
Figure 1.6: Schematic drawing of a LTQ Orbitrap Velos mass spectrometer.
The figure was adapted from Olsen, Schwartz, *et al.*, 2009[260]

Once inside the mass spectrometer, the ion beam passes through the transmission quadrupole which is facilitated by an electromagnetic field. The quadropole acts as another filter mechanism which removes unwanted solvent droplets and solvent clusters from the sample. This is facilitated by a slight bend in the quadropole through which only charged ions will be guided. The ion beam then enters the octopole which works in a similar fashion as the qudrupole but also serves as a passage to the ions. Quadropole and octopole together facilitate the entry of the ions into the low pressure environment of the ion traps. From there, the sample can then be either analysed in the C trap for mass/charge analysis or fragmented in the ion trap and analysed for their MS/MS spectra.

The first scan or MS^1 scan takes places in the Orbitrap after samples have been collected in the C trap. The Orbitrap is a spindle shaped electrode in which the ions are electrostatically trapped in an orbit around the electrode. The ions oscilliate along the length of the Orbitrap electrode and their mass/charge ratios can be obtained from the frequency of these oscilliations via Fourier Transformation. After the MS^1 data has been generated, ions to be fragmented are selected and fragmented in the high-pressure compartment of the linear ion trap. The fragmented ions are then send to the low-

pressure compartment and sequentially send to the detector to generate the MS/MS or MS^2 data. The dual pressure system of the LTQ Orbitrap Velos as well as the Orbitrap electrode are the main factors that provide the increased resolution, sensitivity and fast cycle times when compared to other mass spectrometers. These factors contribute to the high rate of identified ions that enable the application of quantitative mass spectrometry to complex biological samples.

1.8.2. Quantitative mass spectrometry based proteomics

The term proteomics was coined in 1997[261] and describes the goal of achieving a comprehensive and quantitative description of protein expression in a steady-state or its changes due to the effect of perturbations like drugs and diseases[262]. Modern proteomics and quantitative MS are now strongly connected as a number of methodical and technological advances in the field of mass spectrometry as well as international initiatives[263] led to the first near complete characterisations of the total proteome not only of yeast[264] or human cultured cell lines[265] but also more recently to first drafts of the human proteome by combining proteomic data derived from a wide range of tissues[266,267]. Projects that led to the sequencing of the human genome and those of other species form the foundation for recent proteomic advances as these databases are crucial for current mass spectrometry based approaches. The combination of advanced liquid chromatography with new generation tandem mass spectrometers (LC-MS/MS)[268] now allows the identification and quantification of tens of thousands of spectra within several hours which enables mass spectrometry to be used for a wide range of proteomic applications. The high performance liquid chromtatography (HPLC) allows the separation of very small peptide amounts due to columns with very small inner diameters allowing flow rates in the range of nL/min. This ensures that the peptides are

resuspended in a very small volume and at low speeds which in return aids the analysis in the mass spectrometer as it leads to a reduction in sample complexity as well as an increase in signal intensity. Once an ionised peptide is detected it will be recorded as a mass/charge peak over intensity (the MS spectrum) which is then followed by a further fragmentation of a specific number of the most abundant peptide peaks within a given time frame which depends on the type of mass spectrometer used. The pattern of the fragmented ions (the MS/MS spectrum) is also recorded as mass/charge peaks over intensity and generally creates a more complex spectrum than the MS spectrum. The data derived from the MS/MS spectrum ideally contains enough information to be compared to protein databases like Uniprot which serve to generate a library of possible peptides which are matched to the MS/MS spectra. The cycle is repeated several times within the time frame of a second and thus leads to the generation of thousands of MS/MS spectra from a peptide mixture during a run which typically is processed within a couple of hours.

A major problem when using mass spectrometry in proteomic approaches is the fact that mass spectrometry is not inherently quantitative. Major reason for this problem is the fact that peptides can show a range of different physical attributes which affect their 'flyability' in the mass spectrometer caused by different solubility properties, ionisation efficiencies or detector responses. Thus the most abundant peptide ion in a biological sample is not necessarily the one that is detected by the mass spectrometer as the most intense. Furthermore, changes in the digestion efficiency of peptides or fluctuations in the mass spectrometer itself can cause large variations between experiments. Several approaches have thus been developed to minimise variability. The most quantitative approaches involve metabolic labelling of proteins of an organism with amino acids enriched in non-radioactive atoms[269]. Samples labelled this way can be combined right at the beginning of the sample preparation protocol and will behave identically during

cell lysis, degradation, fractionation and will only be distinguished in the actual MS run itself leading to a an accurate relative quantification. The most commonly used strategy of metabolic labelling is called stable isotopic labelling of amino acids in cell culture (SILAC)[270]. In its simplest form it uses two pools of amino acids (usually L-lysine and L-arginine) containing either 'light' – naturally occurring – or 'heavy' isotopes of hydrogen, carbon or nitrogen. Two populations of cells are grown with these different amino acids which will be incorporated into all nascent proteins. Trypsin, which cleaves peptides after L-lysine or L-arginine, is mostly used for the digestion of proteins and thus leads to the generation of peptides which ideally only contain one labelled amino which in turn leads to a defined shift in the mass of the peptides which can easily detected by modern mass spectrometers. However, this difference in mass, which is usually in the range of 2 – 10 Da per peptide, does not affect the general chemical properties of peptides like their pI or intramoleculear structures and thus peptides labelled with 'light' or 'heavy' amino acids have been shown to behave exactly same in equal culture conditions[271,272]. However, SILAC requires complete labelling of all proteins within a cell and thus the cells to undergo at least 5 cell divisions ($2^5 = 32$ fold increase in cell numbers and thus more than 95% incorporation of light or heavy amino acids). Therefore, metabolic approaches can only be used actively proliferating cells like bacteria[273], funghi[274], parasites[275] or human[276] and mice[270] cell lines in tissue cultures but only for a handful of primary non-transformed cells[277,46]. More recently the SILAC approach could also successfully be adopted to label whole organisms like worms[278], flies[279] or even mammals like mice[280]. Further disadvantages of the technique are the relatively high costs of the labelled amino acids required and the fact that the SILAC approach leads to fewer protein identification as the mass spectrometer has to detect peptides ions for both members of a SILAC pair and thus has to effectively detect every peptide twice.

Label-free approaches[281] stand in contrast to metabolic labelling strategies like SILAC. The biological samples are handled and processed in parallel throughout the whole work flow and are only combined at the *in silico* data analysis step. In order to avoid or correct biases that will be introduced by a parallel handling of samples this strategy requires the use of highly reproducible sample handling and fractionation techniques. The strategy used in this chapter is hydrophilic strong anion exchange (SAX) chromatography which is a highly reproducible fractionation method which is also very orthogonal to the reverse phase (RP) chromatography used in the LC-MS/MS stage, i.e. different physical properties of peptides are used for fractionation[282]. This approach has been shown to highly effective in achieving near-complete coverage of mammalian proteomes[283].

1.8.3. Computational analysis of MS-based proteomics

In order to identify the peptides generated by the mass spectrometer the MS/MS spectra are typically compared to a theoretical database of peptides which have been generated by an *in silico* digest of protein sequences[284]. This crucial aspect of MS-based proteomics approaches thus relies on the technological advances in genome sequencing which build the basis for protein databases like Uniprot. A commonly used software analysis suite is MaxQuant[285] which is freely available and developed by the group of Matthias Mann. This mapping of theoretical and observed peptides is performed by the database search engine Andromeda[286] which is part of the MaxQuant software package. The search engine performs an *in silico* digest of the peptide sequences with the relevant protein database and creates a list of peptides with all possible combinations of defined post translational modifications and other chemical modifications or digestions with different endopeptidases. Fragmented ions of these peptides are then calculated as well

as the predicted mass of the precursor ion of the MS spectra. If the mass of an observed precursor ion matches its calculated predicted mass (taking in consideration PTMs and other modification) within a defined deviation the MS/MS spectrum of this ion is then matched to the theoretical fragmentation pattern. This procedure is repeated for each peptide within the database and leads to assignment of a score to each peptide depending on the quality of the match between observed and theoretical spectra. As theoretical and observed peptides are matched in a random and non-ideal fashion, search engines inevitably create false positive identifications. Other factors like the size of the protein database used or the performance of the mass spectrometer affect the whole population of peptides[287] and this problems cannot be fully addressed by a simple matching of peptide fragmentation patterns with a generated database.

In order to assess the extent of false positives identification in MS-based proteomics a target-decoy search is typically used[288]. This approach involves the creation of decoy peptides which are non-existing in the sample but are still representative of the actual peptide sample that is being analysed. This decoy database typically consists of the reversed sequences of the 'target', real database. As the decoy database is representative of the real database the FDR for the decoy and the target database should be the same and thus a number of false positive hits can be estimated. User specified criteria and the amount of decoy hits then leads to the calculation of a false discovery rate which estimates the proportion of falsely identified hits the total population (as opposed to a probability score for each single peptide).

Parallel handling of samples and their MS analysis inevitable introduces variation in the observed peptide ion intensities and also other properties like chromatography retention times. The label-free quantification (LFQ) algorithm within the MaxQuant package addresses this problem by performing several normalisation steps across all MS runs

that are used in the analysis[281,289]. The two most important features of the algorithm are the alignment of retention times of peptides as well as the transfer of identification across runs. This will lead to a maximisation of the number of peptides that can be used for quantification beyond the levels of the identification that is done by the peptide search engine. As the robustness of quantification of proteins is strongly linked to the amount of peptides that can be detected (and thus quantified) in the analysis this approach is crucial for a robust label-free quantification.

Whereas LFQ is used to measure changes in the abundance of the same protein when comparing across samples, intensity based absolute quantification (IBAQ)[290] can be used to estimate the abundance of proteins within a sample. The IBAQ uses the sum of all peak intensities of all peptides matching to a specific protein. As longer proteins generate more peptides than shorter proteins at equal abundance levels, this raw peptide intensity is then divided by the number of theoretically observable peptides to give an IBAQ intensity value which provides an accurate proxy for protein levels[290,283].

2. Materials and Methods

2.1. Transgenic mice

All mice used were bred and maintained under specific pathogen-free conditions in the Biological Resource Unit at the University of Dundee. The procedures used were approved by the University Ethical Review Committee and authorised by a project licence under the UK Home Office Animals (Scientific Procedures) Act 1986.

2.1.1. P14 LCMV

Transgenic mice expressing a Vα2/Vβ28.1 T cell receptor specific for the amino acid sequence KAVYNFATM of the lymphocytic choriomeningitis virus glycoprotein (LCMV-GP33-41)[291]. This peptide was synthesised and purified in the Cancer Research UK production laboratory, London.

2.1.2. PTEN$^{fl/fl}$ Lck$^{Cre+/-}$

Mice carrying PTEN$^{fl/fl}$ alleles with the Cre recombinase under the control of the Lck promotor were generated as described previously[292]. This leads to a deletion of PTEN early in T cell development at the double negative stage[293].

2.1.3. PDK1-K465E

Mice carrying a K465E point mutation in the PH domain of PDK1 that inhibits binding to PIP$_3$ were described previously[150].

2.2. Cell culture

2.2.1. Reagents

reagent	manufacturer
2C11 (hamster anti-mouse CD3)	R&D Systems/CRUK hybridoma unit
anti-CD28 antibody	Life technologies
β-mercaptoethanol	Sigma
Dialysed fetal bovine serum (10 kDa)	Life technologies
Fetal bovine serum	Life technologies
Insulin-transferrin-Selenium-G (100x)	Life technologies
L-arginine	Sigma
L-arginine:HCl "R10" (13C6, 15N4)	CK Gas Products Ltd.
L-glutamine (200 mM)	Life technologies
L-lysine:HCl	Sigma
L-lysine:2HCl "K8" (13C6, 15N2)	CK Gas Products Ltd.
L-proline	Sigma
MEM vitamin solution (100x), liquid	Life technologies
Penicillin/Streptomycin	Life technologies
Recombinant human IL-2 (Proleukin®)	Novartis
Recombinant mouse IL-12 (p35/40)	R&D systems
RPMI 1640 (+L-glutamine, +glucose)	Life technologies
RPMI media for SILAC	Thermo Fisher
Sodium pyruvate	Life technologies
0.22 μm Stericup	Millipore

2.2.2. Cell culture media and solutions

T cell medium: RPMI 1640 pre-supplemented with 25 mM glucose and 300 mg/mL L-glutamine, 10% heat-inactivated FBS, 100 μM β-mercaptoethanol, 100 U/mL penicillin-G, 100 μg/mL streptomycin

SILAC T cell medium: RPMI media for SILAC pre-supplemented with 25 mM glucose and 300 mg/mL L-glutamine, 10% heat-inactivated dialysed FBS, 100 μM β-mercaptoethanol, 100 U/mL penicillin-G, 100 μg/mL streptomycin, 84 mg/mL L-arginine or 106 mg/mL L-arginine:HCl "R10", 40 mg/mL L-lysine:HCl or 49.7 mg/mL L-lysine:2HCl "K8", 200 mg/mL L-proline, 2 mM glutamine, MEM vitamin solution,

Insulin-transferrin-Selenium-G, 1 mM sodium pyruvate. The medium was then filter sterilised using a 0.22 μm filter.

ACK buffer: 155 mM ammonium chloride, 10 mM potassium bicarbonate, 0.1 mM ethelenedieaminetetraacetic acid. Adjusted to pH 7.8 and autoclaved.

2.2.3. *In vitro* cytotoxic T cell generation

Spleens were obtained from mice between 8 and 26 weeks old and passed through a 70μm cell strainer to obtain a single cell suspension. Red blood cells were lysed by resuspension in ACK buffer for 10 seconds. Cells were washed and resuspended in T cell medium. T cells were activated by addition of 100 ng/mL gp33 peptide (for p14 LCMV TCR transgenic T cells) or 500 ng/mL 2C11 and 4 ng/mL αCD28 (for non-TCR transgenic T cells) in the presence of 20 ng/mL IL-2 and 2 ng/mL IL-12. After up to 48 hrs cells were washed and resuspended in T cell medium (or SILAC T cell medium where indicated) and maintained in exponential growth with 20 ng/mL IL-2 and 2 ng/mL IL-12.

2.2.4. Inhibitor treatments and stimulations

Where indicated cells were treated with inhibitors at the following concentrations:

antagonist of	inhibitor	concentration
ATP synthase	oligomycin	1 μM
Cytochrome c reductase	Antimycin A	1 μM
Complex I	rotenone	1 μM
mTOR	KU-0063794	1 μM
mTORC1	rapamycin	20 nM
PKB	Akt inhibitor VII	1 μM

2.3. SDS-PAGE and Western Blotting

2.3.1. Reagents

reagent	manufacturer
4x LDS sample buffer	Life technologies
cOmplete protease inhibitor cocktail	Roche
PhosStop phosphatase inhibitor tablet	Roche
Powdered milk	Marvel
TCEP (tris(2-carboxyethyl)phosphine)	Thermo

2.3.2. Solutions

RIPA buffer: 50 mM HEPES pH 7.4, 150 mM NaCl, 1% (w/v) NP40, 0.5% (w/v) sodium deoxycholate, 0.1% (w/v) SDS, 10% (w/v) glycerol, 1 mM EDTA, 1 mM EGTA, 50 mM NaF, 5 mM sodium pyrophosphate, 10 mM sodium β-Phosphoglycerate, 0.5 mM sodium orthovanadate, 5 mM NEM, 1 mM neutralised TCEP, 1 tablet cOmplete Protease Inhibitor Cocktail tablet per 10 mL

SDS-PAGE gel (resolving): 4-14% acrylamide, 0.1% SDS, 0.375 M Tris-HCl pH 8.8

SDS-PAGE gel (stacking): 4% acrylamide, 0.1% SDS, 0.125 M Tris-HCl pH 6.8

SDS-PAGE running buffer: 25 mM Tris, 192 mM glycine, 0.1% (w/v) SDS

Transfer buffer: 48 mM Tris, 39 mM glycine in 20% (v/v) methanol

PBST: phosphate buffered saline (PBS), 0.05% (w/v) Tween-20

Ponceau S: 0.1% Ponceau S, 0.5% (v/v) acetic acid

Stripping buffer: 0.7% (v/v) β-ME, 2% (w/v) SDS, 62.5 mM Tris (pH 7.4)

2.3.3. Antibodies

antigen	manufacturer
4EBP1	Cell Signaling Technology #9452
p-4EBP1 (Thr37/46)	Cell Signaling Technology #2855
p-4EBP1 (Thr65)	Cell Signaling Technology #9451
PKB	Cell Signaling Technology #9272
p-PKB (Thr308)	Cell Signaling Technology #4056
p-PKB (Ser473)	Cell Signaling Technology #4058
cMyc	Cell Signaling Technology #9402
ERK	Cell Signaling Technology #3372
p-ERK1/2 (	Cell Signaling Technology #4377
FoxO1	Cell Signaling Technology #9454
FoxO3a	Cell Signaling Technology #2497
p-FoxO1/3a (Thr24/Thr32)	Cell Signaling Technology #9464
Glut-1	DSTT
Hif-1α	Santa cruz sc-10790
Histone H3	Cell Signaling Technology #4499
IRS2	Cell Signaling Technology #4502
NDRG1	Cell Signaling Technology #5482
p-NDRG1 (Thr346)	Cell Signaling Technology #9485
Perforin	DSTT
PTEN	Santa cruz sc-7974
RSK	Cell Signaling Technology #9333
p-RSK (Ser227)	Santa cruz sc-12445
S6K	Cell Signaling Technology #9202
p-S6K (Thr389)	Cell Signaling Technology #9239
SMCI	Bethyl Laboratories, Inc A300-055A
T-bet	eBioscience 14-5825

2.3.4. Sample preparation, SDS-PAGE and Western blotting

Cells where washed once with ice cold HBSS and lysed in RIPA buffer at $20x10^6$ cells/mL for 30 minutes and sonicated with a Branson Digital Sonicator to shear DNA. The lysates were spun down in a refrigerated bench mini centrifuge at 16,100 g for 10 minutes to remove non soluble proteins. Samples were mixed with 4x LDS sample buffer and TCEP followed by 5 minutes incubation at 95° to denature and reduce. Samples were loaded on a SDS-PAGE gel with a fixed acrylamide concentration of 4 to 12% depending on the molecular weight of the proteins analysed. A Mini-Protean system (BioRad) was used for electrophoresis and blotting of proteins. Samples were

run at a fixed voltage of 100 V for 2 hrs or until the dye running front had left the gel. The proteins were then transferred onto Hybond-C Extra membranes (Amersham) for 1 ½ h on ice. Transfer and equal loading was confirmed by Poncaeu S staining. The membrane was washed with water and was blocked with 5% milk in PBST or 5% BSA in PBST at room temperature for 1 h. Blots were probed with primary antibodies at optimized concentrations (1 μg/mL in most cases) in 5% milk PBS-T or in 5% BSA PBS-T at 4°C overnight. Membranes were then washed thrice in PBST at room temperature for 10 minutes followed by incubation with HRP tagged secondary antibody diluted in 5% milk or BSA in PBST (1:5000) at room temperature for 1 hour. Membranes were washed thrice with PBST for 20 minutes at room temperature before being visualised using ECL.

2.4. ELISA

2.4.1. Reagents

item	manufacturer
Ready-Set-Go! ELISA mouse CD62L	eBioscience
Ready-Set-Go! ELISA mouse IFN-γ	eBioscience
1x TMB substrate solution	eBioscience

2.4.2. General ELISA protocol for CD62L and IFN-γ

A 96-well plate was coated with a capture antibody (2 μg/mL), sealed and incubated overnight at 4 °C. CTL were seeded at a concentration of 1×10^6 cells/mL in 96-well cell culture plates and cultured in T cell medium and freshly added cytokines and inhibitors for 5 h. After the incubations the plates were centrifuged and the supernatant used for further analysis. The capture antibody was aspirated and the plate was washed twice with PBST. The plate was then blocked for 1 h in room temperature by adding

300 µL of 1% BSA in PBST to each well. Following reagent diluent aspiration, 100 µL of standards and diluted cell supernatants samples were added into each well. The plate was covered with an adhesive strip and incubated two hours at room temperature. After incubation, the samples were aspirated and the plate was washed with PBST. A volume of 100 µL of detection antibody at a concentration of 400 ng/mL was incubated for 20 min at RT in each of the wells. Following this incubation step, the plate was washed with a wash buffer and 50 µL of substrate solution was incubated for 20 min in each well. Once the colour reaction was complete, 50 µL of 1 M H_2SO_4 was added and the absorbance of each well was measured at 450 nm. A standard curve generated using the recombinant protein was used to determine CD62L and IFN-γ concentrations in the samples.

2.5. Metabolic assays

2.5.1. Reagents

item	manufacturer
[U-^{14}C] glutamine	Perkin Elmer
7 mL glass vials	Thermo
Cell-Tak	BD biosciences
Optiphase HiSafe 3	Perkin Elmer
Rubber septum	Thermo
Screw vial	Thermo
Seahorse calibrant solution	Seahorse
Unbuffered RPMI (powdered)	Sigma
XF24 FluxPak	Seahorse

2.5.2. O$_2$ consumption and media acidification

A XF24 cell culture microplate was coated with 50 µL/well of a 22.4 µg/mL Cell-Tak, 0.1 M $NaHCO_3$, pH 8.0 solution for 30 minutes. The plate was then washed twice with sterile H2O and air dried at room temperature overnight. A XF24 cartridge was

equilibrated with 1 mL Seahorse calibrant solution and equilibrated at 37 °C overnight. Unbuffered RPMI media without FBS was prepared as per manufacturer's instruction and sterile filtered. 150,000 cells/well were used in the experiments. The manufacturer's recommended settings for an oxygen conmption rate of 200-500 pmol/min were used (3 minutes mixing, 2 minutes waiting, 3 minutes measuring). A mitochondrial stress test was performed and oligomycin, DNP and roteneone/antimycin were sequentially used to affect the ATP synthase and electron transport chain. Three measurements were taken for the baseline OCR and ECAR and each inhibitor treatment giving a total of 12 measurements. The average for each data point was calculated from at least 3 wells and 3 biological replicates were performed.

2.5.3. Glutaminolysis assay

1×10^6 cells per data point were harvested and resuspended in 1 mL fresh glutamine free media containing appropriate cytokines and required drugs. The cells were then transferred into 7 mL vials with a PCR tube containing 50 µL 1.0M KOH glued to the inner side wall to collect produced CO_2. 50 µL of a 20% [U-^{14}C]-glutamine (equivalent to 0.5 µCi [U-^{14}C] glutamine) were added to each sample and the vial closed with a screw cap with rubber septum. Samples were then incubated for 1 hr at 37 °C and the assay was stopped by injecting 100 µL 5M HCl through the septum with a Hamilton syringe. The vials were then kept at room temperature over night to trap the released CO_2. The KOH solution in the PCR inside the glass vials was then transferred to scintillation vials, 3 mL of Optiphase HiSafe 3 was added and the samples were analysed in a scintillation counter. All measurements were performed in technical triplicates.

2.6. Quantitative Mass spectrometry

2.6.1. Reagents

item	manufacturer
Deepwell Plate 96/500, LoBind	Eppendorf
Deepwell Plate 96/1000, LoBind	Eppendorf
Pierce Detergent Removal Spin Plates	Thermo
Sep-Pak C18 SPE cartridges	Waters
Sep-Pak tC18 96-well µElution Plate	Waters
Subcellular Protein Fractionation Kit for Cultured Cells	Thermo
Trisethanolamine (TEAB)	Sigma

2.6.2. Solutions

Urea lysis buffer: 8 M urea, 100 mM Tris-HCl pH 8.0, 2x complete protease inhibitor tablet per 10 mL buffer, 1x PhosStop phosphatase inhibitor tablet

Digest buffer: 100 mM Tris-HCl pH 8.0, 1 mM $CaCl_2$

Desalting wash buffer: 0.1% TFA

Desalting elution buffer: 0.1% TFA in 50% acetonitrile

SAX sample buffer: 10 mM sodium borate, pH 9.3 in 20% acetonitrile

SEC sample buffer: 4% SDS, 100 mM NaCl, 10 mM phosphate buffer pH 6.0

2.6.3. Strong anion exchange

2.6.3.1. Sample lysis and in-solution digest

25×10^6 CTL treated with either DMSO or rapamycin were harvested in a 50 mL falcon tube and washed three times in cold HBSS and transferred into a 2.0 mL Eppendorf tube. Cells were lysed in 0.5 mL urea lysis buffer and vigorously mixed for 15 minutes at room temperature. The samples were then sonicated with a Branson digital sonicator

before vigorously mixed for another 15 minutes. The protein concentration was determined by BCA assay as per manufacturer's instructions before DTT at a working concentration of 10 mM was added. Lysates were incubated at 30 °C for 30 minutes. Iodoacetamide was added to a working concentration of 50 mM and lysates were incubated in the dark at room temperature for 45 minutes. Lysates were diluted with digest buffer to 4 M urea. LysC was added to the samples in a 50:1 (protein:LysC) ratio and the samples were then incubated at 30 °C over night. The samples were then split in half. One half was diluted to 0.8 M urea with digest buffer and Trypsin was added in a 50:1 ratio. The other half was kept a LysC fraction. The samples were then incubated at 30 °C for a further 8 hours.

2.6.3.2. Sample desalting using Sep-Pak cartridges

Samples were adjusted to 1% TFA using 10% TFA. In case of strong precipitation of urea the samples were spun down to remove the urea. The Sep-Pak cartridges were washed twice with 1 mL elution buffer and equilibrated twice with 1 mL wash buffer before the acidified peptide samples were loaded. The flow through was loaded again to ensure maximal peptide binding. The peptide loaded cartridges were washed three times with 1 mL washing buffer. Peptides were eluted into 2 mL Eppendorf Protein LoBind tubes by 2 subsequent elutions with 600 μL elution buffer each. The eluted samples were reduced to dryness in a vacuum concentrator.

2.6.3.3. Strong anion exchange chromatography

Samples were resuspended in 210 μL SAX sample buffer and the pH was readjusted to pH 9.3 with 1 M NaOH if necessary. Samples were injected and peptides separated by a Dionex Ultimate 3000 HPLC system equipped with an AS24 strong anion exchange

column; similar experimental approaches have been reported recently[282,283]. The following buffers were used for the separation of peptides: 10 mM sodium borate, pH 9.3 (Buffer A) and 10 mM sodium borate, pH 9.3, 500 mM NaCl (Buffer B). An exponential elution gradient starting with Buffer A was used to sepearte the peptides into 12 fractions of 750 µL which were desalted using the protocol described in paragraph 2.6.5.

2.6.4. Size exclusion chromatography

2.6.4.1. Sample lysis and in solution digest

50 x 10^6 CTL grown in 'light' SILAC media and treated with either rapamycin or KU-0063794 were mixed with 50 x 10^6 CTL grown in 'heavy' SILAC treated with DMSO and washed twice with ice cold HBSS. Cells were lysed and fractionated into five different subcellular fractions (cytoplasmic, membrane, soluble nuclear, chromatin-bound nuclear and cytoskeletal fractions) using a Subcellular Fractionation Kit for Cultured Cells (Pierce) following the manufacturer's instructions for a 200 µL packed cell volume. Protein contents for each fraction were measured by BCA assay.

2.6.4.2. Chloroform-methanol precipitation

300 µg of each subcellular fraction were used for the precipitation. Samples were adjusted to a final concentration of 2% SDS, 10 mM TCEP and 20 mM NEM in 1 mL and heated to 65 °C for 10 minutes to denature proteins. 4 mL of methanol was added and samples were vortexed for 5 seconds. 1 mL chloroform was added and samples were mixed before 3 mL H_2O were added and samples vortexed for another 60 seconds. Samples were centrifuged at 9000 x g for 5 minutes with a low deceleration setting.

Approx. 80% of the aqueous upper phase was removed without disturbing the precipitated protein at the interface. 3 mL methanol were added and the samples were centrifuged at 9000 x g for 5 minutes at a low deceleration setting. The supernatant was taken off and the samples air dried.

2.6.4.3. Size exclusion chromatography of proteins

The precipitated cytoplasmic, membrane, nuclear and chromatin bound nuclear fraction were resuspended in 60 µL SEC sample buffer and boiled for 10-30 minutes with vortexing. Samples were separated by a mAbPacSEC column (Dionex) using a 0.2% SDS, 100 mM NaCl, 10 mM sodium phosphate buffer, pH 6.0. The flow rate was 0.2 ml min^{-1} and 8 fractions of 200 µL were collected into Protein LoBind 1 mL 96-deep well plates (Eppendorf) as described previously[294].

2.6.4.4. In solution digest of proteins from denaturing SEC and SDS removal

TEAB was added to the SEC fractions to a final concentration of 0.1 M. Trypsin was resuspended in 0.1 M TEAB and added to the SEC fractions in a 50:1 (protein:trypsin) ratio. The unseparated cytoskeletal fraction was diluted with digest buffer to a urea concentration of 1 M. Trypsin was added in a 50:1 (protein:trypsin) ratio. All samples were incubated at 37 °C over night. The Detergent Removal Spin plates were centrifuged at 1,000 x g at room temperature for 1 minute. The plate was washed three times with 300 µL PBS and centrifuged at 1,000 x g at room temperature for 1 minute. All SDS containing samples were loaded onto the plate and incubated on the resin for 2 minutes. Samples were then collected in a 500 µL low protein binding collection plate by centrifugation at 1,000 x g at room temperature for 1 minute. The detergent free flow

through and the cytoskeletal fraction were then kept for desalting and further sample processing.

2.6.5. Desalting with tC18 Sep-Pak 96-well plate

Fractions from either strong anion exchange or size exclusion chromatography were adjusted to 1% TFA with 10% TFA. Each well of the desalting plate was washed with 0.2 mL acetonitrile and equilibrated with 0.2 mL desalting wash buffer. The samples were then slowly applied onto the columns and washed first with 0.8 mL and then with 0.2 mL desalting wash buffer. The samples were then eluted into an Eppendorf 1000 μL 96-well-plate with 0.2 mL desalting elution buffer. Samples were reduced to dryness in a vacuum concentrator.

2.6.6. Liquid chromatography mass spectrometry analysis (LC-MS/MS)

Samples from desalting were resuspended at a concentration 0.066 μg/μL in 5% formic acid and 15 μL (equivalent to 1 μg of peptides) was used for analysis. A Dionex RSLCnano HPLC was used for the peptide chromatography. A 5 mm PepMap-C18 pre-column with an inner diameter of 0.3 mm was used and a 75 μm x 15 cm PepMap-C18 column was used for the subsequent chromatography. The mobile phase consisted of 2% acetonitrile + 0.1% formic acid (solvent A) and 80% acetonitrile + 0.1% formic acid (solvent B). A constant flow rate of 300 nL/min was used and the linear gradient increased from 5% to 35% solvent B over a runtime of 156 minutes. The eluted peptides were injected into a Velos Orbitrap mass spectrometer (Thermo Fisher, San Jose, CA) through a nanoelectrospray emitter. A typical 'Top15' acquisition method was used. The primary mass spectrometry scan (MS1) was performed at a resolution of 60,000. The aforementioned top 15 most abundant m/z signals from the MS1 scan were selected

for subjected for collision-induced dissociation and MS2 analysis in the Orbitrap mass analyzer at a resolution of 17,500.

2.6.7. Mass Spectrometric Data Analysis by MaxQuant

The data were processed, searched, and quantified using the MaxQuant software package version 1.4.1.2 as described previously[285], using the default settings and employing the mouse Uniprot database from October 2013 and the contaminants database supplied by MaxQuant. The following settings were used: two miscleavages were allowed; for the SAX samples fixed modification was carbamidomethylation on cysteine, for the SEC samples N-ethylmaleimide on cysteine; enzyme specificities were Trypsin and/or LysC were applicable; variable modifications included in the analysis were methionine oxidation, deamidation of glutamine or asparagine, N-terminal pyroglutamic acid formation, and protein N-terminal acetylation. Default MaxQuant settings included a mass tolerance of 7 ppm was for precursor ions, and a tolerance of 0.5 Da for fragment ions. A reverse database was used to apply a maximum false positive rate of 1% for both peptide and protein identification. This cut-off was applied to individual spectra and whole proteins in the MaxQuant output. The match between runs feature was activated with an allowed time window of 2 minutes. All proteins were quantified on the basis of unique proteins with the requantification enabled.

Further down-stream analysed was performed using Microsoft Excel and the programming language R. Student's t-test were performed to determine statistical significance of recurring ratios. Pathway analyses were performed using the Database for Annotation, Visualisation and Integrated Discovery (DAVID)[295,296] bioinformatics tools based on Kyoto Encyclopedia of Genes and Genomes (KEGG).

2.7. Flow Cytometry

Flow cytrometric data was obtained on a FACS Calibur or FACS Verse (Becton Dickinson) with the appropriate machine specific software. A minimum of 20,000 relevant events were collected and stored ungated. Data were analysed FlowJo data analysis software version 10 for Microsoft Windows (Treestar Inc.).

2.7.1. Reagents

item	manufacturer
αCD8 (FITC 1:200)	BD Biosciences
αCD62L (APC 1:200)	BD Biosciences
αIFN-γ (APC 1:200)	BD Biosciences
GolgiPlug^{TM}	BD Biosciences
IC Fixation Buffer	eBioscience
Permeabilization Buffer	eBioscience

2.7.2. Solutions

FACS buffer: 0.5% BSA in PBS

2.7.3. Live cell staining

Cells were stained at $1\text{-}2\text{x}10^6$ cells per mL at 4ºC for 20 min in FACS buffer. Cells were then washed and resuspended in RPMI + 1% FCS prior to acquisition on a FACS Calibur or Verse. Live cells were gated according to their forward light scatter (FCS) and side scatter (SSC)

2.7.4. Fixed cell staining for intracellular IFN-γ staining

CTL were treated with Golgi plug for 4 hours followed by staining for CD8. Cells were then washed and fixed using fixation buffer while mixing the tubes and followed by

incubation in the dark at room temperature for 20 min. The fixed cells were then permeabilised and washed once with permeabilization Buffer. The samples were then stained with IFN-γ antibody resuspended in Permeabilization Buffer in the dark for 20 minutes. Cells were then washed twice with 1 mL of Permeabilization Buffer and resuspended in FACS buffer.

2.8. Data analysis and statistical evaluation

All quantified data were processed in Microsoft Excel 2010 for PC. Generation of scatter and bar diagrams, histograms and heatmaps was done using Excel. Statistical tests to determine significant differences were two-tailed t-tests and one-way ANOVA. Differences were considered significant for p-values < 0.05 with exception for some mass spectrometry data.

Unless stated otherwise, experiments were performed in at least biological triplicates.

3. Proteomic characterisation of Cytotoxic T Lymphocytes

3.1. Introduction

We decided to use an unbiased quantitative mass spectrometry based approach to not only map the global changes caused by mTORC1 inhibition but also to gain information about the undisturbed CTL proteome. The aim of this chapter is to investigate whether a label-free proteomics approach based on fractionating cell lysates using strong anion exchange chromatography can be used to assess the total proteome of a CD8 cytotoxic T lymphocyte. We will then describe and discuss the results obtained from the proteome of an undisturbed CTL while Chapter 4 will summarise our observation of the mTORC1 controlled CTL proteome.

3.2. Results

3.2.1. Label-free quantification (LFQ) based proteomics with strong anion exchange chromatography (SAX) fractionation is robust and highly reproducible

We used a well establish protocol to generate CD8 cytotoxic T lymphocytes *in vitro* based on P14 LCMV T cell receptor transgenic mice. The TCR of these mice recognises the peptide sequence KAVYNFATM derived from the lymphocytic choriomeningitis virus (LCMV) presented by the MHC class I molecule H-2D[b]. Naïve T cells expressing this TCR can be activated by this peptide-MHC complex and differentiate into a homogenous population of CTL when cultured in the presence of interleukin-2 and interleukine-12[131,158,159]. An important aspect of the massive clonal expansion of CTL with several cell divisions per day is the fact that relative high cell numbers are required for MS based proteomic approaches. The approach we followed (Figure 3.1) required approx. 2 mg of cell lysate per condition which is equivalent to 40-50 x 10^6 CTL. Cells were activated for 2 days with the TCR ligand in the presence of IL-2 and IL-12 and then cultivated in IL-2 and IL-12 for another 4 days for clonal expansion. Cells were then lysed and subjected to the MS sample processing workflow (Figure 3.1).

We initially assessed the robustness of our LFQ SAX approach. Three biological replicates derived from the spleens of different mice were performed in the timeframe of approximately 4 months. The first biological replicate was performed on its own, whereas biological replicates 2 and 3 were processed in parallel 4 months later. We thus plotted the IBAQ values obtained for each protein from each of the three replicates and correlated the obtained values to each other (Figure 3.2, A-C). All three replicates show very strong Spearman correlations of 0.95 to 0.97 with very few outliers. There was no significant difference in the correlation of the samples despite parallel handling of

samples 2 and 3. Typically proteins with higher IBAQ intensity showed a higher correlation than less abundant proteins. We furthermore looked at the overlap between the replicates in terms of detected proteins (Figure 3.2, D) We identified more than 6500 protein groups in each replicate, leading to a total number of protein groups of 6792. A core subset of 6288 proteins (93% of all proteins) was detected in all replicates whereas 159 proteins (2% of all proteins) were only detected in only one of the three replicates with the remaining 341 (5%) protein groups detected in 2 of the 3 replicates.
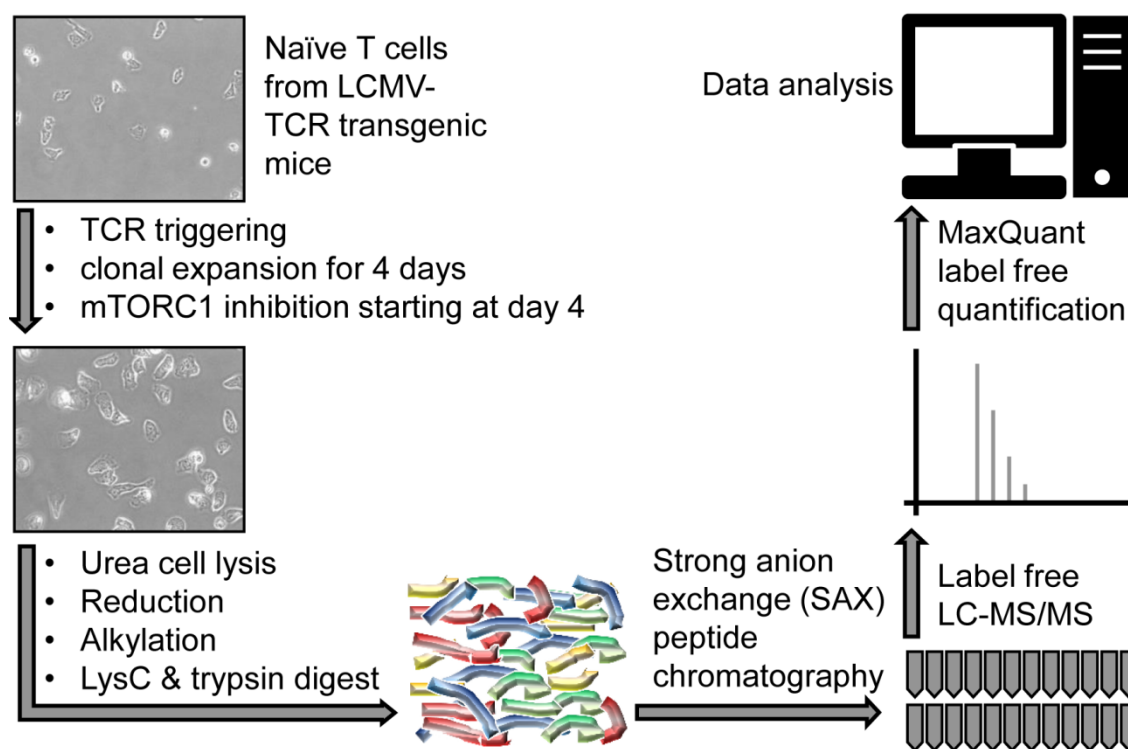
Figure 3.1: Experimental workflow.
T cells were isolated from LCMV TCR transgenic mice and activated with cognate peptide. Antigen was washed out after 48 hours and CTL were clonally expanded for 96 hours. Cells were treated with DMSO (control) or Rapamycin for the last 48 hrs of culture. Cells were collected, lysed and processed prior to digest with LysC or LysC/Trypsin double digest. Peptides were separated by strong anion and reverse phase chromatography prior to analysis by an Orbitrap Velos mass spectrometer. The generated data was analysed using MaxQuant.
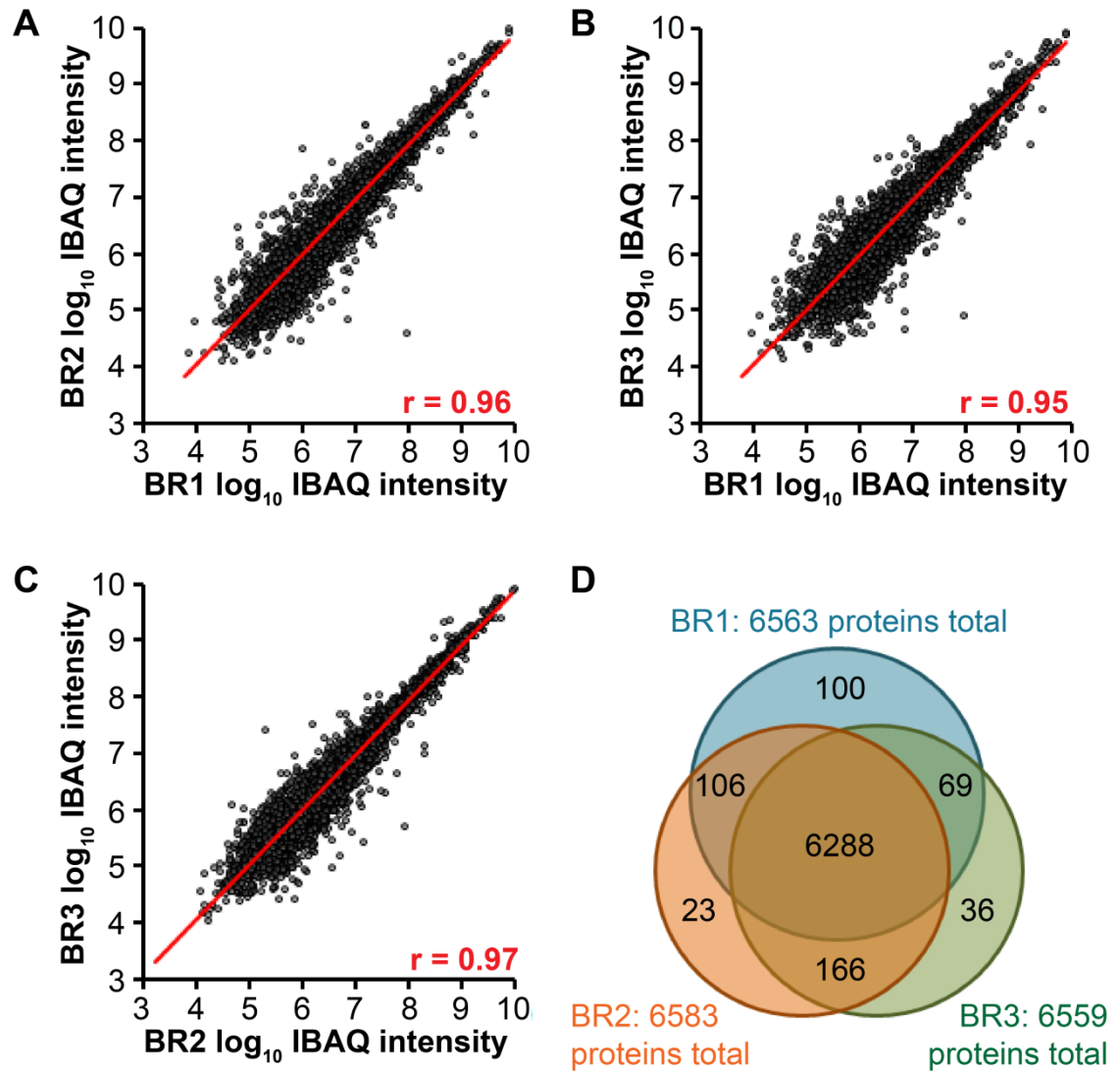
Figure 3.2: Reproducibility of LFQ approach
(A-C) Log-transformed IBAQ intensities for each replicate are plotted against each other and the Spearman correlation coefficient (r) is depicted in red. The calculated linear regression is depicted as red line. (D) Venn diagram showing the overlap of identified proteins in biological replicates.

3.2.2. LFQ based proteomics with SAX fractionation is unbiased

We next investigated whether our approach showed any bias toward different classes of proteins occurring in the cell. We thus calculated the frequencies of several Gene Ontology[297] terms that the protein groups in our data set were annotated with and compared these frequencies with the frequencies of these terms in the complete Uniprot

protein data set that was used for our analysis (Figure 3.3). The frequencies show very strong positive correlation as indicated by Spearman coefficients of 0.98 and more. Of the three terms analysed (biological process (GOBP), cellular compartment (GOCC) and molecular function (GOMF)) only the cellular function annotation showed a few outliers which were associated with a localisation to the membrane and were underrepresented in our dataset (Figure 3.3, B). Thus the frequencies with which these terms occur in the proteins detected by our approach are very similar to the frequencies of the total mouse proteome and therefore indicate that our dataset is an unbiased representation of the total theoretically achievable proteome.
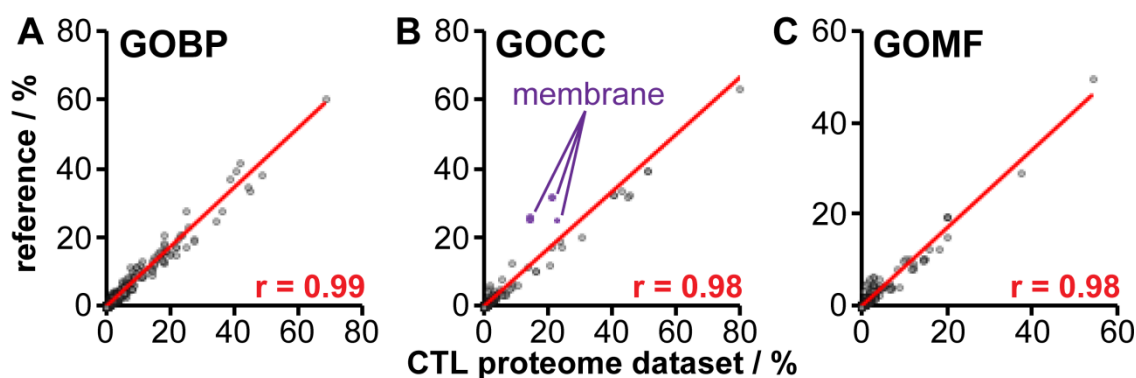
Figure 3.3: Estimation of detection bias in LFQ approach
Frequencies of GO terms in this dataset were compared with predicted frequencies based on total mouse proteome. GO terms for (A) biological process (B) cell compartment (C) molecular function are shown. Spearman correlation coefficient (r) is depicted in red, red lines indicates calculated linear regression. Outliers are indicated by purple label.

3.2.3. Transcript and protein levels show a moderate correlation

In parallel to sampling replicates for our proteomics approach we also prepared samples for a transcriptional analysis using the affymetrix platform[298]. We compared protein abundance as estimated by the IBAQ value for each protein with the transcript intensity of their corresponding mRNA by using the probe intensities derived from micro arrays as reported previously[299]. The values for RNA and proteins show a moderate correlation

according to a Spearman correlation of 0.56 (Figure 3.4) which is similar to previous reports in other cells systems[299].
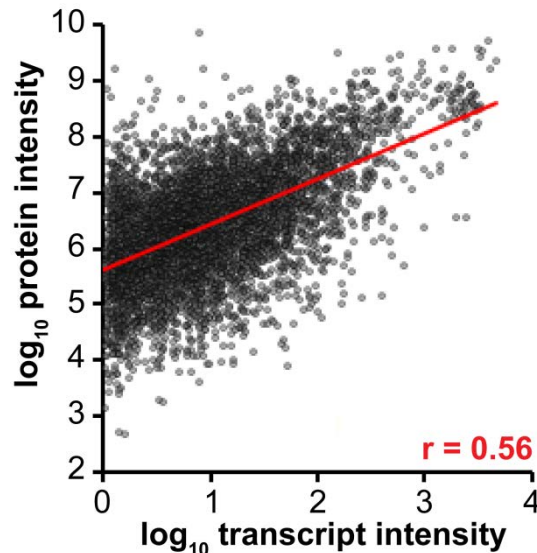
Figure 3.4: Correlation between transcript and proteins levels in CTL
Log-transformed micro array probe intensities and log-transformed IBAQ-scaled protein intensities are plotted. The calculated Spearman correlation coefficient (r) is depicted. The red line indicates the linear regression of the data.

We then investigated the correlation between transcript and protein for cytoplasmic and mitochondrial ribosomes and the 26S proteasome as the subunits of the multi protein complexes appear in equal abundances and should thus form a subset of proteins with tightly regulated abundances[265]. There is a clear difference in the protein abundance between cytoplasmic and mitochondrial isoforms with the cytoplasmic isoforms being one of the most abundant proteins in CTL and approx. 100 times more abundant than the mitochondrial isoforms (Figure 3.5, A and Figure 3.6) The protein abundances of the two populations are very tight and show a very low coefficient of variation of less than 5%. The same tight regulation of protein abundance can be seen for subunits of the 26S proteasome (Figure 3.5, B). In contrast to the tight protein levels the corresponding transcript levels for the ribosomal and proteasomal complexes show a wide spread over

the whole range of detected transcript intensities (Figure 3.4) which is illustrated by the

high CV values associated with the average of the transcript intensities.
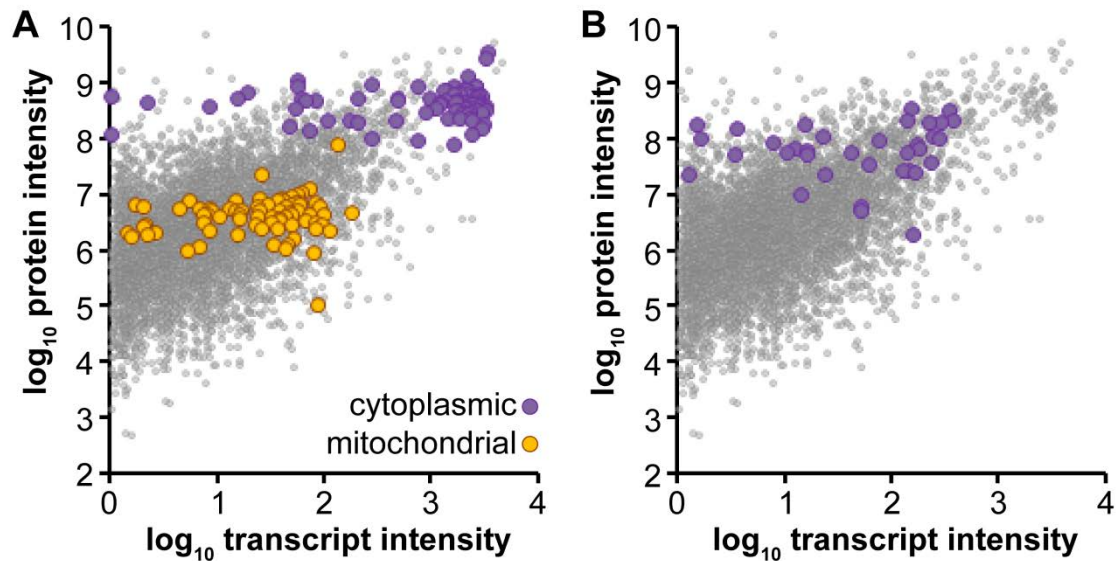
Figure 3.5: Correlation between transcript and proteins levels of ribosomal and the 26S proteasome subunits.
Log-transformed micro array probe intensities and log-transformed IBAQ-scaled protein intensities are plotted. (A) Cytoplasmic (purple) and mitochondrial (yellow) ribosomal subunits are highlighted. (B) Subunits of the 26S proteasome are shown. Grey dots: background data points.

protein complex	transcript		protein	
	average	CV	average	CV
ribosome (cytoplasmic)	2.8	30%	8.6	3%
ribosome (mitochondrial)	1.3	41%	6.6	5%
26S proteasome	1.6	45%	7.8	7%

Figure 3.6: Comparison of variation between transcript and protein levels of protein complexes.
Average $\log_{10}$ transformed transcript and protein intensities as well as coefficients of variation are shown.

3.2.4. Characterisation of CTL proteome

When we analysed the contribution of each protein to the total mass of cell we saw that

only a small subset of protein (21 proteins) contributed to 25% of the bulk total cell

mass. The 100 most abundant proteins make up over 50% of the cell mass and 75% of

the total cell mass is made up the 346 most abundant proteins. The least abundant 6446

taken together only contribute to 25% of the total cell mass.
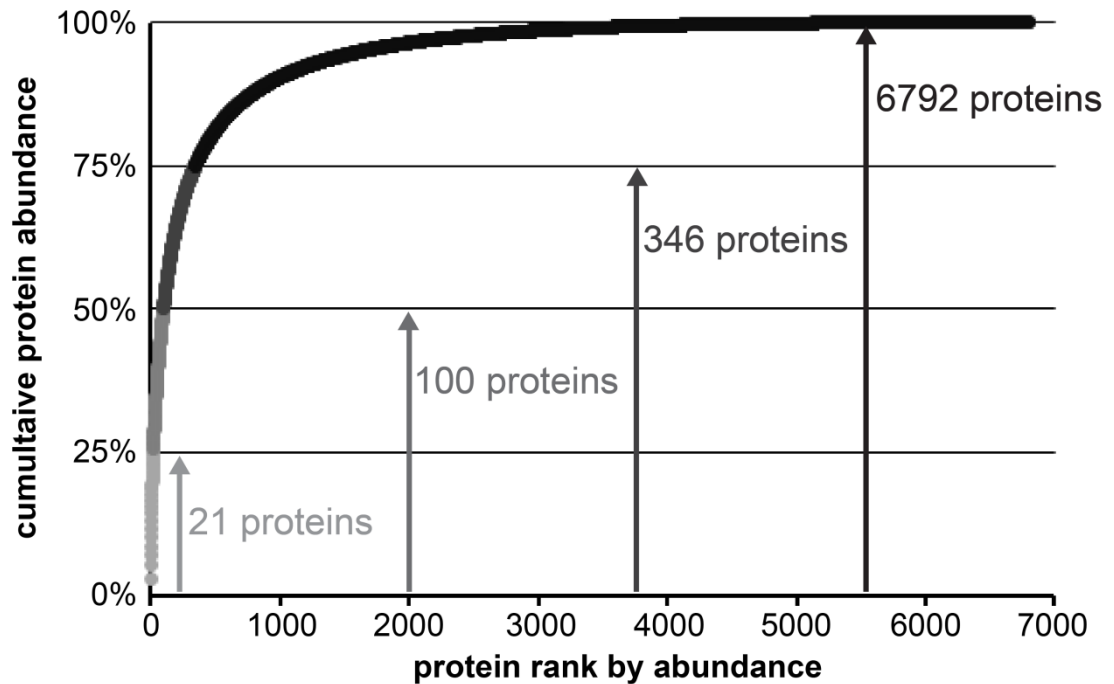
Figure 3.7: Cumulative plot of protein abundance.
Proteins were ranked by abundance as estimated by IBAQ intensities and plotted
against the cumulative mass of the whole dataset. Proteins follow an exponential
increase in abundance, with the 21 most abundant proteins constituting 25% of the bulk
cell protein mass and 346 proteins constituting 75% of the total mass. 6446 proteins
contribute to the remaining 25% of the cell mass.

A list of the 20 most abundant proteins in CTL is shown in Figure 3.8. Among the list

are histones (histone H4 and H3.2), components of the cytoskeleton (several thymosin

isoforms, vimentin, cofilin, protein S100-4) components of the translational machinery

(petidyl-petidyl cis-trans isomerase A, ribosomal proteins, initiation and elongation

factors, chaperones) and glycolytic enzymes (enolase, GAPDH, LDH). Granzyme B is

an effector molecule expressed by CTL, γδT and NKT cells[300]. With the exception of

granzyme B the list is similar to studies performed in several cancer cell lines[265,283].

Vimentin is also known to be major component and marker of cells of the mesenchymal lineage like cells of the lymphocytic and circulatory systems[301]. Many of the proteins in this list also show very high transcript intensities with the histones being notable exceptions.

protein rank	transcript rank	Protein name	fracti. abund.	cumul. abund.
1	2778	Histone H4	3%	3%
2	3	Isoform Short of Thymosin beta-4	2%	5%
3	64	Vimentin	2%	7%
4	47	Prothymosin alpha	2%	9%
5	9	Peptidyl-prolyl cis-trans isomerase A	2%	10%
6	4	60S acidic ribosomal protein P2	1%	12%
7	348	Cofilin-1	1%	13%
8	96	Alpha-enolase	1%	14%
9	7	60S acidic ribosomal protein P1	1%	16%
10	120	Eukaryotic translation initiation factor 5A-1	1%	17%
11	1	Granzyme B(G,H)	1%	18%
12	75	Glyceraldehyde-3-phosphate dehydrogenase	1%	19%
13	56	L-lactate dehydrogenase A chain	1%	19%
14	2642	Putative RNA-binding protein 3	1%	20%
15	2	Elongation factor 1-alpha 1	1%	21%
16	5301	Histone H3.2	1%	21%
17	201	Protein S100-A4	1%	22%
18	100	Heat shock protein HSP 90-beta	1%	23%
19	173	Fructose-bisphosphate aldolase A	1%	23%
20	76	Phosphoglycerate kinase 1	1%	24%

Figure 3.8: List of 20 most abundant proteins in a CTL.
The list shares many proteins with similar studies published in different cell lines with proteins involved in chromatin and cytoskeletal organisation, translation and glycolysis. The high expression of granzyme B is specific to effector immune cells.
fract. abund.: fractional abundance for specific protein; cum. abund.: cumulative abundance

As depicted in Figure 3.9 the abundance of proteins ranges of seven orders of magnitudes. We used the KEGG DAVID bioinformatics tool[295,296] to perform a pathway enrichment analysis on our dataset. The highest intensity quartile was enriched

in pathways involved in transcription and translation (ribosomes, aminoacyl-tRNA synthetases) and metabolic pathways involved in oxidative phosphorylation, glycolysis, the TCA cycle and glycolysis. Pathways involved in the replication of DNA and other anabolic pathways like the pentose phosphate pathway are also enriched in this quartile. In contrast to the cytoplasmic aminoacyl-tRNA synthases the mitochondrial isoforms of these enzymes are much less abundant. The low abundance quartile does not show any enriched pathway apart from regulators of the cell cycle.
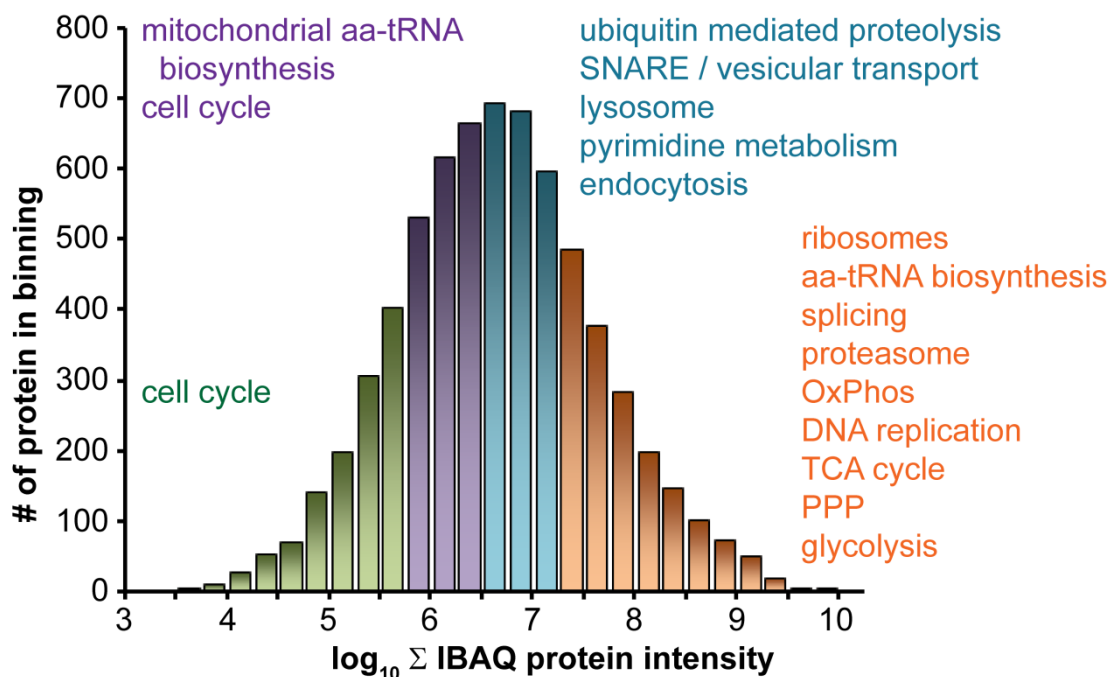
Figure 3.9: Histogram of log-transformed protein abundance as estimated by IBAQ intensity.
Protein abundances span seven orders of magnitude. Enriched KEGG ontology terms (p < 0.05) are depicted above each quartile. The highest expressed quartile is enriched in proteins involved in several metabolic pathways whereas transcription factors and cell cycle regulator are expressed at lower levels.

3.2.5. Relative quantification of key CTL molecules, nutrient transporters and protein isoforms

We then looked specifically at the expression of selected groups of molecules (Figure 3.11) namely surface proteins (A), molecules important for CTL effector function (B), nutrient receptors (C) and kinase isoforms (D). We detected all three subunits of the IL-2 receptor in a ratio that correlates to previous reports. All IL-2 receptor subunits are also more abundant than the detected IL-7 receptor subunit. We furthermore detected the constant regions of the TCRα and TCRβ subunits at roughly the same levels. All CD3 receptor subunits were detected (at slightly higher abundance than the TCR subunits) with the CD3ε subunit being the most abundant. With the exception of the IL-2Rα subunit all molecules are detected at levels that roughly correspond to the median protein abundance. IL-2Rα, CD45 and Thy1 are expressed at high levels. CD4 was not detected in our dataset. Of all effector molecules depicted in Figure 3.11 (B) granzyme B is expressed at extremely high levels (see Figure 3.8), whereas the transcription factor Eomes is expressed at very low levels. The balance between the transcription factor Eomes and T-Bet has been reported to be important for CD8 effector T cell fate [302,303]; according to our data T-bet is significantly more abundant than eomesodermin.

protein	transcript abundance	protein abundance
Eomes	30	1.4×10^5
T-bet	38	4.9×10^6
Glut1	103	1.2×10^7
Glut3	5	1.4×10^7
PKM1	207*	3.3×10^6
PKM2	207*	2.0×10^8

Figure 3.10: Comparing expression levels of selected protein isoforms and transcription factors
Transcript and proteins levels for Glut1/3, PKM1/2 and Eomesdodermin/T-bet are shown. *: The Affymetrix microarray probes are directed again a shared region of PKM1 and PKM2 and thus no PKM1/2 specific intensities are available.

Interestingly, the differences in the Eomesodermin:T-bet-ratio were more evident on the protein level than on the transcript level (Figure 3.10).
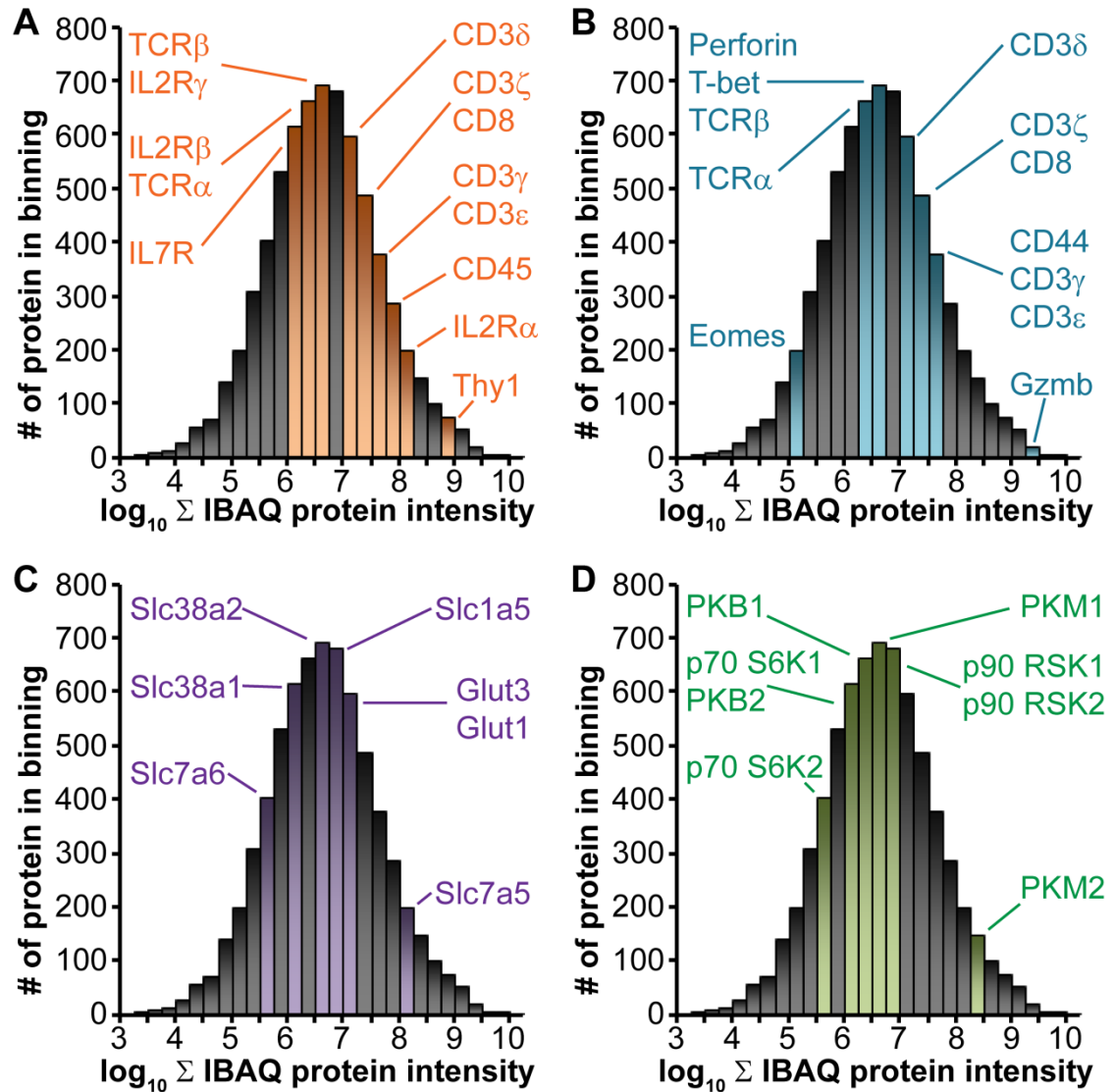
Figure 3.11: Histograms of log-transformed protein abundance as estimated by IBAQ intensity with key CTL molecules highlighted.
Distribution of a selection of receptor subunits expressed by CTL. (**B**) Histogram showing the distribution of markers used to characterise CTL in flow cytometry based assys. (**C**) Expression of selected nutrient transporters in CTL showing equal expression of the glucose transporters Glut1 and Glut3. (**D**) Comparison of isoform expression in CTL. Levels of PKM2 are more than 80x higher than PKM1 levels. The p90 RSK isoforms 1 and 2 are expressed at equal levels whereas Akt1 and p70 S6K1 are expressed at higher levels than their respective isoforms.

As rapidly proliferating cells CTL require a steady supply of nutrients in order to fulfil the metabolic demand of the rate of proliferation. In this context, the glucose receptor Glut1 and the large amino acid transporter Slc7a5 have been shown to be crucial for CTL clonal expansion[81,84,227]. Slc7a5 is indeed expressed at high levels whereas several other known amino acid transporters (Slc7a6, Slc38a/1, Slc5a1) were only expressed at average levels. The glucose transporters Glut1 and Glut3 were also expressed at average levels whereas their corresponding transcripts suggest a more than 20-fold excess of Glut1 over Glut3 (Figure 3.10).

The overexpression of pyruvate kinase M2 isoform has been reported to be hallmark of cancer and other rapidly proliferating cells[304,305] so we assessed its expression and compared it to the levels of the PKM1 isoform. PKM2 is highly expressed in CTL and approximately 60 times more abundant than the PKM1 isoform. As the Affymetrix micro array platform used does not include PKM1 or PKM2 specific probes this difference could only be picked up in our proteomics approach. Other pyruvate kinase isoforms were not detected in our data. We furthermore compared expression of several kinases of the AGC family, namely p90 RSK, p70 S6K and PKB. We could detect RSK1 and RSK2 at approximately equal levels whereas the RSK3 isoforms could not be detected. PKB1 and PKB2 were also expressed at approximately equal levels whereas the PKB3 was not detected. Both known homologues of p70 S6K were detected with S6K1 being expressed at slightly higher levels.

3.3. Discussion

The results presented in this chapter show that our LFQ mass spectrometry approach in conjunction with SAX chromatography could successfully be adapted to the use with CTL. The approach proved to be robust and highly reproducible (Figure 3.2) and showed only little detection bias (Figure 3.3). One explanation for the slight underrepresentation of membrane proteins might be the use of a urea based lysis buffer which does not contain any detergents which might have aided the solubilisation of the hydrophobic membranes. However, detergents like SDS are not compatible with the subsequent fractionation as the detergent will bind irreversibly to the fractionation column and thereby render it useless.

We detected 6800 proteins in our 3 biological replicates with more than 6500 proteins found in each single replicate, with an instrument time of 1 ½ days per replicate. We know this is not complete coverage. For example we failed to detect the transcription factor Hif1α, which is known to be expressed in CTL[85]. Previous studies with a similar instrumental approach of the proteome of mouse macrophage[282] or human promyelocytic cell lines[283] led to the identification of 9469 or more than 10,000 proteins, respectively and thus approached near-total coverage of the predicted proteome . It is thus estimated that the number of proteins expressed by mammalian cells is in the order of 10,000[265,306]. However, these studies used slightly different fractionation strategies nearly tripling the samples numbers analysed by the machine and thus increasing run time to one week[282] or used the same fractionation strategy but increased the sample size by pre-fractionating the human cell line used according to their cell cycle stage[283]. Moreover, these experiments used human cells and the human Uniprot database contains more database entries than the mouse database (approx. 20,000 entries for the human versus 16,000 entries for the mouse database). There is hence a bigger library of peptides to match any identified MS/MS spectra for peptides from human cells compared to the options for mouse cells. This enables

higher identification rates of studies of human peptides. However, the study by Ritorto et al.[282] also illustrates the scalability of our approach which might help to close the gap of missing identifications of proteins. It should be noted that one limitation is practical: there would be better peptide identifications with longer run times but machine access time is limited by funding and the need to share access with other users.

The results depicted in Figure 3.4 show the importance of our proteomics approach. Transcriptional analyses have been used for a long time and are a powerful tool to study changes in global gene expression. However, the approximations for transcript intensities gained from these experiments cannot be used to predict the abundance of the corresponding protein as the low correlation in our experiment showed and which has been reported for other cell lines as well[299,307,308,309,310,311,283].

The wide range of proteins abundance spanning over seven or more orders of magnitude (Figure 3.7, Figure 3.8) is typical for eukaryotic cells and has been reported previously[265,283]. Despite this wide range of protein abundances, several macromolecular complexes like the ribosomal and 26S proteasomal complex show a tight and seemingly coupled regulation of the abundance of their respective subunits to effectively maintain the defined stoichiometry of these complexes. A similar behaviour can be seen with other macromoulcar complexes with a defined stoichiometry like the TCR (the constant regions of the α and β subunits are expressed at a roughly equimolar ratio) as well as the CD3 subunits whose expression levels comply with the reported stoichiometry of the complex. The list of the most abundant proteins acquired by our experiment is also similar to previous studies. However, the high expression of granzyme B is unique to CTL (NKT and $\gamma\delta$ T cells) and emphasises the importance of this protein for effector function. Granzyme B is also the protein with the highest transcript levels in CTL. With the exception of the histones many of the proteins in Figure 3.8 also show high transcript levels indicated that high protein levels usually

correlate with high transcript levels which is also illustrated by the tight ribosomal cluster in the high transcript-high protein part of Figure 3.5, A. The discrepancy between the abundance of histone mRNA and protein levels can be explained by the lack of polyadenylation at the 3'-end of their mRNA[312]. As oligo(dT) primers are used in the generation of the cDNA which is analysed by the micro array, a lack of polyadenylation will inevitably lead to a underrepresentation of these transcript in the analysis.

The high abundance of glycolytic enzymes also emphasises the importance of this metabolic pathway for CTL. Naïve T cells perform a glycolytic switch when their TCR is stimulated and massively up regulate glycolysis and maintain high glycolytic rates during their clonal expansion[313,314]. Nevertheless, our pathway analysis showed that enzymes involved in oxidative phosphorylation are also still highly expressed. The translational machinery of the cells is also strongly expressed and enables the rapid proliferation of CTL together with anabolic pathways like the pentose phosphate pathway. Subunits of the 26S proteasome are also expressed at very high levels which might indicate that the high rate of protein biosynthesis requires high proteasomal activity to serve as a quality control for nascent proteins as well as a regulator of intracellular amino acid pools[315]. Misfolds and other errors occurring during protein translation can stress a cell and lead to apoptosis[316] so resolving these problems is crucial for cells which employ strategies like the ubiquitin-proteasome system to deal with the aggregation of misfolded proteins. The high levels of proteasomal subunits might reflect a high activity of this quality control system due to an equally high translational activity.

The balance between the transcription factors T-bet and Eomesodermin is crucial for the formation of CD8 effector or memory T cells, with T-bet favouring an effector and

Eomesodermin a memory phenotype[302,303,317]. Our data suggests that T-bet is more than 30 times more abundant than Eomesdermin (Figure 3.11, B) which supports this hypothesis. Interestingly, the transcript levels of these two proteins are roughly the same which suggest that non-transcriptional mechanisms are regulating the balance between these two proteins. The importance of other molecules is also illustrated by their high abundance: Slc7a5 which is essential for CTL differentiation[227] is expressed at very high levels, particularly when compared to other amino acid transporters (Figure 3.11, C). As high levels of glucose are required to fuel the high proliferation rates of CTL[228,318] glucose has to be transported into the cells at high rates by glucose transporters like Glut1. Glut3, which has a higher affinity as well as a higher transport capacity than other glucose transporters and is important in neuronal glucose transport[319], is expressed at equal levels to Glut1 which might indicate that Glut3 is the most important glucose transporter in CTL and might thus be critical in maintaining high metabolic rates in CTL. Interestingly, transcript levels of Glut1 are 20 times higher than those of Glut3, indicating that differences in translational efficiency or posttranslational regulation are responsible for the equal protein levels of the glucose transporters. Another enzyme involved in glucose metabolism, pyruvate kinase is also expressed in the form of two different isoforms which could be distinguished in the proteomic analysis. The highly similar splice variants PKM1 and PKM2 are expressed at very different levels, with PKM2 expressed at an approximately 60-fold higher level than PKM1 (Figure 3.11, D). This is important as high levels of PKM2 are typical for cancer and other highly proliferative cells as PKM2 (and not PKM1) can exist in a dimeric form with low catalytic activity. At the cost of ATP generation, this lower catalytic activity leads to the accumulation of phosphoenolpyruvate and other glycolytic intermediates and thus aids cell proliferation as it supplies building blocks required for the synthesis of amino acids and phospholipids[304]. The tetrameric forms of PKM1 and

PKM2 show a high catalytic activity which does not show a proliferative phenotype as it maintains high glycolytic flux and thus does not cause the accumulation of glycolytic intermediates.

Despite the high coverage of our proteome and the detection of nearly 7000 proteins, we noticed that we were not able to detect some proteins known to play a key role in T cell biology. We discussed the slight underrepresentation of membrane protein before and an example for a membrane protein that we were not able to identify in our approach is PD-1, which has emerged as an important negative regulator of the immune response of CTL[320]. But we also struggled to find several key transcription factors like Hif1-α[85] which are also known to fulfil critical roles in CD8$^+$ effector function. This failed identification of these proteins further illustrates the importance of high coverage in quantitative mass spectrometry experiments.

Based on this proteomic approach, the following chapter will describe the global effects of mTORC1 inhibition with rapamycin on the CTL proteome.

4. Characterisation of the mTORC1 controlled CTL proteome

4.1. Introduction

Whereas the previous chapter described our approach to define the global proteome of a cytotoxic T cell, the following chapter will investigate the effects that mTORC1 inhibition causes in CTL. The mTORC1 complex serves as an integrator for nutrient availability and cytokines signalling[321] and controls CTL trafficking[155] as well as CD8 T cell differentiation[200,322,177]. mTORC1 is widely considered a regulator of translation[323] and hence analysis of the role of mTORC1 in regulating the CTL proteome should give insights as to how this drug control CTL function.

Global proteomics approaches in the context of mTORC1 inhibition have been used before[324], however these experiments were done using transformed cell lines and not primary lymphocytes thus missing cell specific effects of mTORC1 signalling regulation in these specific cell types.

We therefore wished to examine the proteome of CTL exposed to rapamycin, a highly specific inhibitor of the mTORC1 complex. We wished to assess the impact of long term mTORC1 inhibition on the proteome of CTL and accordingly, the following chapter will describe the effects of 2 days inhibition of mTORC1 on the CTL proteome.

4.2. Results

4.2.1. mTORC1 inhibition in CTL leads to decreased cell proliferation, translation rates and cell size

As mentioned before, we used a well-established *in vitro* model of CTL differentiation based on LCMV P14 TCR-transgenic mice for our approach. Treatment of these cells with 20 nM of rapamycin led to the dephosphorylation of ribosomal protein kinase S6 (S6K) at Thr389 and the translational inhibitor 4EBP1 at several sites (Figure 4.1, A) showing that treatment of CTL with rapamycin inhibits these established mTORC1 substrates[325]. It has been proposed that long term inhibition of the mTORC1 complex can disrupt the activity of the mTORC2 complex[195]. The data in Figure 4.1, A show that long term treatment of CTL with rapamycin did not prevent the phosphorylation of PKB on the mTORC2 substrate sequence Ser473. Rapamycin thus selectively targets the activity of the mTORC1 complex in CTL even after prolonged treatment.

mTORC1 can control cell cycle progression and thus cell proliferation in transformed cell lines[326] and early studies showed a complete block of IL-2 driven proliferation of the *in vitro* CTL clone CTL[327]. We therefore examined whether IL-2 induced proliferation of the primary murine CTL used in the present experiments was effected by mTORC1 inhibition (Figure 4.1, B). CTL can undergo several cell divisions per day which is illustrated by the nearly 10-fold increase in cell numbers from day 4 to day 6 in culture. In contrast to that, the rapamycin treated CTL increased their cell numbers approximately 5-fold and thus showed a reduced proliferation rate. However, this rate still corresponds to more than one cell doubling per 24 hrs. Inhibition of mTORC1 thus slows down but does not fully prevent CTL proliferation.

mTORC1 phosphorylation of 4EBP1 and S6K1 has been proposed to control protein synthesis in transformed cell models[238] but it is not known how mTORC1 inhibition

affects protein translation rates in CTL. We measured the effects of rapamycin on the global translation rate in CTL in a time dependent manner by monitoring the incorporation of a short pulse (15 mins) of radio labelled L-methionine into nascent proteins[328]. Long term inhibition with rapamycin decreased the incorporation rate of L-methionine into proteins by 50% in a time dependant manner and thus indicates that mTORC1 controls protein synthesis rates in CTL. The maximal inhibition of methionine incorporation was achieved between the 24 h and 48 h time point. Thus we decided to treat CTL with rapamycin for 48 h in order to examine the steady state effect of mTORC1 inhibition; the term 'long term treatment' will thus refer to a 48 h treatment.

The ability of rapamycin to decrease rates of protein synthesis made us explore the impact of rapamycin treatment on the cell size of CTL. The analysis of rapamycin treated CTL by flow cytometry indicated that these cells had reduced forward (Figure 4.1, F) and side light scatter (Figure 4.1, E) characteristics compared to control cells which is indicative that these cells have reduced cell size although it could also reflect that rapamyicn treated CTL change in cell shape or cell granularity. We therefore quantified the protein content of rapamycin treated CTL compared to control CTL. These data (Figure 4.1, F) show a 15% reduction in the total protein content of 48 hour rapamycin treated CTL compared to controls. We also examined the cytoplasmic protein content of rapamycin treated CTL and determined a 35% reduction in cytoplasmic protein of long term rapamycin treated CTL compared to controls.
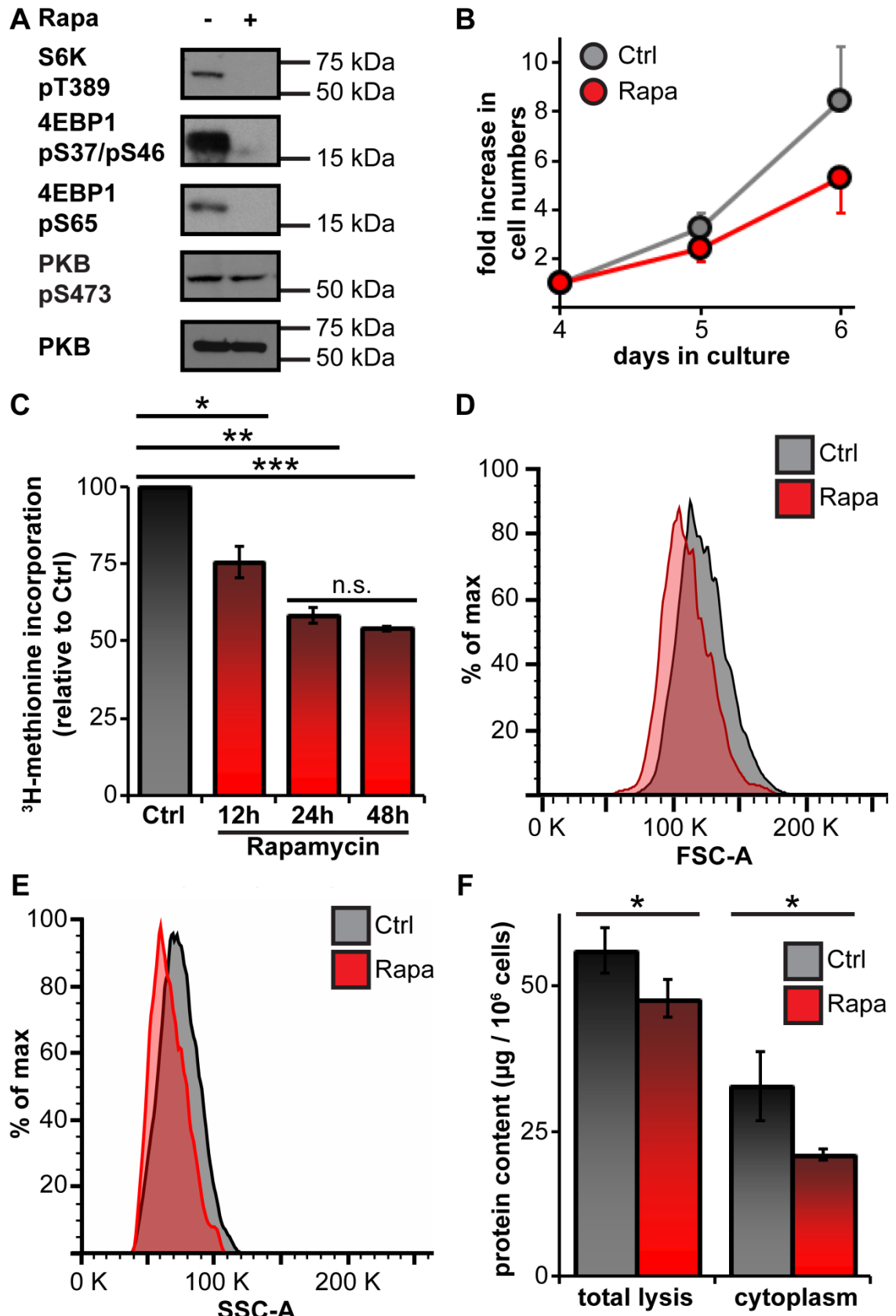
Figure 4.1: Effects of rapamycin on mTORC1 kinase activity, cell proliferation, protein biosynthesis and cell size

(A) immunoblot analysis of mTOR activity in Ctrl and Rapamycin treated cells. Phospho-S6K and phospho-4EBP1 used as a measure of mTORC1 activity. PKB was used as a loading control. (B) Growth curve showing effects of mTORC1 inhibition on

CTL growth. Rapamycin was given from day 4 on. (C) Analysis of protein biosynthesis rate by methionine incorporation. (D) Flow cytometric analysis of effect of mTORC1 inhibition on CTL forward scatter. (E) Flow cytometric analysis of effect of mTORC1 inhibition on CTL side scatter. (F) Cell mass determination of vehicle and rapamycin treated cells. Comparison of total lysis (8M urea buffer) and cytoplasmic fraction (low detergent lysis). Data are mean ±SD or representative of at least three experiments (*, p ≤ 0.05; **, p ≤ 0.01; ***, p ≤ 0.001)

4.2.2. Long term inhibition leads to translational reprogramming of the CTL proteome and not a general down regulation

As the data in Figure 4.1, F demonstrated that long term rapamycin treatment leads to a decrease in overall cell mass we sought to identify the proteins down regulated due to mTORC1 inhibition. The protein synthesis data could thus indicate that there was a global reduction in the production of all cellular proteins or that there were selective losses of very rapidly synthesised abundant proteins. We chose a proteomic approach based on quantitative mass spectrometry to address the problem. We used a label-free quantification strategy similar to the approach chosen in the previous chapter. In short, we used the P14 LCMV TCR-transgenic model for *in vitro* generation of CTL by activating TCR-transgenic splenocytes with the cognate peptide KAVYNFATM for 2 days in the presence of IL-2 and IL-12. Cells were then washed and clonally expanded in IL-12/IL-12 for a further 4 days. 20 nM Rapamycin or DMSO (control) were added to the cell culture for the last 48 hrs of clonal expansion. Cells were then urea lysed and digested and the resulting peptides were separated using strong anion exchange (SAX) chromatography. Control and rapamycin treated samples were further processed and submitted to reverse phase (RP) liquid chromatography coupled to Orbitrap Velos mass spectrometer. The data was then analysed using the label-free quantification algorithm of the MaxQuant package. Ratios for each protein were calculated comparing the peptide intensities of control and rapamycin treated samples. Three biological replicates

of control and rapamycin treated cells derived from three different LCMV mice were used for the subsequent data analysis.

By following the aforementioned approach we could calculate the changes in protein expression upon rapamycin treatment for 6733 proteins in our three replicates. The global proteomic analyses indicated that rapamycin treatment regulated expression of 719 proteins (as judged by a p-value of < 0.05) of which 376 proteins were decreased in expression and 343 proteins showed increased expression following the rapamycin treatment (Figure 4.2). Proteins that could only be detected in either the control or the untreated samples due to sensitivity issues were considered 'not detected' for that particular replicate and thus no ratio was assigned. Previous studies have shown that inhibition of mTORC1 with rapamycin causes CTL to decrease perforin expression and increase expression of CD62L (L-Selectin). Both perforin and L-Selectin were amongst the significant changed proteins identified in the dataset or mTORC1 regulated proteins (Figure 4.2).
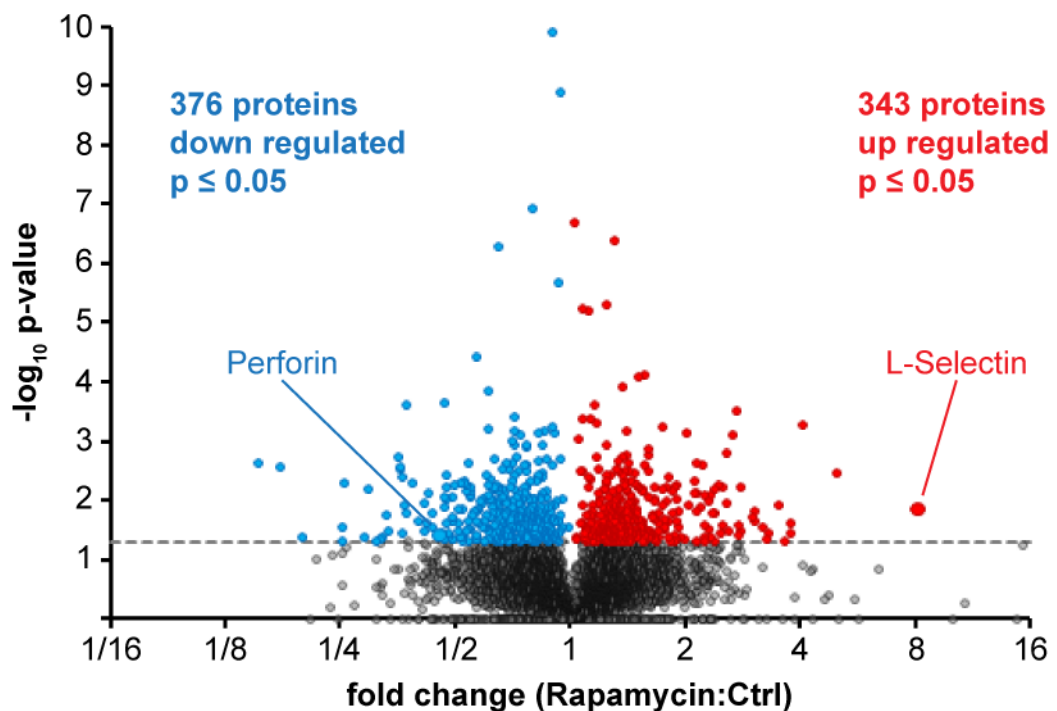
Figure 4.2: global changes in the CTL proteome induced by mTORC1 inhibition as

determined by LFQ SAX

6733 protein groups were detected in 3 biological replicates. Blue/red circles represent reproducibly down/up regulated proteins respectively. The dashed line indicates the p ≤ 0.05 threshold. Perforin and L-Selectin, known mTOR regulated proteins[329], are marked in the plot.

The changes in expression levels of perforin and L-Selectin/CD62L were then confirmed by orthogonal approaches. Flow cytometry analysis confirms the increased expression of CD62L on the CTL plasma membrane (Figure 4.3, A). These data have been previously reported[155]. However, CD62L is rapidly cleaved at the plasma membrane of CTL and thus released into the extra cellular medium. Therefore measuring CD62L levels in the cell culture supernatants is a more accurate way to monitor cellular production of CD62L. The ELISA (Figure 4.3, B) shows a more than 100-fold increase of CD62L levels in the supernatant derived from rapamycin treated cells compared to control cells.
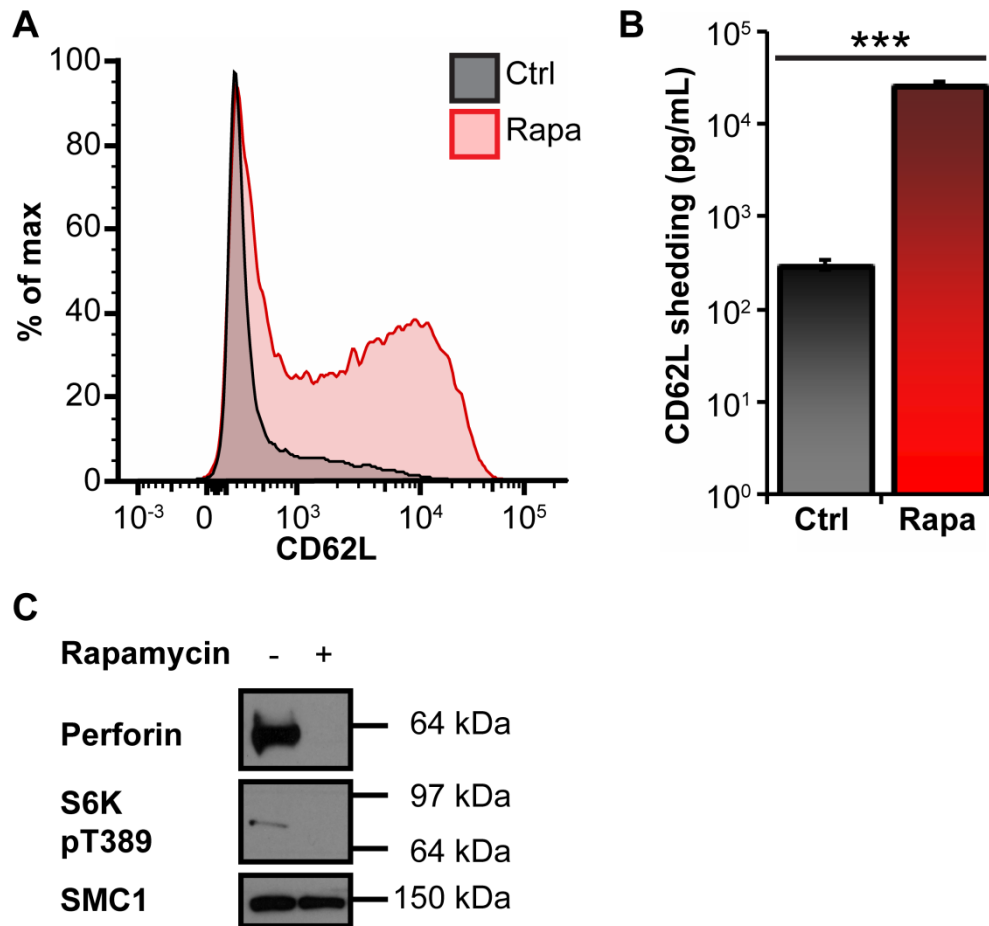
Figure 4.3: Effect of rapamycin on CD62L and perforin expression in CTL.
(A) flow cytometric analysis of intracellular CD62L levels in control and rapamycin treated CTL. (B) ELISA analysis of CD62L cleaved from CTL surface. (C) Immunoblot analysis of perforin expression in CTL. SMC1 was used as a loading control.
Data are mean ±SD or representative of at least three experiments (*, $p \leq 0.05$; ***, $p \leq 0.001$)

Even though we could derive a ratio for most of the proteins detected in the comparison between control and rapamycin treated samples, there was a sub-class of proteins for which this was not possible as these proteins were consistently only detected in one of the conditions and thus showed a theoretically infinite up or down regulation. A list with these proteins can be found in Figure 4.4. In order to be listed, proteins had to be found in one condition in at least two biological replicates but not detected in any of the replicates of the other condition. This was done to filter out proteins with generally low abundance which might have fallen below the detection limit by chance and not due to a genuine regulation upon mTORC1 inhibition.

Protein name	Up / down regulated	# of repl.
Ig lambda-3 chain C region	Up	2
Isoform 2 of Zinc finger protein 1	Up	3
Ubiquitin-conjugating enzyme E2 D1	Up	2
Isoform Short of Extracellular matrix protein 1	Up	3
DNA polymerase sigma	Up	2
Pre-miRNA 5-monophosphate methyltransferase	Up	2
Napsin-A	Down	2
Tumor necrosis factor	Down	2
B-cell differentiation antigen CD72	Down	2
JmjC domain-containing protein 8	Down	2
Zinc finger and BTB domain-containing protein 17	Down	2
RNA exonuclease 1 homolog	Down	2
SH2 domain-containing protein 5	Down	3
Isoform 2 of Transmembrane protein 129	Down	2
Bifunctional apoptosis regulator	Down	2
Sprouty-related, EVH1 domain-containing protein 2	Down	2
UBX domain-containing protein 8	Down	3

Figure 4.4: Protein only found only in control or rapamycin treated cells.
Proteins found only in control or rapamycin treated CTL. Proteins had to be detected in at least 2 biological replicates of the corresponding condition but not detected in any biological replicate of the other conditions.

Among the proteins with drastic down regulation due to mTORC1 inhibition is TNF (tumor necrosis factor), a crucial CTL effector molecule. Another example is the UBX domain-containing protein 8, a protein involved in the protein proof-reading-mechanism of cells.

Despite the decreased overall protein synthesis in CTL upon mTORC1 inhibition we found equal numbers of up and down regulated proteins in rapamycin treated cells. In order to understand this phenomenon we investigated the relationship between regulation of expression and protein abundance. The average down regulated protein is more than twice as abundant as the average up regulated protein (Figure 4.5) and thus leads to a net loss in protein content.
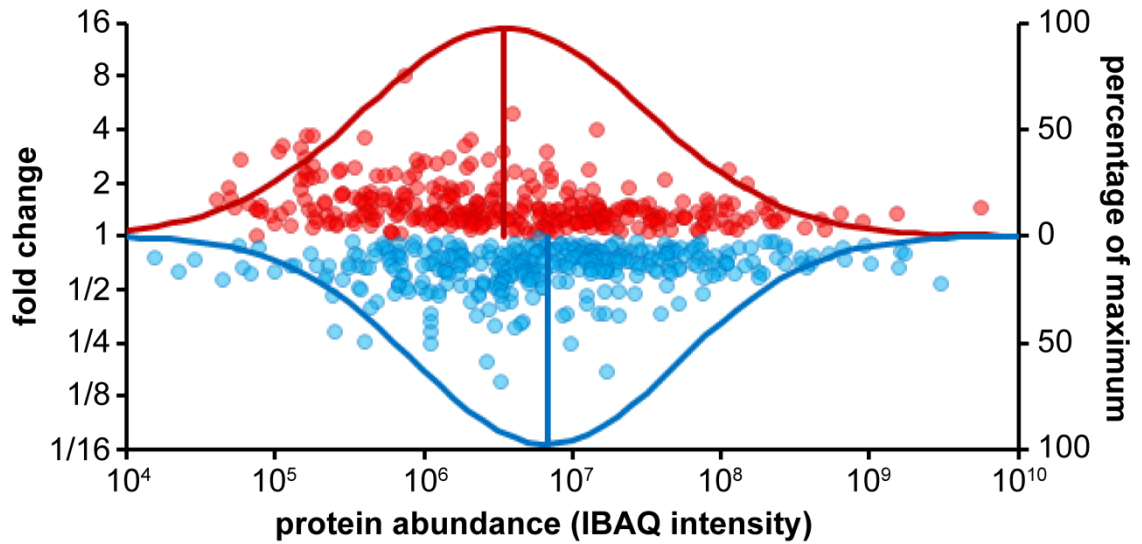
Figure 4.5: proteins down regulated due to rapamycin treatment are more abundant then up regulated proteins.
Fold change of significantly changed proteins is plotted against their abundance as estimated by IBAQ intensity. Up regulated proteins are shown in red, down regulated protein in blue. Average distribution of the two populations is indicated by bell curves.

4.2.3. Rapamycin treatment decreases the expression of CTL effector molecules

As perforin is not the only effector molecule important for CTL function, we mined our dataset for potential changes in other effector molecules. As discussed above, rapamycin also decreased expression of TNFα (Figure 4.4). The data in Figure 4.6 show that rapamycin treatment also regulated expression of granzymes, a family of serine proteases which induce apoptosis in targeted cells[330].

			protein name	fold change	p-value
			Granzyme A	1.7	0.07
			Granzyme B	0.7	0.075
			Granzyme C	2.3	0.01
			Granzyme D	1.0	< 0.001
			Granzyme E	0.89	0.2
			Granzyme G	0.23	1
			Lymphotoxin A	0.78	0.2
			Lymphotoxin B	0.90	0.8
			Tumor necrosis factor	1/∞	N/A
			Perforin	0.44	0.04
			Interferon-γ	0.17	0.002
			Interleukin-12 receptor β-1	0.48	0.009
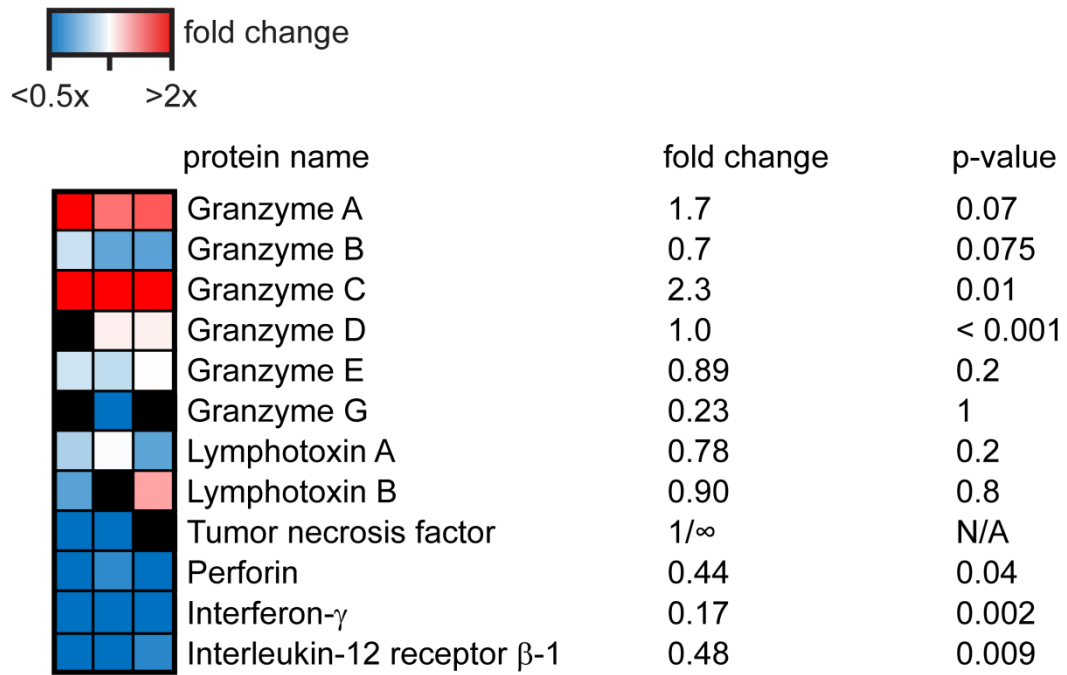
Figure 4.6: Effect of mTORC1 inhibition on effector molecule expression.
Heatmap illustration of affected protein levels of granzyme family members, Lymphotoxins, perforin, Interferon-γ and IL-12 receptor subunit β-1. Red hues indicate up regulation of protein, white no regulation and blue down regulation. Fold changes and associated p-values are given. Black fields indicate no ratio determined in replicate.

Rapamycin treatment of CTL led to differential regulation of effector molecules. granzyme A and granzyme C show up regulation, whereas perforin, Interferon-γ and IL-12 receptor subunit β-1 are down regulated. The granzyme isoforms D, E and G are not affected by rapamycin treatment. In contrast to TNFα itself, other members of the TNF family, like lymphotoxin A and B, are not significantly down regulated upon rapamycin treatment.

In order to validate the indicated drastic down regulation of IFN-γ picked up in the mass spectrometry experiments, we performed intracellular staining of control and rapamycin treated CTL (Figure 4.7, A) and measured the levels of IFN-γ secreted into CTL tissue culture supernatant (Figure 4.7, B). The FACS analysis confirmed the decreased IFN-γ expression as mTORC1 inhibition leads to a reduction in IFN-γ positive cells as well as reduced levels of IFN-γ in these IFN-γ positive cells. Rapamycin treatment also led to a

4-fold decrease of IFN-γ levels in the CTL supernatant. The proteomics experiments furthermore indicated a down regulation of the IL-12 receptor subunit β-1 so we used the phosphorylation of STAT at the Tyrosine residue 693 as a read out for functional IL-12 signalling[331]. IL-12 induces the phosphorylation of STAT4 on Y693 in the presence of IL-12 (Figure 4.7, C), and the phosphorylation level of STAT4 Y693 is slightly decreased when cells were treated with rapamycin indicative for decreased signalling through the IL-12 receptor and its downstream kinases. Interestingly, IL-12 stimulation down regulates total STAT4 levels in CTL.
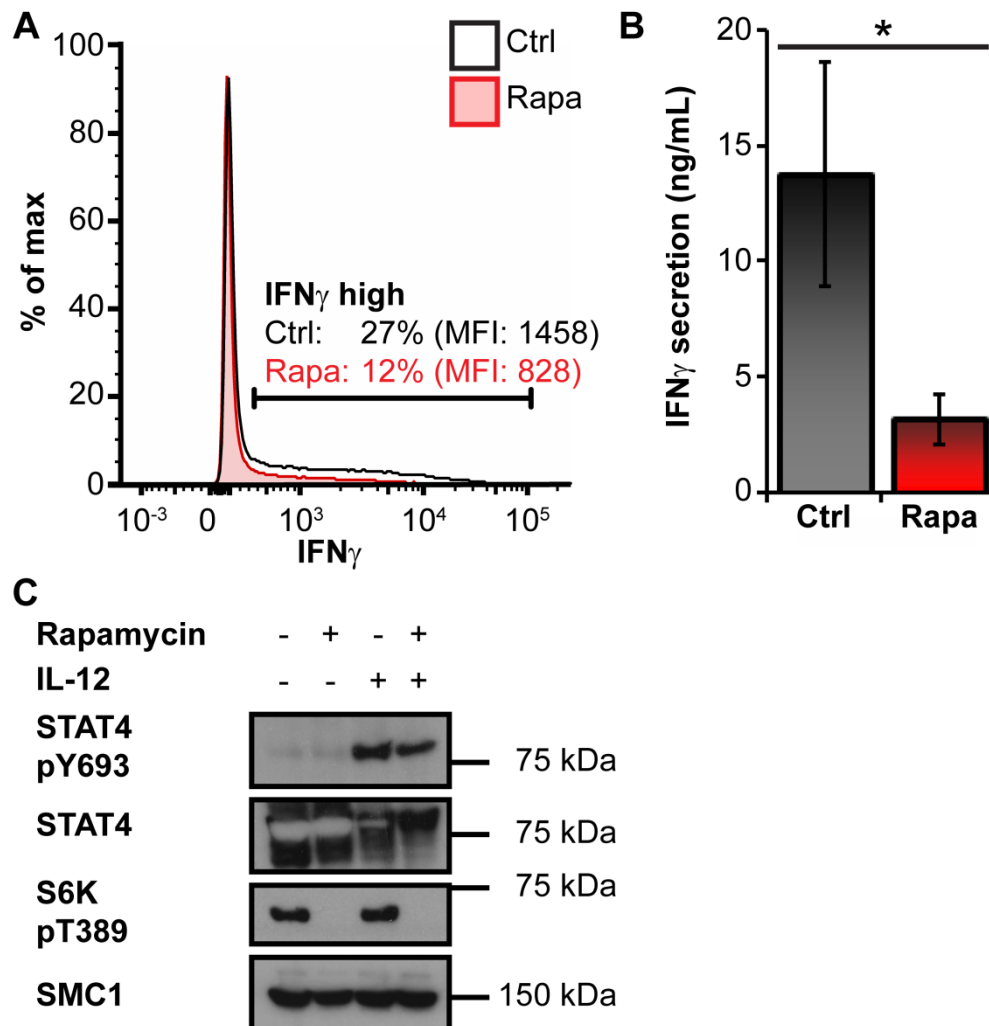
Figure 4.7: Validation of selected mTORC1 regulated proteins.
(A) Flow cytometric analysis of intracellular IFN-γ levels in control and rapamycin treated CTL. (B) ELISA analysis of IFN-γ secretion by CTL. (C) immunoblot analysis of mTOR activity in Ctrl and Rapamycin treated cells. STAT4 pY693 phosphorylation was used as a readout for IL-12 receptor activity. SMC1 was used as a loading control.

Data are mean ±SD or representative of at least three experiments (*, p ≤ 0.05)

4.2.4. Inhibition of mTORC1 leads to the up regulation of pathways involved in catabolic pathways and oxidative phosphorylation and down regulation of glycolytic and anabolic pathways

We next performed a pathway analysis of mTORC1 regulated genes (as defined by the p-value obtained from student's t-test) using the DAVID Bioinformatics resource[295,296]. The pathways which are enriched among the up (Figure 4.8) and down regulated (Figure 4.9) proteins are displayed. The pathway analysis revealed that several metabolic pathways were affected by the treatment in a distinctive way: Catabolic pathways like the degradation pathway of the terpenoids limonene and pinene (which includes enzymes responsible for the metabolism of fatty acids) and several amino acids degradation pathways are up regulated whereas anabolic pathways involved in protein translation, nucleotide biosynthesis steroid biosynthesis are down regulated.

KEGG pathway identifier	# of genes	p-value
Mismatch repair	5	4×10^{-4}
Oxidative phosphorylation	9	1×10^{-3}
Parkinson's disease	9	2×10^{-3}
Limonene and pinene degradation	4	2×10^{-3}
DNA replication	5	3×10^{-3}
Huntington's disease	10	3×10^{-3}
Valine, leucine and isoleucine degradation	5	7×10^{-3}
Alzheimer's disease	9	1×10^{-2}
Ether lipid metabolism	4	2×10^{-2}
Lysine degradation	4	3×10^{-2}

Figure 4.8: pathways up regulated by mTORC1 inhibition as determined by LFQ SAX

KEGG pathway identifier	# of genes	p-value
Aminoacyl-tRNA biosynthesis	9	4×10^{-6}
Terpenoid backbone biosynthesis	5	2×10^{-4}
Pentose phosphate pathway	5	3×10^{-3}
Steroid biosynthesis	4	6×10^{-3}
Ubiquitin mediated proteolysis	9	1×10^{-2}
Glycolysis / Gluconeogenesis	6	2×10^{-2}
Proteasome	5	2×10^{-2}
Galactose metabolism	4	2×10^{-2}
Porphyrin and chlorophyll metabolism	4	3×10^{-2}
Endocytosis	10	4×10^{-2}

Figure 4.9: pathways down regulated by mTORC1 inhibition as determined by LFQ SAX

A striking result was the impact of mTORC1 inhibition due to rapamycin treatment on proteins that control glucose metabolism in T cells. CTL treated with rapamycin down regulate the expression of both glucose transporters Glut1 and Glut3 and they also show a consequent down-regulation of multiple enzymes that control glycolysis (Figure 4.10).
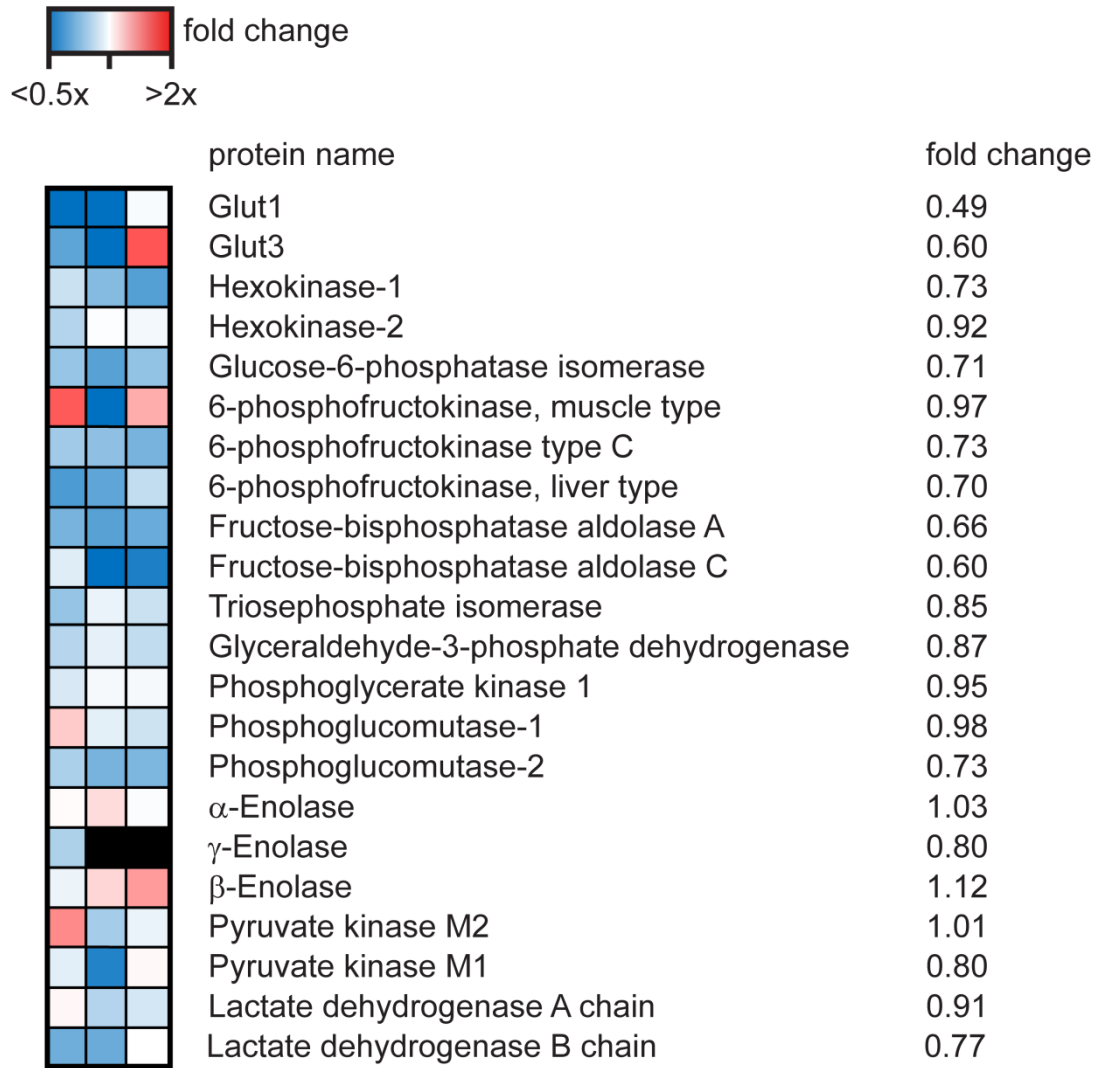
Figure 4.10: Effects of rapamycin treatment on glycolytic enzymes in CTL as determined by label-free proteomics approach
Heat map representation of enzymes involved in glycolysis and the fold changes in protein levels due to rapamycin treatment are shown. Red hues indicate up regulation of protein, white no regulation and blue down regulation. Fold changes for each protein are given. Black fields indicate no ratio determined in replicate.

These data indicate that CTL treated with rapamycin may undergo a metabolic switch as enzymes in oxidative phosphorylation are up regulated and glycolytic enzymes are down regulated, the opposing regulation of these two metabolic pathways is highlighted in Figure 4.13, A.

As rapamycin decreased the expression of the glucose transporters Glut1 and Glut3 we next investigated the effects of mTORC1 inhibition on the expression of all detected

Solute carrier (Slc) family of membrane transport families expressed by CTL. We also had a closer look at the expression of the system L amino acid transport system subunits and the transferrin transporter. We identified the expression of all subunits of the system L and y^+L amino acid transporters, the transferrin receptor as well as 66 further Slc family members with varying coverage. The CD98 subunit was consistently down regulated by nearly 40%, and the transferrin receptor also showed a slight down regulation. Recent studies have shown that ASCT is an important glutamine transporter in T cells[229] but the expression of this transporter and other possible glutamine transporters Slc7a6 or the large neutral amino acid transporer showed no change in expression due to the rapamycin treatment. The heat map for the other members of the Slc family members show that mTORC1 inhibition leads to both up and down regulation of receptors.
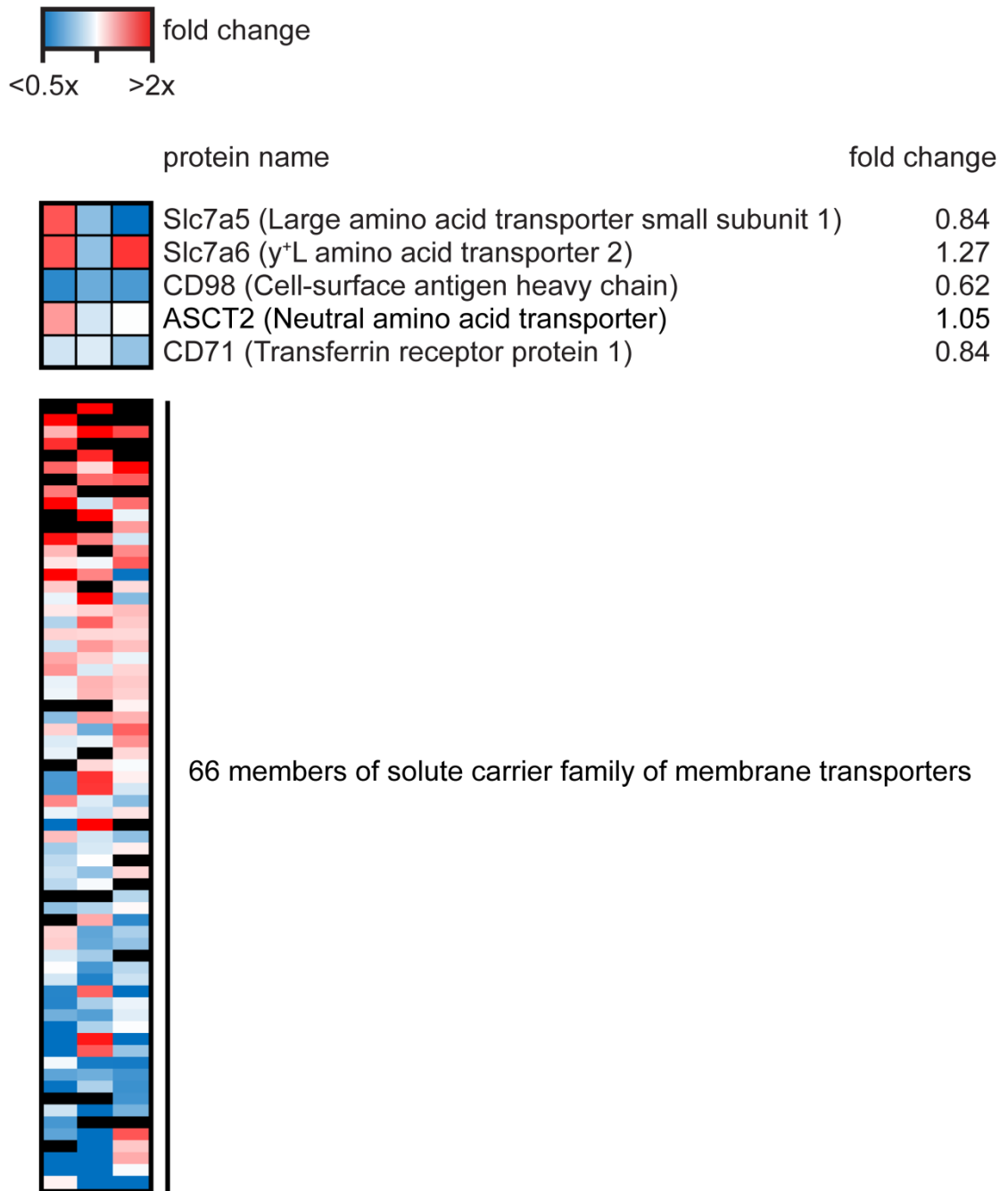
Figure 4.11: Effects of mTORC1 inhibition on expression on system L-amino acid transporters, the transferrin transporter and other members of the solute carrier membrane transport proteins.
Heat map representation of the system L amino acid transporter subunits, transferrin receptor and other members of the solute carrier family of membrane transporters is shown. Red hues indicate up regulation of protein, white no regulation and blue down regulation. Black fields indicate no ratio determined in replicate.

Glutaminolysis utilises reactions performed by the TCA to metabolise glutamine and is known to play a crucial role in activated lymphocytes[83]. The primary L-glutamine transporter in T cells, ASCT2[229] was not affected by rapamycin treatment (Figure 4.11), in contrast to the glucose transporters Glut1 and Glut3 which were drastically down regulated by the drug. We thus investigated whether enzymes performing the rate limiting steps of glutaminolysis, which feed L-glutamine into the TCA cycle by converting it into α-ketoglutarate, were affected by mTORC1 inhibition (Figure 4.12).

	protein name	fold change
	Glutaminase kidney isoform, mitochondrial	1.39
	Glutamate dehydrogenase, mitochondrial	1.37
	Alanine aminotransferase	1.33
	Aspartate aminotransferase, mitochondrial	1.16
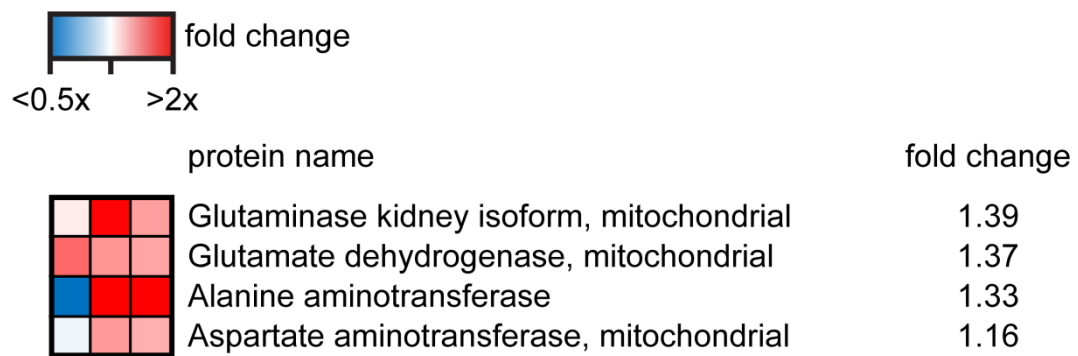
Figure 4.12: Effect of mTORC1 inhibition up regulates key enzymes in glutaminolysis as determined by LFQ SAX
Heat map representation of the enzymes facilitating the conversion of L-glutamine into α-ketoglutarate. Red hues indicate up regulation of protein, white no regulation and blue down regulation.

We saw a consistent up regulation of all relevant enzymes upon mTORC1 inhibition, indicating increased glutaminolysis rates.

We also noted that rapamycin treatment caused changes in expression of the family of aminoacyl-tRNA synthetases in CTL. These enzymes are involved in the esterification of amino acid to their cognate tRNA and thus are critical regulators of protein biosynthesis. The pathway analysis suggested that enzymes of this category are significantly enriched in the group of proteins down regulated upon mTORC1 inhibition. However at closer inspection it became clear that rapamycin treatment of CTL caused down regulation of the expression of cytoplasmic isoforms of these

enzymes, whereas the mitochondrial isoforms of the aminoacyl-tRNA synthetases family show a trend towards up regulation (Figure 4.13, B). The aforementioned effect of mTORC1 inhibition on the anabolic pathways involved in terpenoid and steroid biosynthesis is further illustrated in (Figure 4.13, C). Enzymes of the pentose phosphate pathway, as another major anabolic pathway in CTL does not show any change upon mTORC1 inhibition.
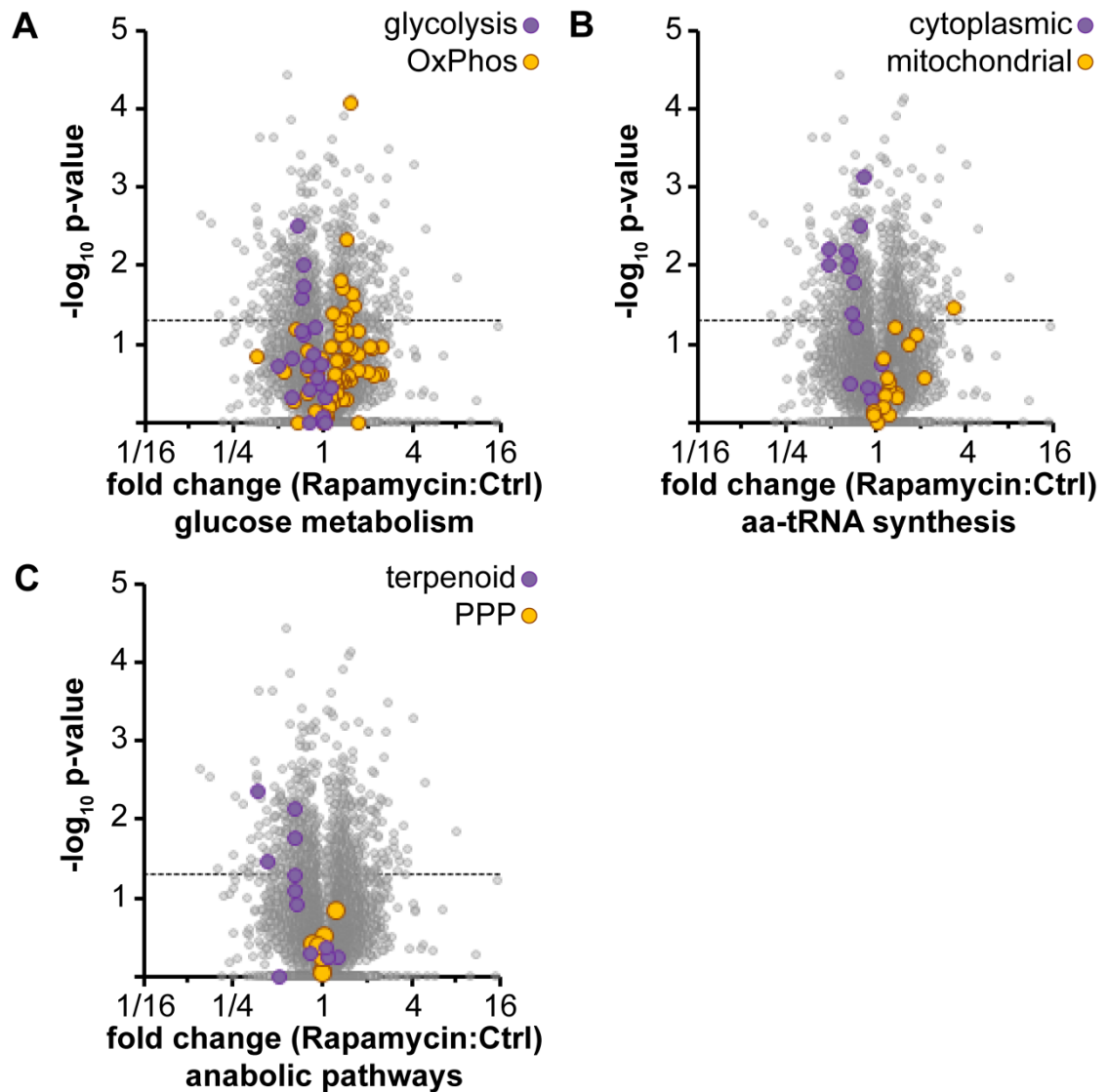
Figure 4.13: Selected pathways affected by mTORC1 inhibition as determined by KEGG analysis of LFQ dataset.
Plots showing regulation of (A) glucose metabolism, (B) aminoacyl-tRNA biosynthesis in cytoplasm and mitochondria and (C) anabolic pathways.

In conclusion, our label-free mass spectrometry approach enabled us to detect global changes in genes expression of 6733 proteins induced by mTORC1 inhibition. Despite an even number of up and down regulated proteins we discovered a net decrease in protein content of rapamycin treated cells due to the preferred down regulation of high abundance proteins. We discovered that mTORC1 controls the expression of several CTL effector molecules like granzymes, Interferon-γ, perforin and affects IL-12 signalling in CTL. Rapamycin treatment furthermore led to decreased rates of protein biosynthesis and other anabolic pathways. mTORC1 inhibition also led to a profound effect on CTL metabolism as evident by decreased levels of glycolytic enzymes but increased levels of proteins involved in in Glutaminolysis and OxPhos as well as reprogramming of nutrient transporter expression.

4.2.5. Our LFQ proteomics approach shows comparable results to a SILAC quantification based approach.

Proteomic approaches using metabolic labelling strategies like SILAC (stable isotope labelling of amino acids in cell culture) are reported to be more quantitative than label free approaches as the combined sample processing minimises variation during the sample processing and analysis; these approaches are thus considered the gold standard in terms of accurate quantification.

In order to use SILAC as a quantification strategy in mass spectrometry cells are grown in the presence of regular 'light' or modified 'heavy' amino acids, which differ in their molecular weight due to the incorporation of heavy H, C or N isotopes. The 'heavy' amino acids are incorporated into nascent proteins like the normal amino acids and thus lead to the generation of heavy peptides and proteins. Modern mass spectrometers are capable of distinguishing 'light' and 'heavy' peptides within in a sample and thus enable measurements of different experimental conditions within the same sample run. Biological samples that are metabolically labelled this way can be combined right from the beginning of the sample processing procedure and thus eliminate any bias introduced by different sample handling. This stands in stark contrast to our aforementioned label-free approach in which samples derived from different experimental conditions are completely run in parallel and are not combined at any point before the *in silico* data analysis. These approaches thus rely heavily on standardised and robust sample processing procedures to avoid introduction of any kind of bias.

We wished to see if the use of quantitative SILAC proteomics would enable us to gain additional insights about the role of mTORC1 in regulating the T cell proteome that might have been missed in the label free proteomic experiments. We thus followed an

established protocol for the generation of SILAC labelled CTL *in vitro*[46] and combined it with a subcellular fractionation followed by size exclusion chromatography (SEC) which separates proteins under denaturing conditions according to their molecular size [294,332] to increase the coverage of our experiments.

In order to control precise amino acids levels in the media used for growing and metabolically labelling of CTL dialysed FBS, which does not contain amino acids and other small molecules with a molecular weight smaller than 10 kDa, has to be used as naturally occurring amino acids in the FBS would interfere with the SILAC labelling. Previous studies in the lab had shown that CTL grown in SILAC proliferate normally and show normal expression of surface molecules. However, we noted that the cells showed decreased forward scatter when compared to cells grown in media supplemented with regular FBS (Figure 4.14, A). Moreover, CTL cultured in media where FBS was substituted with dialysed FBS show down regulated expression of perforin (Figure 4.14, B). This indicated to us that the SILAC labelling protocol was not optimal for CTL cultures. Nevertheless, cells grown in SILAC media with the dialysed FBS show the expected response to rapamycin treatment. For example, the data in Figure 4.14 show that rapamycin treatment caused a further decrease in forward scatter of CTL and the cells also lost mTORC1 activity as judged by a decrease in the phosphorylation of S6K T389 in the rapamycin treated cells compared to controls. Rapamycin treatment also causes CTL grown in SILAC media to further decrease levels of perforin (Figure 4.14, B). Accordingly we judged that it would still be useful to use SILAC to explore the role of mTORC1 in regulating the CTL proteome.
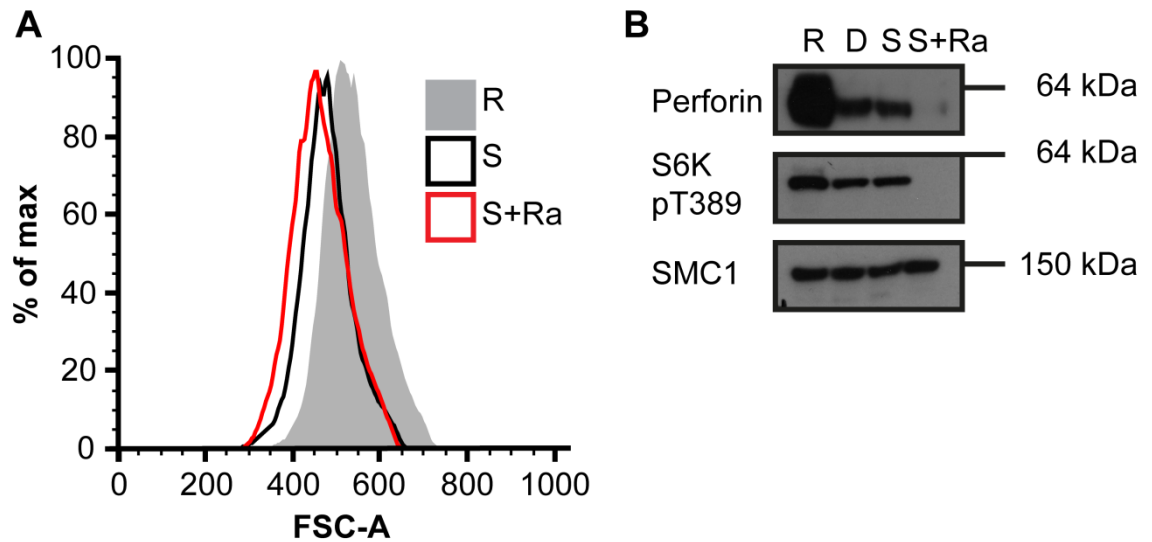
Figure 4.14: Effects of SILAC media on CTL forward scatter and effector protein expression.
The effects of limited nutrient availability due to dialysed FBS are shown. (A) Flow cytometry analysis of CTL grown in different media. (B) Immunoblot analysis of perforin expression of CTL grown under different nutrient conditions. R: RPMI medium with FBS, D: RPMI medium with dialysed FBS, S: RPMI medium with dialysed FBS plus additional supplements, S+Ra: like S, but additional long term rapamycin treatment.

The experimental approach used the same P14 LCMV TCR transgenic mouse model as the label-free approach. In order to facilitate the metabolic labelling of the cells, CTL were cultured in SILAC T cell medium after activation and clonally expanded for 4 days. The cells were treated with rapamycin for 48 hrs before harvesting. Cells were then combined in a 1:1 ratio and subjected to subcellular fraction before being separated by size exclusion chromatography into 33 fractions and analysed via LC-MC/MS and analysed by the MaxQuant software package (Figure 4.15).
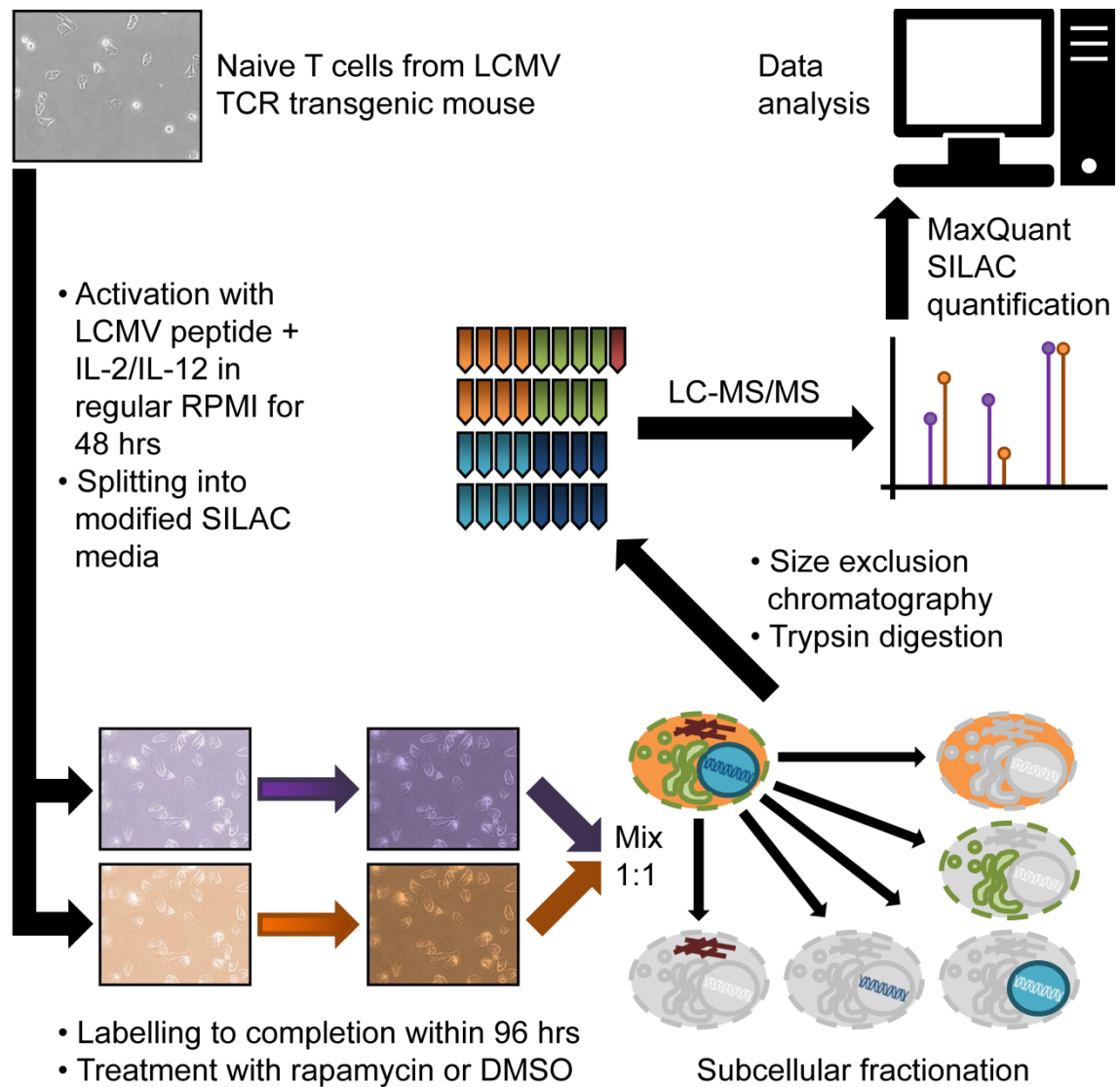
Figure 4.15: Experimental approach for SILAC quantification
T cells were isolated from LCMV TCR transgenic mice and activated with cognate peptide. Antigen was washed out after 48 hours and CTL were clonally expanded for 96 hours in 'light' and 'heavy' SILAC T cell medium. Cells were treated with DMSO (control) or Rapamycin for the last 48 hrs of culture. Cells were combined in a 1:1 ratio and subjected to a subcellular fractionation (Subcellular Protein Fractionation Kit for Cultured Cells, Thermo). Peptides were separated by size exclusion chromatography prior to analysis by an Orbitrap Velos mass spectrometer. The generated data was analysed using MaxQuant.

We compared the different subcellular fractions obtained by the subcellular fractionation kit by separating the lysates via SDS-PAGE. All five band fractions showed different patterns of protein bands indicating that the subcellular fractionation indeed led to differential extraction of proteins (Figure 4.16).
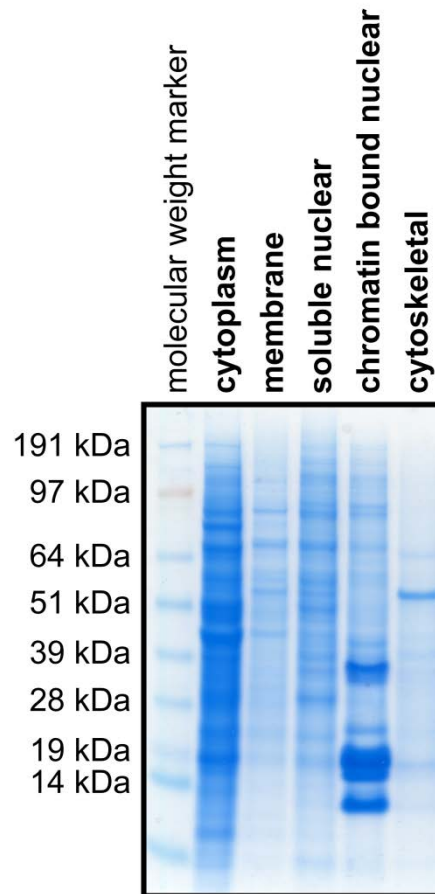
Figure 4.16: subcellular fractionation of CTL
Coomassie stained SDS PAGE gel showing the separation of protein via the fractionation protocol. CTL were separated into cytoplasmic, membrane, soluble nuclear, chromatin bound nuclear and cytoskeletal fraction using a commercially available subcellular fractionation kit.

However, upon initial data analysis it became clear that the fractionations of the different biological replicates were not consistent enough to be confidently compared with each other. We thus decided to combine the protein ratios derived from each fraction to a total cell protein ratio. Ratios derived from each fraction were weighted according to the number of quantifiable events in each subcellular fraction.

The SILAC approach led to the identification and quantification of 4795 proteins, of which 278 were down and 440 were up regulated (Figure 4.17). The mTORC1 regulated effector molecule perforin was detected among the down regulated proteins,

albeit with a high p-value (0.22, detected in 2 out of the 3 replicates), whereas L-selectin, whose expression is known to be suppressed by mTORC1 activity[155], could not be detected in the experiment.
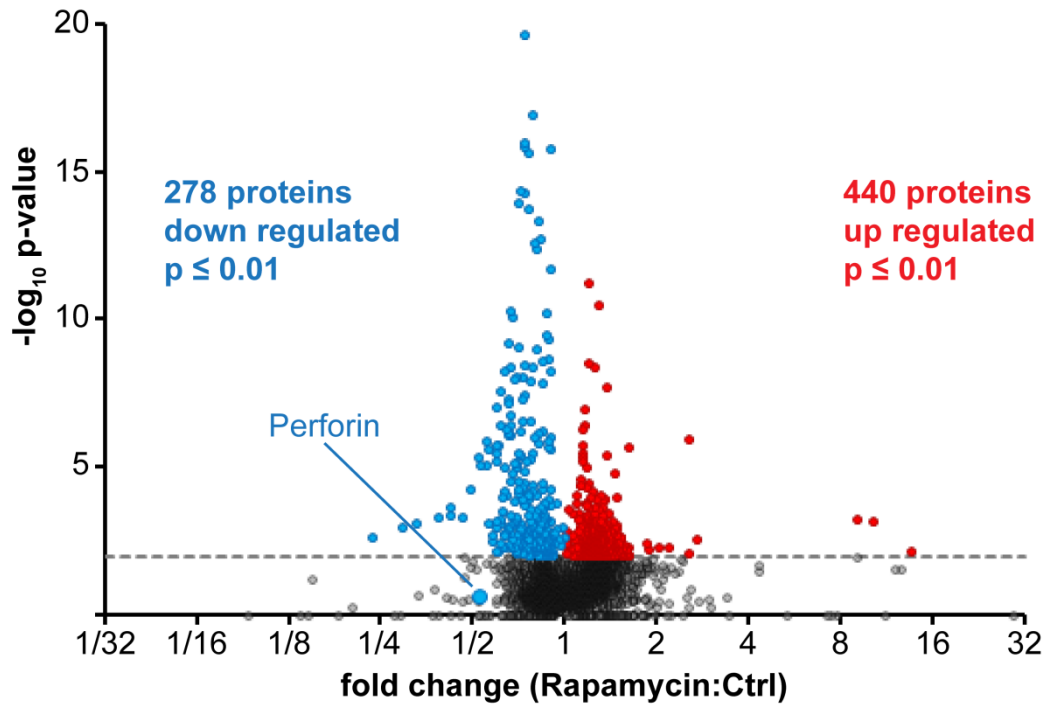
Figure 4.17: global changes in protein expression as measured by SILAC approach.
4895 protein groups were detected in 3 biological replicates. Blue/red circles represent reproducibly down/up regulated proteins respectively. The dashed line indicates the $p \leq 0.05$ threshold. Perforin as a known mTORC1 regulated protein is highlighted.

Apart from perforin we detected a robust decrease in the expression of several CTL effector molecules (Figure 4.18). Granzyme family members B and F showed significantly decreased protein levels as well as the cytokines Lymphotoxin A and Interferon-γ. We furthermore observed a decrease in the level of the IL-12 receptor subunit β-1.
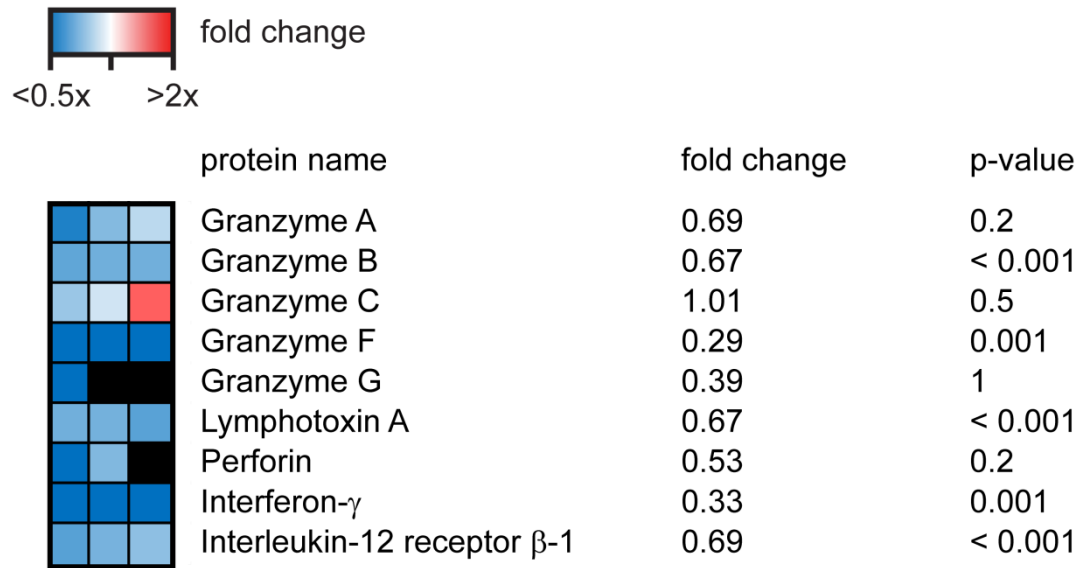
Figure 4.18: Effects of mTORC1 inhibition on the expression of CTL effector molecules as determined by SILAC quantification.
Heatmap illustration of affected protein levels of granzyme family members, Lymphotoxin A, perforin, Interferon-γ and IL-12 receptor subunit β-1. Red hues indicate up regulation of protein, white no regulation and blue down regulation. Fold changes and associated p-values are given. Black fields indicate no ratio determined in replicate.

We performed a pathway analysis using the DAVID bioinformatics tool to assess which pathways in a CTL are over represented in the up (Figure 4.19) or down regulated (Figure 4.20) proteins of our SILAC approach. Oxidative Phosphorylation and the Citrate cycle are among the proteins up regulated upon rapamycin treatment. Several other catabolic pathways related to fatty acid and amino acid metabolism were also included in the list. Pathways involved in DNA maintenance and replication are also among the up regulated proteins.

KEGG pathway identifier	# of genes	p-value
Oxidative phosphorylation	63	4×10^{-46}
Parkinson's disease	62	4×10^{-44}
Huntington's disease	68	8×10^{-41}
Alzheimer's disease	62	2×10^{-34}
DNA replication	25	2×10^{-23}
Citrate cycle (TCA cycle)	15	1×10^{-10}
Mismatch repair	13	1×10^{-10}
Propanoate metabolism	13	1×10^{-08}
Valine, leucine and isoleucine degradation	15	5×10^{-08}
Nucleotide excision repair	14	2×10^{-07}
Cardiac muscle contraction	18	4×10^{-07}
Cell cycle	19	1×10^{-04}
Base excision repair	10	2×10^{-04}
Limonene and pinene degradation	6	8×10^{-04}
Lysine degradation	9	1×10^{-03}
Butanoate metabolism	8	3×10^{-03}
beta-Alanine metabolism	6	5×10^{-03}
Pyruvate metabolism	8	5×10^{-03}
Fatty acid elongation in mitochondria	4	7×10^{-03}

Figure 4.19: pathways up regulated by mTORC1 inhibition as determined by SILAC

On the other hand, the list of down regulated pathways (Figure 4.20) is dominated by pathways involved in transcription and translation (ribosome, aminocacyl-tRNA biosynthesis, spliceosome), and anabolic fatty acid synthesis and glycan biosynthesis. Glycolysis is also down regulated.

KEGG pathway identifier	# of genes	p-value
Ribosome	59	1×10^{-53}
Aminoacyl-tRNA biosynthesis	13	1×10^{-06}
Terpenoid backbone biosynthesis	7	4×10^{-05}
Protein export	5	5×10^{-04}
Proteasome	10	7×10^{-04}
SNARE interactions in vesicular transport	8	3×10^{-03}
Glycolysis / Gluconeogenesis	10	9×10^{-03}
N-Glycan biosynthesis	8	1×10^{-02}
Spliceosome	14	1×10^{-02}

Figure 4.20: pathways down regulated by mTORC1 inhibition as determined by SILAC

As glycolytic and other metabolic enzymes were among the list of pathways regulated by rapamycin treatment, we focussed on these pathways and investigated the whole full extent of their regulation.

fold change			protein name	fold change
			Glut1	0.66
			Glut3	0.52
			Hexokinase-1	0.90
			Hexokinase-2	0.74
			Hexokinase-3	1.4
			Glucose-6-phosphatase isomerase	0.83
			6-phosphofructokinase, muscle type	1.33
			6-phosphofructokinase, liver type	0.80
			6-phosphofructokinase type C	0.79
			Fructose-bisphosphatase aldolase A	0.74
			Fructose-bisphosphatase aldolase C	0.60
			Triosephosphate isomerase	0.87
			Glyceraldehyde-3-phosphate dehydrogenase	0.73
			Phosphoglycerate kinase 1	0.88
			Phosphoglycerate kinase 2	0.68
			Phosphoglucomutase-1	1.0
			Phosphoglucomutase-2	1.1
			α-Enolase	0.74
			γ-Enolase	1.1
			β-Enolase	0.99
			Pyruvate kinase M1	1.11
			Pyruvate kinase M2	0.83
			Lactate dehydrogenase A chain	0.79

Figure 4.21: Effects of mTORC1 inhibition on expression of glycolytic enzymes as determined by SILAC.
Heat map representation of enzymes involved in glycolysis and the fold changes in protein levels due to rapamycin treatment are shown. Red hues indicate up regulation of protein, white no regulation and blue down regulation. Fold changes for each protein are given. Black fields indicate no ratio determined in replicate.

Figure 4.21 shows the consequent down regulation of glycolytic of nearly every glycolytic enzyme. The glucose transporters Glut1 and Glut3 show the highest decrease in protein levels due to rapamycin treatment.

Due to the striking effect on Glut1 and Glut3 we then examined the global effect on nutrient transporter expression CTL. We determined changes in the protein ratio of the system L and y^+L amino acid transporters subunits, ASCT2, the transferrin receptor and 46 other members of the family of solute carrier membrane transport proteins (Figure 4.22).

	fold change
protein name	fold change
Large amino acid transporter small subunit 1	0.65
Slc7a6 (y^+L amino acid transporter 2)	1.13
CD98 (Cell-surface antigen heavy chain)	0.71
ASCT2 (Neutral amino acid transporter)	0.85
CD71 (Transferrin receptor protein 1)	0.83

46 members of solute carrier family of membrane transporters
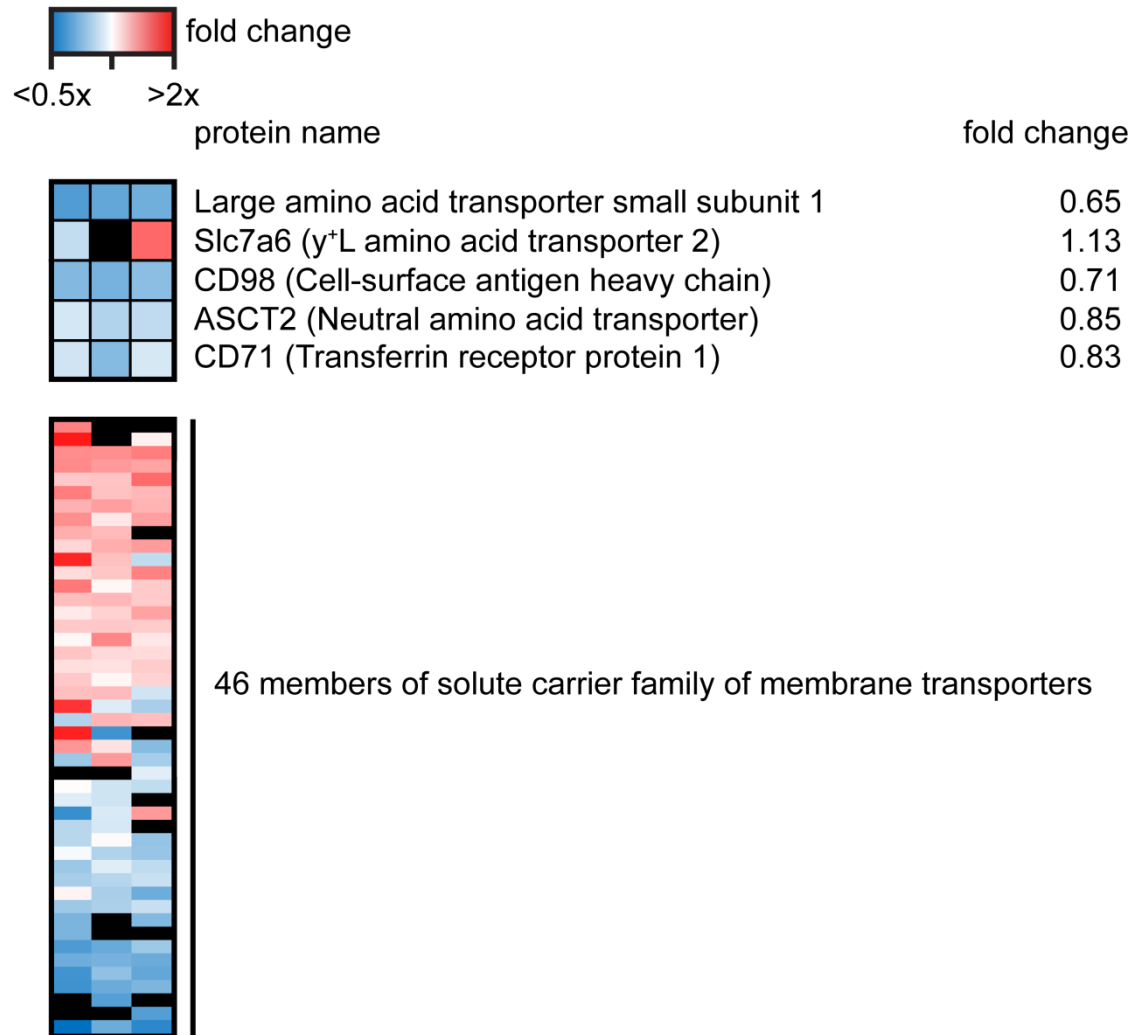
Figure 4.22: mTORC1 inhibition leads to reprogramming of nutrient transporter expression in CTL

Heat map representation of the system L amino acid transporter subunits, transferrin receptor and other members of the solute carrier family of membrane transporters is shown. Red hues indicate up regulation of protein, white no regulation and blue down regulation. Black fields indicate no ratio determined in replicate.

Rapamycin treatment of CTL led to a down regulation of the Large amino acid transporter subunit 1 (Slc7a5) as well as CD98, both protein together form the System L

amino acid transporter. The glutamine transporter ASCT2 and transferrin receptor CD71 were also slightly down regulated. mTORC1 inhibition also led to changes in the expression of many members of the Slc family as illustrated by different proteins being up and down regulated due to the drug treatment.

We further investigated whether enzymes involved in glutaminolysis were up regulated as an effect of the mTORC1 inhibition, as the slight effect on ASCT2 indicated an effect on L-glutamine uptake.

protein name	fold change
Glutaminase kidney isoform, mitochondrial	1.21
Glutamate dehydrogenase, mitochondrial	1.30
Aspartate aminotransferase, mitochondrial	1.26
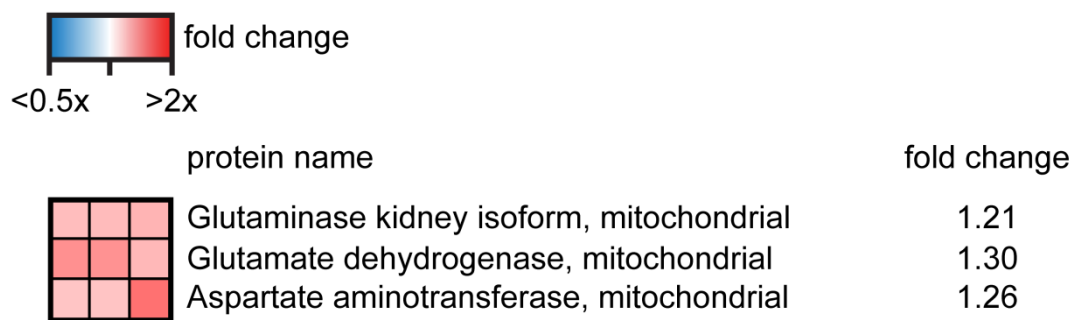
Figure 4.23: Effect of mTORC1 inhibition up regulates key enzymes in glutaminolysis as determined by LFQ SAX
Heat map representation of the enzymes facilitating the conversion of L-glutamine into α-ketoglutarate. Red hues indicate up regulation of protein, white no regulation and blue down regulation.

All enzymes detected by our SILAC experiment showed increased expression by approx. 25% upon rapamycin treatment.

Figure 4.24 further highlights some of the findings regarding findings of the pathway analysis of the SILAC (A-C) dataset. The differential regulation of OxPhos when compared to glycolytic enzymes can be seen (Figure 4.24, A), with the importance of mitochondrial pathways further emphasised by up regulation of the mitochondrial translational machinery in from of ribosomal subunits (Figure 4.24, B) and, to a certain

extent, members of the aa-tRNA synthetases (Figure 4.24, C). Cytoplasmic subunits on

the other hand tend to be down regulated.
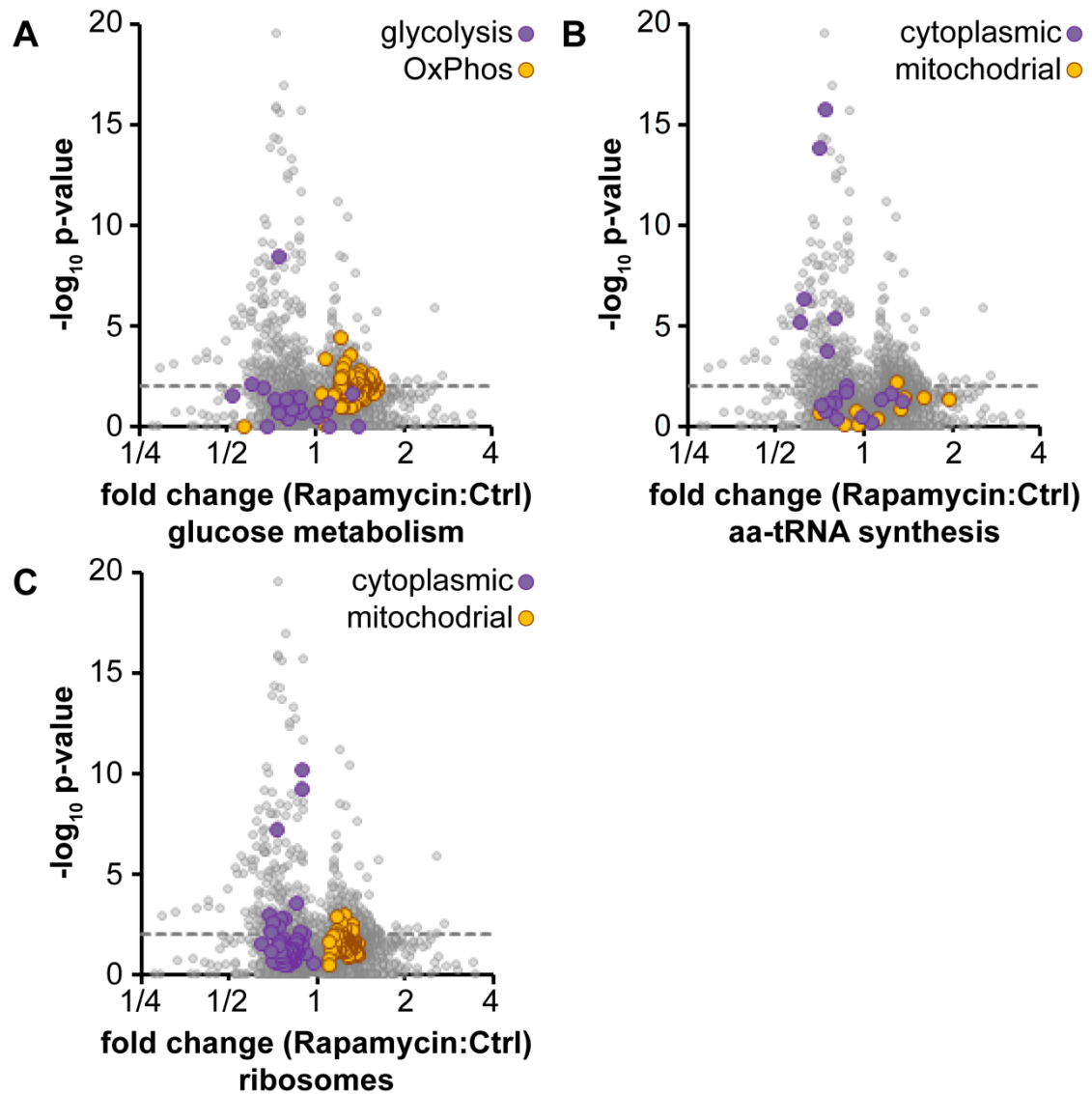
Figure 4.24: Selected pathways affected by mTORC1 inhibition as determined by KEGG analysis of SILAC dataset.
Plots showing regulation of (A) effector molecules, (B) glucose metabolism, (C) ribosomes and (D) aminoacyl-tRNA biosynthesis in cytoplasm and mitochondria.

4.2.6. mTORC1 does not control Eomesodermin or T-bet expression

It has been reported that the mTORC1 complex controls the balance of the two crucial transcription factors Eomesodermin and T-bet[177] by supressing Eomesodermin and promoting T-bet expression. We thus analysed our datasets to see whether we could find any evidence for this hypothesis of CD8 differentiation control (Figure 4.25). Neither the label-free nor the SILAC data set showed any robust up regulation of Eomesodermin. The SILAC data showed a slight increase of T-Bet upon mTORC1 inhibition which contradicts previous studies[177].

protein name	gene name	fold change SAX (p-value)	fold change SILAC (p-value)
Eomesodermin	Eomes	1.56 (0.17)	0.92 (0.36)
T-bet	Tbx21	1.14 (0.42)	1.47 (0.04)

Figure 4.25: effect of mTORC1 inhibition on expression levels of Eomoesdermin and T-bet
The fold changes derived from LFQ and SILAC approach for the transcription factors Eomesodermin and T-bet are shown.

We further validated the results derived from the proteomic approaches by immunoblotting (Figure 4.26). The western blot analysis confirmed the MS data and showed no difference in T-bet expression upon mTORC1 inhibition with rapamycin.
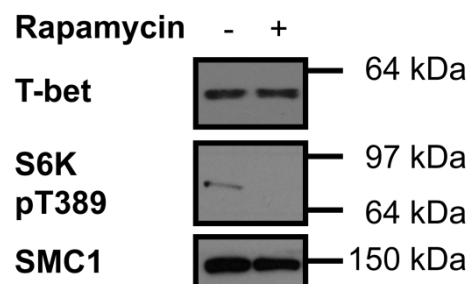
Figure 4.26: mTORC1 inhibition does not affect expression levels of T-bet.
Immunoblot to investigated T-bet expression levels in control and rapamycin treated CTL.

4.2.7. Validation of metabolic changes induced by mTORC1 inhibition

We then wanted to validate the effects of sustained rapamycin treatment on CTL metabolism. The mass spectrometry based approaches showed a decrease in the glucose transporters Glut1 and Glut3, so we used immunoblotting to validate the control of Glut1 expression by mTORC1 (Figure 4.27).

As an increase in enzymes involved in oxidative phosphorylation predicts increased oxygen consumption we used a Seahorse analyser to measure the oxygen consumption rate of control and rapamycin treated CTL (Figure 4.27, B). However, we could not find any differences in the two populations at any time of the mitochondrial stress test, which not only determines the baseline oxygen consumption rate (first three time points) but also the maximally possible cellular respiration rate and (and thus the spare respiratory capacity as determined at time points 7 - 9). In contrast to this finding, we could detect changes in the extracellular acidification rate (ECAR) which was measured in parallel to the oxygen consumption rate and is an indicator for the glycolytic activity of cells due to the excretion of lactic acid. There was a twofold decrease in the baseline ECAR as a result of rapamycin treatment (Figure 4.27, C, first three time points) and also a significant difference in the total glycolytic capacity (as seen by ECAR values at later time points). In a published study[85] we furthermore directly measured the levels of lactate secretion by CTL treated with rapamycin as well as the uptake of glucose by measuring the uptake of radio labelled 2-deoxyglucose. Both measures of glycolytic activity were decreased by more than 2-fold, and thus further validate our findings.

CTL maintain high proliferation rates even when long term treated with rapamycin (Figure 4.1, B) despite down regulation of the glycolytic pathway (Figure 4.13, B; Figure 4.27, A, C) and glucose uptake[85] and a lack of compensation of ATP generation by other mechanisms (Figure 4.27, B). On the other hand, while glycolysis was down

regulated due to rapamycin treatment, we noticed an up regulation of the enzymes in the conversion of L-glutamate into α-ketoglutarate (Figure 4.12, Figure 4.23), indicative for higher glutaminolytic activity. We thus measured the glutaminolysis activity in CTL treated with or without Rapamycin by measuring the formation of $^{14}CO_2$ derived from L-glutamine[83] and detected a more than 50% higher glutaminolytic rate in the rapamycin treated cells (Figure 4.27, D).
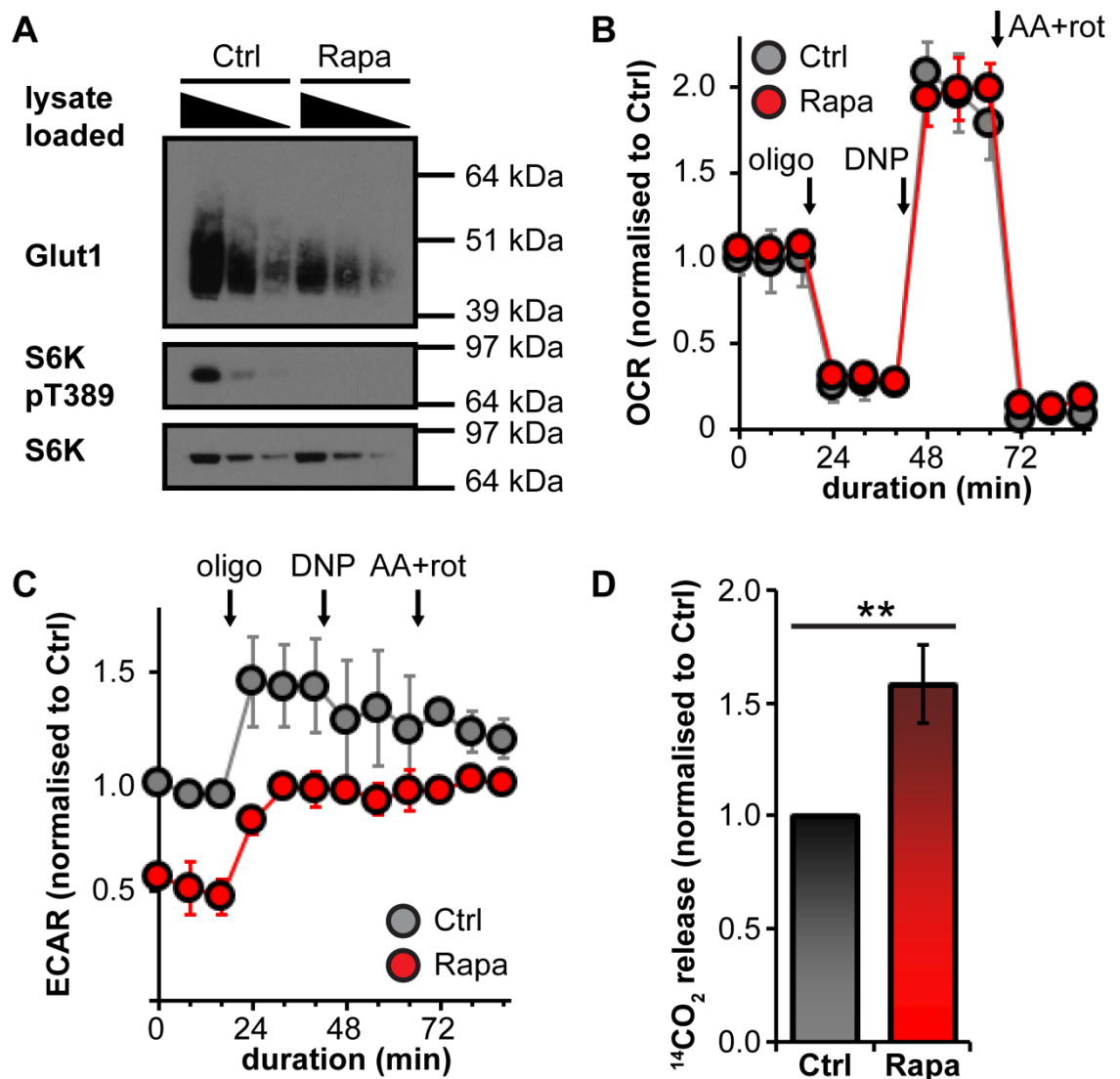
Figure 4.27: Effects of mTORC1 on CTL metabolism.
(A) Immunoblotting for the glucose transporter Glut1 validates down regulation of expression upon rapamycin treatment. (B) Oxygen consumption rate (OCR) and (C) extracellular acidification rate (ECAR) as indicators for oxidative phosphorylation and glycolytic rates were determined using a Seahorse Analyser. Rates for control (grey

circles) and rapamycin treated (red circles) are shown. Arrows in (B) and (C) indicate the addition of inhibitors of the electron transport chain; oligo: oligomycin; DNP: 2,4-dinitrophenol; AA: antimycin A; rot: rotenone (D) glutaminolytic rates of CTL were determined by measuring $^{14}CO_2$ release from $[1\text{-}^{14}C]$-glutamine Data are mean $\pm$SD or representative of at least three experiments (**, $p \leq 0.01$)

4.3. Discussion

This is the first time to our knowledge that the impact of mTORC1 inhibition on global protein expression levels has been assessed using a proteomics work flow.

The results above describe the impact of mTORC1 inhibition on the CTL proteome. The most striking result from the data is that mTORC1 is not a global regulator of translation in T cells. It has very selective effects and only controls expression of a very small subset of the CTL proteome.

4.3.1. Comparison between SILAC and label-free approach

Two different strategies were used to probe the role of mTORC1 on the CTL proteome: A SILAC and a label-free quantification approach. The SILAC approach relies on the metabolic labelling of protein *in vitro* which requires high proliferation rates of the desired cells in suboptimal tissue culture media. However, the metabolic labelling enables very robust quantification, as samples can be combined right from the beginning of the sample processing work flow and thus avoid technical bias. SILAC is thus considered to be the gold standard in quantitative proteomics. The label-free approach on the hand does not require any metabolic or chemical labelling of the protein to be analysed and is thus adoptable to any protein sample, so primary, quiescent cells can be quantified and compared to highly proliferative transformed tumour cell lines. This flexibility comes at a cost, as label-free approaches require a highly reproducible and robust work flow to introduce as little bias as possible into the analysis and thus cannot compete with the accuracy of a SILAC approach.

However, the data presented in this chapter illustrate that using a label-free quantification approach yielded very similar results as a SILAC based quantification. The LFQ approach also led to the identification of a significant higher number of

protein ratios (6733 for LFQ vs 4795 for SILAC) for which the more complicated MS/MS spectra in SILAC approaches can be held responsible. A relevant example for a protein that had been missed in the SILAC analysis is L-selectin, emphasising the importance of a high coverage of the proteome. The effects of the SILAC media on perforin expression (Figure 4.14) illustrates another disadvantage of the SILAC approach: As the less nutritious SILAC media is affecting baseline expression levels of perforin (and probably a range of other proteins as well) it impedes the detection of these proteins in the proteomics experiments which is also exemplified by the fact that perforin could only be detected in two out of three SILAC experiments but in all three replicates of the SAX approach. However, the higher accuracy of the SILAC approach is shown by the fact that the average statistical significance of the obtained proteins ratios was higher than in the LFQ approach. This increased accuracy did nevertheless not lead to major differences on the outcome of the subsequent analysis.

One problem that was apparent from the label free analysis when analysing the effect of mTORC1 on the expression of nutrient transporters was the amount of missing data points, i.e. problems with the robust identification of these protein. This can be explained by the fact in the label free experiments we used urea based lysis buffers and this may not be optimal for solubilisation of membrane spanning proteins that contain hydrophobic stretches which lead to a poor solubility of these proteins in urea based lysis buffers. Thus biophysical properties are most likely the reason for the underrepresentation of membrane spanning proteins as mentioned in the previous chapter which ultimately explains the missing data points. In the SILAC protocol we used a subcellular fractionation approach which made use of different detergent based buffers including a dedicated membrane fraction buffer. Hence the identification of membrane proteins was not as big a problem in the SILAC approach. The SILAC approach allowed the usage of detergent based lysis buffers as the subsequent size

exclusion chromatography was compatible with detergents, whereas the strong anion exchange chromatography used for the label free approach was not. However, alternative lysing techniques are now enabling the usage of detergents, as they allow the removal of these substances after cell lysis.

4.3.2. What were the major conclusions from the mTORC1 proteomic experiments?

Firstly, inhibition of mTORC1 causes down regulation of a whole range of CTL effector molecules like several granzymes, perforin, Interferon-γ and the IL-12 receptor. The term "foot soldiers" has been used to describe CTL and sticking to 'foot soldier' analogy inhibition of mTORC1 in CTL has the effect of disarming the troops of the immune system.

Our CTL do not show a significant effect on mTORC2 signalling due to long term mTORC1 inhibition with rapamycin whereas reports in the literature have shown that long term inhibition of mTORC1 also disrupts mTORC2 signalling[195] in transformed cell lines. The authors propose a mechanism by which prolonged inhibition of the mTOR-Raptor leads to the removal of available mTOR subunits and thus eventually decreases free mTOR levels so that mTORC2 signalling is also affected. However, the authors of the study also conclude that the magnitude of this effect depends on the cell-line and relative expression levels of mTOR, Raptor and Rictor subunits and is thus not necessary a general phenomenon. We know from our experiments in the previous chapter that mTOR is approx. twice as abundant as Rictor which in turn is expressed at more than 5-fold higher levels than Raptor. Thus even inactivating all mTOR-Raptor complexes by rapamycin treatment in a CTL would not be sufficient to remove all available mTOR molecules in order to affect mTORC2 signalling.

One of the most striking effects of mTORC1 inhibition of the T cell proteome was the effect of rapamycin on glucose uptake and glycolysis. A key finding was that mTORC1 activity is required for immune-activated CD8$^+$ T cells to sustain high rates of glucose uptake. mTORC1 activity is also necessary for CD8$^+$ T cells to initiate and sustain a switch to a glycolytic metabolism. One way in which mTORC1 controls glucose uptake in CD8$^+$ T cells is by controlling expression of the glucose transporter Glut1. CD8$^+$ T cells also show mTORC1 dependence for the expression of hexokinase 2, a key enzyme which phosphorylates glucose to produce glucose-6-phosphate, an essential intermediate in most pathways for glucose metabolism. Importantly, mTORC1 controls expression of key rate-limiting glycolytic enzymes in CD8$^+$ T cells such as phosphofructokinase 1, lactate dehydrogenase, and pyruvate kinase M2.

The high glycolytic rate of CTL is thought to be essential to meet the metabolic demands caused by the rapid proliferation of clonally expanding CD8$^+$ T cells. However, despite the down regulated glycolytic enzymes and decreased glucose uptake, rapamycin treated CTL still maintain an impressive proliferation rate. How do rapamycin treated cells fuel their proliferation? Glutaminolysis has been reported to be important in the proliferation and effector function of T cells[83,229]. At the same time that CTL down regulate glycolysis rates due to mTORC1 inhibition they also show an up regulation of glutaminolysis as an alternative measure of generating ATP and supplying substrates for anabolic pathways. L-glutamine is the most abundant free amino acid in the blood stream[333] and might represent an important energy for source for cells when blood glucose levels are low. It has been shown that mTOR signalling controls the trafficking of T cells[155] and that T cells treated with rapamycin home to lymph nodes. The rapamycin induced switch from the utilisation of glucose to glutamine might thus also represent a mechanism by which T cells adapt to the different nutrient levels in blood and lymph. Unfortunately, not much is known about nutrient levels in the lymph

to further support this possibility. TORC1 inhibition also led to a diverse regulation of nutrient transporters as illustrated by the different effects of long term rapamycin treatment on the expression of solute carrier membrane transporters. In combination with the increased expression of subunits of the electron transport chain this illustrates that mTORC1 inhibition leads to a complicated regulation of CTL metabolism rather than a general down regulation. However, this reprogramming does not justify the term "metabolic switch" as CTL do not completely switch from using glycolysis to OxPhos to fulfil their energetic demand but merely show a shift in the relative importance of these pathways, as OxPhos levels are not changed upon mTORC1 inhibition.

One of the frequent generalisations about the role of mTORC1 is that it controls protein synthesis. The impact of rapamycin on methionine incorporation rates into nascent proteins is consistent with this idea. However, the conclusions from the global proteomic data show that rapamycin effects on the proteome are complex. There was a decrease in the total protein content of a rapamycin treated cell but in mTORC1 caused loss of only 300-400 of the proteins that make up a CTL approx. 6000 either remained expressed at the same level and 350 were actually increased in expression.

We had a closer look at the abundance levels of up and down regulated proteins. Despite up and down regulating approximately equal numbers of proteins, the abundance levels of the affected pathways are very different. We have shown in the previous chapter that some of the most abundant proteins of a CTL are enzymes involved in glycolysis or the splicing apparatus as well as the subunits of ribosomes and the proteasome. All these pathways and protein complexes are down regulated upon rapamycin treatment and thus explain the decrease in overall cell size in rapamycin treated CTL.

The coordinated down regulation of ribosomal subunits and the aminoacyl-tRNA loading apparatus also illustrates that CTL down regulate their whole translational machinery to adapt to decreased protein translation demands. It has been shown in transformed cell lines that mTOR regulates the transcription of ribosomal RNA (rRNA) and mRNA[334] the consequences of this regulation had never been shown on the protein level on a global scale before, particularly not for CTL. Thoreen *et al.*[239] illustrate in another study in mouse embryonic fibroblasts that mTORC1 signalling regulates the translation efficiency of mRNA containing a 5' terminal oligopyrimidine (TOP) motif. This study also highlights the differences between expression control of cytoplasmic and mitochondrial ribosomes, as only the cytoplasmic isoforms, which are known to contain a 5'-TOP motif[335], showed a decrease in expression upon mTORC1 inhibition. The mitochondrial isoforms of both ribosomes and aa-tRNA synthetases on the other hand are not affected or even show a slight up regulation (Figure 4.13; Figure 4.24). This suggests a) a different mechanism by which these isoforms are regulated and b) a special role for mitochondria in the context of mTORC1 inhibition.

One of the more surprising results from the proteome work was that inhibition of mTORC1 caused increases in the expression of a subset of proteins and in some cases e.g. in the case of CD62L the increases in expression were quite large (Figure 4.3, A - B). These data could reflect that certain proteins are more effectively translated in the absence of mTORC1 activity. It could also reflect that mTORC1 controls protein degradation pathways. In this respect, a recent study by Zhang, *et al.*[240] illustrated the role of the 26S proteasome in protein homeostasis by regulation general global protein half-life. This study showed that proteasomal expression is regulated by mTORC1 signalling and that mTORC1 inhibition led to a global decrease in protein turnover. However, the down regulation of the proteasome is unlikely to be the sole the mechanism by which proteins are up regulated upon mTORC1 inhibition as it is not the

26S proteasome itself that targets specific proteins for degradation but the interplay of ubiquitin-activating (E1), -conjucating (E2) and ligating (E3) enzymes[336]. The pathway analysis of proteins down regulated upon rapamycin treatment (Figure 4.9) shows indeed that proteins involved in "ubiquitin mediated proteolysis" are affected and Figure 4.4 also contains several enzymes involved in the regulation of ubiquitinylation. Recent studies have shown how sophisticated mass spectrometry based approaches[310,337] can be used to assess global turnover rates of protein in a cell which would tell us whether differences in translation efficiencies or protein half-lives are indeed the mechanism by which mTORC1 inhibition leads to the up regulation of proteins.

Another obvious mechanism by which protein levels could be regulated is the control of transcription of the corresponding mRNA. The following chapter will thus present the data we obtained from a global transcriptomic analysis of long term rapamycin treated cells using the Affymetrix micro array platform.

5. Control of gene CTL gene transcription by mTORC1

5.1. Introduction

The previous chapter described the changes induced by long term mTORC1 inhibition on the total proteome of CTL. However, these experiments did not tell us how mTORC1 controls protein levels in CTL. mTORC1 is usually perceived as a regulator of translation and less so of transcription. However, as the long term mTORC1 inhibition might have induced changes on the transcriptome (due to indirect effects) as well as on the proteome, we decided to use a global transcriptomic approach to investigate the role of mTORC1 in controlling the CTL transcriptional program.

5.2. Results

After having described the effects of rapamycin treatment on the proteome of CTL we used a transcriptional approach to investigate the effects of mTORC1 inhibition on global transcription in CTL. We used the Affymetrix Mouse genome 430.2 platform to measure the expression levels of thousands of transcripts in parallel. The assay utilises oligonucleotide probes which hybridise to targeted transcripts and thus enable an *in vitro* transcription to generate a library of reverse transcripts complementary to the cDNA generated from the biological sample. The complimentary RNA is then biotinylated, fragmented and hybridised to an array of approx. 45000 probes immobilised on the array. The array is then stained with fluorescent tags which bind to the biotinylated samples. The samples are then excited by a laser source and the resulting fluorescence can be used to assign intensity values to each probe set which can be linked to specific genes.

We generated cDNA samples derived from control and long term rapamycin treated CTL from three different mice; differences in cell size and lack of S6K Thr389 phosphorylation were used as validation for effective mTORC1 inhibition. The Affymetrix analysis was performed by Eveliina Vertanen at the Turku Centre for Biotechnology, Finland.

5.2.1. mTORC1 leads to reprogramming of CTL transcription

The mouse genome 430.2 platform includes 45000 probes corresponding to approximately 34000 genes, of which 10521 were expressed in our dataset. The levels of 618 transcripts were robustly affected by the rapamycin treatments by more than 1.5-fold, with 327 transcripts being up and 291 transcripts being down regulated (Figure 5.1). mTORC1 inhibition thus led to equal up and down regulation of transcripts in

CTL. The most up regulated transcript were those of L-Selectin which has been shown to be controlled by mTORC signalling[155] whereas the most down regulated transcripts were those of several granzyme isoforms as well as Interferon-γ and perforin which are all essential for cytolytic effector function. The glucose transporters Glut1 and Glut3 are also ranked among the most down regulated transcripts.
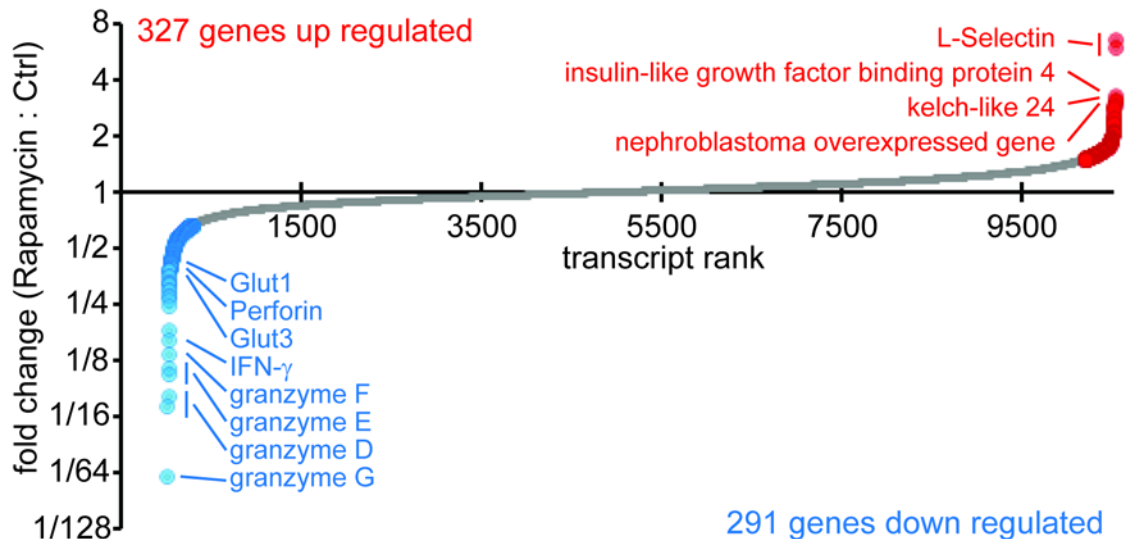
Figure 5.1: micro array analysis of mTORC1 controlled transcriptome.
Transcripts are ranked by their fold change upon rapamycin treatments in ascending order. Down regulated transcripts are highlighted in blue, up regulated transcript in red. A selection of the most regulated genes is annotated.

All significantly changed genes with a difference in expression of more than 1.5-fold were then subjected to pathway analysis using the DAVID tools which is based on the KEGG databank. The up regulated genes are enriched in pathways involved in the regulation of the cell cycle and general DNA maintenance (Figure **5.2**).

KEGG pathway identifier	# of genes	p-value
Cell cycle	17	2×10^{-11}
DNA replication	5	2×10^{-3}
Oocyte meiosis	7	6×10^{-3}
Homologous recombination	4	7×10^{-3}
Progesterone-mediated oocyte maturation	6	7×10^{-3}
Base excision repair	4	2×10^{-2}
Mismatch repair	3	4×10^{-2}
Ubiquitin mediated proteolysis	6	5×10^{-2}
Pyrimidine metabolism	5	5×10^{-2}

Figure 5.2: Pathway analysis of up regulated transcripts.

The down regulated genes on the other hand (Figure 5.3) are enriched in genes which are either components of glycolysis (including Glut1, Glut3, hexokinase 2, phosphofructokinase and the aldolase isoforms 1 and 3) and other metabolic pathways or anabolic pathways involved in the biosynthesis of terpenoids and steroids, including HMG-CoA reductase, a major rate limiting enzyme of these pathways.

KEGG pathway identifier	# of genes	p-value
Steroid biosynthesis	5	2×10^{-4}
Terpenoid backbone biosynthesis	4	2×10^{-3}
Glycolysis / Gluconeogenesis	6	6×10^{-3}
Valine, leucine and isoleucine degradation	5	8×10^{-3}
Alanine, aspartate and glutamate metabolism	4	1×10^{-2}
Fructose and mannose metabolism	4	3×10^{-2}
Insulin signaling pathway	7	3×10^{-2}
Pyruvate metabolism	4	3×10^{-2}

Figure 5.3: Pathway analysis of down regulated transcripts

Closer interrogation of the results of the pathways analyses revealed that mTORC1 activity is required for the expression of many effector molecules (Figure 5.1), as many of these molecules were down regulated upon rapamycin treatment. However, we saw quantitative differences between several granzyme family members. The family

members A, B and C only show moderate down regulations whereas D, E, F and G are down regulated by at least seven-fold (Figure 5.4). Tumor necrosis factor showed a slight decrease in transcript levels upon rapamycin treatment, whereas Lymphotoxin A, another member of the TNF family, showed a strong transcriptional down regulation due to the drug treatment. Lymphotoxin B was not affected. Other effector molecules down regulated by the rapamycin treatment are IFN-γ and the IL-12 receptor subunit β-1.

	fold change
	fold change
Granzyme A	0.74
Granzyme B	0.84
Granzyme C	0.86
Granzyme D	0.08
Granzyme E	0.11
Granzyme F	0.14
Granzyme G	0.03
Interleukin-12 receptor subunit beta-1	0.67
Interferon γ	0.16
Lymphotoxin A	0.59
Lymphotoxin B	1.08
Tumor necrosis factor	0.78
Perforin	0.36
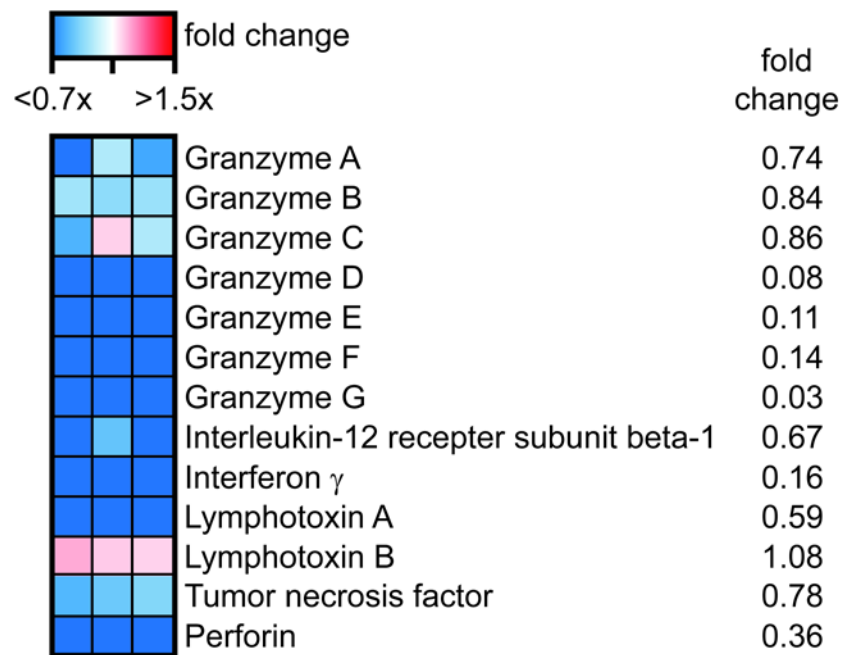
Figure 5.4: mTORC1 controls CTL effector molecule transcription.
Heat map showing the fold changes in transcript levels of selected effector molecules. The fold change of each molecule is also indicated. Red hues indicate up regulated genes, blue hues down regulated genes.

We then investigated the effect of mTORC1 inhibition on the transcription of metabolic enzymes as these pathways were enriched in the pathway analysis (Figure 5.5, A). Rapamycin treatment led to a general decrease in glycolytic gene transcription with an average decrease in transcription levels by 25%. However, several transcript levels were significantly decreased by more than 50%; in fact, the two glucose transporters Glut1 and Glut3 are amongst the most down regulated transcripts in a CTL upon mTORC1

inhibition. We then compared the effect on glycolytic gene transcriptions with the effects on the level of genes transcribing genes of the electron transport chain (Figure 5.5, B). There was no effect on the transcription on any of the complexes I – IV or the ATP synthase subunits. There was however, an effect on all three micro array probes of a single subunit of complex IV, Cox7a2l, which was consistently up regulated by approximately 50%.
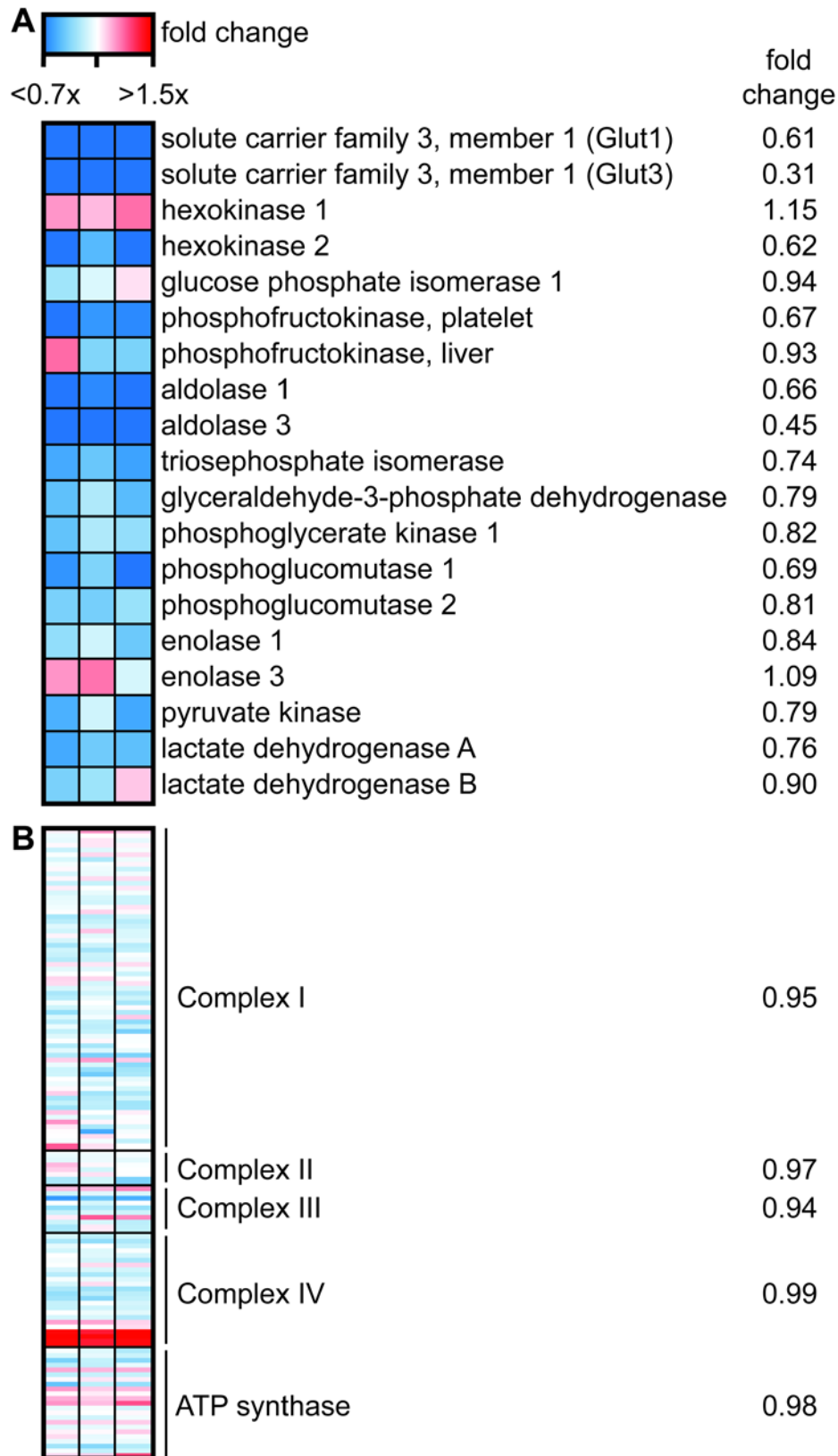
Figure 5.5: Transcriptional regulation of glycolysis but not OxPhos by mTORC1.
Heat map showing the fold changes in transcript levels of glycolytic enzymes and subunits of the complexes I – IV of the electron transport chain and the ATP synthase. The fold change of each molecule is also indicated. Red hues indicate up regulated genes, blue hues down regulated genes.

As we noticed a drastic down regulation of the glucose transporters Glut1 and Glut3 upon mTORC1 inhibition, we examined whether other members of the Solute Carrier transport protein family which are expressed in CTL (Figure 5.6). We were particularly interested in the changes of transcription of the LAT1 (Slc7a5/CD98 heterodimer) and y^+LAT (Slc7a6/CD98 heterodimer) amino acid transporter subunits, the glutamine ASCT2 and the transferrin receptor CD71 as these transporters are known to be important for T cell biology. Apart from the three aforementioned SLC members and the transferrin receptor our micro array revealed the expression of another 83 members of the SLC membrane transporter family (Figure 5.6).

The LAT1 amino acid transporter showed a down regulation of both complex subunits due to mTORC1 inhibition whereas the y^+LAT2 subunit was not affected. ASCT was also consistently down regulated. The transferrin receptor was not affected by rapamycin treatment.

Of all up and down regulated transporters that we say in our micro array experiment, the two glucose transporters mentioned before showed the strongest down regulation due to rapamycin treatment. On the other hand, Slc30a4, a zinc transporter, was the most up regulated transporter detected when CTL were treated with the drug.
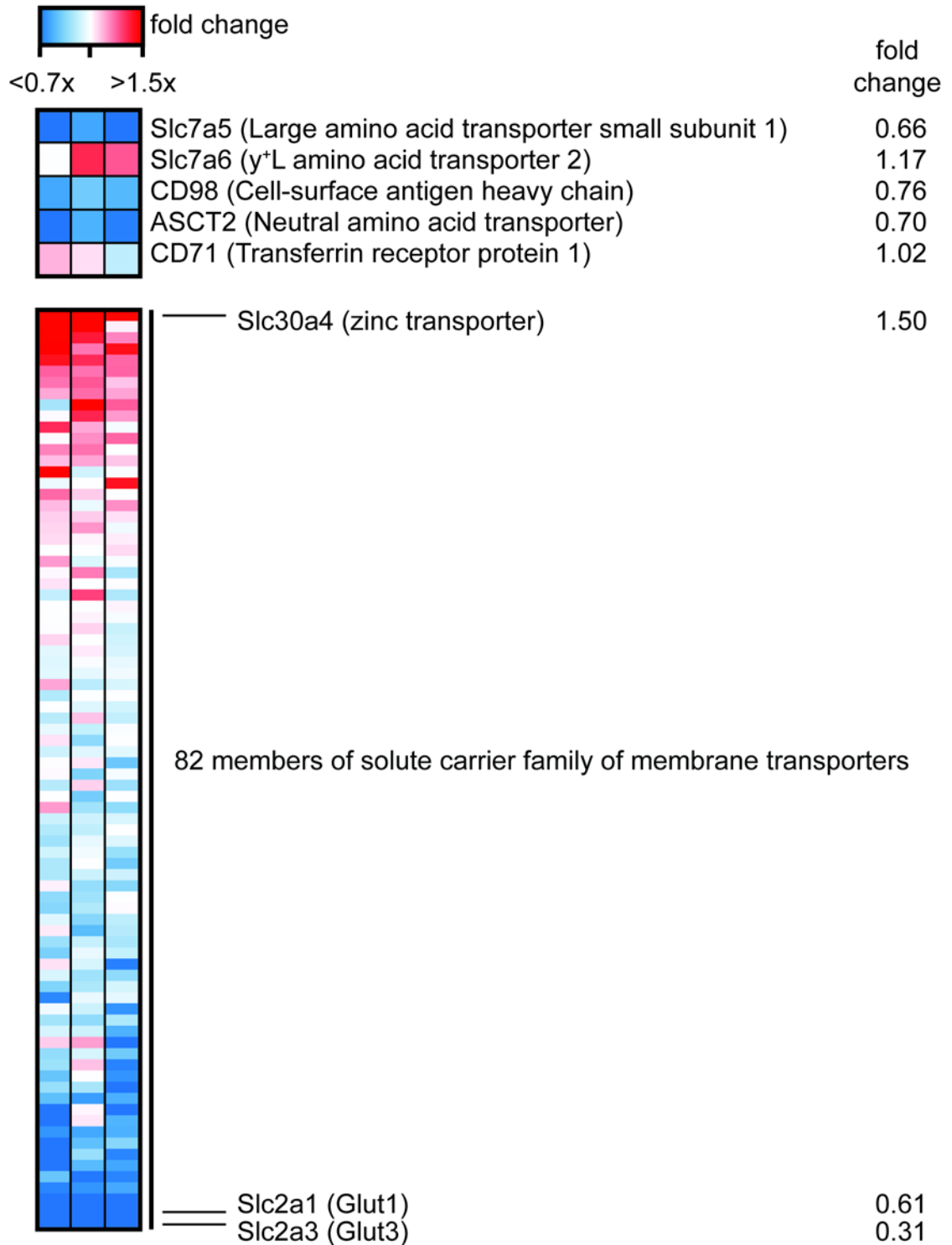
Figure 5.6: mTORC1 inhibition leads to a reprogramming of nutrient transporter transcription

Heatmap representation of all solute carrier family members expressed in CTL. The fold change of each molecule is also indicated. Red hues indicate up regulated genes, blue hues down regulated genes.

We noted some decrease in the expression of mRNA encoding the principal L-glutamine transporter ASCT2 in rapamycin treated CTL. We therefore wondered whether there were changes in transcript levels of enzymes faciliting the reactions which convert L-glutamine into α-ketoglutarate which initiate the glutaminolytic pathway (Figure 5.7).

	gene title	gene symbol	fold change
	Glutaminase kidney isoform, mitochondrial	Gls	1.00
	Glutamate dehydrogenase, mitochondrial	Glud1	1.22
	Alanine aminotransferase	Gpt2	0.42
	Aspartate aminotransferase, mitochondrial	Got2	0.92
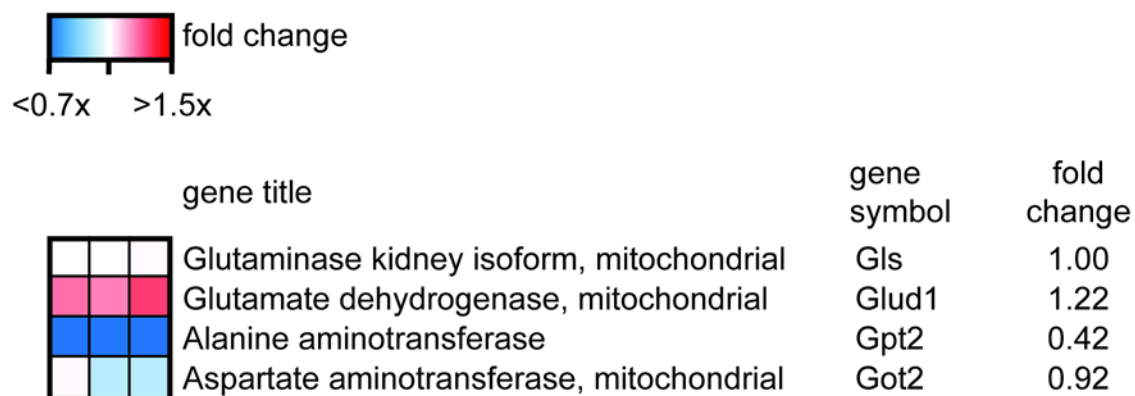
Figure 5.7: Effect of rapamycin treatment on the transcript levels of proteins initiating glutaminolysis.
Heatmap representation of the enzymes involved in the conversion of L-glutamine into α-ketoglutarate. The fold change of each molecule is also indicated. Red hues indicate up regulated genes, blue hues down regulated genes.

The transcript levels of Gls, which catalyses the first reaction of glutaminolysis, were not affected by mTORC1 inhibition. Got2 was also not affected by rapamycin treatment, whereas Glud1 and Gpt reproducibly showed moderate up or strong down regulation, respectively.

We then further investigated the expression of mRNA encoding proteins that mediate the synthesis of the anabolic intermediate isopentenyl pyrophosphate as well as transcripts encoding for enzymes involved in the biosynthesis of cholesterol.The proteomic data had shown loss of expression of proteins in these pathways in CTL treated with rapamycin. Figure 5.8 shows a moderate but consistent regulation of the corresponding transcripts.
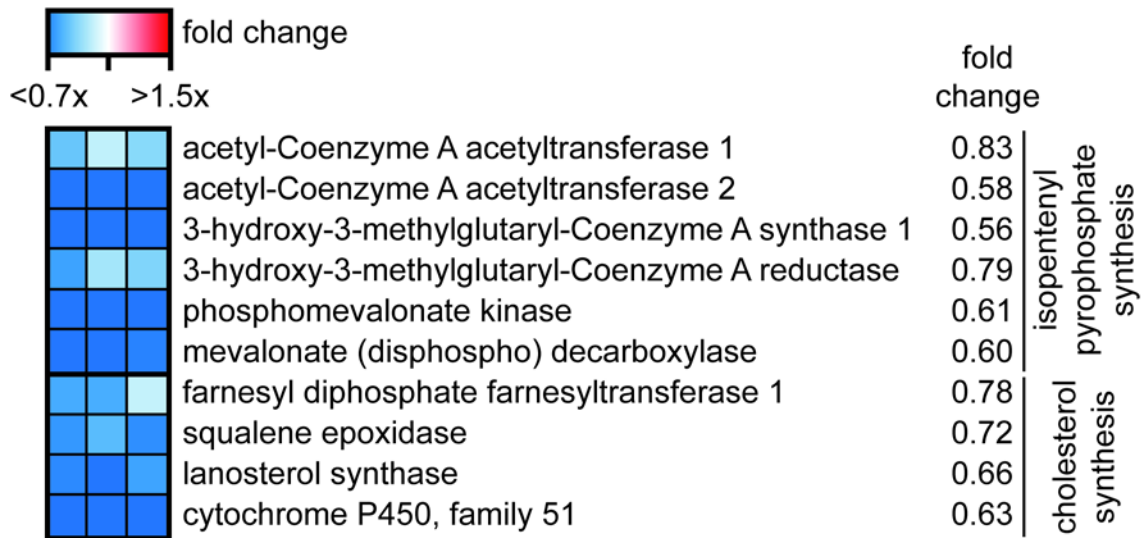
Figure 5.8: Terpenoid and steroid biosynthesis enzymes transcription is reduced upon mTORC1 inhibition.
Heat map representation of the effects on mTORC1 inhibition on the transcription of genes involved in terpenoid and steroid biosnyhtesis. The fold change of each molecule is indicated. Red hues indicate up regulated genes, blue hues down regulated genes.

It has been reported before that mTORC1 inhibition of CTL leads to increased expression of the adhesion molecule L-Selectin/CD62L[155], and transcripts encoding CD62L are indeed the most drastically up regulated transcript in our micro array data. CD62L controls T cell trafficking[338] and we thus investigated whether CTL expression of mRNA encoding other adhesion molecules or chemokines and chemokine receptors are affected by mTORC1 inhibition (Figure 5.9).
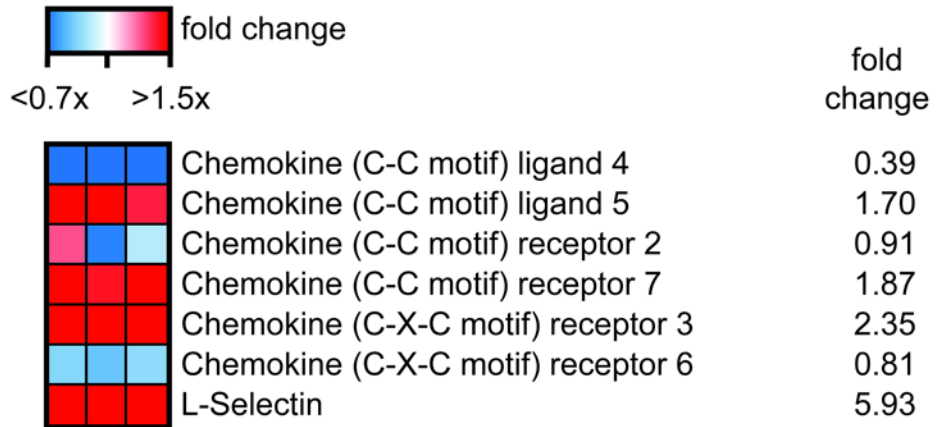
Figure 5.9: mTORC1 controls the expression of chemokines, chemokines receptor and adhesion molecules.
Heat map representation of changes in transcription of selected chemokines, chemokine receptors and adhesion molecules. The fold change of each molecule is indicated. Red hues indicate up regulated genes, blue hues down regulated genes.

Of all molecules that are potentially involved in chemotaxis and trafficking of CTL, CCL5, CCR7, CXCR3 and CD62L showed increased transcript levels upon rapamycin treatment, whereas CCL4 was transcribed at lower rates in rapamycin treated cells.

5.2.2. Comparison between transcriptome and proteome analyse

We described the changes on protein expression in a CTL treated with rapamycin in the previous chapter and investigated the mTORC1 controlled transcriptome in the beginning of this chapter. How do the data compare? The biological samples for our micro array analysis were generated from the same cells used for the SILAC proteomics, so we will compare these two data sets with each other.

Generally speaking, we detected 10521 transcribed genes in our micro array of which 327 transcripts were up and 291 transcripts down regulated. On the other hand, our SILAC quantified 4795 proteins, of which 278 were down and 440 were up regulated. Out of the up regulated proteins, 72 were up regulated on the transcriptome (16%), whereas 68 (24%) out of significantly down regulated proteins were also down regulated on the transcriptome.

We then looked at the most drastically changed proteins within our SILAC data set to investigate the correlation between transcript and protein correlation in more detail. 2 out of the 10 most up regulated proteins were already up regulated on the transcript level (Figure 5.10), whereas 7 out of the 10 most down regulated proteins were also down regulated on the transcript (Figure 5.11). At this point it is worthwhile to point out, that for 4 out of these 20 proteins no micro array probe was available.

Protein name	Gene name	SILAC fold change	transcript regulated?
PDZ domain-containing protein	Pdzd11	13.5	NO
Uncharacterised protein KIAA2022	Kia2022	10.2	N/A
Dymeclin	Dym	9.1	NO
Programmed cell death protein 4	Pdcd4	2.7	YES
Interferon-induced guanylate-binding protein 2	Gbp2	2.5	YES
O-acetyl-ADP-ribose deacetylase MACROD1	Macrod1	2.5	NO
SUN domain-containing protein 2	Sun2	2.2	N/A
C-type lectin domain family 2 member D	Clec2d	2.0	NO
Epimerase family protein SDR39U1	Sdr39u1	1.9	N/A
Placenta-specific gene 8 protein	Plac8	1.9	NO

Figure 5.10: Correlation between transcript and protein levels of most up regulated proteins.
Comparison between protein changes and underlying transcript changes for 10 most up regulated proteins upon rapamycin treatment. N/A indicates missing micro array probes for that specific protein.

Protein name	Gene name	SILAC fold change	transcript regulated?
Protein slowmo homolog 2	Slmo2	0.24	NO
Granzyme F	Gzmf	0.29	YES
Interferon gamma	Ifng	0.33	YES
Hydroxymethylglutaryl-CoA synthase, cytoplasmic	Hmgcs1	0.39	YES
Asparagine synthetase [glutamine-hydrolyzing]	Asns	0.43	YES
Complement component C1q receptor	Cd93	0.43	YES
Glia-derived nexin	Serpine2	0.47	YES
Protein FAM134B	Fam134b	0.50	N/A
Fos-related antigen 2	Fosl2	0.53	YES
E3 ubiquitin-protein ligase ZNRF2	Znrf2	0.53	NO

Figure 5.11: Correlation between transcript and protein levels of most down regulated proteins.
Comparison between protein changes and underlying transcript changes for 10 most down regulated proteins upon rapamycin treatment. N/A indicates missing micro array probes for that specific protein.

Moving away from single protein comparison we were then wondering how CTL

regulate the different pathways that we detected to be controlled by mTORC1. We

compiled all pathways that we found to be regulated by mTORC1 and investigated

whether these pathways were found to be regulated on the transcriptional, translational or both levels.

Up regulated pathway	transcriptome	proteome
Cell cycle	YES	YES
DNA replication	YES	YES
Base excision repair	YES	YES
Mismatch repair	YES	YES
Oocyte meiosis	YES	NO
Homologous recombination	YES	NO
Progesterone-mediated oocyte maturation	YES	NO
Ubiquitin mediated proteolysis	YES	NO
Pyrimidine metabolism	YES	NO
Oxidative phosphorylation	NO	YES
Parkinson's disease	NO	YES
Huntington's disease	NO	YES
Alzheimer's disease	NO	YES
Citrate cycle (TCA cycle)	NO	YES
Propanoate metabolism	NO	YES
Valine, leucine and isoleucine degradation	NO	YES
Nucleotide excision repair	NO	YES
Cardiac muscle contraction	NO	YES
Limonene and pinene degradation	NO	YES
Lysine degradation	NO	YES
Butanoate metabolism	NO	YES
beta-Alanine metabolism	NO	YES
Pyruvate metabolism	NO	YES
Fatty acid elongation in mitochondria	NO	YES

Figure 5.12: Differential expression control of pathways up regulated due to mTORC1 inhibition.
All pathways that were found in either the transcriptional or the proteomic analysis to be up regulated are displayed. 'YES' and 'NO' indicate whether pathways were detected in transcriptional or proteomic analysis.

Of all 24 pathway found to be up regulated (Figure 5.12), 4 (17%) pathways (cell cycle, DNA replication, Base excision repair, mismatch) were detected in the micro array and the mass spectrometry approaches. 5 (21%) were specific for the transcriptomic and 15 (62%) specific for the proteomic experiment.

Down regulated pathway	transcriptome	proteome
Terpenoid backbone biosynthesis	YES	YES
Glycolysis / Gluconeogenesis	YES	YES
Steroid biosynthesis	YES	NO
Valine, leucine and isoleucine degradation	YES	NO
Alanine, aspartate and glutamate metabolism	YES	NO
Fructose and mannose metabolism	YES	NO
Insulin signaling pathway	YES	NO
Pyruvate metabolism	YES	NO
Ribosome	NO	YES
Aminoacyl-tRNA biosynthesis	NO	YES
Protein export	NO	YES
Proteasome	NO	YES
SNARE interactions in vesicular transport	NO	YES
N-Glycan biosynthesis	NO	YES
Spliceosome	NO	YES

Figure 5.13: Differential expression control of pathways down regulated due to mTORC1 inhibition.
All pathways that were found in either the transcriptional or the proteomic analysis to be up regulated are displayed. 'YES' and 'NO' indicate whether pathways were detected in transcriptional or proteomic analysis.

15 pathways were detected to be down regulation upon rapamycin treatment (Figure 5.13). 2 (13%) pathways were detected by both approaches (glycolysis, and terpenoid backbone biosynthesis) whereas 6 (40%) pathways were only detected by changes in transcript levels and 7 (47%) detected on the protein level only.

To further illustrate the relation between changes in transcript and proteins for a selected set of pathways, we plotted the changes in transcript and protein levels for selected pathways to visualise correlations that way (Figure 5.14). The effector molecules detected in both pathways show a very strong correlation between the approaches (Figure 5.14, A), as the changes in the effector protein levels are likely the results of the transcriptional control. A different situation can be seen when examining the glycolytic and OxPhos pathways (Figure 5.14, B). Whereas the glycolytic enzymes (purple) are already affected on the transcript level, the OxPhos components (yellow)

only show a change on the protein, but not transcript level, with the exception of Cox7a2l, which is up regulated on the transcript level as well (cf. Figure 5.5, B). The actual effect on the protein expression of this subunit is comparable to and within the range of the other OxPhos subunits. Cytoplasmic and mitochondrial subunits of the ribosomal complexes (Figure 5.14, C) are are only affected on the protein level but do not show any signs of transcriptional regulation upon mTORC1 inactivation. Furthermore, a clear separation between cytoplasmic (down regulated) and mitochondrial subunits (up regulated) can be seen. A further disconnection between cytoplasmic and mitochondrial isoforms of the same class of proteins can be seen for the different isoforms of aminoacyl-tRNA synthetases (Figure 5.14, D). The cytoplasmic isoforms show a trend towards down regulation on the transcriptional as well as the translational level, whereas the cytoplasmic isoforms are up regulated solely on the translational level.
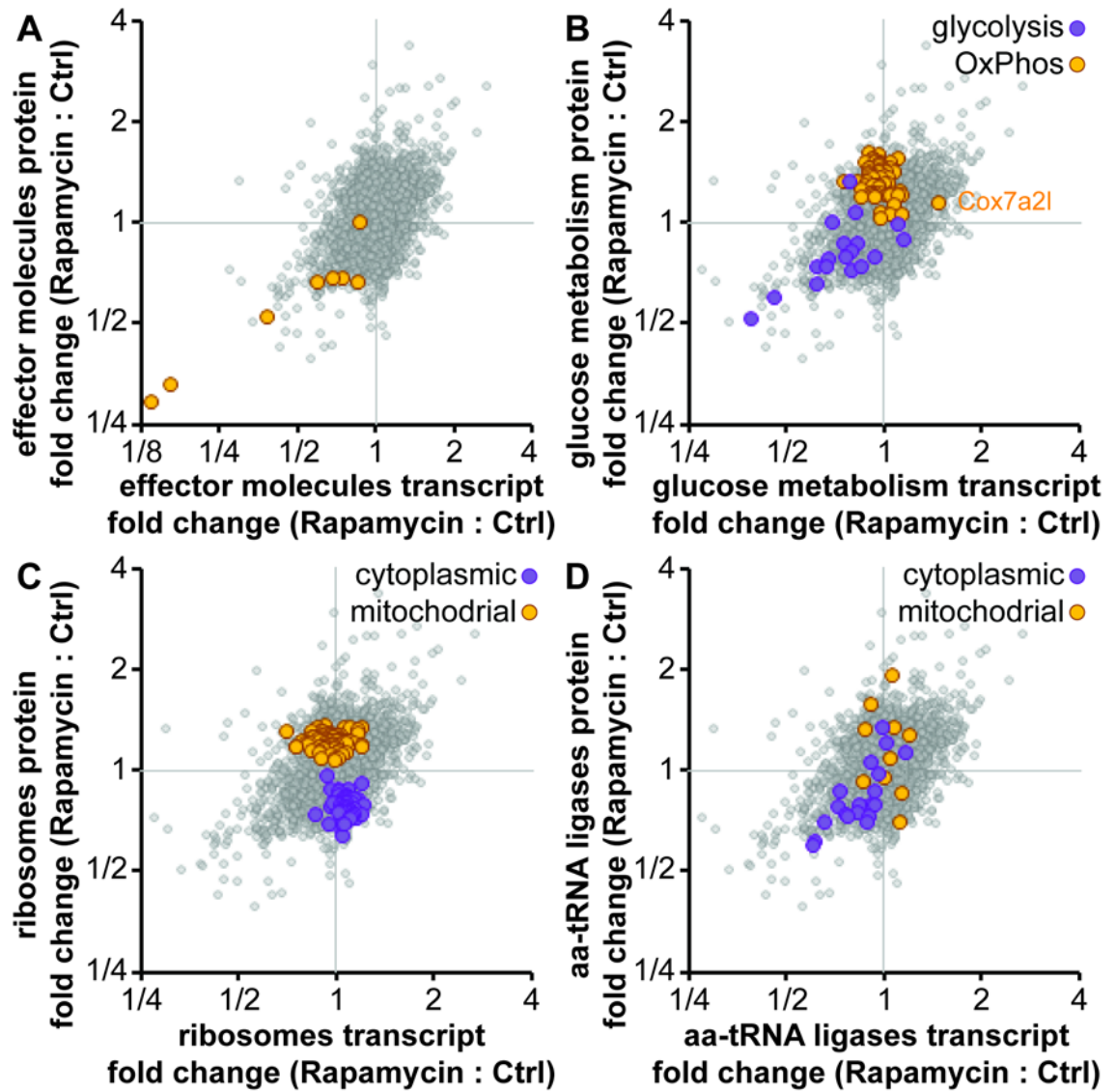
Figure 5.14: Comparison between of transcript and protein level changes upon mTORC1 inhibition for selected pathways.
Regulation of (A) effector molecules, (B) glucose metabolic enzymes, (C) ribosomal subunits and (D) aminoacyl-tRNA synthetases.

5.3. Discussion

The present data show that rapamycin treatment of CTL caused reduced expression of mRNA encoding multiple CTL effector molecules e.g. several granzyme isoforms, interferon-γ, the IL-12 receptor beta subunit 1 and TNF family members like TNF-α and lymphotoxin A. This concerted down regulation of mRNA transcripts encoding these effector molecules explains why rapamycin treatment reduces expression of effector proteins in T cells. These effector molecules are paramount to CTL function and hence the present data give some insight as to basis for the immunosuppressive effects of rapamycin. But how can the effects on the transcription of these genes and genes in general be explained when mTORC1 and its downstream effector like 4EBP1 and S6K are mostly effecting translation by interfering with translational initiation[339] or ribosomal biogenesis? One strategy with which mTORC1 can exert its control gene transcription is by (post-)translationally controlling the expression of key transcription factors, which in turn control the transcription of their substrate genes.

The expression of the genes encoding enzymes that control glucose metabolism can be controlled by the HIF1-α and HIF1-β (also known as ARNT or Aryl hydrocarbon receptor [AHR] nuclear translocator) complex[340]. Do CD8$^+$ T cells express HIF1 complexes? We did not find HIF1-α in our proteomics experiments but found ARNT to be expressed in CTL. The coordinated down regulation of a number of HIF-1α target genes by rapamycin treatment prompted us to look at HIF directly using immunblotting. We showed[85] that CTL maintain high levels of Hif-α even under normoxic conditions and mTORC1 inhibition leads to a repression of Hif1-α protein levels. However, we found no difference in HIF1-α transcript levels in cells treated with rapamycin, indicating that its expression is regulated by non-transcriptional mechanism. As HIF1-α and ARNT are both required for the function of the transcription factor complex we used CTL deficient in ARNT to look at the effects of HIF down-stream signaling. Using

these CTL we showed that the loss of HIF function led to decreased transcript levels of the glucose transporters Glut1 and Glut3 and enzymes involved in glycolysis. Thus HIF1-α acts like a switch that is used by mTORC1 to convert its translational regulation of a single protein into the transcriptional regulation of many proteins. This study also showed a marked decrease in the expression of effector molecules like perforin, granzymes in the ARNT deficient CTL. However, it was evident that the change in perforin levels was not directly caused by the loss of HIF activity but rather indirectly by the decreased glycolytic activity, an effect that had been noticed in earlier studies[318]. HIF deletion furthermore led to altered trafficking behaviour of CTL increasing transcription levels of several chemokines, chemokine receptors and cell adhesion molecules like CD62L. Overall, the HIF transcription factor complex is a critical down-stream target of mTORC1 signalling that controls aspects of CTL metabolism, effector function and trafficking.

However, the transcription of the effector molecules IFN-γ, the IL-12 receptor and TNF family members was not affected by the loss of HIF activity and must thus be controlled by a different, HIF-independent, mechanism. We have no precise mechanism for this yet, but it is known that Interleukin-12 supports high expression of IFN-γ[177] so the observed down regulation of IFN-γ expression due to rapamycin treatment might be at least partially due the observed reduction in IL-12 signalling caused by the down regulation of its receptor.

Another transcription factor that has been shown to be controlled by mTORC1 signalling in human transformed and fly cell lines is SREBP1/2[241]. In conditions with high mTORC1 activity, SREBP1/2 accumulates in the nucleus of a cell and drives the transcription of genes involved in lipid and cholesterol biogenesis[241]. Our rapamycin treated cell on the other hand showed a decrease in the transcript level of these genes,

indicating decreased SREBP transcriptional activity. However, SREBP transcript levels are not affected in experiments. How does mTORC1 signalling control SREBP1/2 transcription? An explanation might be given by studies performed in other cell systems which show elevated SREBP1/2 levels in cells with a Tsc2$^{-/-}$ background[341]. The authors demonstrate an involvement of S6K in the SREBP1/2 up regulation but the exact mechanism is still not known. However, a mechanism involving postranslational control of this transcription factor would explain why we are not able to change differences in the micro array experiment. A recent study by Kidani *et al.*[342] further supports this idea. They showed that expression of SREBP proteins required intact mTORC1 signalling and that failure to up regulate SREBPs led to impaired T cell activation and reduced effector function of CTL.

Other metabolic pathways, like the oxidative phosphorylation pathway as a whole was not affected by rapamycin, apart from one subunit of Complex IV, Cox7a2l, which showed a more than 50% increase in transcript levels. It has been reported that this subunit can be directly regulated by p53[343]. As presented before, CTL treated with rapamycin show a decreased proliferation rate which is accompanied by an up regulation of transcript involved in cell cycle control (Figure 5.2). The complex network of cell cycle regulators might lead to the stabilisation of p53 which in return would lead to an increase in Cox7a2l transcription. However, this increase in transcript levels does not translate into higher protein levels than the other OxPhos subunits (Figure 5.14, B) meaning that the expression of this subunit is mostly controlled on a posttranscriptional level.

How do the changes in transcript and protein levels compare? In this and in the previous chapter we already established that mTORC1 inhibition lead to the down regulation of the transcripts of several pathways (glycolysis, lipid biosynthesis) and effector

molecules (granzymes, perforin, Lymphotoxins) which ultimately leads to the down regulation of the corresponding proteins as well. However, most of the proteins changed in our SILAC approach were only changed on the protein but not on the transcript level. In addition to that, our pathway analysis of the proteome also revealed several pathways which do not seem to be transcriptionally regulated, but on solely on the protein level.

Examples of rapamycin caused effects that were only detected in the MS based experiments are the changes in ribosome levels. All (cytoplasmic) ribosomal subunits show a coordinated down regulation solely due to non-transcriptional effects. This can be explained by a mechanism by which mTORC1 controls the translation efficiency of transcripts containing a 5'-TOP domain without affecting their abundance[239], as it is the case for nearly all cytoplasmic ribosomal subunits. Several mitochondrial pathways (OxPhos, TCA cycle, glutaminolyis specific reactions) are also at least partially uncoupled from the transcriptional regulation and even override potential changes of transcript levels (cf. Cox7a2l in Figure 5.14, B). Even though most mitochondrial proteins are encoded by the nuclear genome and are subject to the regulation of the cytoplasmic translational machinery, once incorporated into the mitochondria their fate is controlled by the complex mechanism regulating mitochondrial protein homeostasis which is completely uncoupled from the corresponding transcript levels[344,345,346].

We also noticed differences between the gene expression control of up and down regulated proteins. Up regulated proteins and up regulated pathways showed a stronger disconnect between transcript and protein levels than the down regulated proteins/pathways. This indicates that the increase of proteins due to mTORC1 inhibition is often likely due to posttranscriptional effects like increased translational efficiency or increased protein half-lives, whereas the down regulation of proteins is more likely to be caused by a down regulation of the corresponding transcripts. Our

results from the previous chapter indicated that proteasome levels in the cell are down regulated upon mTORC1 inhibition, which would lead to an increase of general protein half-live and might be an explanation for this observed effect. Another reason might be that many increases that we only see on the protein levels correspond to mitochondrial pathways (electron transport chain, TCA cycle, mitochondrial subunits of ribosomes) which are subject to the complex, transcriptionally independent regulation of mitochondrial homeostasis.

What did we learn from the proteomics that we did not learn from the micro array experiments?

We found more proteins to be regulated on the protein level than on the transcript level, many of which are most likely caused by non-transcriptional control of these proteins. This fact illustrates that using proteomic approaches is indispensable to fully understand the effects of rapamycin treatment on CTL. This is not surprising as transcriptional approaches are intrinsically limited to observe effects on the transcript levels, unless they are used in the context of ribosomal profiling which can also give insights into translational efficiency. But even these approaches will never be able to detect changes in protein levels caused by altered protein half-lives or changes in protein trafficking.

Apart from this crucial intrinsic disadvantage of our micro array approach, it did show a more robust quantification which does not suffer from detection problems due to low protein abundances or problematic chemical properties of peptides. The micro array analysis was thus able to detect changes in the transcripts of proteins which were not robustly quantified in the proteomics approach like the adhesion molecules. The micro array also helped answering questions about the mechanism by which mTORC1 controls certain pathways, e.g. the transcriptional control of glycolysis and several

effector molecules via the Hif1-α/ARNT complex. However, we showed in previous sections of this thesis that there is only a weak correlation between transcript and protein levels. Thus only quantitative proteomic approaches are suitable to answer questions involving protein abundances or stoichiometries. Furthermore, we already showed in earlier chapters that recent advances in chromatography and mass spectrometers are helping to close the gap between transcriptomics and proteomics in regard to sensitivity and coverage and the first studies achieving near-complete coverage of proteomes have been published[309,283]. And already now we were able to highlight differences in protein levels that we would have not detected by just using the transcriptomics approach, examples for this are whole complexes like ribosomes but also specific regulatory proteins, which will be discussed in the following chapters of this thesis.

6. The role of mTORC2 signalling in CTL

6.1. Introduction

mTOR is the catalytic component of two protein kinase complexes, mTORC1 and mTORC2. The immunosuppressive drug rapamycin inhibits mTORC1 activity but does not directly affect activity of the mTORC2 complex. Genetic approaches using Raptor (to disturb mTORC1 signalling) and Rictor (to inhibit mTORC2 signalling) knockouts have been used to show the importance of mTORC2 signalling for CD4 T cell differentiation[347,348]. These studies showed that mTORC1 signalling was indispensable for the generation of T_H1 and T_H17 cells, while knocking out Rictor and thus inhibiting mTORC2 signalling lead to defects in the generation of T_H2 cells. However, not much is known about the role of mTORC2 signalling for CD8 T cell biology. We will thus discuss the effects of a specific catalytic inhibitor of mTOR, KU-006374, which inhibits mTORC1 and mTORC2 on CTL. We will use the same approaches that were used in the previous two chapters, namely our transcriptomic analysis via Affymetrix micro array and SILAC based quantitative mass spectrometry.

6.2. Results

We analysed our mass spectrometry data of the CTL proteome to see whether the canonical components of the mTORC2 pathway are expressed and thus potentially active in CTL. The data are presented in Figure 6.1.

protein name	complex	detected
Raptor		YES
PRAS40		YES
Rheb	mTORC1	YES
RagA		YES
RagC		YES
mTOR		YES
mLST8		YES
Deptor	mTORC1/2	NO
TTI1		YES
Telo2		YES
Rictor		YES
mSIN1	mTORC2	YES
Protor		NO

Figure 6.1: mTORC1/2 subunits detected by mass spectrometry
Proteins involved in the formation of mTORC1 and mTORC2 are shown. YES/NO indicate whether the specific protein as found in the LFQ MS experiment.

Apart from the inhibitory subunit Deptor, which is shared by both mTORC1 and mTORC2, and Protor, which is an mTORC2 specific subunit, all canonical mTORC1 and mTORC2 subunit could be detected in our mass spectrometry data sets.

As in the previous chapters we used the P14 TCR transgenic mouse model to generate CTL in *vitro*. Long term treatment with 20 nM rapamycin or 1 μM KU-0063796 led in both cases to the dephosphorylation of the mTORC1 substrate S6K Thr389 (Figure 6.2, A). Several phosphorylation sites on another mTORC1 substrate, 4EBP1, were also affected be either treatment, however, only KU-0063794 led to the complete dephosphorylation of the phosphosites. KU-0063794 also affected the phosphorylation of the mTORC2 substrate PKB Ser473 and of NDRG1 Thr346.

NDRG1 is a direct substrate of serum and glucocorticoid kinase 1 (SGK1) which in turn is a substrate of mTORC2. We described the effect of rapamycin treatment on the proliferation rate of CTL in chapter 2. KU-0063794 treatment decreased, but not stopped, the proliferation rate of CTL to the same extent as rapamycin (Figure 6.2, B). The forward scatter profile of CTL treated with rapamycin or KU-0063794 also indicated that KU-0063794 and rapamycin had similar effects on CTL cell size and morphology (Figure 6.2, C). It has been proposed that mTORC1 controls protein synthesis rates by its effects on its down-stream effectors S6K and 4EBP1, an effect which we already illustrated in previous chapters. In order to see whether the complete loss of phosphorylation of 4EBP1 due to KU-0063794 treatment led to additional effects on the protein synthesis rate of CTL, we monitored the incorporation of a short pulse (15 minutes) of radiolabelled L-methionine into nascent proteins (Figure 6.2, D). Long term (> 24 h) treatment with either rapamycin or KU-0063794 led to similar decreases by 50% in the protein synthesis rate of CTL. However, the two compounds showed different kinetics regarding their inhibition of CTL protein synthesis rate. The rapamycin effect took approximately 24 hrs to reach its maximum inhibition, whereas the effect of KU-0063794 already plateaued after our first time point at 12 h of treatment.
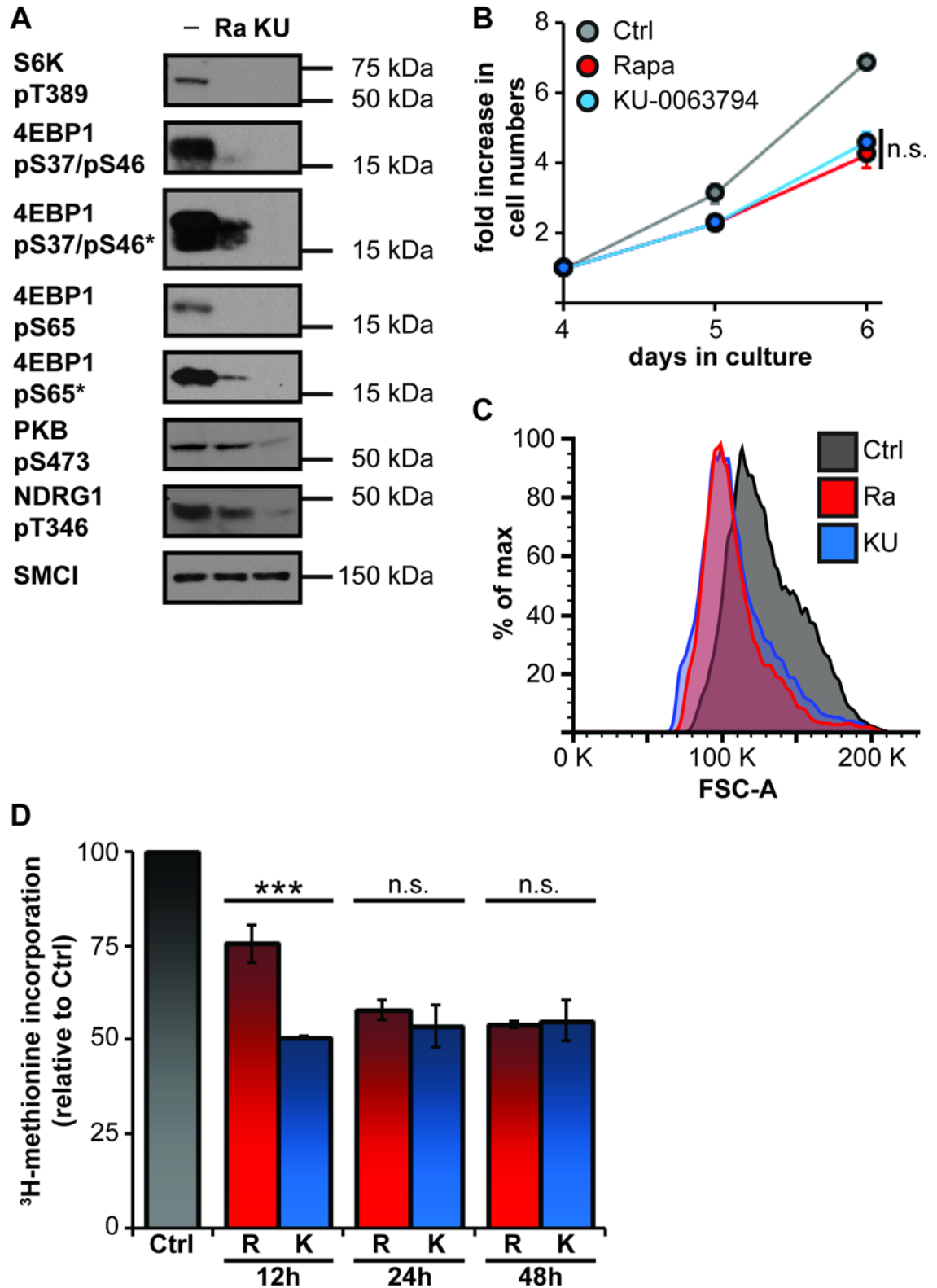
Figure 6.2: Effects of rapamycin and KU-0063794 on mTORC1 and mTORC2 kinase activity, cell proliferation, cell size and protein biosynthesis rate.
(A) Immunoblot analysis of CTL treated with either rapamycin or KU-0063794. S6K and 4EBP1 were used as measure of mTORC1 activity. PKB Ser473 and NDRG1 T346 as direct and indirect indicators for mTORC2 activity. SMCI was used as a loading control. * indicate overexposure of films to highlight differenecs between rapamycin and KU-0063794 treatment. (B) Growth curve of control cells and cells treated with either inhibitor. (C) Comparison of forward scatter or inhibitor treated CTL. (D)

Analysis of protein biosynthesis rate as determined by incorporation of L-methionine into nascent proteins. R: Rapamycin treated CTL, K: KU-0063794 treated cells.

6.2.1. Comparison of rapamycin and KU-0063794 induced changes of the CTL transcriptome

The transcriptional analysis of the previous chapter revealed that rapamycin treatment of CTL led to changes in the transcript levels of 618, with 327 transcripts being up and 297 transcripts being down regulated. In order to see whether the inhibition of mTORC2 in addition to mTORC1 due to KU-0063794 treatment led to further effects on CTL transcript levels we repeated our transcriptomic analysis with the mTOR catalytic inhibitor. As previously described for the rapamycin treatment we used the Affymetrix 430.2 platform to detect changes in transcript levels. Both treatments caused very similar effects in CTL, as indicated by the general high correlation coefficients (Figure 6.3). Strikingly, all transcripts changed in the KU-0063794 treated CTL were also regulated in the rapamycin treated samples (Figure 6.3, B). Vice versa, all transcripts changed due to rapamycin treatment were also affected by the combined mTORC1/mTORC2 treatment to the same extent (Figure 6.3, C). The only exceptions are two micro array probes for nephroblastoma overexpressed gene (Nov), which were only up regulated in the rapamycin but not KU-0063794 treatment (highlighted in red).
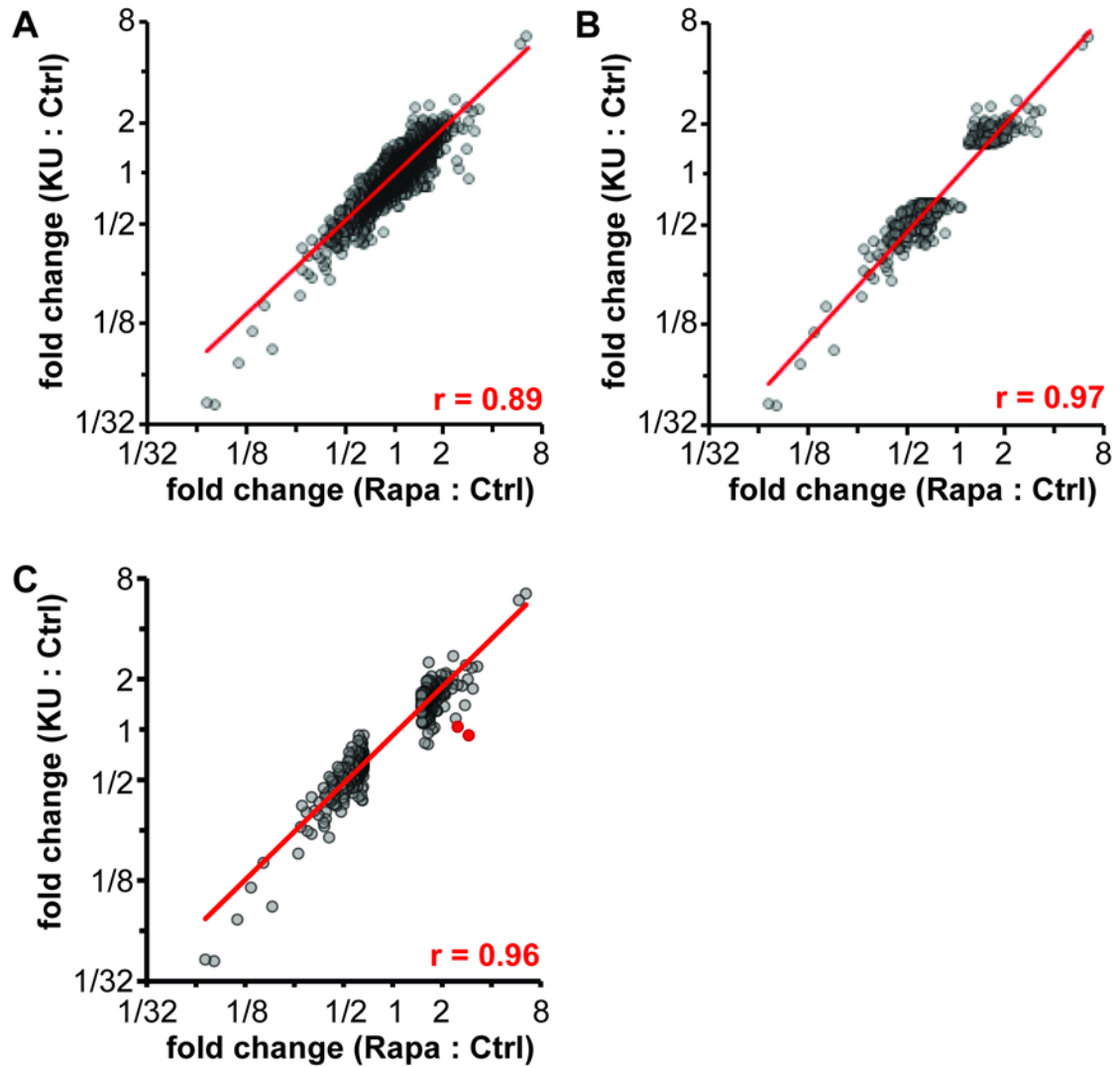
Figure 6.3: Comparison of the effects of long term rapamycin and KU-0063794 on CTL transcript level.
(A) Correlation all genes detected. (B) Like (A), but filtered for transcript due to KU-0063794. (C) Like (A), but filtered for transcripts changed in rapamycin treated cells. Values in red indicate spearman coefficient of correlation.

Due to the effects of KU-0063794 on the phosphorylation on PKB Ser473 we expected changes in the transcription of genes regulated by PKB. The PKB controlled transcriptional program in CTL has been described previously[86]. We were particularly interested in the effects of the mTOR inhibitor on expression of the gene targets of the transcription factor FoxO1, which regulates the expression of several genes including Klf2, IL7r, Ccr7 and S1pr1[86]. FoxO1 is phosphorylated by protein kinase B on several

sites and these phosphorylations lead to the translocation of FoxO1 into the cytoplasm and sequestering by 14-3-3 proteins. High PKB activity thus switches off the expression of these FoxO1 controlled genes. KU-0063794 leads to the dephosphorylation of PKB Ser473 and we thus expect a re-expression of Foxo target genes.

We thus compared the changes in transcript levels for these five genes in our rapamycin and KU-0063794 treated CTL and compared them to previously published data of CTL treated with AktI, an inhibitor specific for Akt/PKB[349] (Figure 6.4). We furthermore investigated the effects of the inhibitor treatments on mRNA levels of the transcription factors T-bet and Eomesodermin, which have also been reported to be controlled by FoxO transcription factors[350].

	fold change			
	Rapa	KU	AktI	gene
Klf2	0.93	1.3	5.8	Klf2
Il7r	0.88	0.95	2.2	Il7r
Ccr7	1.9	1.3	3.1	Ccr7
S1pr1	0.91	0.89	2.6	S1pr1
Eomes	1.2	1.0	0.77	Eomes
Tbx21	1.1	1.0	1.0	Tbx21
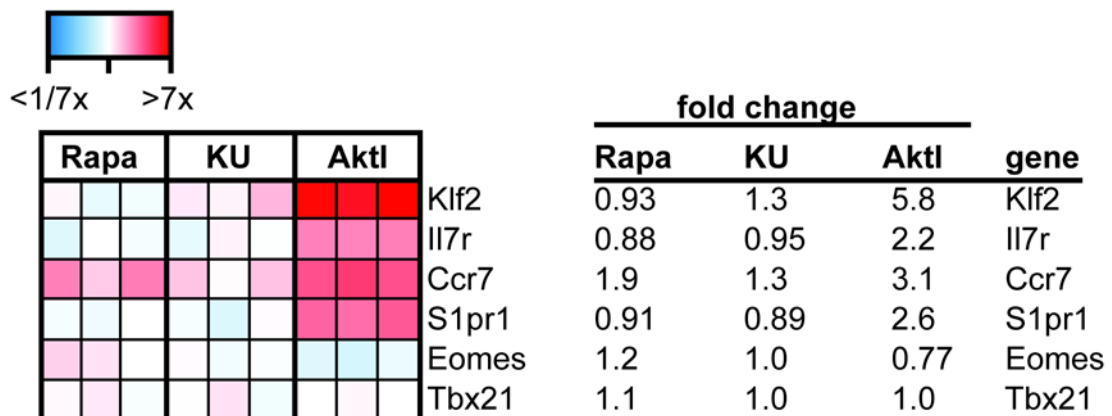
Figure 6.4: Effects of rapamycin and KU-0063794 treatment on the transcription of FoxO targets and comparison to PKB inhibited cells.
Heat map representation of transcript changed to due to mTORC1, mTORC1/2 or PKB/Akt inhibition. Red hues indicate up regulated, blue hues down regulated transcript. Fold changes are given as well.

The transcription of the FoxO targets Klf2, Il7r, CCr7 and S1pr1 was not affected by any treatment other than the PKB inhibition, indicating that neither mTORC1 nor mTORC2 control the transcription of these genes. The two transcription factors T-bet and Eomesodermin were also not affected by any of the inhibitor treatments. The results

thus indicate that FoxO1 activity is still repressed despite the effects of mTORC2 inhibition on the phosphorylation on PKB S473.

6.2.2. Comparison of the mTORC1 and mTORC1/2 controlled proteomes

As we demonstrated in the previous chapter that mTORC1 controls the expression of many proteins independent of their corresponding transcript levels, we wanted to know whether the same is also true for mTORC2. We thus decided to use the SILAC approach described in the previous chapter to investigate whether combined mTORC1/mTORC2 inhibition led to the regulation of any proteins that are not already regulated by mTORC1 inhibition alone.

The experimental approach as the same as previously described. We used P14 LCMV TCR transgenic mouse model to generate CTL *in vitro*. In order to facilitate the metabolic labelling of the cells, CTL were cultured in SILAC T cell medium after activation and clonally expanded for 4 days. The cells were treated with rapamycin or KU-0063794 for 48 hrs before harvesting. Cells were then combined in a 1:1 ratio with controls cells and subjected to subcellular fraction before being separated by size exclusion chromatography into 33 fractions and analysed via LC-MC/MS and analysed by the MaxQuant software package.

As with the transcriptomic analysis earlier, both treatments show a strong correlation (Figure 6.5, A), in particular when filtering only proteins that were robustly changed in any of the conditions (Figure 6.5, B). Using the SILAC approach we could thus not detected any significant changes between the two conditions.
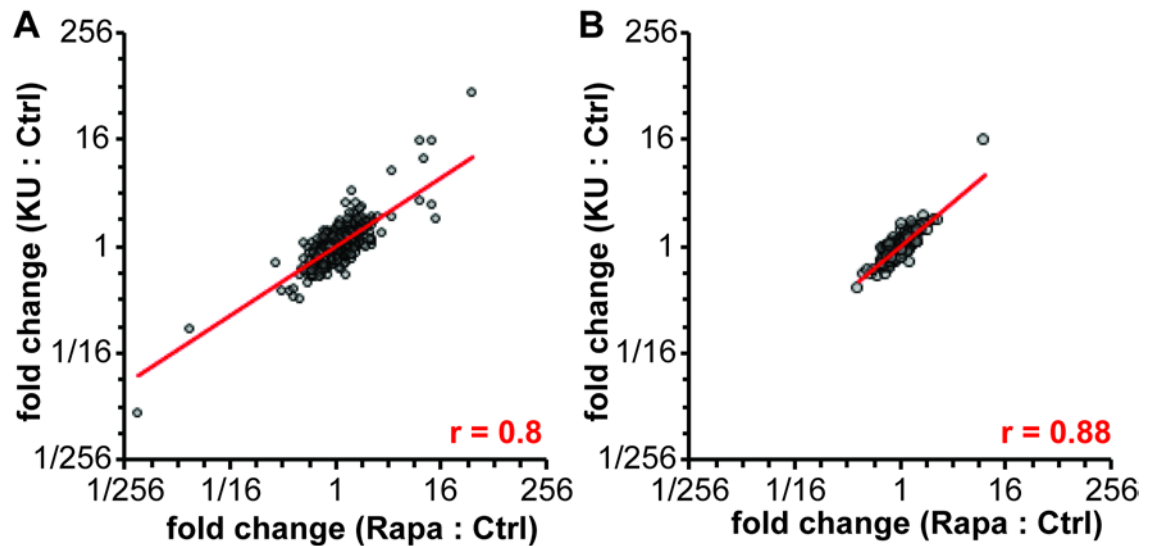
Figure 6.5: Comparison of rapamycin and KU-0063794 effects of the proteome of CTL.
(A) Observed ratios for all proteins detected in at least replicates for each condition are shown. (B) Only protein that are robustly changed in at least one inhibitor treatment are shown.

We know from previous studies that protein kinase B activity is important for the expression of Interferon-γ, as inhibition of PKB leads to the down regulation of IFN-γ transcript resulting in reduced protein levels[86]. However, it has been reported that SGK1, a down-stream kinase of mTORC2, represses the expression of Interferon-γ in CD4 cells[351]. We have also shown in earlier chapters of this thesis that mTORC1 inhibition led to the decreased expression of Interferon-γ in CTL. Combined mTORC1/mTORC2 inhibition should affect all three aforementioned mechanisms of IFN-γ expression controls. We thus compared the effects of rapamycin and KU-0063794 treatment on CTL to see whether the two treatments cause different effects on IFN-γ levels.

We performed a flow cytometric analysis of intracellular levels of IFN-γ in CTL treated with rapamycin and KU-0063794 to compare the effects of both inhibitors (Figure 6.6, A). We could not detect any changes in either frequency of IFN+ cells or in the MFI of the intracellular IFN-γ stainings when comparing the two inhibitor treatments. We also

saw no differences between mTORC1 and combined mTORC1/2 inhibition, as both inhibitors reduce the secretion of IFN-γ by approximately 70% of the untreated cells.
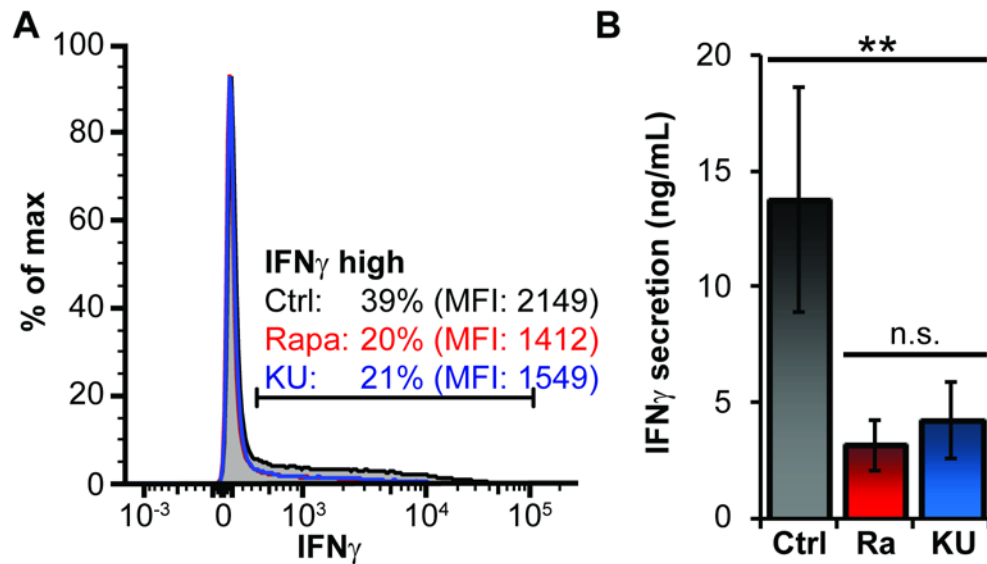
Figure 6.6: effects of Rapamycin and KU-0063794 inhibition on expression of IFN-γ

(A) Flow cytometry analysis of intracellular levels of IFN-γ in CTL. (B) ELISA analysis of IFN-γ secreted by CTL.

Data are mean ±SD or representative of three experiments (**, p ≤ 0.01)

6.3. Discussion

The aforementioned results describe the role of mTORC2 signalling in the context of a combined mTORC1 and mTORC2 inhibition using an mTOR catalytic inhibitor. Despite completely abrogating 4EBP1 phosphorylation and inhibiting mTORC2 signalling we were not able to detect any differences on the transcriptome or proteome between long term rapamycin and KU-0063794 inhibited CTL. These data indicate that mTORC2 does not play a major role in CTL in the context of simultaneous mTORC1 inhibition. This stands in stark contrast to CD4 T cells, for which it has been shown that mTORC2 signalling is indispensable for the generation of T_H2 cells[347]. Other studies used genetic approaches to abrogate either just mTORC1 signalling (by knocking out the mTORC1 activator Rheb) or knocked out mTOR to prevent both mTORC1 and mTORC2 signalling[352]. This study proposed different phenotypes for the two different models: T cells generated from mTOR deficient mice did showed normal activation and initial IL-2 production. However, these cells failed to differentiate into T_H1, T_H2 or T_H17 cells but differentiated to Tregs instead. On the other hand, T cells generated from the Rheb deficient mice are still able to generate T_H2 T cells[348]. Thus mTORC2 seems to play a more important role in CD4$^+$ T cells than it does in CD8$^+$ T cells.

However, we were particularly surprised that the inhibition of mTORC2 did not affect the expression of FoxO1 target genes. FoxO1 can be phosphorylated by PKB on several sites which leads to its translocation form the nucleus to the cytoplasm and binding to 14-3-3 proteins and consequently to the inhibition of the transcription factor activity.

As mTORC2 phosphorylates PKB on the hydrophobic motif site Ser473 we expected to see a change in the transcription in FoxO1 genes as KU-0063794 inhibition of mTOR led to decreased phosphorylation levels on that site. PKB Ser473 is required for the activation of PKB as it serves as a binding site for the phosphoinositide-dependent

kinase-1 (PDK1) which upon binding to that site phosphorylates PKB on the T-loop site Thr308 which leads to activation of PKB[146]. Thus Ser473 is important for the full kinase of activity of PKB. However, FoxO function as still repressed in the long term KU-0063794 treatments indicating that PKB activity is not impaired under these conditions despite the loss of the phosphorylation at Ser473.

Unfortunately, there are no inhibitors available that specifically inhibit mTORC2 activity without affecting mTORC1 signalling. Therefore we are forced to use catalytic inhibitors which lead to the inhibition of both signalling complexes. It is thus possible that potential effects of mTORC2 are overridden and thus masked by the simultaneous inhibition of mTORC1. One potential example is the proposed role of SGK1 in suppressing IFN-γ transcription in CD4$^+$ T cells[351]. These studies used mice deficient in SGK1 to describe its role in controlling T$_H$1 and T$_H$2 differentiation and suppressing IFN-γ production by controlling the expression of an isoform of the transcription factor TCF-1. It is possible that a similar mechanism by which SGK controls IFN-γ exists in CTL. However, we do not see a difference in the IFN-γ levels of CTL treated with rapamycin or KU-0063794, indicating that the mechanism by which the mTORC1 inhibition down regulates IFN-γ levels overrides any potential SGK control of IFN-γ expression. Genetic approaches were also used in the past to selectively interrupt mTORC1 (by deleting Rheb) or mTORC2 (by deleting Rictor) signalling in CD4 T cells to describe their function[348]. However, it is not known whether Rheb or Rictor are involved in mTOR independent complexes and thus their deletion might not reflect impaired mTORC1 or mTORC2 function.

Apart from the combined inhibition of mTORC1 and mTORC2, catalytic inhibitors of mTOR also show a more complete inhibition of mTORC1 than rapamycin as evident by the complete dephosphorylation of the partially rapamycin-resistant 4EBP1. As 4EBP1,

which is an inhibitor of the translation initiation factor eIF4e, is known a regulator of translation[353], we expected a further reduction of protein synthesis of KU-0063794 treated cells when compared to rapamycin treated cells. However, apart from the faster onset of the mTOR inhibition we were not able to see a difference in either protein biosynthesis rate or a general decrease of protein levels as evident by the SILAC approach. A recent study in a transformed cell line has shown that cells became resistant to a catalytic mTOR inhibitor by up regulating the expression of eIF4E upon chronic mTOR inhibition in order to maintain cell growth and protein translation[354]. CTL also up regulate eIF4e, type 3 upon long term rapamycin or KU-0063794 treatment as analysis of our SILAC data of both inhibitor treatments revealed. This up regulation might counter-act the 4EBP1 mediated inhibition in CTL with sustained mTORC1 inhibition and furthermore level out the differences between the incomplete dephosphorylation of 4EBP1 due to rapamycin and the complete dephosphorylation by KU-0063794.

Another mechanism by which CTL adapt to long term mTORC1 inhibition and which involves the S6K will be discussed in the next chapter. This mechanism will explain why rapamycin and KU-0063794 treatments showed such a similar phenotype despite the expected effects mediated by the mTORC2 substrate PKB.

7. Links between mTOR and PIP$_3$ signalling in CTL

7.1. Introduction

In the previous chapter we demonstrated that combined long term inhibition of mTORC1 and mTORC2 with catalytic inhibitors of mTOR like KU-0063794 did not lead to major differences in the CTL transcriptome or proteome compared to just inhibiting mTORC1 signalling with rapamycin. We were particularly surprised that we did not see a difference between the two inhibitor treatments in the expression of genes controlled by the transcription factor FoxO1, whose transcriptional activity is regulated by protein kinase B (PKB) activity. PKB is activated by phosphorylation of Thr308 by PDK1 and on Ser473 by mTORC2 and both phosphorylations are required for full activity[146]. As mTORC2 inhibition leads to the loss of phosphorylation at Ser473 we expected that mTORC2 inhibition would thus cause loss of PKB activity, decreased phosphorylation of FoxO1 and therefore re-expression of its target genes. However, we did not see a re-expression of Foxo1 controlled genes in CTL treated with an mTOR catalytic inhibitor indicating that PKB activity was not affected by sustained mTORC1/2 inhibition. In this respect, Delgoffe and colleagues have examined this issue and shown that in T cells lacking mTORC2 complexes there is no TCR-induced phosphorylation of Akt-Ser473[348]. However, Akt-Thr308 phosphorylation is reduced but not ablated arguing that AktS473 phosphorylation may not be obligatory for Akt activation[348]. These experiments used genetic deletion of Rictor to study the role of the mTORC2 complex in T cells. In the following chapter we will investigate the effects of mTORC1 and combined mTORC1/2 catalytic inhibition on PKB activity in CTL in more detail.

7.2. Results

7.2.1. Long term mTOR inhibition leads to dephosphorylation of PKB Ser473, but not PKB T308 and does not disrupt PKB activity

We demonstrated in the previous chapter that inhibition of mTORC2 activity drastically reduces phosphorylation of the hydrophobic motif site Ser473 of PKB. However, we did not probe for the T-loop site Thr308 of PKB, which is phosphorylated by PDK1 and is required for PKB activity[146]. We thus performed immunoblot analyses of lysates of CTL generated from splenocytes derived from P14 TCR transgenic mice and probed for these two phosphorylation sites of PKB (Figure 7.1, A). CTL treated with KU-0063794 for 48 hours showed no detectable PKB Ser473 phosphorylation. However, the phosphorylation of PKB Thr308 was not decreased by either rapamycin or KU-0063794 treatment (Figure 7.1, A). In fact, Thr308 phosphorylation of PKB was increased when mTORC1 was inhibited for longer periods of time.

We then performed a time course experiment using KU-0063794 (Figure 7.1, B). The data show that KU-0063794 led to the dephosphorylation of mTORC1 substrates like Thr389 on S6K and Ser65 on 4EBP1 as well as mTORC2 substrates like Ser473 on PKB within 10 minutes. This immediate de-phosphorylation of PKB Ser473 was accompanied by the de-phosphorylation of PKB Thr308. We also monitored the impact of KU-0063794 on PKB activity by measuring the phosphorylation of Thr24/32 on FoxO1/3a, a PKB substrate sequence[86]. These data showed that treatment of CTL with a catalytic mTOR inhibitor causes loss of PKB activity. However, the dephosphorylation of PKB Thr308 is only transient as normal phosphorylation levels are regained after approximately 6 hrs of KU-0063794 treatment. This re-phosphorylation of PKB is also mirrored by restoration of PKB activity as judged by corresponding FoxO1/3a phosphorylation at Thr24/32.
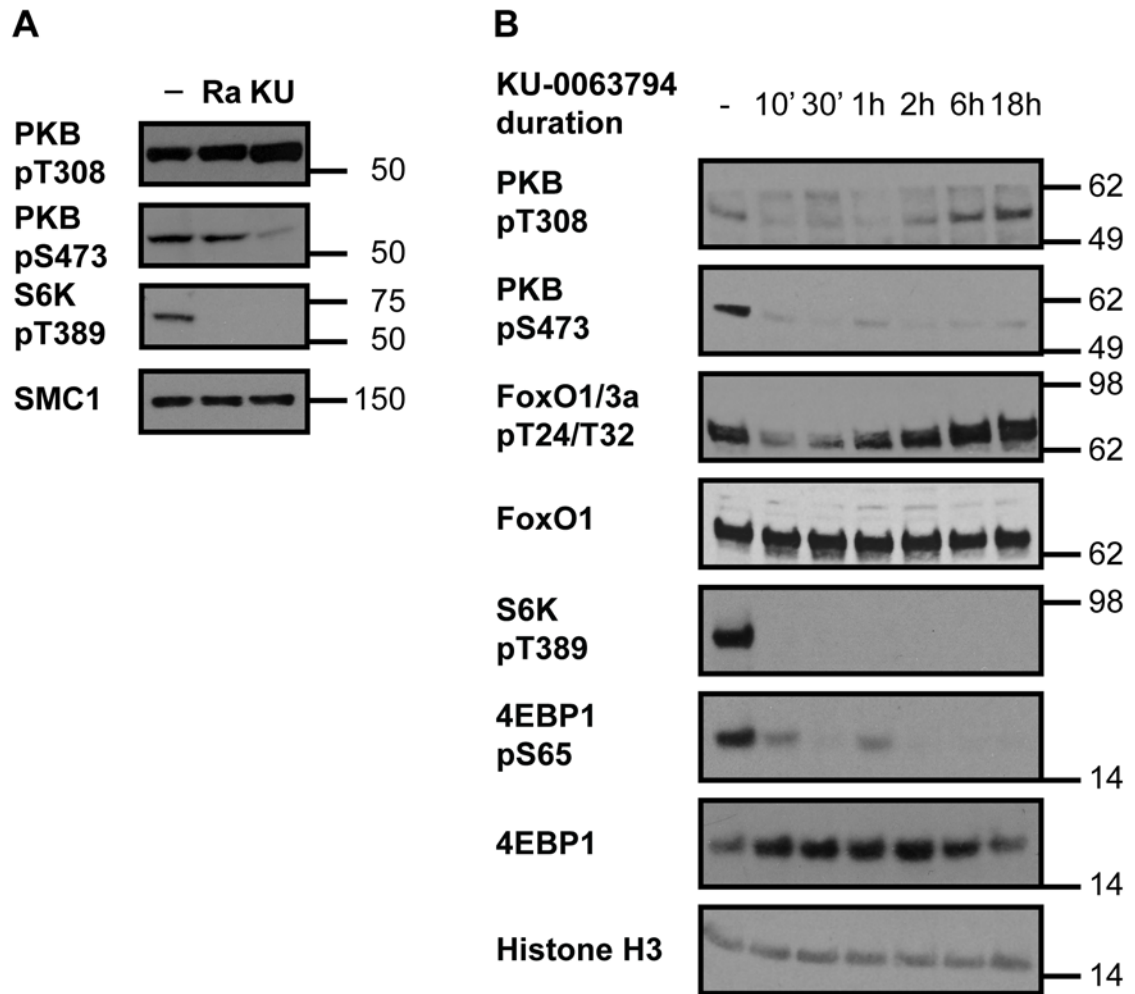
Figure 7.1: Time course of KU-0063794 treatment of CTL
Immunoblotting of CTL generated from P14 LCM TCR transgenic mice. (A) Comparison of long term Rapamycin and KU-0063794 treatment on phosphorylation of Thr308 and Ser473 of PKB. SMCI was used as a loading control. (B) Time course of CTL treated with 1 μM KU-0063794 for 10 minutes to 18 hrs. Histone H3 was used as a loading control. Numbers on the right indicate molecular size (in kDa)

7.2.2. The re-activation of PKB is dependent on the translocation of PDK1 to the plasma membrane via binding to phosphatidylinositol (3,4,5)-trisphosphate

The interaction of PKB with the phospholipid phosphatidylinositol (3,4,5)-trisphosphate (PIP$_3$) via its Pleckstrin homology (PH) domain is required for the activation of PKB. The interaction induces a conformational shift in PKB that enables 3-phosphoinosotide

dependent protein kinase-1 (PDK1) to phosphorylate Thr308 within the T-loop of PKB[146]. PDK1 itself is believed to be constitutively active and the phosphorylation of its substrates like PKB is predominantly regulated by controlling the kinase-substrate interaction[148]. Two mechanisms that promote the interaction of PKD1 and PKB and the subsequent phosphorylation of Thr308 on PKB have been proposed[355]. The first is a phosphatidyl-(3,4,5)-trisphosphate (PIP$_3$) dependent mechanism which relies on elevated levels of PIP$_3$ in the cell membrane generated by high phosphatidyl-3,4-bisphosphate 3-kinase (PI3K) activity. PDK1, like PKB, contains a PH domain which facilitates the recruitment of the kinase to the plasma membrane by high PIP$_3$ levels. In contrast to PKB however, the association of PDK1 with the PIP$_3$ is not required for PDK1 activity[148]. Recruitment of both PKB and PDK1 to the plasma membrane leads to the interaction of the two kinases and enables the efficient phosphorylation of PKB Thr308 by PDK1. The second mechanism by which PKB and PDK1 can interact with each other is the so-called PIF-pocket dependent mechanism. This mechanism depends on the phosphorylation of PKB Ser473 rather than high PIP$_3$ levels. If PKB Ser473 is phosphorylated by mTORC2 it can recruit PDK1 by the PIF-pocket domain of PDK1 and this interaction leads to the subsequent phosphorylation of PKB Thr308. However, even though high PIP$_3$ levels are not required for the PIF-pocket mediated interaction of PKB and PDK1, binding of PKB to PIP$_3$ via its PH domain is still essential for the induction of the conformational shift necessary for PKB Thr308 phosphorylation. Both mechanisms are illustrated in Figure 7.2.
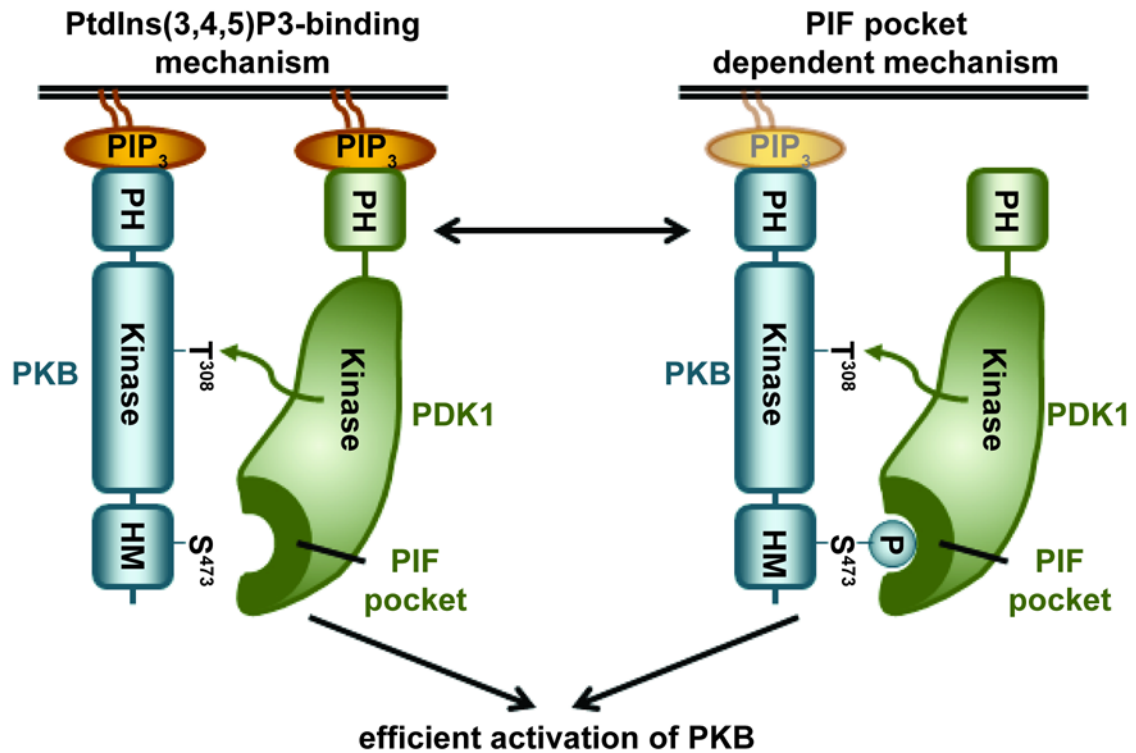
Figure 7.2: Models of PKB activation by PDK1
PIP_3 and PIF-pocket dependent mechanism of PKB activation by PDK1 according to Najafov et al.[355]. PDK1 either associates with PKB via PH domains or via PIF-pocket dependent association via phosphorylation at Ser473 of PKB.

At earlier time points of the KU-0063794 treatment we see a decrease in both Thr308 and Ser473 of PKB (Figure 7.1, B). This indicates that at these time points the Ser473 phosphorylation is required for Thr308 to be phosphorylated which can be explained with the aforementioned PIF-pocket dependent mechanism. Thr308 is then rephosphorylated whereas Ser473 levels remain low. The phosphorylation of PKB on Thr308 in the absence of phosphorylated Ser473 could happen if the cells switched from using the PIF-pocket dependent mechanism to co-localise PDK1 and PKB to using the PIP_3-dependent mechanism.

Why would cells switch to the PIP_3 dependent mechanism for the co-localisation of PDK1 and PKB? One explanation could be that mTOR signalling restrains PIP_3 levels and subsequently PIP_3 signalling such that in the presence of mTOR inhibitors the

levels of PIP_3 increase. This type of mTOR controlled negative feedback pathway has been described extensively before[247,248,249]. For example, the insulin receptor substrate (IRS) 1/2 has been shown to be involved in an mTORC1 negative feedback pathway controlling PIP_3 levels in mouse embryonic fibroblasts[247] and later in the context of multiple myeloma[356]. IRS1/2 are adaptor molecules that can be phosphorylated on tyrosine residues and thus serve as a docking site for the PI3K p85 SH2 domain, leading to the membrane recruitment of the p85/p110 PI3K complex. IRS1/2 can also be phosphorylated on serine/threonine residues by S6K which targets the protein for proteasomal degradation[357]. High mTORC1-S6K activity thus causes cells to down regulate IRS2 levels which restrains PI3K membrane recruitment and thus restricts the generation of PIP_3. More recently, phospho-proteomic studies in mouse embryonic fibroblasts have revealed that the expression of another adaptor molecule, Grb10, a negative regulator of receptor tyrosine kinases (RTK), is also controlled by mTORC1[248,249]: Elevated mTORC1 activity leads to stabilisation of this protein which in turn down regulates RTK activity and consequently PI3K activity.

However neither the Grb10 nor the IRS1/2 mediated mechanisms have been described in CTL before. We thus wanted to know whether pronged mTORC1 inhibition leads to increased level of PIP_3 in CTL. Hence we treated CTL with rapamycin or KU-0063794 for different periods of time and determined intracellular PIP_3 levels. These measurements were performed by Dr. Karen Anderson at the Babraham Institute in Cambridge using a HPLC-MS-based approach[358]. CTL treated with rapamycin or KU-0063794 for 24h or longer showed a strong increase in PIP_3 levels, indicating that chronic mTORC1 inhibition leads to increased PIP_3 generation in CTL (Figure 7.3, A). CTL treated with either inhibitor for only 1 hour did not show this increase in PIP_3.
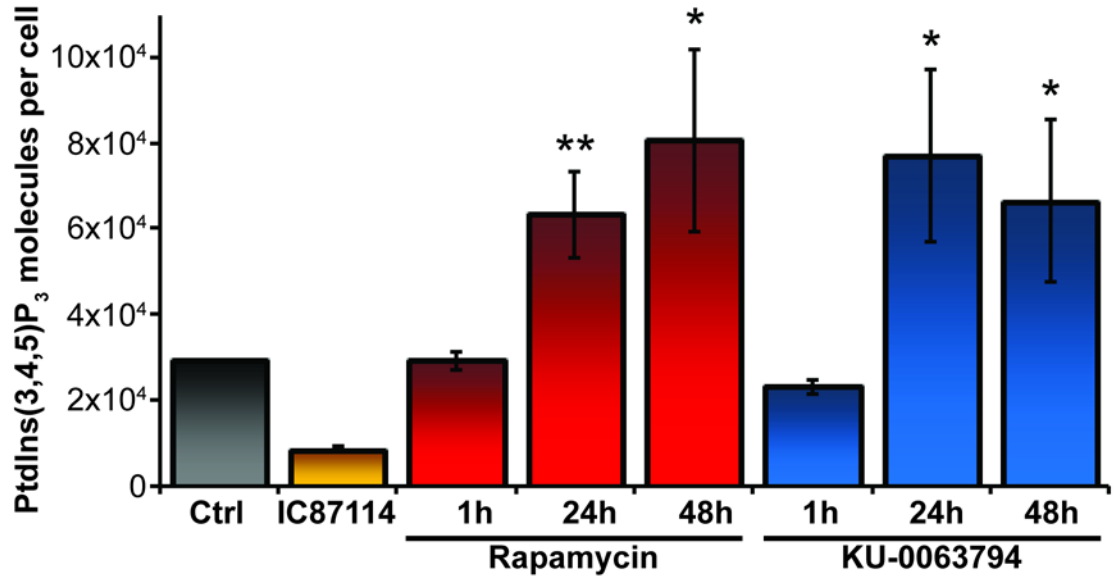
Figure 7.3: prolonged mTORC1 inhibition leads to increased PIP$_3$ levels in CTL
Measurements of PIP$_3$ levels in CTL treated for 1h, 24h or 48 h with rapamycin or KU-0063794. PI3K inhibitor IC87714 was used as negative control. PIP$_3$ levels were measured by HPLC-MS. *: $p<0.05$, **: $p<0.01$.

To further test whether the co-localisation of PKB and PDK1 via PIP$_3$ was important for the increased PKB activity seen in mTORC1 inhibited CTL, we assessed whether the PKB activity in CTL treated with rapamycin or KU-0063794 was still sensitive to PI3K inhibition or compounds that inhibit the PH-domain mediated interaction of PKB with PIP$_3$.

PI3K can be inhibited using a specific inhibitor for the p110δ subunit of PI3K, IC87114. P110δ is the predominant p110 isoform in CTL and is important for the activation of PKB[86]. Inhibiting PI3K activity with IC87114 led to the complete loss of PKB phosphorylation on both Thr308 and Ser473 (Figure 7.4, A), indicating that PI3K activity and thus PIP$_3$ is required for the hyperphosphorylation of PKB Thr308 due to prolonged mTORC1 inhibition.

PKB inhibitors like Akt-1/2 (AktI) bind to and inhibit the function of the PH domain of PKB and thus effectively inhibit PKB activity[359]. Treatment with AktI in CTL with

intact or disturbed mTORC1 signalling completely inhibited phosphorylation on both

PKB Thr308 and Ser473 (Figure 7.4, B). This shows that the mechanism by which

mTORC1 inhibition elevates PKB activity still requires PKB to bind to PIP$_3$ via its PH

domain in order to be phosphorylated on the two sites. However, inhibiting PKB

activity with either IC87114 or AktI did not lead to a significant inhibition of mTORC1

activity as Thr389 on S6K is still phosphorylated in these conditions.
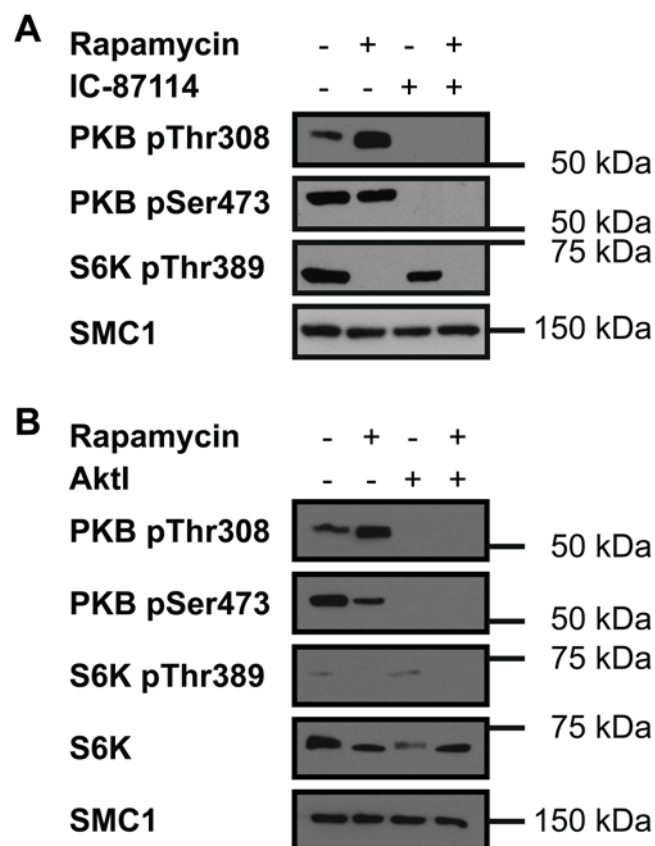
Figure 7.4: PI3K activity is required for hyperphosphorylation of PKB following long term mTORC1 inhibition.
(A) Immunoblot analysis showing the effects of PI3K inhibition on CTL treated with rapamycin. CTL were treated with rapamycin for 48 hrs and IC87114 was added to the culture for 1 h before lysis. (B) Immunoblot analysis showing the effects of disturbed PH domain function of PKB in CTL treated with rapamycin. CTL were treated with rapamycin for 48 hrs and AktI was added to the culture for 1 h before lysis.

We then examined the impact of mTORC1 inhibition on PKB activity in CTL expressing PDK1 with a point mutation in its PH domain. This PDK1-K464E mutant is not able to bind PIP_3[360] and are thus not able to phosphorylate PKB Thr308 via the PIP_3-dependant mechanism. The mutant therefore relies solely on the PIF-pocket dependent mechanism of PKB activation. It is important to remember that the function of the PH domain of PKB is not affected in these CTL and thus PKB will bind normally to PIP_3 and perform the conformational shift required for the PDK1 interaction.

We treated CTL derived from WT and PDK1-K465E splenocytes with rapamycin or KU-0063794 for 1 h or 48 h and compared the effects of chronic mTORC1 and combined mTORC1/2 inhibition on the activity of PKB (Figure 7.5).
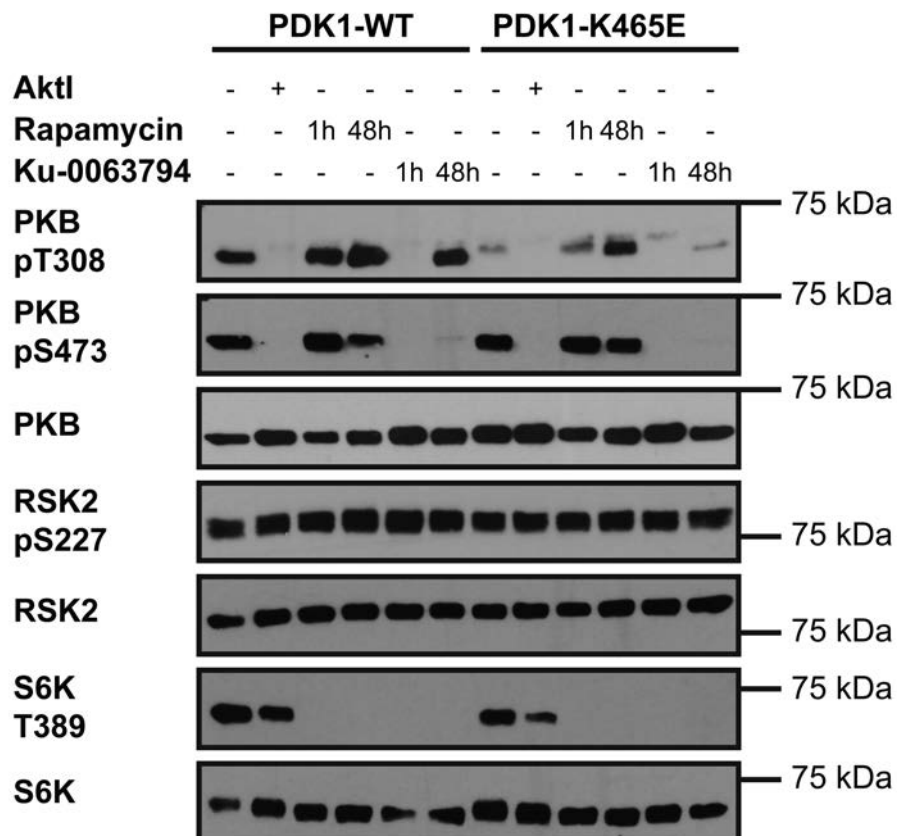
Figure 7.5: hyper-phosphorylation of PKB T308 is dependent on binding of PDK1 to PIP_3
Western blotting of CTL derived from OT-I TCR transgenic splenocytes activated with SIINFEKL peptide. CTL are expressing either wild type PDK1 or a K465E mutant which is unable to bind PIP_3.

CTL carrying the PDK1-K465E mutant showed lower baseline levels of PKB Thr308 which has been shown previously[150]. Phosphorylation of RSK2 Ser227, another substrate of PDK1, was not impaired, as the PH domain of PDK1 is not involved in the phosphorylation of this site[146]. CTL expressing wild type PDK1 alleles initially lost PKB Thr308 phosphorylation when treated with KU-0063794 but were able to rephosphorylate the site after long term treatment as mentioned before. PKB Ser473 remained dephosphorylated even after long term mTOR inhibition. In contrast to that, CTL expressing PDK1-K465E failed to rephosphorylate Thr308 after chronic mTOR inhibition. This shows that association of PDK1 with PIP_3 is required for the rephosphorylation of PKB Thr308 if PKB Ser473 is not phosphorylated and thus cannot aid in the association of PKB and PDK1 via the PIF-pocket dependent mechanism. Therefore PDK1-K465E can neither bind to Ser473 on PKB in KU-0063794 treated CTL nor can it be translocated to the plasma membrane via PIP_3-PH domain interaction due to the mutation and despite elevated PIP_3 levels.

Long term rapamycin treatment led to hyperphosphorylation of PKB Thr308 in both PDK1-WT and the PDK1-K465E mutant. Increased PIP_3 levels thus lead to increased phosphorylation of Thr308 even if PDK1 cannot be recruited to the membrane any longer. However, the increased PIP_3 levels could cause more PKB to associate with the plasma membrane and perform the conformational shift and thus priming it for PDK1 to phosphorylate PKB Thr308. Thus as long as PKB is phosphorylated on Ser473 the PDK1-K465E is still able to phosphorylate more PKB molecules, despite being limited to the PIF-pocket dependent mechanism for its interaction with PKB.

7.2.3. PTEN expression is reduced by mTORC1 inhibition but is not required for PKB hyperactivation.

We then investigated how CTL up regulate their PIP_3 levels upon mTORC1 inhibition. We thus analysed our mass spectrometry data for potential candidates. We discovered that Phosphatase and Tensin homolog (PTEN) was down regulated in our long term rapamycin treated CTL on the protein, but not in the transcript level (Figure 7.6, top). We further validated this finding via immunoblotting (Figure 7.6, bottom).

Protein name	Gene name	Label-free ratio (Rapamycin:Ctrl)	Micro-array ratio (Rapamycin:Ctrl)
Phosphatase and Tension homolog PTEN	PTEN	0.47	1.09
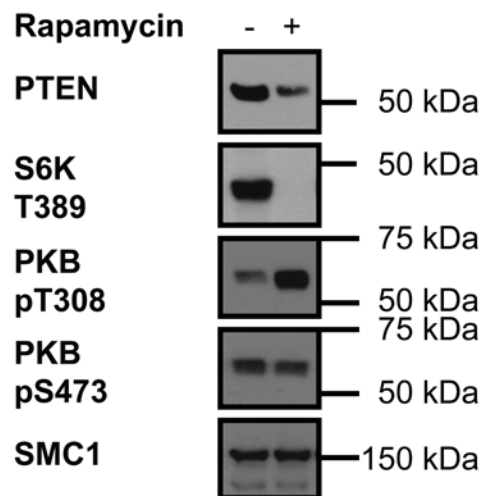
Figure 7.6: mTORC1 activity sustains PTEN expression.
Top: PTEN down regulation due to mTORC1 inhibition as evident by mass spectrometry and micro array data. Bottom: Immunblots of CTL derived from P14 TCR transgenic mice activated with gp33 and treated with rapamycin for 48 hrs or control cells. SMC was used as a loading control.

PTEN is a lipid phosphatase with specificity for the 3′ position of $PI(3,4,5)P_3$. PTEN thus dephosphorylates PIP_3, leading to the formation of phosphatidylinositol-4,5-bisphosphate[361,362] ($PtdIns(4,5)P_2$). PTEN thus negatively regulates $PI(3,4,5)P_3$ signalling. By using CTL derived from splenocytes lacking either one or both alleles of

PTEN we wanted to investigate whether reduction of PTEN levels on its own is sufficient to increase PKB Thr308 levels (Figure 7.7).
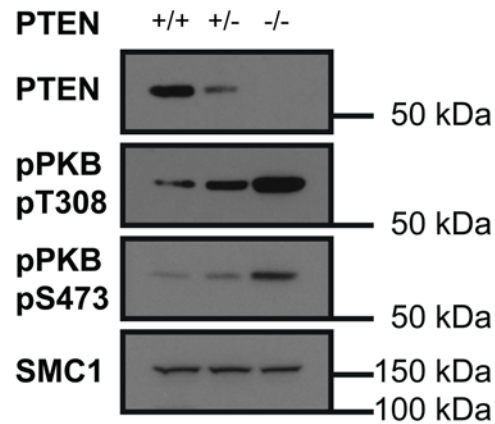
Figure 7.7: Expression of PTEN limits PKB activity.
Immunoblotting of CTL derived from polyclonal splenocytes activated with CD3CD/28 antibody. Comparison of CTL derived from PTEN$^{-/-}$ X CD4-Cre$^{+/-}$ (PTEN$^{+/+}$), PTEN$^{fl/-}$ X CD4-Cre$^{+/-}$ (PTEN$^{+/-}$) and PTEN$^{fl/fl}$ X CD4-Cre$^{+/-}$ (PTEN$^{-/-}$). SMCI was used as a loading control.

The data in Figure 7.7 show that reducing PTEN levels in CTL by 50% is sufficient to increase both PKB Thr308 as well as PKB Ser473 phosphorylation with the homozygous knockout showing even higher phosphorylation levels than the heterozygous knockout.

We then examined whether PTEN null CTL could further hyperactivate PKB Thr308 phosphorylation following long term mTORC1 inhibition. We thus treated CTL lacking PTEN with rapamycin and KU-0063794 and compared the effects of PKB phosphorylation to control CTL (Figure 7.8).
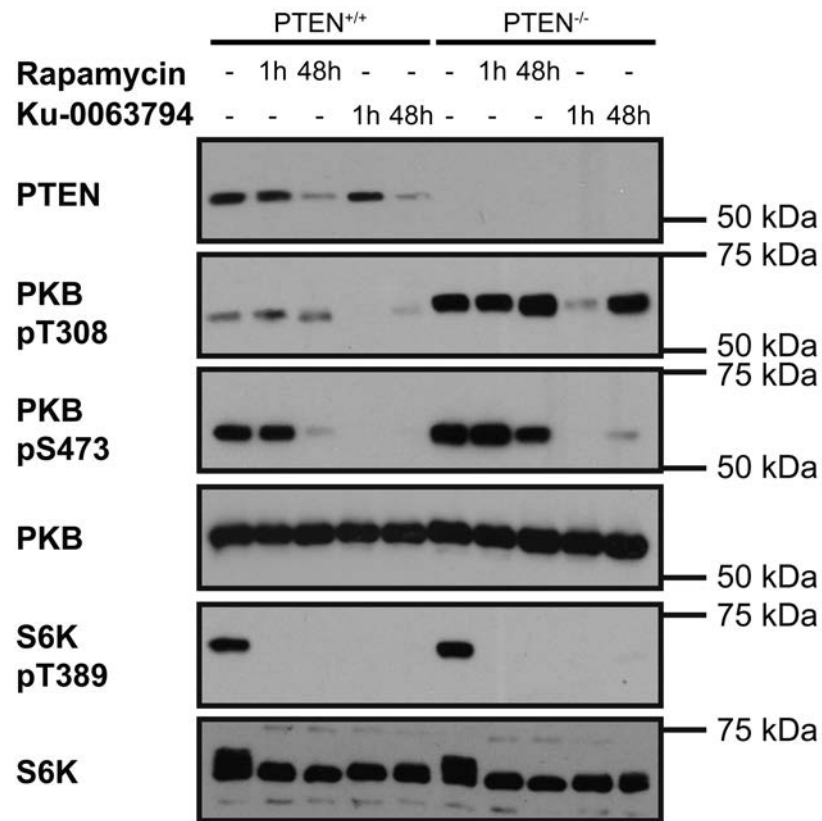
Figure 7.8: PTEN down regulation is not required for hyper activation of PKB due to long term mTORC1 inhibition.
Immunoblotting of CTL derived from polyclonal splenocytes activated with CD3CD/28 antibody. Comparison of CTL derived from PTEN$^{-/-}$ X CD4-Cre$^{+/-}$ (PTEN$^{+/+}$) and PTEN$^{fl/fl}$ X CD4-Cre$^{+/-}$ (PTEN$^{-/-}$). CTL treated with either rapamycin or KU-0063794 for the indicated duration.

As shown previously in Figure 7.7, PTEN deletion leads to elevated baseline PKB Thr308 and Ser473 phosphorylation levels in CTL. However, upon chronic exposure to either rapamycin or KU-0063794, CTL lacking PTEN increased Thr308 phosphorylation even further. This indicates that the down regulation of PTEN expression due to chronic mTORC1 inhibition is not the sole mechanism to hyperactivate PKB activity and that other mechanisms are involved as well.

7.2.4. mTORC1 inhibition leads to elevated levels of insulin receptor substrate 2

As mentioned before, the mTORC1 mediated negative feedback pathway controlling PI3K signalling has been studied extensively. Two mechanisms have been proposed: The first mechanism is mediated by Grb10, a negative regulator of PI3K activity whose expression is controlled by mTORC1 activity[248],[249]. Chronic inhibition of mTORC1 leads to the degradation of Grb10 and thus activates PIP_3 signalling. However, analysis of our micro array and proteomics data did not indicate expression of Grb10 in CTL.

The other mechanism by which mTORC1 could control PI3K signalling is via the insulin receptor substrate $1/2^{247}$. As mentioned earlier, IRS1/2 is an adaptor molecule and positive regulator of PI3K as it is required for the targeting of the p85 subunit of PI3K to the plasma membrane. If mTORC1 activity is high, it leads to the phosphorylation of IRS1/2 via S6K which targets it for proteasomal degradation. Chronic mTORC1 inhibition on the other hand leads to the accumulation of IRS1/2 and thus elevates PI3K activity. We were thus wondering whether IRS1 or IRS2 is expressed and phosphorylated in CTL.

Previous members of the lab have performed global phospho-proteomic studies on CTL, detecting several thousand phosphorylated peptides in these experiments[46]. Analysis of these data as well as our transcriptomic and proteomics data sets revealed that the IRS isoform 2 is expressed and phosphorylated on several residues in CTL, including sites corresponding to the S6K phosphorylation consensus site. According to our data sets, IRS1 is not expressed in CTL.

Our mass spectrometry data further indicated that IRS2 levels are indeed increased upon long term rapamycin treatment while IRS2 transcript levels were not affected by the drug treatment (Figure 7.9, top). We validated these findings using immunoblotting for IRS2 in CTL treated with rapamycin for 48 h. (Figure 7.9, A). Monitoring the time-

dependent effects of rapamycin inhibition on the expression of IRS2 and phosphorylation of PKB 308 furthermore showed a correlation between IRS2 levels and PKB Thr308 phosphorylation in CTL (Figure 7.9, B), as both levels increase with prolonged exposure of CTL to the drug.

Protein name	Gene name	Label-free ratio (Rapamycin:Ctrl)	Micro-array ratio (Rapamycin:Ctrl)
Insulin receptor substrate 2	Irs2	2.1	1.2

Figure 7.9: mTORC1 activity limits IRS2 expression in CTL.
Top: PTEN down regulation due to mTORC1 inhibition as evident by mass spectrometry and micro array data. Bottom: Immunoblotting of CTL derived from P14 TCR transgenic splenoytes activated with gp33. (A) CTL treated with or without rapamycin for 48 hrs. (B) Time course of effects induced by rapamycin treatment of CTL.

7.2.5. Chronic mTORC1 inhibition leads to activation of ERK signalling

PI3K signalling is not the only signalling pathway demonstrated to be negatively regulated by mTORC1. Recent studies indicate that mTORC1 signalling also negatively regulates MAPK signalling[363,249] in mouse embryonic fibroblasts and transformed cell lines and that this mTORC1-MAPK negative feedback pathway also relies on the ability of mTORC1 to control IRS1/2 expression[363].

MAPK kinase signalling plays an important role in CD8 T cell activation, proliferation and survival[364]. We thus investigated whether chronic mTORC1 inhibition increased ERK phosphorylation levels in CTL.
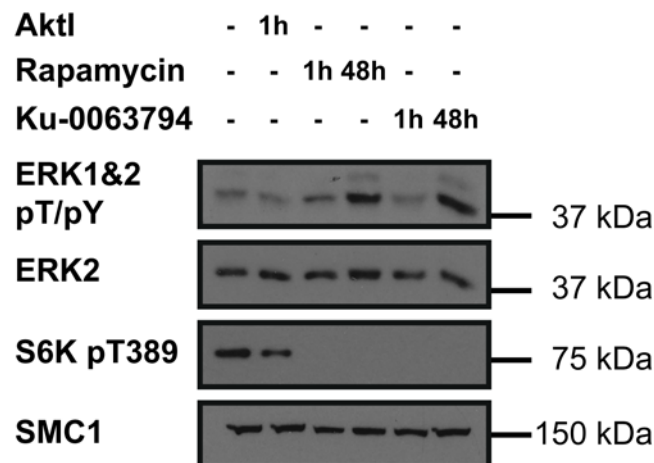
Figure 7.10: Chronic mTORC1 inhibition leads to increased ERK phosphorylation levels.
Immuoblotting of CTL treated with AktI, rapamycin or KU-0063794 for the indicated durations. SMC1 was used as a loading control.

Chronic treatment of CTL with rapamycin or KU-0063794 led to increased levels of phosphorylation of threonine and tyrosine residues within the activation loop of both ERK1 and ERK2. Interestingly, the increased phosphorylation of ERK did not induce increased expression of known ERK regulated genes like CD69, Egr1/3, Fos and Jun.

7.3. Discussion

In this chapter we demonstrated a crosstalk between mTORC1 and PI3K signalling in CTL. We could show that chronic mTORC1 inhibition leads to an increase in intracellular PIP_3 levels and consequently in a hyper-activation of PKB activity. This surge of PIP_3 was also able to overcome the initial dephosphorylation of PKB Thr308 and consequent inactivation of PKB activity induced by combined mTORC1/2 inhibition. PKB Thr308 is re-phosphorylated by PDK1 via a mechanism that no longer relies on the mTORC2 facilitated phosphorylation of Ser473 on PKB, but solely on increased PIP_3 levels. This mechanism explains why we did not observe a re-expression of FoxO target genes in our long-term KU-0063794 treated cells as one would expect if PKB activity was impaired. We do not know the exact mechanism for this up-regulation of PIP_3 levels, but we know that it is sensitive to PI3K inhibition. Studies in other cell models as well as our experiments also indicate that the adaptor protein IRS2 might be involved in this negative feedback mechanism. On the other hand, the down regulation of the tumour suppressor PTEN upon mTORC1 inhibition also increased PKB activity but is ultimately not solely responsible for the described feedback mechanism. We also showed that chronic mTORC1 inhibition leads to increased MAPK signalling activity as indicated by increased ERK activity.

The results shown in this chapter thus clearly illustrate that mTORC2 activity is not necessarily required for PKB function. This is particularly important as several studies examining the role of mTORC2 in T cell function consider PKB as the main down-stream effector of mTORC2 signalling[347,321,365]. mTORC2 is thought to be an important regulator of PKB activity as Ser473 phosphorylation of PKB is considered to be indispensable for PKB activity. However, the results presented in this chapter clearly demonstrate that Ser473 phosphorylation is not required for PKB activity in the context of high PIP_3 levels. These elevated PIP_3 levels enable the cells to switch from a PIF-

pocket dependent mechanism of PKB activation which depends on intact mTORC2 signalling to a PIP$_3$ dependent mechanism, which is uncoupled from mTORC2 signalling. Thus monitoring Ser473 phosphorylation is not sufficient in order to assess PKB activity and that monitoring Thr308 or PKB substrate phosphorylation is a more reliable readout.

Due to the ability of PKB to inhibit the activity of the TSC1/TSC2 complex, a negative regulator of mTORC1 signalling[366], many signalling models consider PI3K-PKB signalling to be indispensable for mTORC1 activity. However, the results presented here together with data previously published by the lab[85] show that mTORC1 signalling in CTL is in fact independent of PI3K and PKB activity, as inhibition of PKB does not abrogate mTORC1 signalling. Furthermore, the data presented in this chapter show that it is actually mTORC1 signalling that is able to control PI3K and PKB activity.

This link between mTORC1 and PI3K signalling is particularly interesting as it might present yet another mechanism by which rapamycin exerts its immunosuppressive effects. It has been recently shown that human patients carrying activating mutations in the p110δ subunit of PI3K leading to increased PIP$_3$ levels suffer from several immundefects[367,368]. This is surprising as increased PIP$_3$ levels are usually considered a positive signal for cells, however the authors argue that the increased PIP$_3$ levels caused the cells to be more prone to activation-induced cell death and thus caused lymphopenia in the patients. This phenotype could be reversed by the use of PI3K inhibitors and thus reducing PIP$_3$ levels. The elevated levels of PIP$_3$ due to chronic mTORC1 inhibition might thus be another mechanism explaining the immunosuppressive effects of rapamycin. Studies have shown that mTORC1 controls T cell trafficking via regulation of adhesion molecules like CD62L and chemokine receptors[155]. However, PIP$_3$ is also known to be a modulator of chemotaxis as it regulates the activity of the family of Rac

proteins, members of the Rho family of small GTPases which control actin dynamics and thus cell motility[369]. Furthermore, the PI3K-PKB-FoxO axis also controls the expression of several chemokine receptors, ligands, adhesion molecules, integrins and other proteins involved in CTL trafficking[86]. Thus the altered trafficking behaviour of CTL treated with rapamycin may not only be caused by direct effects of mTORC1 signalling but also due to the indirect effects of prolonged mTORC1 inhibition on PIP_3 levels.

Due to the lack of genetic models or suitable inhibitors we were unfortunately not able to further dissect the mechanism by which mTORC1 controls PIP_3 levels. The proposed mTORC1-S6K-IRS2 feedback mechanism has been well established in other cells, however, no evidence of the existence of this pathway in lymphocytes has been reported before. As mentioned earlier, we do not have access to T cells lacking IRS2 so we cannot fully confirm the role of this protein in the feedback mechanism. We also tried using S6K specific inhibitors to test the involvement of this down-stream effector of mTORC1 in the regulation of IRS2. However, the effects of these inhibitors on S6K activity were inconclusive.

Interestingly, the studies examining the effects of mTOR deletion in $CD4^+$ T cells[352] also observed increased Thr308 phosphorylation of PKB upon mTOR deletion indicating that the mTOR-PI3K feedback mechanism is also relevant for CD4 T cell biology.

We also demonstrated that mTORC1 signalling is required to sustain PTEN expression in CTL. The regulation of PTEN by mTORC1 in mouse embryonic fibroblasts has been demonstrated before[370], however, the authors of the study suggest a role of the transcription factor HIF1α in the transcriptional regulation of PTEN by mTORC1. We could not see a regulation of PTEN transcript level in our rapamycin treated CTL

(Figure 7.6) or CTL deficient in HIF1 transcriptional activity, indicating that mTORC1 controls PTEN levels by non-transcriptional mechanisms. On the other hand, PTEN deficient CTL treated with either rapamycin or KU-0063794 were still able to hyperphosphorylate PKB Thr308 indicating that PTEN is not crucial for the mTORC1 mediated control of PIP$_3$ levels.

The effects on ERK signalling caused by chronic mTORC1 inhibition are also noteworthy. As mentioned before, we have no exact mechanism for this regulation and studies in other systems were also not able to fully understand the connection between the two signalling pathways, even though the involvement of IRS1/2 has been suggested[371,363]. ERK plays an important role in the activation of T cells and is activated down-stream of the T cell receptor[372] or by IL-2 signalling[373]. Despite its role as a positive regulator of T cell activation, elevated levels of ERK signalling represent an early event during activation-induced cell death[374] and inhibition of this signalling pathway is observed in many malignant lymphocytes[375]. Thus the elevated ERK signalling upon chronic mTORC1 inhibition might be another facet of the immunosuppressive effects of rapamycin, similar to the elevated PIP$_3$ levels mentioned earlier.

Lastly, the effects of mTORC1 inhibition on the expression of both PTEN and IRS2 are examples of how just using our transcriptomic data would not have been sufficient to detect this regulation. Both proteins appear to be regulated by non-transcriptional mechanisms which could not be addressed by the micro array analysis but required methods which detect protein level directly like the quantitative mass spectrometry based approaches utilised in the previous chapters.

8. Concluding remarks and outlook

The title of this thesis is "The Role of the Mammalian Target of Rapamycin (mTOR) in Cytotoxic T Lymphocytes". What is its role? Using high resolution quantitative mass spectrometry and micro array analysis we have shown that mTOR is an important regulator of CTL transcription and translation controlling the expression of several hundred genes in CTL. Importantly, inhibition of mTORC1 does not just lead to a general down regulation of gene expression in CTL but it rather reprograms gene expression CTL and thus up- and down-regulates equal numbers of proteins in CTL. It particularly regulates the expression of metabolic regulators, effector molecules, adhesion molecules and adaptor molecules.

CTL have been described as "The Foot Soldiers of the Immune System"[372] so the role of mTOR is to supply the logistics (by regulating the metabolism), weaponry (control of effector molecules) and facilitate the mobilisation of the troops (control of CTL trafficking). We now know how mTOR facilitates some of these effects, e.g. the control of metabolic pathways and some effector molecules by controlling Hif1α expression[85]. However, we still do not know how mTOR signalling controls the expression of other important effector molecules like IFN-γ and preliminary experiments in the lab have shown a complex regulation of these molecules.

We also showed that the traditional linear PI3K-PKB-mTOR pathway postulated for other cell models does not apply to CTL. On the contrary, the inhibition of mTORC1 led to a dramatic increase in PIP_3 levels and changed the way how CTL activate PKB.

We have also mapped the abundance and isoform specificity for more than 6700 protein in CTL. These data constitute a valuable resource which will aid the future research in the lab. One such example might be the role of Glut1 and Glut3 in CTL. Whereas recent papers have emphasized the importance of Glut1 for T cell differentiation and

function[376], not much research has been dedicated to explore the role of Glut3 which is expressed at equal levels in CTL and thus might play an equally important role in CTL. As it is becoming easier and cheaper to perform high resolution quantitative mass spectrometry on all kinds of tissue, hopes are high that the systematic mapping of tissue specific proteomes might change the research in a similar way as the wide-spread availability of the genomes of humans and other species did. The first studies drafting maps of the human proteome have been published recently[266,267], collating the proteomic data for dozens of human tissue samples, including several haematopoietic cells. A comparable project mapping transcript levels for different kind of immune cells already exists in the form of the Immunological Genome Project. Expanding this initiative by mapping the specific proteomes of immune cells would be an equally invaluable resource and would help the immunological community tremendously.

References

1.Schatz, D. G. & Ji, Y. Recombination centres and the orchestration of V(D)J recombination. *Nature reviews. Immunology* **11,** 251-63 (2011).

2.Palmer, E. & Naeher, D. Affinity threshold for thymic selection through a T-cell receptor-co-receptor zipper. *Nature reviews. Immunology* **9,** 207-13 (2009).

3.Wang, H. *et al.* ZAP-70: an essential kinase in T-cell signaling. *Cold Spring Harbor perspectives in biology* **2,** a002279 (2010).

4.Iwashima, M., Irving, B. A., van Oers, N. S., Chan, A. C. & Weiss, A. Sequential interactions of the TCR with two distinct cytoplasmic tyrosine kinases. *Science (New York, N.Y.)* **263,** 1136-9 (1994).

5.Samelson, L. E., Davidson, W. F., 3rd, H. C. M. & Klausner, R. D. Abnormal tyrosine phosphorylation on T-cell receptor in lymphoproliferative disorders. *Nature* **324,** 674-6 (1986).

6.Straus, D. B. & Weiss, A. Genetic evidence for the involvement of the lck tyrosine kinase in signal transduction through the T cell antigen receptor. *Cell* **70,** 585-93 (1992).

7.van Oers, N. S., Killeen, N. & Weiss, A. Lck regulates the tyrosine phosphorylation of the T cell receptor subunits and ZAP-70 in murine thymocytes. *The Journal of experimental medicine* **183,** 1053-62 (1996).

8.Xu, C. *et al.* Regulation of T cell receptor activation by dynamic membrane binding of the CD3epsilon cytoplasmic tyrosine-based motif. *Cell* **135,** 702-13 (2008).

9.Fernandes, R. A. *et al.* What controls T cell receptor phosphorylation? *Cell* **142,** 668-9 (2010).

10.Chow, L. M., Fournel, M., Davidson, D. & Veillette, A. Negative regulation of T-cell receptor signalling by tyrosine protein kinase p50csk. *Nature* **365,** 156-60 (1993).

11.McNeill, L. *et al.* The differential regulation of Lck kinase phosphorylation sites by CD45 is critical for T cell receptor signaling responses. *Immunity* **27,** 425-37 (2007).

12.Veillette, A., Rhee, I., Souza, C. M. & Davidson, D. PEST family phosphatases in immunity, autoimmunity, and autoinflammatory disorders. *Immunological reviews* **228,** 312-24 (2009).

13.Chan, A. C., Irving, B. A., Fraser, J. D. & Weiss, A. The zeta chain is associated with a tyrosine kinase and upon T-cell antigen receptor stimulation associates with ZAP-70, a 70-kDa tyrosine phosphoprotein. *Proceedings of the National Academy of Sciences of the United States of America* **88,** 9166-70 (1991).

14.Chan, A. C., Iwashima, M., Turck, C. W. & Weiss, A. ZAP-70: a 70 kd protein-tyrosine kinase that associates with the TCR zeta chain. *Cell* **71,** 649-62 (1992).

15.Wange, R. L., Malek, S. N., Desiderio, S. & Samelson, L. E. Tandem SH2 domains of ZAP-70 bind to T cell antigen receptor zeta and CD3 epsilon from activated Jurkat T cells. *The Journal of biological chemistry* **268,** 19797-801 (1993).

16.Chan, A. C. *et al.* Activation of ZAP-70 kinase activity by phosphorylation of tyrosine 493 is required for lymphocyte antigen receptor function. *The EMBO journal* **14,** 2499-508 (1995).

17.Paz, P. E. *et al.* Mapping the Zap-70 phosphorylation sites on LAT (linker for activation of T cells) required for recruitment and activation of signalling proteins in T cells. *The Biochemical journal* **356,** 461-71 (2001).

18.Zhang, W. *et al.* Association of Grb2, Gads, and phospholipase C-gamma 1 with phosphorylated LAT tyrosine residues. Effect of LAT tyrosine mutations on T cell angigen receptor-mediated signaling. *The Journal of biological chemistry* **275,** 23355-61 (2000).

19.Liu, S. K., Fang, N., Koretzky, G. A. & McGlade, C. J. The hematopoietic-specific adaptor protein gads functions in T-cell signaling via interactions with the SLP-76 and LAT adaptors. *Current biology : CB* **9,** 67-75 (1999).

20.Gilliland, L. K. *et al.* Lymphocyte lineage-restricted tyrosine-phosphorylated proteins that bind PLC gamma 1 SH2 domains. *The Journal of biological chemistry* **267,** 13610-6 (1992).

21.Joseph, R. E., Min, L., Xu, R., Musselman, E. D. & Andreotti, A. H. A remote substrate docking mechanism for the tec family tyrosine kinases. *Biochemistry* **46,** 5595-603 (2007).

22.Bogin, Y., Ainey, C., Beach, D. & Yablonski, D. SLP-76 mediates and maintains activation of the Tec family kinase ITK via the T cell antigen receptor-induced association between SLP-76 and ITK. *Proceedings of the National Academy of Sciences of the United States of America* **104,** 6638-43 (2007).

23.Gonen, R., Beach, D., Ainey, C. & Yablonski, D. T cell receptor-induced activation of phospholipase C-gamma1 depends on a sequence-independent function of the P-I region of SLP-76. *The Journal of biological chemistry* **280,** 8364-70 (2005).

24.Carpenter, G. & Ji, Q. S. Phospholipase C-gamma as a signal-transducing element. *Experimental cell research* **253,** 15-24 (1999).

25.Streb, H., Irvine, R. F., Berridge, M. J. & Schulz, I. Release of Ca2+ from a nonmitochondrial intracellular store in pancreatic acinar cells by inositol-1,4,5-trisphosphate. *Nature* **306,** 67-9 (1983).

26.Barr, V. A., Bernot, K. M., Shaffer, M. H., Burkhardt, J. K. & Samelson, L. E. Formation of STIM and Orai complexes: puncta and distal caps. *Immunological reviews* **231,** 148-59 (2009).

27.Clapham, D. E. Calcium signaling. *Cell* **131,** 1047-58 (2007).

28.Hogan, P. G., Chen, L., Nardone, J. & Rao, A. Transcriptional regulation by calcium, calcineurin, and NFAT. *Genes & development* **17,** 2205-32 (2003).

29.Calne, R. Y. *et al.* Cyclosporin A in patients receiving renal allografts from cadaver donors. *Lancet* **2,** 1323-7 (1978).

30.Tamás, P. *et al.* Regulation of the energy sensor AMP-activated protein kinase by antigen receptor and Ca2+ in T lymphocytes. *The Journal of experimental medicine* **203,** 1665-70 (2006).

31.Hardie, D. G., Ross, F. A. & Hawley, S. A. AMPK: a nutrient and energy sensor that maintains energy homeostasis. *Nature reviews. Molecular cell biology* **13,** 251-62 (2012).

32.Matthews, S. A. & Cantrell, D. A. New insights into the regulation and function of serine/threonine kinases in T lymphocytes. *Immunological reviews* **228,** 241-52 (2009).

33.Jun, J. E., Rubio, I. & Roose, J. P. Regulation of ras exchange factors and cellular localization of ras activation by lipid messengers in T cells. *Frontiers in immunology* **4,** 239 (2013).

34.Monks, C. R., Kupfer, H., Tamir, I., Barlow, A. & Kupfer, A. Selective modulation of protein kinase C-theta during T-cell activation. *Nature* **385,** 83-6 (1997).

35.Dustin, M. L. & Depoil, D. New insights into the T cell synapse from single molecule techniques. *Nature reviews. Immunology* **11,** 672-84 (2011).

36.Quann, E. J., Merino, E., Furuta, T. & Huse, M. Localized diacylglycerol drives the polarization of the microtubule-organizing center in T cells. *Nature Immunology* **10,** 627-35 (2009).

37.Rosse, C. *et al.* PKC and the control of localized signal dynamics. *Nature reviews. Molecular cell biology* **11,** 103-12 (2010).

38.Ma, J. S. Y., Haydar, T. F. & Radoja, S. Protein kinase C delta localizes to secretory lysosomes in CD8+ CTL and directly mediates TCR signals leading to granule

exocytosis-mediated cytotoxicity. *Journal of immunology (Baltimore, Md. : 1950)* **181,** 4716-22 (2008).

39.Matsumoto, R. *et al.* Phosphorylation of CARMA1 plays a critical role in T Cell receptor-mediated NF-kappaB activation. *Immunity* **23,** 575-85 (2005).

40.Letschka, T. *et al.* PKC-theta selectively controls the adhesion-stimulating molecule Rap1. *Blood* **112,** 4617-27 (2008).

41.Fagerholm, S., Morrice, N., Gahmberg, C. G. & Cohen, P. Phosphorylation of the cytoplasmic domain of the integrin CD18 chain by protein kinase C isoforms in leukocytes. *The Journal of biological chemistry* **277,** 1728-38 (2002).

42.Matthews, S. A., Rozengurt, E. & Cantrell, D. Protein kinase D. A selective target for antigen receptors and a downstream target for protein kinase C in lymphocytes. *The Journal of experimental medicine* **191,** 2075-82 (2000).

43.Rozengurt, E. Protein kinase D signaling: multiple biological functions in health and disease. *Physiology (Bethesda, Md.)* **26,** 23-33 (2011).

44.Spitaler, M., Emslie, E., Wood, C. D. & Cantrell, D. Diacylglycerol and protein kinase D localization during T lymphocyte activation. *Immunity* **24,** 535-46 (2006).

45.Matthews, S. A. *et al.* Unique functions for protein kinase D1 and protein kinase D2 in mammalian cells. *The Biochemical journal* **432,** 153-63 (2010).

46.Navarro, M., Goebel, J., Feijoo-Carnero, C., Morrice, N. & Cantrell, D. Phosphoproteomic analysis reveals an intrinsic pathway for the regulation of histone deacetylase 7 that controls the function of cytotoxic T lymphocytes. *Nature Immunology* **12,** 352-61 (2011).

47.Simon, M. A., Bowtell, D. D., Dodson, G. S., Laverty, T. R. & Rubin, G. M. Ras1 and a putative guanine nucleotide exchange factor perform crucial steps in signaling by the sevenless protein tyrosine kinase. *Cell* **67,** 701-16 (1991).

48.Moodie, S. A., Willumsen, B. M., Weber, M. J. & Wolfman, A. Complexes of Ras.GTP with Raf-1 and mitogen-activated protein kinase kinase. *Science (New York, N.Y.)* **260,** 1658-61 (1993).

49.Genot, E. & Cantrell, D. A. Ras regulation and function in lymphocytes. *Current opinion in immunology* **12,** 289-94 (2000).

50.Harriague, J. & Bismuth, G. Imaging antigen-induced PI3K activation in T cells. *Nature Immunology* **3,** 1090-6 (2002).

51.Huppa, J. B., Gleimer, M., Sumen, C. & Davis, M. M. Continuous T cell receptor signaling required for synapse maintenance and full effector potential. *Nature Immunology* **4,** 749-55 (2003).

52.Garçon, F. *et al.* CD28 provides T-cell costimulation and enhances PI3K activity at the immune synapse independently of its capacity to interact with the p85/p110 heterodimer. *Blood* **111,** 1464-71 (2008).

53.Costello, P. S., Gallagher, M. & Cantrell, D. A. Sustained and dynamic inositol lipid metabolism inside and outside the immunological synapse. *Nature Immunology* **3,** 1082-9 (2002).

54.Vanhaesebroeck, B. *et al.* P110delta, a novel phosphoinositide 3-kinase in leukocytes. *Proceedings of the National Academy of Sciences of the United States of America* **94,** 4330-5 (1997).

55.Fukazawa, T. *et al.* T cell activation-dependent association between the p85 subunit of the phosphatidylinositol 3-kinase and Grb2/phospholipase C-gamma 1-binding phosphotyrosyl protein pp36/38. *The Journal of biological chemistry* **270,** 20177-82 (1995).

56.Shim, E. K. *et al.* Association of the Src homology 2 domain-containing leukocyte phosphoprotein of 76 kD (SLP-76) with the p85 subunit of phosphoinositide 3-kinase. *FEBS letters* **575,** 35-40 (2004).

57. Rodriguez-Viciana, P. *et al.* Phosphatidylinositol-3-OH kinase as a direct target of Ras. *Nature* **370,** 527-32 (1994).

58. Wabnitz, G. H., Nebl, G., Klemke, M., Schröder, A. J. & Samstag, Y. Phosphatidylinositol 3-kinase functions as a Ras effector in the signaling cascade that regulates dephosphorylation of the actin-remodeling protein cofilin after costimulation of untransformed human T lymphocytes. *Journal of immunology (Baltimore, Md. : 1950)* **176,** 1668-74 (2006).

59. Castellino, F. & Germain, R. N. Cooperation between CD4+ and CD8+ T cells: when, where, and how. *Annual review of immunology* **24,** 519-40 (2006).

60. Mosmann, T. R., Cherwinski, H., Bond, M. W., Giedlin, M. A. & Coffman, R. L. Two types of murine helper T cell clone. I. Definition according to profiles of lymphokine activities and secreted proteins. *Journal of immunology (Baltimore, Md. : 1950)* **136,** 2348-57 (1986).

61. Wan, Y. Y. Multi-tasking of helper T cells. *Immunology* **130,** 166-71 (2010).

62. Harrington, L. E. *et al.* Interleukin 17-producing CD4+ effector T cells develop via a lineage distinct from the T helper type 1 and 2 lineages. *Nature Immunology* **6,** 1123-32 (2005).

63. Stockinger, B., Veldhoen, M. & Martin, B. Th17 T cells: linking innate and adaptive immunity. *Seminars in immunology* **19,** 353-61 (2007).

64. Hirota, K., Ahlfors, H., Duarte, J. H. & Stockinger, B. Regulation and function of innate and adaptive interleukin-17-producing cells. *EMBO reports* **13,** 113-20 (2012).

65. Saraiva, M. & O'Garra, A. The regulation of IL-10 production by immune cells. *Nature reviews. Immunology* **10,** 170-81 (2010).

66. Hirota, K. *et al.* Fate mapping of IL-17-producing T cells in inflammatory responses. *Nature Immunology* **12,** 255-63 (2011).

67. Vahedi, G. *et al.* Helper T-cell identity and evolution of differential transcriptomes and epigenomes. *Immunological reviews* **252,** 24-40 (2013).

68. Sakaguchi, S., Yamaguchi, T., Nomura, T. & Ono, M. Regulatory T cells and immune tolerance. *Cell* **133,** 775-87 (2008).

69. Brunkow, M. E. *et al.* Disruption of a new forkhead/winged-helix protein, scurfin, results in the fatal lymphoproliferative disorder of the scurfy mouse. *Nature genetics* **27,** 68-73 (2001).

70. Hori, S., Nomura, T. & Sakaguchi, S. Control of regulatory T cell development by the transcription factor Foxp3. *Science (New York, N.Y.)* **299,** 1057-61 (2003).

71. Fontenot, J. D. *et al.* Regulatory T cell lineage specification by the forkhead transcription factor foxp3. *Immunity* **22,** 329-41 (2005).

72. Bennett, C. L. *et al.* The immune dysregulation, polyendocrinopathy, enteropathy, X-linked syndrome (IPEX) is caused by mutations of FOXP3. *Nature genetics* **27,** 20-1 (2001).

73. Pandiyan, P., Zheng, L., Ishihara, S., Reed, J. & Lenardo, M. J. CD4+CD25+Foxp3+ regulatory T cells induce cytokine deprivation-mediated apoptosis of effector CD4+ T cells. *Nature Immunology* **8,** 1353-62 (2007).

74. Read, S., Malmström, V. & Powrie, F. Cytotoxic T lymphocyte-associated antigen 4 plays an essential role in the function of CD25(+)CD4(+) regulatory cells that control intestinal inflammation. *The Journal of experimental medicine* **192,** 295-302 (2000).

75. Shevach, E. M., McHugh, R. S., Piccirillo, C. A. & Thornton, A. M. Control of T-cell activation by CD4+ CD25+ suppressor T cells. *Immunological reviews* **182,** 58-67 (2001).

76. Boehmer, von, H. Mechanisms of suppression by suppressor T cells. *Nature Immunology* **6,** 338-44 (2005).

77. Michalek, R. D. & Rathmell, J. C. The metabolic life and times of a T-cell. *Immunological reviews* **236,** 190-202 (2010).

78.Badovinac, V. P., Haring, J. S. & Harty, J. T. Initial T cell receptor transgenic cell precursor frequency dictates critical aspects of the CD8(+) T cell response to infection. *Immunity* **26,** 827-41 (2007).

79.van Stipdonk, M. J. B. *et al.* Dynamic programming of CD8+ T lymphocyte responses. *Nature Immunology* **4,** 361-365 (2003).

80.Yoon, H., Kim, T. S. & Braciale, T. J. The cell cycle time of CD8+ T cells responding in vivo is controlled by the type of antigenic stimulus. *PloS one* **5,** e15423 (2010).

81.vander Heiden, M. G., Cantley, L. C. & Thompson, C. B. Understanding the Warburg effect: the metabolic requirements of cell proliferation. *Science (New York, N.Y.)* **324,** 1029-33 (2009).

82.WARBURG, O. On the origin of cancer cells. *Science (New York, N.Y.)* **123,** 309-14 (1956).

83.Wang, R. *et al.* The Transcription Factor Myc Controls Metabolic Reprogramming upon T Lymphocyte Activation. *Immunity* **35,** 871-882 (2011).

84.Marko, A. J., Miller, R. A., Kelman, A. & Frauwirth, K. A. Induction of glucose metabolism in stimulated T lymphocytes is regulated by mitogen-activated protein kinase signaling. *PloS one* **5,** e15425 (2010).

85.Finlay, D. K. *et al.* PDK1 regulation of mTOR and hypoxia-inducible factor 1 integrate metabolism and migration of CD8+ T cells. *The Journal of experimental medicine* **209,** 2441-53 (2012).

86.Macintyre, A. N. *et al.* Protein kinase B controls transcriptional programs that direct cytotoxic T cell fate but is dispensable for T cell metabolism. *Immunity* **34,** 224-36 (2011).

87.McMichael, A. J., Gotch, F. M., Noble, G. R. & Beare, P. A. Cytotoxic T-cell immunity to influenza. *The New England journal of medicine* **309,** 13-7 (1983).

88.Harty, J. T., Tvinnereim, A. R. & White, D. W. CD8+ T cell effector mechanisms in resistance to infection. *Annual review of immunology* **18,** 275-308 (2000).

89.Lee, S., Dunmire, S. & McSorley, S. J. MHC class-I-restricted CD8 T cells play a protective role during primary Salmonella infection. *Immunology letters* **148,** 138-43 (2012).

90.White, D. W., Wilson, R. L. & Harty, J. T. CD8+ T cells in intracellular bacterial infections of mice. *Research in immunology* **147,** 519-24 (1996).

91.Monks, C. R., Freiberg, B. A., Kupfer, H., Sciaky, N. & Kupfer, A. Three-dimensional segregation of supramolecular activation clusters in T cells. *Nature* **395,** 82-6 (1998).

92.Cemerski, S. *et al.* The balance between T cell receptor signaling and degradation at the center of the immunological synapse is determined by antigen quality. *Immunity* **29,** 414-22 (2008).

93.Dustin, M. L., Chakraborty, A. K. & Shaw, A. S. Understanding the structure and function of the immunological synapse. *Cold Spring Harbor perspectives in biology* **2,** a002311 (2010).

94.Kuhné, M. R. *et al.* Linker for activation of T cells, zeta-associated protein-70, and Src homology 2 domain-containing leukocyte protein-76 are required for TCR-induced microtubule-organizing center polarization. *Journal of immunology (Baltimore, Md. : 1950)* **171,** 860-6 (2003).

95.Tschopp, J., Masson, D. & Stanley, K. K. Structural/functional similarity between proteins involved in complement- and cytotoxic T-lymphocyte-mediated cytolysis. *Nature* **322,** 831-4 (1986).

96.Thiery, J. *et al.* Perforin pores in the endosomal membrane trigger the release of endocytosed granzyme B into the cytosol of target cells. *Nature Immunology* **12,** 770-7 (2011).

97.Odake, S. *et al.* Human and murine cytotoxic T lymphocyte serine proteases: subsite mapping with peptide thioester substrates and inhibition of enzyme activity and cytolysis by isocoumarins. *Biochemistry* **30,** 2217-27 (1991).

98.Atkinson, E. A. *et al.* Cytotoxic T lymphocyte-assisted suicide. Caspase 3 activation is primarily the result of the direct action of granzyme B. *The Journal of biological chemistry* **273,** 21261-6 (1998).

99.Heibein, J. A., Barry, M., Motyka, B. & Bleackley, R. C. Granzyme B-induced loss of mitochondrial inner membrane potential (Delta Psi m) and cytochrome c release are caspase independent. *Journal of immunology (Baltimore, Md. : 1950)* **163,** 4683-93 (1999).

100.Balaji, K. N., Schaschke, N., Machleidt, W., Catalfamo, M. & Henkart, P. A. Surface cathepsin B protects cytotoxic lymphocytes from self-destruction after degranulation. *The Journal of experimental medicine* **196,** 493-503 (2002).

101.Baran, K. *et al.* Cytotoxic T lymphocytes from cathepsin B-deficient mice survive normally in vitro and in vivo after encountering and killing target cells. *The Journal of biological chemistry* **281,** 30485-91 (2006).

102.Bossi, G. & Griffiths, G. M. Degranulation plays an essential part in regulating cell surface expression of Fas ligand in T cells and natural killer cells. *Nature medicine* **5,** 90-6 (1999).

103.Algeciras-Schimnich, A. *et al.* Molecular ordering of the initial signaling events of CD95. *Molecular and Cellular Biology* **22,** 207-20 (2002).

104.Tanaka, M., Itai, T., Adachi, M. & Nagata, S. Downregulation of Fas ligand by shedding. *Nature medicine* **4,** 31-6 (1998).

105.Suda, T., Hashimoto, H., Tanaka, M., Ochi, T. & Nagata, S. Membrane Fas ligand kills human peripheral blood T lymphocytes, and soluble Fas ligand blocks the killing. *The Journal of experimental medicine* **186,** 2045-50 (1997).

106.Kriegler, M., Perez, C., DeFay, K., Albert, I. & Lu, S. D. A novel form of TNF/cachectin is a cell surface cytotoxic transmembrane protein: ramifications for the complex physiology of TNF. *Cell* **53,** 45-53 (1988).

107.Black, R. A. *et al.* A metalloproteinase disintegrin that releases tumour-necrosis factor-alpha from cells. *Nature* **385,** 729-33 (1997).

108.Palladino, M. A., Bahjat, F. R., Theodorakis, E. A. & Moldawer, L. L. Anti-TNF-alpha therapies: the next generation. *Nature reviews. Drug discovery* **2,** 736-46 (2003).

109.Kägi, D. *et al.* Fas and perforin pathways as major mechanisms of T cell-mediated cytotoxicity. *Science (New York, N.Y.)* **265,** 528-30 (1994).

110.Lowin, B., Hahne, M., Mattmann, C. & Tschopp, J. Cytolytic T-cell cytotoxicity is mediated through perforin and Fas lytic pathways. *Nature* **370,** 650-2 (1994).

111.Ratner, A. & Clark, W. R. Role of TNF-alpha in CD8+ cytotoxic T lymphocyte-mediated lysis. *Journal of immunology (Baltimore, Md. : 1950)* **150,** 4303-14 (1993).

112.Wohlleber, D. *et al.* TNF-induced target cell killing by CTL activated through cross-presentation. *Cell reports* **2,** 478-87 (2012).

113.Lukacs, N. W., Strieter, R. M., Chensue, S. W., Widmer, M. & Kunkel, S. L. TNF-alpha mediates recruitment of neutrophils and eosinophils during airway inflammation. *Journal of immunology (Baltimore, Md. : 1950)* **154,** 5411-7 (1995).

114.Osborn, L. *et al.* Direct expression cloning of vascular cell adhesion molecule 1, a cytokine-induced endothelial protein that binds to lymphocytes. *Cell* **59,** 1203-11 (1989).

115.Cemerski, S. & Shaw, A. Immune synapses in T-cell activation. *Current opinion in immunology* **18,** 298-304 (2006).

116.Schroder, K., Hertzog, P. J., Ravasi, T. & Hume, D. A. Interferon-gamma: an overview of signals, mechanisms and functions. *Journal of leukocyte biology* **75,** 163-89 (2004).

117.Müllbacher, A. *et al.* Antigen-dependent release of IFN-gamma by cytotoxic T cells up-regulates Fas on target cells and facilitates exocytosis-independent specific target cell lysis. *Journal of immunology (Baltimore, Md. : 1950)* **169,** 145-50 (2002).

118.Kaech, S. M. & Cui, W. Transcriptional control of effector and memory CD8+ T cell differentiation. *Nature reviews. Immunology* **12,** 749-61 (2012).

119.Ahmed, R. & Gray, D. Immunological memory and protective immunity: understanding their relation. *Science (New York, N.Y.)* **272,** 54-60 (1996).

120.Kaech, S. M. & Wherry, E. J. Heterogeneity and cell-fate decisions in effector and memory CD8+ T cell differentiation during viral infection. *Immunity* **27,** 393-405 (2007).

121.Cui, W. & Kaech, S. M. Generation of effector CD8+ T cells and their conversion to memory T cells. *Immunological reviews* **236,** 151-66 (2010).

122.Morgan, D. A., Ruscetti, F. W. & Gallo, R. Selective in vitro growth of T lymphocytes from normal human bone marrows. *Science (New York, N.Y.)* **193,** 1007-8 (1976).

123.Gillis, S. & Smith, K. A. Long term culture of tumour-specific cytotoxic T cells. *Nature* **268,** 154-6 (1977).

124.Bazan, J. F. Structural design and molecular evolution of a cytokine receptor superfamily. *Proceedings of the National Academy of Sciences of the United States of America* **87,** 6934-8 (1990).

125.Taniguchi, T. *et al.* Structure and expression of a cloned cDNA for human interleukin-2. *Nature* **302,** 305-10 (1983).

126.Leonard, W. J. *et al.* Molecular cloning and expression of cDNAs for the human interleukin-2 receptor. *Nature* **311,** 626-31 (1984).

127.Nikaido, T. *et al.* Molecular cloning of cDNA encoding human interleukin-2 receptor. *Nature* **311,** 631-5 (1984).

128.Wang, H. M. & Smith, K. A. The interleukin 2 receptor. Functional consequences of its bimolecular structure. *The Journal of experimental medicine* **166,** 1055-69 (1987).

129.Johnson, K. *et al.* Soluble IL-2 receptor beta and gamma subunits: ligand binding and cooperativity. *European cytokine network* **5,** 23-34 (1994).

130.Noguchi, M. *et al.* Interleukin-2 receptor gamma chain mutation results in X-linked severe combined immunodeficiency in humans. *Cell* **73,** 147-57 (1993).

131.Cornish, G., Sinclair, L. & Cantrell, D. Differential regulation of T-cell growth by IL-2 and IL-15. *Blood* **108,** 600-8 (2006).

132.Boussiotis, V. A. *et al.* Prevention of T cell anergy by signaling through the gamma c chain of the IL-2 receptor. *Science (New York, N.Y.)* **266,** 1039-42 (1994).

133.Miyazaki, T. *et al.* Functional activation of Jak1 and Jak3 by selective association with IL-2 receptor subunits. *Science (New York, N.Y.)* **266,** 1045-7 (1994).

134.Friedmann, M. C., Migone, T. S., Russell, S. M. & Leonard, W. J. Different interleukin 2 receptor beta-chain tyrosines couple to at least two signaling pathways and synergistically mediate interleukin 2-induced proliferation. *Proceedings of the National Academy of Sciences of the United States of America* **93,** 2077-82 (1996).

135.Liao, W. *et al.* Priming for T helper type 2 differentiation by interleukin 2-mediated induction of interleukin 4 receptor alpha-chain expression. *Nature Immunology* **9,** 1288-96 (2008).

136.Liao, W., Lin, J., Wang, L., Li, P. & Leonard, W. J. Modulation of cytokine receptors by IL-2 broadly regulates differentiation into helper T cell lineages. *Nature Immunology* **12,** 551-9 (2011).

137.Lin, J. *et al.* Critical Role of STAT5 transcription factor tetramerization for cytokine responses and normal immune function. *Immunity* **36,** 586-99 (2012).

138.Yao, Z. *et al.* Stat5a/b are essential for normal lymphoid development and differentiation. *Proceedings of the National Academy of Sciences of the United States of America* **103,** 1000-5 (2006).

139.Nakajima, H. *et al.* An indirect effect of Stat5a in IL-2-induced proliferation: a critical role for Stat5a in IL-2-mediated IL-2 receptor alpha chain induction. *Immunity* **7,** 691-701 (1997).

140.Imada, K. *et al.* Stat5b is essential for natural killer cell-mediated proliferation and cytolytic activity. *The Journal of experimental medicine* **188,** 2067-74 (1998).

141.Remillard, B. *et al.* Interleukin-2 receptor regulates activation of phosphatidylinositol 3-kinase. *The Journal of biological chemistry* **266,** 14167-70 (1991).

142.Okkenhaug, K. Signaling by the phosphoinositide 3-kinase family in immune cells. *Annual review of immunology* **31,** 675-704 (2013).

143.Ravichandran, K. S., Igras, V., Shoelson, S. E., Fesik, S. W. & Burakoff, S. J. Evidence for a role for the phosphotyrosine-binding domain of Shc in interleukin 2 signaling. *Proceedings of the National Academy of Sciences of the United States of America* **93,** 5275-80 (1996).

144.Gu, H. *et al.* New role for Shc in activation of the phosphatidylinositol 3-kinase/Akt pathway. *Molecular and Cellular Biology* **20,** 7109-20 (2000).

145.Ciprés, A., Gala, S., Martinez-A, C., Mérida, I. & Williamson, P. An IL-2 receptor beta subdomain that controls Bcl-X(L) expression and cell survival. *European Journal of Immunology* **29,** 1158-67 (1999).

146.Pearce, L., Komander, D. & Alessi, D. The nuts and bolts of AGC protein kinases. *Nature reviews. Molecular cell biology* **11,** 9-22 (2010).

147.Calleja, V. *et al.* Intramolecular and intermolecular interactions of protein kinase B define its activation in vivo. *PLoS biology* **5,** e95 (2007).

148.Mora, A., Komander, D., van Aalten, D. M. F. & Alessi, D. R. PDK1, the master regulator of AGC kinase signal transduction. *Seminars in cell & developmental biology* **15,** 161-70 (2004).

149.Sarbassov, D. D., Guertin, D. A., Ali, S. M. & Sabatini, D. M. Phosphorylation and regulation of Akt/PKB by the rictor-mTOR complex. *Science (New York, N.Y.)* **307,** 1098-101 (2005).

150.Waugh, C., Sinclair, L., Finlay, D., Bayascas, J. & Cantrell, D. Phosphoinositide (3,4,5)-triphosphate binding to phosphoinositide-dependent kinase 1 regulates a protein kinase B/Akt signaling threshold that dictates T-cell migration, not proliferation. *Molecular and Cellular Biology* **29,** 5952-62 (2009).

151.3rd, W. H. B., Meisenhelder, J., Hunter, T., Cavenee, W. K. & Arden, K. C. Protein kinase B/Akt-mediated phosphorylation promotes nuclear exclusion of the winged helix transcription factor FKHR1. *Proceedings of the National Academy of Sciences of the United States of America* **96,** 7421-6 (1999).

152.Calnan, D. R. & Brunet, A. The FoxO code. *Oncogene* **27,** 2276-88 (2008).

153.Kerdiles, Y. M. *et al.* Foxo1 links homing and survival of naive T cells by regulating L-selectin, CCR7 and interleukin 7 receptor. *Nature Immunology* **10,** 176-84 (2009).

154.Cyster, J. G. & Schwab, S. R. Sphingosine-1-phosphate and lymphocyte egress from lymphoid organs. *Annual review of immunology* **30,** 69-94 (2012).

155.Sinclair, L. V. *et al.* Phosphatidylinositol-3-OH kinase and nutrient-sensing mTOR pathways control T lymphocyte trafficking. *Nature Immunology* **9,** 513-521 (2008).

156.Hand, T. W. *et al.* Differential effects of STAT5 and PI3K/AKT signaling on effector and memory CD8 T-cell survival. *Proceedings of the National Academy of Sciences of the United States of America* **107,** 16601-6 (2010).

157. Barata, J. T. *et al.* Activation of PI3K is indispensable for interleukin 7-mediated viability, proliferation, glucose use, and growth of T cell acute lymphoblastic leukemia cells. *The Journal of experimental medicine* **200,** 659-69 (2004).

158. Manjunath, N. *et al.* Effector differentiation is not prerequisite for generation of memory cytotoxic T lymphocytes. *The Journal of clinical investigation* **108,** 871-8 (2001).

159. Weninger, W., Crowley, M. A., Manjunath, N. & Andrian, von, U. H. Migratory properties of naive, effector, and memory CD8(+) T cells. *The Journal of experimental medicine* **194,** 953-66 (2001).

160. Duke, R. C. & Cohen, J. J. IL-2 addiction: withdrawal of growth factor activates a suicide program in dependent T cells. *Lymphokine research* **5,** 289-99 (1986).

161. Collison, L. W. & Vignali, D. A. A. Interleukin-35: odd one out or part of the family? *Immunological reviews* **226,** 248-62 (2008).

162. Jones, L. L. & Vignali, D. A. A. Molecular interactions within the IL-6/IL-12 cytokine/receptor superfamily. *Immunologic research* **51,** 5-14 (2011).

163. Presky, D. H. *et al.* A functional interleukin 12 receptor complex is composed of two beta-type cytokine receptor subunits. *Proceedings of the National Academy of Sciences of the United States of America* **93,** 14002-7 (1996).

164. Oppmann, B. *et al.* Novel p19 protein engages IL-12p40 to form a cytokine, IL-23, with biological activities similar as well as distinct from IL-12. *Immunity* **13,** 715-25 (2000).

165. Pflanz, S. *et al.* WSX-1 and glycoprotein 130 constitute a signal-transducing receptor for IL-27. *Journal of immunology (Baltimore, Md. : 1950)* **172,** 2225-31 (2004).

166. Collison, L. W. *et al.* The composition and signaling of the IL-35 receptor are unconventional. *Nature Immunology* **13,** 290-9 (2012).

167. Delgoffe, G. M., Murray, P. J. & Vignali, D. A. A. Interpreting mixed signals: the cell's cytokine conundrum. *Current opinion in immunology* **23,** 632-8 (2011).

168. Vignali, D. A. A. & Kuchroo, V. K. IL-12 family cytokines: immunological playmakers. *Nature Immunology* **13,** 722-8 (2012).

169. Ma, X. & Trinchieri, G. Regulation of interleukin-12 production in antigen-presenting cells. *Advances in immunology* **79,** 55-92 (2001).

170. van de Vosse, E. *et al.* IL-12Rβ1 deficiency: mutation update and description of the IL12RB1 variation database. *Human mutation* **34,** 1329-39 (2013).

171. Airoldi, I. *et al.* Lack of Il12rb2 signaling predisposes to spontaneous autoimmunity and malignancy. *Blood* **106,** 3846-53 (2005).

172. Cooper, A. M. *et al.* Mice lacking bioactive IL-12 can generate protective, antigen-specific cellular responses to mycobacterial infection only if the IL-12 p40 subunit is present. *Journal of immunology (Baltimore, Md. : 1950)* **168,** 1322-7 (2002).

173. Curtsinger, J. M. *et al.* Inflammatory cytokines provide a third signal for activation of naive CD4+ and CD8+ T cells. *Journal of immunology (Baltimore, Md. : 1950)* **162,** 3256-62 (1999).

174. Keppler, S. J., Theil, K., Vucikuja, S. & Aichele, P. Effector T-cell differentiation during viral and bacterial infections: Role of direct IL-12 signals for cell fate decision of CD8(+) T cells. *European Journal of Immunology* **39,** 1774-83 (2009).

175. Starbeck-Miller, G. R., Xue, H. & Harty, J. T. IL-12 and type I interferon prolong the division of activated CD8 T cells by maintaining high-affinity IL-2 signaling in vivo. *The Journal of experimental medicine* **211,** 105-20 (2014).

176. Wilson, D. C., Matthews, S. & Yap, G. S. IL-12 signaling drives CD8+ T cell IFN-gamma production and differentiation of KLRG1+ effector subpopulations during Toxoplasma gondii Infection. *Journal of immunology (Baltimore, Md. : 1950)* **180,** 5935-45 (2008).

177. Rao, R. R., Li, Q., Odunsi, K. & Shrikant, P. A. The mTOR Kinase Determines Effector versus Memory CD8+ T Cell Fate by Regulating the Expression of Transcription Factors T-bet and Eomesodermin. *Immunity* **32,** 67-78 (2010).

178. Vézina, C., Kudelski, A. & Sehgal, S. N. Rapamycin (AY-22,989), a new antifungal antibiotic. I. Taxonomy of the producing streptomycete and isolation of the active principle. *The Journal of antibiotics* **28,** 721-6 (1975).

179. Martel, R. R., Klicius, J. & Galet, S. Inhibition of the immune response by rapamycin, a new antifungal antibiotic. *Canadian journal of physiology and pharmacology* **55,** 48-51 (1977).

180. Hori, T. *et al.* Establishment of an interleukin 2-dependent human T cell line from a patient with T cell chronic lymphocytic leukemia who is not infected with human T cell leukemia/lymphoma virus. *Blood* **70,** 1069-72 (1987).

181. Bierer, B. E. *et al.* Two distinct signal transmission pathways in T lymphocytes are inhibited by complexes formed between an immunophilin and either FK506 or rapamycin. *Proceedings of the National Academy of Sciences of the United States of America* **87,** 9231-5 (1990).

182. Kuo, C. J. *et al.* Rapamycin selectively inhibits interleukin-2 activation of p70 S6 kinase. *Nature* **358,** 70-3 (1992).

183. Terada, N., Franklin, R. A., Lucas, J. J., Blenis, J. & Gelfand, E. W. Failure of rapamycin to block proliferation once resting cells have entered the cell cycle despite inactivation of p70 S6 kinase. *The Journal of biological chemistry* **268,** 12062-8 (1993).

184. Brennan, P., Babbage, J. W., Thomas, G. & Cantrell, D. p70(s6k) integrates phosphatidylinositol 3-kinase and rapamycin-regulated signals for E2F regulation in T lymphocytes. *Molecular and Cellular Biology* **19,** 4729-38 (1999).

185. Breslin, E. M., White, P. C., Shore, A. M., Clement, M. & Brennan, P. LY294002 and rapamycin co-operate to inhibit T-cell proliferation. *British journal of pharmacology* **144,** 791-800 (2005).

186. Heitman, J., Movva, N. R. & Hall, M. N. Targets for cell cycle arrest by the immunosuppressant rapamycin in yeast. *Science (New York, N.Y.)* **253,** 905-9 (1991).

187. Brown, E. J. *et al.* A mammalian protein targeted by G1-arresting rapamycin-receptor complex. *Nature* **369,** 756-8 (1994).

188. Sabatini, D. M., Erdjument-Bromage, H., Lui, M., Tempst, P. & Snyder, S. H. RAFT1: a mammalian protein that binds to FKBP12 in a rapamycin-dependent fashion and is homologous to yeast TORs. *Cell* **78,** 35-43 (1994).

189. Chiu, M. I., Katz, H. & Berlin, V. RAPT1, a mammalian homolog of yeast Tor, interacts with the FKBP12/rapamycin complex. *Proceedings of the National Academy of Sciences of the United States of America* **91,** 12574-8 (1994).

190. Sabers, C. J. *et al.* Isolation of a protein target of the FKBP12-rapamycin complex in mammalian cells. *The Journal of biological chemistry* **270,** 815-22 (1995).

191. Lempiäinen, H. & Halazonetis, T. D. Emerging common themes in regulation of PIKKs and PI3Ks. *The EMBO journal* **28,** 3067-73 (2009).

192. Loewith, R. *et al.* Two TOR complexes, only one of which is rapamycin sensitive, have distinct roles in cell growth control. *Molecular Cell* **10,** 457-68 (2002).

193. Laplante, M. & Sabatini, D. M. Regulation of mTORC1 and its impact on gene expression at a glance. *Journal of Cell Science* **126,** 1713-9 (2013).

194. Yang, H. *et al.* mTOR kinase structure, mechanism and regulation. *Nature* **497,** 217-23 (2013).

195. Sarbassov, dos, D. D. *et al.* Prolonged Rapamycin Treatment Inhibits mTORC2 Assembly and Akt/PKB. *Molecular Cell* **22,** 159-168 (2006).

196. García‑Martínez, J. *et al.* Ku-0063794 is a specific inhibitor of the mammalian target of rapamycin (mTOR). *Biochemical Journal* **421,** 29-42 (2009).

197.Porta, C., Paglino, C. & Mosca, A. Targeting PI3K/Akt/mTOR Signaling in Cancer. *Frontiers in oncology* **4,** 64 (2014).

198.Campistol, J. M. *et al.* Practical recommendations for the early use of m-TOR inhibitors (sirolimus) in renal transplantation. *Transplant international : official journal of the European Society for Organ Transplantation* **22,** 681-7 (2009).

199.Garg, S., Bourantas, C. & Serruys, P. W. DES the year in review: controversies. *Minerva cardioangiologica* **61,** 99-123 (2013).

200.Araki, K. *et al.* mTOR regulates memory CD8 T-cell differentiation. *Nature* **460,** 108-112 (2009).

201.Li, Q. *et al.* A Central Role for mTOR Kinase in Homeostatic Proliferation Induced CD8+ T Cell Memory and Tumor Immunity. *Immunity* **34,** 541-553 (2011).

202.Battaglia, M., Stabilini, A. & Roncarolo, M. Rapamycin selectively expands CD4+CD25+FoxP3+ regulatory T cells. *Blood* **105,** 4743-8 (2005).

203.Jones, R. G. & Thompson, C. B. Revving the engine: signal transduction fuels T cell activation. *Immunity* **27,** 173-8 (2007).

204.Pearce, E. L. Metabolism in T cell activation and differentiation. *Current opinion in immunology* **22,** 314-20 (2010).

205.Pearce, E. L., Poffenberger, M. C., Chang, C. & Jones, R. G. Fueling Immunity: Insights into Metabolism and Lymphocyte Function. *Science (New York, N.Y.)* **342,** 1242454 (2013).

206.Sancak, Y. *et al.* The Rag GTPases bind raptor and mediate amino acid signaling to mTORC1. *Science (New York, N.Y.)* **320,** 1496-501 (2008).

207.Kim, E., Goraksha-Hicks, P., Li, L., Neufeld, T. P. & Guan, K. Regulation of TORC1 by Rag GTPases in nutrient response. *Nature cell biology* **10,** 935-45 (2008).

208.Tee, A. R. *et al.* Tuberous sclerosis complex-1 and -2 gene products function together to inhibit mammalian target of rapamycin (mTOR)-mediated downstream signaling. *Proceedings of the National Academy of Sciences of the United States of America* **99,** 13571-6 (2002).

209.Dibble, C. C. *et al.* TBC1D7 is a third subunit of the TSC1-TSC2 complex upstream of mTORC1. *Molecular Cell* **47,** 535-46 (2012).

210.Manning, B. D. & Cantley, L. C. Rheb fills a GAP between TSC and TOR. *Trends in biochemical sciences* **28,** 573-6 (2003).

211.Yee, W. M. & Worley, P. F. Rheb interacts with Raf-1 kinase and may function to integrate growth factor- and protein kinase A-dependent signals. *Molecular and Cellular Biology* **17,** 921-33 (1997).

212.Saucedo, L. J. *et al.* Rheb promotes cell growth as a component of the insulin/TOR signalling network. *Nature cell biology* **5,** 566-71 (2003).

213.Betz, C. & Hall, M. N. Where is mTOR and what is it doing there? *The Journal of Cell Biology* **203,** 563-74 (2013).

214.Manning, B. D., Tee, A. R., Logsdon, M. N., Blenis, J. & Cantley, L. C. Identification of the tuberous sclerosis complex-2 tumor suppressor gene product tuberin as a target of the phosphoinositide 3-kinase/akt pathway. *Molecular Cell* **10,** 151-62 (2002).

215.Inoki, K., Li, Y., Zhu, T., Wu, J. & Guan, K. TSC2 is phosphorylated and inhibited by Akt and suppresses mTOR signalling. *Nature cell biology* **4,** 648-57 (2002).

216.Menon, S. *et al.* Spatial control of the TSC complex integrates insulin and nutrient regulation of mTORC1 at the lysosome. *Cell* **156,** 771-85 (2014).

217.Demetriades, C., Doumpas, N. & Teleman, A. A. Regulation of TORC1 in response to amino acid starvation via lysosomal recruitment of TSC2. *Cell* **156,** 786-99 (2014).

218.Cai, S. *et al.* Activity of TSC2 is inhibited by AKT-mediated phosphorylation and membrane partitioning. *The Journal of Cell Biology* **173,** 279-89 (2006).

219. Ma, L., Chen, Z., Erdjument-Bromage, H., Tempst, P. & Pandolfi, P. P. Phosphorylation and functional inactivation of TSC2 by Erk implications for tuberous sclerosis and cancer pathogenesis. *Cell* **121,** 179-93 (2005).

220. Sancak, Y. *et al.* PRAS40 is an insulin-regulated inhibitor of the mTORC1 protein kinase. *Molecular Cell* **25,** 903-15 (2007).

221. Wang, L., Harris, T. E., Roth, R. A. & Lawrence, J. C., Jr. PRAS40 regulates mTORC1 kinase activity by functioning as a direct inhibitor of substrate binding. *The Journal of biological chemistry* **282,** 20036-44 (2007).

222. vander Haar, E., Lee, S., Bandhakavi, S., Griffin, T. J. & Kim, D. Insulin signalling to mTOR mediated by the Akt/PKB substrate PRAS40. *Nature cell biology* **9,** 316-23 (2007).

223. Smith, E. M., Finn, S. G., Tee, A. R., Browne, G. J. & Proud, C. G. The tuberous sclerosis protein TSC2 is not required for the regulation of the mammalian target of rapamycin by amino acids and certain cellular stresses. *The Journal of biological chemistry* **280,** 18717-27 (2005).

224. Roccio, M., Bos, J. L. & Zwartkruis, F. J. T. Regulation of the small GTPase Rheb by amino acids. *Oncogene* **25,** 657-64 (2006).

225. Bar-Peled, L., Schweitzer, L. D., Zoncu, R. & Sabatini, D. M. Ragulator is a GEF for the rag GTPases that signal amino acid levels to mTORC1. *Cell* **150,** 1196-208 (2012).

226. Sancak, Y. *et al.* Ragulator-Rag complex targets mTORC1 to the lysosomal surface and is necessary for its activation by amino acids. *Cell* **141,** 290-303 (2010).

227. Sinclair, L. *et al.* Control of amino-acid transport by antigen receptors coordinates the metabolic reprogramming essential for T cell differentiation. *Nature Immunology* **14,** 500-8 (2013).

228. Cham, C. M. & Gajewski, T. F. Glucose availability regulates IFN-gamma production and p70S6 kinase activation in CD8+ effector T cells. *Journal of immunology (Baltimore, Md. : 1950)* **174,** 4670-7 (2005).

229. Nakaya, M. *et al.* Inflammatory T cell responses rely on amino acid transporter ASCT2 facilitation of glutamine uptake and mTORC1 kinase activation. *Immunity* **40,** 692-705 (2014).

230. Waickman, A. T. & Powell, J. D. mTOR, metabolism, and the regulation of T-cell differentiation and function. *Immunological reviews* **249,** 43-58 (2012).

231. Carr, E. L. *et al.* Glutamine uptake and metabolism are coordinately regulated by ERK/MAPK during T lymphocyte activation. *Journal of immunology (Baltimore, Md. : 1950)* **185,** 1037-44 (2010).

232. Bar-Peled, L. & Sabatini, D. M. Regulation of mTORC1 by amino acids. *Trends in cell biology* **24,** 400-6 (2014).

233. Rolf, J. *et al.* AMPKα1: A glucose sensor that controls CD8 T-cell memory. *European Journal of Immunology* **43,** 889-896 (2013).

234. Sengupta, S., Peterson, T. R. & Sabatini, D. M. Regulation of the mTOR complex 1 pathway by nutrients, growth factors, and stress. *Molecular Cell* **40,** 310-22 (2010).

235. Dibble, C. C. & Manning, B. D. Signal integration by mTORC1 coordinates nutrient input with biosynthetic output. *Nature cell biology* **15,** 555-64 (2013).

236. Bain, J. *et al.* The selectivity of protein kinase inhibitors: a further update. *The Biochemical journal* **408,** 297-315 (2007).

237. Yang, K., Neale, G., Green, D. R., He, W. & Chi, H. The tumor suppressor Tsc1 enforces quiescence of naive T cells to promote immune homeostasis and function. *Nature Immunology* **12,** 888-97 (2011).

238. Ma, X. M. & Blenis, J. Molecular mechanisms of mTOR-mediated translational control. *Nature reviews. Molecular cell biology* **10,** 307-18 (2009).

239. Thoreen, C. C. *et al.* A unifying model for mTORC1-mediated regulation of mRNA translation. *Nature* **485,** 109-13 (2012).

240. Zhang, Y. *et al.* Coordinated regulation of protein synthesis and degradation by mTORC1. *Nature* (2014). doi:10.1038/nature13492

241. Porstmann, T. *et al.* SREBP activity is regulated by mTORC1 and contributes to Akt-dependent cell growth. *Cell metabolism* **8,** 224-36 (2008).

242. Boya, P., Reggiori, F. & Codogno, P. Emerging regulation and functions of autophagy. *Nature cell biology* **15,** 713-20 (2013).

243. Korolchuk, V. I. *et al.* Lysosomal positioning coordinates cellular nutrient responses. *Nature cell biology* **13,** 453-60 (2011).

244. Poüs, C. & Codogno, P. Lysosome positioning coordinates mTORC1 activity and autophagy. *Nature cell biology* **13,** 342-4 (2011).

245. Ganley, I. G. *et al.* ULK1.ATG13.FIP200 complex mediates mTOR signaling and is essential for autophagy. *The Journal of biological chemistry* **284,** 12297-305 (2009).

246. Weichhart, T. *et al.* The TSC-mTOR signaling pathway regulates the innate inflammatory response. *Immunity* **29,** 565-77 (2008).

247. Harrington, L. *et al.* The TSC1-2 tumor suppressor controls insulin-PI3K signaling via regulation of IRS proteins. *The Journal of Cell Biology* **166,** 213-23 (2004).

248. Hsu, P. P. *et al.* The mTOR-Regulated Phosphoproteome Reveals a Mechanism of mTORC1-Mediated Inhibition of Growth Factor Signaling. *Science* **332,** 1317-1322 (2011).

249. Yu, Y. *et al.* Phosphoproteomic Analysis Identifies Grb10 as an mTORC1 Substrate That Negatively Regulates Insulin Signaling. *Science* **332,** 1322-1326 (2011).

250. He, S. *et al.* Characterization of the metabolic phenotype of rapamycin-treated CD8+ T cells with augmented ability to generate long-lasting memory cells. *PloS one* **6,** e20107 (2011).

251. Arbonés, M. L. *et al.* Lymphocyte homing and leukocyte rolling and migration are impaired in L-selectin-deficient mice. *Immunity* **1,** 247-60 (1994).

252. Springer, T. A. Traffic signals on endothelium for lymphocyte recirculation and leukocyte emigration. *Annual review of physiology* **57,** 827-72 (1995).

253. Galkina, E. *et al.* T lymphocyte rolling and recruitment into peripheral lymph nodes is regulated by a saturable density of L-selectin (CD62L). *European Journal of Immunology* **37,** 1243-53 (2007).

254. Mora, J. R. & Andrian, von, U. H. T-cell homing specificity and plasticity: new concepts and future challenges. *Trends in immunology* **27,** 235-43 (2006).

255. Nier, A. Some reminiscences of mass spectrometry and the Manhattan Project. *Journal of Chemical Education* (1989).

256. Karas, M. & Hillenkamp, F. Laser desorption ionization of proteins with molecular masses exceeding 10,000 daltons. *Analytical chemistry* **60,** 2299-301 (1988).

257. Fenn, J. B., Mann, M., Meng, C. K., Wong, S. F. & Whitehouse, C. M. Electrospray ionization for mass spectrometry of large biomolecules. *Science (New York, N.Y.)* **246,** 64-71 (1989).

258. Fenn, J. B. Electrospray wings for molecular elephants (Nobel lecture). *Angewandte Chemie (International ed. in English)* **42,** 3871-94 (2003).

259. Steen, H. & Mann, M. The ABC's (and XYZ's) of peptide sequencing. *Nature reviews. Molecular cell biology* **5,** 699-711 (2004).

260. Olsen, J. V. *et al.* A dual pressure linear ion trap Orbitrap instrument with very high sequencing speed. *Molecular & cellular proteomics : MCP* **8,** 2759-69 (2009).

261. James, P. Protein identification in the post-genome era: the rapid rise of proteomics. *Quarterly reviews of biophysics* **30,** 279-331 (1997).

262. Anderson, N. L. & Anderson, N. G. Proteome and proteomics: new technologies, new concepts, and new words. *Electrophoresis* **19,** 1853-61 (1998).

263.Lamond, A. I. *et al.* Advancing cell biology through proteomics in space and time (PROSPECTS). *Molecular & cellular proteomics : MCP* **11,** O112.017731 (2012).

264.Nagaraj, N. *et al.* System-wide perturbation analysis with nearly complete coverage of the yeast proteome by single-shot ultra HPLC runs on a bench top Orbitrap. *Molecular & cellular proteomics : MCP* **11,** M111.013722 (2012).

265.Geiger, T., Wehner, A., Schaab, C., Cox, J. & Mann, M. Comparative proteomic analysis of eleven common cell lines reveals ubiquitous but varying expression of most proteins. *Molecular & cellular proteomics : MCP* **11,** M111.014050 (2012).

266.Kim, M. *et al.* A draft map of the human proteome. *Nature* **509,** 575-81 (2014).

267.Wilhelm, M. *et al.* Mass-spectrometry-based draft of the human proteome. *Nature* **509,** 582-7 (2014).

268.Makarov, A. & Scigelova, M. Coupling liquid chromatography to Orbitrap mass spectrometry. *Journal of chromatography. A* **1217,** 3938-45 (2010).

269.Ong, S. & Mann, M. Mass spectrometry-based proteomics turns quantitative. *Nature chemical biology* **1,** 252-62 (2005).

270.Ong, S. *et al.* Stable isotope labeling by amino acids in cell culture, SILAC, as a simple and accurate approach to expression proteomics. *Molecular & cellular proteomics : MCP* **1,** 376-86 (2002).

271.Mann, M. Functional and quantitative proteomics using SILAC. *Nature reviews. Molecular cell biology* **7,** 952-8 (2006).

272.Trinkle-Mulcahy, L. *et al.* Identifying specific protein interaction partners using quantitative mass spectrometry and bead proteomes. *The Journal of Cell Biology* **183,** 223-39 (2008).

273.Soufi, B. *et al.* Stable isotope labeling by amino acids in cell culture (SILAC) applied to quantitative proteomics of Bacillus subtilis. *Journal of proteome research* **9,** 3638-46 (2010).

274.de Godoy, L. M. F. *et al.* Status of complete proteome analysis by mass spectrometry: SILAC labeled yeast as a model system. *Genome biology* **7,** R50 (2006).

275.Urbaniak, M. D., Guther, M. L. S. & Ferguson, M. A. J. Comparative SILAC proteomic analysis of Trypanosoma brucei bloodstream and procyclic lifecycle stages. *PloS one* **7,** e36619 (2012).

276.Everley, P. A., Krijgsveld, J., Zetter, B. R. & Gygi, S. P. Quantitative cancer proteomics: stable isotope labeling with amino acids in cell culture (SILAC) as a tool for prostate cancer research. *Molecular & cellular proteomics : MCP* **3,** 729-35 (2004).

277.Loyet, K. M., Ouyang, W., Eaton, D. L. & Stults, J. T. Proteomic profiling of surface proteins on Th1 and Th2 cells. *Journal of proteome research* **4,** 400-9 (2005).

278.Larance, M. *et al.* Stable-isotope labeling with amino acids in nematodes. *Nature methods* **8,** 849-51 (2011).

279.Sury, M. D., Chen, J. & Selbach, M. The SILAC fly allows for accurate protein quantification in vivo. *Molecular & cellular proteomics : MCP* **9,** 2173-83 (2010).

280.Zanivan, S., Krueger, M. & Mann, M. In vivo quantitative proteomics: the SILAC mouse. *Methods in molecular biology (Clifton, N.J.)* **757,** 435-50 (2012).

281.Luber, C. A. *et al.* Quantitative proteomics reveals subset-specific viral recognition in dendritic cells. *Immunity* **32,** 279-89 (2010).

282.Ritorto, M. S., Cook, K., Tyagi, K., Pedrioli, P. G. & Trost, M. Hydrophilic strong anion exchange (hSAX) chromatography for highly orthogonal peptide separation of complex proteomes. *Journal of proteome research* **12,** 2449-57 (2013).

283.Ly, T. *et al.* A proteomic chronology of gene expression through the cell cycle in human myeloid leukemia cells. *eLife* **3,** e01630 (2014).

284.Colinge, J. & Bennett, K. L. Introduction to computational proteomics. *PLoS computational biology* **3,** e114 (2007).

285. Cox, J. & Mann, M. MaxQuant enables high peptide identification rates, individualized p.p.b.-range mass accuracies and proteome-wide protein quantification. *Nature Biotechnology* **26,** 1367-72 (2008).

286. Cox, J. *et al.* Andromeda: a peptide search engine integrated into the MaxQuant environment. *Journal of proteome research* **10,** 1794-805 (2011).

287. Nesvizhskii, A. I., Vitek, O. & Aebersold, R. Analysis and validation of proteomic data generated by tandem mass spectrometry. *Nature methods* **4,** 787-97 (2007).

288. Elias, J. E. & Gygi, S. P. Target-decoy search strategy for increased confidence in large-scale protein identifications by mass spectrometry. *Nature methods* **4,** 207-14 (2007).

289. Cox, J. *et al.* MaxLFQ allows accurate proteome-wide label-free quantification by delayed normalization and maximal peptide ratio extraction. *Molecular & cellular proteomics : MCP* (2014). doi:10.1074/mcp.M113.031591

290. Schwanhäusser, B. *et al.* Global quantification of mammalian gene expression control. *Nature* **473,** 337-42 (2011).

291. Pircher, H., Bürki, K., Lang, R., Hengartner, H. & Zinkernagel, R. M. Tolerance induction in double specific T-cell receptor transgenic mice varies with antigen. *Nature* **342,** 559-61 (1989).

292. Hagenbeek, T. J. *et al.* Murine Pten(-/-) T-ALL requires non-redundant PI3K/mTOR and DLL4/Notch1 signals for maintenance and γc/TCR signals for thymic exit. *Cancer letters* 1-12 (2013). doi:10.1016/j.canlet.2013.12.027

293. Lee, P. P. *et al.* A critical role for Dnmt1 and DNA methylation in T cell development, function, and survival. *Immunity* **15,** 763-74 (2001).

294. Larance, M. *et al.* Characterization of MRFAP1 turnover and interactions downstream of the NEDD8 pathway. *Molecular & cellular proteomics : MCP* **11,** M111.014407 (2012).

295. Da Huang, W., Sherman, B. T. & Lempicki, R. A. Systematic and integrative analysis of large gene lists using DAVID bioinformatics resources. *Nature protocols* **4,** 44-57 (2009).

296. Da Huang, W., Sherman, B. T. & Lempicki, R. A. Bioinformatics enrichment tools: paths toward the comprehensive functional analysis of large gene lists. *Nucleic acids research* **37,** 1-13 (2009).

297. Ashburner, M. *et al.* Gene ontology: tool for the unification of biology. The Gene Ontology Consortium. *Nature genetics* **25,** 25-9 (2000).

298. Liu, G. *et al.* NetAffx: Affymetrix probesets and annotations. *Nucleic acids research* **31,** 82-6 (2003).

299. Tian, Q. *et al.* Integrated genomic and proteomic analyses of gene expression in Mammalian cells. *Molecular & cellular proteomics : MCP* **3,** 960-9 (2004).

300. Lord, S. J., Rajotte, R. V., Korbutt, G. S. & Bleackley, R. C. Granzyme B: a natural born killer. *Immunological reviews* **193,** 31-8 (2003).

301. Leader, M., Collins, M., Patel, J. & Henry, K. Vimentin: an evaluation of its role as a tumour marker. *Histopathology* **11,** 63-72 (1987).

302. Pearce, E. L. *et al.* Control of effector CD8+ T cell function by the transcription factor Eomesodermin. *Science (New York, N.Y.)* **302,** 1041-3 (2003).

303. Intlekofer, A. M. *et al.* Effector and memory CD8+ T cell fate coupled by T-bet and eomesodermin. *Nature Immunology* **6,** 1236-44 (2005).

304. Mazurek, S., Boschek, C. B., Hugo, F. & Eigenbrodt, E. Pyruvate kinase type M2 and its role in tumor growth and spreading. *Seminars in cancer biology* **15,** 300-8 (2005).

305. Dombrauckas, J. D., Santarsiero, B. D. & Mesecar, A. D. Structural basis for tumor pyruvate kinase M2 allosteric regulation and catalysis. *Biochemistry* **44,** 9417-29 (2005).

306.Beck, M. *et al.* The quantitative proteome of a human cell line. *Molecular systems biology* **7,** 549 (2011).

307.Maier, T., Güell, M. & Serrano, L. Correlation of mRNA and protein in complex biological samples. *FEBS letters* **583,** 3966-73 (2009).

308.Lundberg, E. *et al.* Defining the transcriptome and proteome in three functionally different human cell lines. *Molecular systems biology* **6,** 450 (2010).

309.Nagaraj, N. *et al.* Deep proteome and transcriptome mapping of a human cancer cell line. *Molecular systems biology* **7,** 548 (2011).

310.Schwanhäusser, B. *et al.* Global quantification of mammalian gene expression control. *Nature* **473,** 337-342 (2011).

311.Vogel, C. & Marcotte, E. M. Insights into the regulation of protein abundance from proteomic and transcriptomic analyses. *Nature reviews. Genetics* **13,** 227-32 (2012).

312.López, M. D. & Samuelsson, T. Early evolution of histone mRNA 3' end processing. *RNA (New York, N.Y.)* **14,** 1-10 (2008).

313.Fox, C. J., Hammerman, P. S. & Thompson, C. B. Fuel feeds function: energy metabolism and the T-cell response. *Nature reviews. Immunology* **5,** 844-52 (2005).

314.Maciver, N. J. *et al.* Glucose metabolism in lymphocytes is a regulated process with significant effects on immune cell function and survival. *Journal of leukocyte biology* **84,** 949-57 (2008).

315.Brodsky, J. L. & McCracken, A. A. ER protein quality control and proteasome-mediated protein degradation. *Seminars in cell & developmental biology* **10,** 507-13 (1999).

316.Sontag, E. M., Vonk, W. I. M. & Frydman, J. Sorting out the trash: the spatial nature of eukaryotic protein quality control. *Current Opinion in Cell Biology* **26,** 139-46 (2014).

317.Joshi, N. S. *et al.* Increased numbers of preexisting memory CD8 T cells and decreased T-bet expression can restrain terminal differentiation of secondary effector and memory CD8 T cells. *Journal of immunology (Baltimore, Md. : 1950)* **187,** 4068-76 (2011).

318.Cham, C. M., Driessens, G., O'Keefe, J. P. & Gajewski, T. F. Glucose deprivation inhibits multiple key gene expression events and effector functions in CD8+ T cells. *European Journal of Immunology* **38,** 2438-50 (2008).

319.Simpson, I. A. *et al.* The facilitative glucose transporter GLUT3: 20 years of distinction. *American journal of physiology. Endocrinology and metabolism* **295,** E242-53 (2008).

320.Freeman, G. J. *et al.* Engagement of the PD-1 immunoinhibitory receptor by a novel B7 family member leads to negative regulation of lymphocyte activation. *The Journal of experimental medicine* **192,** 1027-34 (2000).

321.Powell, J. D. & Delgoffe, G. M. The Mammalian Target of Rapamycin: Linking T Cell Differentiation, Function, and Metabolism. *Immunity* **33,** 301-311 (2010).

322.Pearce, E. L. *et al.* Enhancing CD8 T-cell memory by modulating fatty acid metabolism. *Nature* **460,** 103-7 (2009).

323.Kim, D. *et al.* mTOR interacts with raptor to form a nutrient-sensitive complex that signals to the cell growth machinery. *Cell* **110,** 163-75 (2002).

324.Bandhakavi, S. *et al.* Quantitative nuclear proteomics identifies mTOR regulation of DNA damage response. *Molecular & cellular proteomics : MCP* **9,** 403-14 (2010).

325.Fingar, D. C., Salama, S., Tsou, C., Harlow, E. & Blenis, J. Mammalian cell size is controlled by mTOR and its downstream targets S6K1 and 4EBP1/eIF4E. *Genes & development* **16,** 1472-87 (2002).

326.Fingar, D. C. *et al.* mTOR controls cell cycle progression through its cell growth effectors S6K1 and 4E-BP1/eukaryotic translation initiation factor 4E. *Molecular and Cellular Biology* **24,** 200-16 (2004).

327. Kay, J. E., Kromwel, L., Doe, S. E. & Denyer, M. Inhibition of T and B lymphocyte proliferation by rapamycin. *Immunology* **72,** 544-9 (1991).

328. SIRLIN, J. L. On the incorporation of methionine 35S into proteins detectable by autoradiography. *The journal of histochemistry and cytochemistry : official journal of the Histochemistry Society* **6,** 185-90 (1958).

329. Sinclair, L. *et al.* Phosphatidylinositol-3-OH kinase and nutrient-sensing mTOR pathways control T lymphocyte trafficking. *Nature Immunology* **9,** 513-21 (2008).

330. Ewen, C. L., Kane, K. P. & Bleackley, R. C. A quarter century of granzymes. *Cell death and differentiation* **19,** 28-35 (2012).

331. Athié-M, V., Flotow, H., Hilyard, K. L. & Cantrell, D. A. IL-12 selectively regulates STAT4 via phosphatidylinositol 3-kinase and Ras-independent signal transduction pathways. *European Journal of Immunology* **30,** 1425-34 (2000).

332. Kirkwood, K. J., Ahmad, Y., Larance, M. & Lamond, A. I. Characterisation of Native Protein Complexes and Protein Isoform Variation using Size-Fractionation Based Quantitative Proteomics. *Molecular & cellular proteomics : MCP* 1-55 (2013). doi:10.1074/mcp.M113.032367

333. Brosnan, J. T. Interorgan amino acid transport and its regulation. *The Journal of nutrition* **133,** 2068S-2072S (2003).

334. Mayer, C. & Grummt, I. Ribosome biogenesis and cell growth: mTOR coordinates transcription by all three classes of nuclear RNA polymerases. *Oncogene* **25,** 6384-91 (2006).

335. Yamashita, R. *et al.* Comprehensive detection of human terminal oligo-pyrimidine (TOP) genes and analysis of their characteristics. *Nucleic acids research* **36,** 3707-15 (2008).

336. Schrader, E. K., Harstad, K. G. & Matouschek, A. Targeting proteins for degradation. *Nature chemical biology* **5,** 815-22 (2009).

337. Boisvert, F. *et al.* A quantitative spatial proteomics analysis of proteome turnover in human cells. *Molecular & cellular proteomics : MCP* **11,** M111.011429 (2012).

338. Ley, K. & Kansas, G. S. Selectins in T-cell recruitment to non-lymphoid tissues and sites of inflammation. *Nature reviews. Immunology* **4,** 325-35 (2004).

339. Pause, A. *et al.* Insulin-dependent stimulation of protein synthesis by phosphorylation of a regulator of 5'-cap function. *Nature* **371,** 762-7 (1994).

340. Semenza, G. L. HIF-1: upstream and downstream of cancer metabolism. *Current opinion in genetics & development* **20,** 51-6 (2010).

341. Düvel, K. *et al.* Activation of a metabolic gene regulatory network downstream of mTOR complex 1. *Molecular Cell* **39,** 171-83 (2010).

342. Kidani, Y. *et al.* Sterol regulatory element-binding proteins are essential for the metabolic programming of effector T cells and adaptive immunity. *Nature Immunology* **14,** 489-99 (2013).

343. Krieg, A. J., Hammond, E. M. & Giaccia, A. J. Functional analysis of p53 binding under differential stresses. *Molecular and Cellular Biology* **26,** 7030-45 (2006).

344. Hoppins, S. The regulation of mitochondrial dynamics. *Current Opinion in Cell Biology* **29C,** 46-52 (2014).

345. Jensen, M. B. & Jasper, H. Mitochondrial Proteostasis in the Control of Aging and Longevity. *Cell metabolism* **20,** 214-225 (2014).

346. Hällberg, B. M. & Larsson, N. Making Proteins in the Powerhouse. *Cell metabolism* **20,** 226-240 (2014).

347. Lee, K. *et al.* Mammalian target of rapamycin protein complex 2 regulates differentiation of Th1 and Th2 cell subsets via distinct signaling pathways. *Immunity* **32,** 743-53 (2010).

348. Delgoffe, G. M. *et al.* The kinase mTOR regulates the differentiation of helper T cells through the selective activation of signaling by mTORC1 and mTORC2. *Nature Immunology* **12,** 295-303 (2011).

349. Lindsley, C. W. *et al.* Allosteric Akt (PKB) inhibitors: discovery and SAR of isozyme selective inhibitors. *Bioorganic & medicinal chemistry letters* **15,** 761-4 (2005).

350. Rao, R., Li, Q., Bupp, M. . & Shrikant, P. Transcription Factor Foxo1 Represses T-bet-Mediated Effector Functions and Promotes Memory CD8+ T Cell Differentiation. *Immunity* **36,** 374-387 (2012).

351. Heikamp, E. B. *et al.* The AGC kinase SGK1 regulates TH1 and TH2 differentiation downstream of the mTORC2 complex. *Nature Immunology* **15,** 457-64 (2014).

352. Delgoffe, G. M. *et al.* The mTOR kinase differentially regulates effector and regulatory T cell lineage commitment. *Immunity* **30,** 832-44 (2009).

353. Gingras, A. C., Kennedy, S. G., O'Leary, M. A., Sonenberg, N. & Hay, N. 4E-BP1, a repressor of mRNA translation, is phosphorylated and inactivated by the Akt(PKB) signaling pathway. *Genes & development* **12,** 502-13 (1998).

354. Cope, C. L. *et al.* Adaptation to mTOR kinase inhibitors by amplification of eIF4E to maintain cap-dependent translation. *Journal of Cell Science* **127,** 788-800 (2014).

355. Najafov, A., Shpiro, N. & Alessi, D. R. Akt is efficiently activated by PIF-pocket- and PtdIns(3,4,5)P3-dependent mechanisms leading to resistance to PDK1 inhibitors. *The Biochemical journal* **448,** 285-95 (2012).

356. Shi, Y., Yan, H., Frost, P., Gera, J. & Lichtenstein, A. Mammalian target of rapamycin inhibitors activate the AKT kinase in multiple myeloma cells by up-regulating the insulin-like growth factor receptor/insulin receptor substrate-1/phosphatidylinositol 3-kinase cascade. *Molecular cancer therapeutics* **4,** 1533-40 (2005).

357. Briaud, I. *et al.* Insulin receptor substrate-2 proteasomal degradation mediated by a mammalian target of rapamycin (mTOR)-induced negative feedback down-regulates protein kinase B-mediated signaling pathway in beta-cells. *The Journal of biological chemistry* **280,** 2282-93 (2005).

358. Clark, J. *et al.* Quantification of PtdInsP3 molecular species in cells and tissues by mass spectrometry. *Nature methods* **8,** 267-72 (2011).

359. Barnett, S. F. *et al.* Identification and characterization of pleckstrin-homology-domain-dependent and isoenzyme-specific Akt inhibitors. *The Biochemical journal* **385,** 399-408 (2005).

360. Bayascas, J. R. *et al.* Mutation of the PDK1 PH domain inhibits protein kinase B/Akt, leading to small size and insulin resistance. *Molecular and Cellular Biology* **28,** 3258-72 (2008).

361. Myers, M. P. *et al.* The lipid phosphatase activity of PTEN is critical for its tumor supressor function. *Proceedings of the National Academy of Sciences of the United States of America* **95,** 13513-8 (1998).

362. Wu, X., Senechal, K., Neshat, M. S., Whang, Y. E. & Sawyers, C. L. The PTEN/MMAC1 tumor suppressor phosphatase functions as a negative regulator of the phosphoinositide 3-kinase/Akt pathway. *Proceedings of the National Academy of Sciences of the United States of America* **95,** 15587-91 (1998).

363. Carracedo, A. *et al.* Inhibition of mTORC1 leads to MAPK pathway activation through a PI3K-dependent feedback loop in human cancer. *The Journal of clinical investigation* **118,** 3065-74 (2008).

364. D'Souza, W. N., Chang, C., Fischer, A. M., Li, M. & Hedrick, S. M. The Erk2 MAPK regulates CD8 T cell proliferation and survival. *Journal of immunology (Baltimore, Md. : 1950)* **181,** 7617-29 (2008).

365.Rao, R. R., Li, Q., Bupp, M. R. G. & Shrikant, P. A. Transcription factor Foxo1 represses T-bet-mediated effector functions and promotes memory CD8(+) T cell differentiation. *Immunity* **36,** 374-87 (2012).

366.Huang, J. & Manning, B. D. A complex interplay between Akt, TSC2 and the two mTOR complexes. *Biochemical Society transactions* **37,** 217-22 (2009).

367.Angulo, I. *et al.* Phosphoinositide 3-kinase δ gene mutation predisposes to respiratory infection and airway damage. *Science (New York, N.Y.)* **342,** 866-71 (2013).

368.Lucas, C. L. *et al.* Dominant-activating germline mutations in the gene encoding the PI(3)K catalytic subunit p110δ result in T cell senescence and human immunodeficiency. *Nature Immunology* **15,** 88-97 (2014).

369.Ridley, A. J. Rho GTPases and actin dynamics in membrane protrusions and vesicle trafficking. *Trends in cell biology* **16,** 522-9 (2006).

370.Falguni, das *et al.* Unrestrained mammalian target of rapamycin complexes 1 and 2 increase expression of phosphatase and tensin homolog deleted on chromosome 10 to regulate phosphorylation of Akt kinase. *The Journal of biological chemistry* **287,** 3808-22 (2012).

371.Yu, Y. *et al.* Phosphoproteomic analysis identifies Grb10 as an mTORC1 substrate that negatively regulates insulin signaling. *Science (New York, N.Y.)* **332,** 1322-6 (2011).

372.Zhang, N. & Bevan, M. CD8+ T Cells: Foot Soldiers of the Immune System. *Immunity* **35,** 161-168 (2011).

373.Karnitz, L. M., Burns, L. A., Sutor, S. L., Blenis, J. & Abraham, R. T. Interleukin-2 triggers a novel phosphatidylinositol 3-kinase-dependent MEK activation pathway. *Molecular and Cellular Biology* **15,** 3049-57 (1995).

374.Zhu, L., Yu, X., Akatsuka, Y., Cooper, J. A. & Anasetti, C. Role of mitogen-activated protein kinases in activation-induced apoptosis of T cells. *Immunology* **97,** 26-35 (1999).

375.Despouy, G., Joiner, M., Le Toriellec, E., Weil, R. & Stern, M. H. The TCL1 oncoprotein inhibits activation-induced cell death by impairing PKCtheta and ERK pathways. *Blood* **110,** 4406-16 (2007).

376.Macintyre, A. N. *et al.* The glucose transporter Glut1 is selectively essential for CD4 T cell activation and effector function. *Cell metabolism* **20,** 61-72 (2014).

Supplementary tables

protein rank	transcipt rank	protein names	fract. abund.	cumul. abund.
1	2778	Histone H4	3.1%	3.1%
2	3	Isoform Short of Thymosin beta-4	2.2%	5.4%
3	64	Vimentin	1.7%	7.0%
4	47	Prothymosin alpha	1.6%	8.7%
5	9	Peptidyl-prolyl cis-trans isomerase A	1.6%	10.3%
6	4	60S acidic ribosomal protein P2	1.5%	11.8%
7	348	Cofilin-1	1.4%	13.2%
8	96	Alpha-enolase	1.2%	14.4%
9	7	60S acidic ribosomal protein P1	1.2%	15.6%
10	120	Eukaryotic translation initiation factor 5A-1	1.0%	16.7%
11	1	Granzyme B(G,H)	1.0%	17.7%
12	75	Glyceraldehyde-3-phosphate dehydrogenase	0.9%	18.6%
13	56	L-lactate dehydrogenase A chain	0.7%	19.3%
14	2642	Putative RNA-binding protein 3	0.7%	20.0%
15	2	Elongation factor 1-alpha 1	0.7%	20.7%
16	5301	Histone H3.2	0.7%	21.4%
17	201	Protein S100-A4	0.6%	22.1%
18	100	Heat shock protein HSP 90-beta	0.6%	22.7%
19	173	Fructose-bisphosphate aldolase A	0.6%	23.4%
20	76	Phosphoglycerate kinase 1	0.6%	24.0%
21	116	Triosephosphate isomerase	0.6%	24.6%
22	228	Transgelin-2	0.6%	25.2%
23	34	40S ribosomal protein S8	0.5%	25.8%
24	78	Heat shock cognate 71 kDa protein	0.5%	26.3%
25		Histone H2A type 1-F	0.5%	26.8%
26	2092	Vesicle-trafficking protein SEC22b	0.5%	27.3%
27	4269	Actin, alpha skeletal muscle	0.5%	27.8%
28	97	GTP-binding nuclear protein Ran	0.5%	28.3%
29	834	14-3-3 protein zeta/delta	0.5%	28.8%
30	37	Galectin-1	0.5%	29.2%
31	808	40S ribosomal protein SA	0.5%	29.7%
32	744	Translationally-controlled tumor protein	0.4%	30.1%
33		Thioredoxin	0.4%	30.5%
34	70	Elongation factor 2	0.4%	30.9%
35	275	Phosphoglycerate mutase 1	0.4%	31.3%
36	197	Profilin-1	0.4%	31.7%
37	260	Plastin-2	0.4%	32.1%
38	194	40S ribosomal protein S25	0.4%	32.5%
39	203	SH3 domain-binding glutamic acid-rich-like protein 3	0.4%	32.9%
40	22	40S ribosomal protein S14	0.4%	33.3%
41	52	40S ribosomal protein S17	0.4%	33.6%
42	787	40S ribosomal protein S20	0.4%	34.0%

43	20	60S ribosomal protein L23a	0.4%	34.4%
44	84	60S ribosomal protein L27	0.4%	34.7%
45	57	Nucleoside diphosphate kinase B	0.4%	35.1%
46		Histone H1.5	0.4%	35.4%
47	72	Nucleophosmin	0.4%	35.8%
48	40	40S ribosomal protein S28	0.3%	36.1%
49	219	Heat shock protein HSP 90-alpha	0.3%	36.5%
50	105	Coronin-1A	0.3%	36.8%
51	186	78 kDa glucose-regulated protein	0.3%	37.1%
52	253	Rho GDP-dissociation inhibitor 2	0.3%	37.5%
53	62	40S ribosomal protein S12	0.3%	37.8%
54	5489	Histone H1.4	0.3%	38.1%
55	63	60S ribosomal protein L18	0.3%	38.4%
56	33	40S ribosomal protein S7	0.3%	38.7%
57	1539	Protein disulfide-isomerase A3	0.3%	39.0%
58	1021	Nucleolin	0.3%	39.3%
59	259	10 kDa heat shock protein, mitochondrial	0.3%	39.7%
60	35	Ubiquitin-40S ribosomal protein S27a	0.3%	40.0%
61	575	Rho GDP-dissociation inhibitor 1	0.3%	40.3%
62		Beta-actin-like protein 2	0.3%	40.5%
63		Heterogeneous nuclear ribonucleoprotein A1	0.3%	40.8%
64	1739	60S ribosomal protein L31	0.3%	41.1%
65	153	Calmodulin	0.3%	41.4%
66	375	Guanine nucleotide-binding protein subunit beta-2-like 1	0.3%	41.7%
67	163	High mobility group protein B2	0.3%	41.9%
68	4022	Annexin A2	0.3%	42.2%
69	15	40S ribosomal protein S3a	0.3%	42.5%
70	109	Isoform Smooth muscle of Myosin light polypeptide 6	0.3%	42.8%
71	36	40S ribosomal protein S11	0.3%	43.0%
72	44	60S ribosomal protein L17	0.3%	43.3%
73	93	Peroxiredoxin-1	0.3%	43.6%
74	43	Isoform HF2 of Granzyme A	0.3%	43.8%
75	54	60S ribosomal protein L12	0.3%	44.1%
76	79	Proliferating cell nuclear antigen	0.3%	44.3%
77	732	Chromobox protein homolog 3	0.3%	44.6%
78	919	14-3-3 protein epsilon	0.3%	44.9%
79	123	Ran-specific GTPase-activating protein	0.3%	45.1%
80		Heterogeneous nuclear ribonucleoprotein A/B	0.2%	45.4%
81	12	40S ribosomal protein S4, X isoform	0.2%	45.6%
82		60S acidic ribosomal protein P0	0.2%	45.8%
83	174	Transketolase	0.2%	46.1%
84	85	Thy-1 membrane glycoprotein	0.2%	46.3%
85	17	60S ribosomal protein L38	0.2%	46.6%

86	266	Peptidyl-prolyl cis-trans isomerase FKBP1A	0.2%	46.8%
87	748	60S ribosomal protein L11	0.2%	47.0%
88	258	60S ribosomal protein L3	0.2%	47.3%
89	220	Endoplasmin	0.2%	47.5%
90		Histone H1.3	0.2%	47.7%
91	108	ATP synthase subunit beta, mitochondrial	0.2%	47.9%
92	73	60S ribosomal protein L22	0.2%	48.1%
93	1978	40S ribosomal protein S3	0.2%	48.4%
94	119	40S ribosomal protein S6	0.2%	48.6%
95	1029	Chloride intracellular channel protein 1	0.2%	48.8%
96	21	60S ribosomal protein L9	0.2%	49.0%
97	5416	Macrophage migration inhibitory factor	0.2%	49.2%
98	588	40S ribosomal protein S18	0.2%	49.4%
99	87	Histidine triad nucleotide-binding protein 1	0.2%	49.7%
100	694	40S ribosomal protein S19	0.2%	49.9%

Figure S1: List of 100 most abundant proteins in CTL.
100 most abundant in CTL are shown sorted by descending abundance. Corresponding ranking according to mRNA levels is also shown.
fract. abund.: fractional abundance for specific protein; cum. abund.: cumulative abundance

protein name	gene name	protein fold change	t-test	ratio Exp1	ratio Exp2	ratio Exp3	transcript fold change	transcript significant
Ubiquinone biosynthesis monooxygenase COQ6	Coq6	15.3	0.058	38.4	4.0	23.4	1.0	NO
Sideroflexin-2	Sfxn2	14.9	1.000	14.9		1/∞	1.0	NO
Limbin	Evc2	10.9	0.533	∞	152.9	0.8	0.9	NO
Tyrosine-protein kinase Fyn	Fyn	10.0	1.000		10.0		1.0	NO
L-selectin	Sell	8.1	0.014	12.2	5.2	8.5	6.2	YES
Tetratricopeptide repeat protein 5	Ttc5	6.4	0.141	1.4	15.7	12.7	0.9	NO
Cellular retinoic acid-binding protein 2	Crabp2	5.7	1.000		5.7		1.2	NO
Isoform ICAD-S of DNA fragmentation factor subunit alpha	Dffa	5.6	0.465	1.2	1/∞	25.8	0.8	NO
Isoform 2 of Serine/threonine-protein kinase MRCK alpha	Cdc42bpa	5.1	1.000			5.1	1.0	NO
Programmed cell death protein 4	Pdcd4	5.0	0.003	5.8	4.2	5.1	1.8	YES
Probable palmitoyltransferase ZDHHC19	Zdhhc19	4.8	0.390		14.2	1.6	1.0	NO
Isoform 2 of Kinesin-like protein KIF20B	Kif20b	4.6	0.448		17.0	1.3		
Isoform 3 of Interleukin enhancer-binding factor 3	Ilf3	4.3	1.000		4.3		1.0	NO
Histone H2A.V	H2afv	4.3	0.143		3.1	6.0	1.9	YES
Muscleblind-like protein 3	Mbnl3	4.3	0.153	12.9	4.2	1.4	1.3	NO
Interferon-induced guanylate-binding protein 2	Gbp2	4.1	0.001	3.8	4.3	4.1	2.8	YES
Lymphocyte antigen 6C2	Ly6c2	4.1	0.120	8.3	5.7	1.4		
Transmembrane protein 14C	Tmem14c	3.9	1.000	∞	3.9		1.0	NO
Numb-like protein	Numbl	3.9	0.438	61.7	0.7	1.3	1.0	NO
Cysteine and histidine-rich protein 1	Cyhr1	3.8	0.036	4.3	2.3	5.5	1.0	NO
Isoform Short of H-2 class II histocompatibility antigen gamma chain	Cd74	3.8	0.024	2.6	5.4	3.8	1.0	NO
Transgelin-3	Tagln3	3.6	0.049		4.0	3.3	0.9	NO
Protein APCDD1	Apcdd1	3.6	1.000			3.6	1.1	NO
C-type lectin domain family 2 member D	Clec2d	3.5	0.012	3.6	2.7	4.4	1.5	YES
Aspartate--tRNA ligase, mitochondrial	Dars2	3.3	0.034	4.3	2.1	4.0	1.4	YES
Integrin alpha-E	Itgae	3.3	1.000	3.3			1.8	NO

Protein	Gene							
Isoform 2 of Protein piccolo	Pclo	3.3	0.044	2.8	5.3	2.3	1.1	NO
G-protein coupled receptor 161	Gpr161	3.2	0.136	3.1	1.4	7.4	1.0	NO
Keratin, type II cytoskeletal 2 oral	Krt76	3.2	0.029	2.9	4.7	2.4	1.3	YES
Isoform 2 of Phosphatidylinositol 4-phosphate 5-kinase type-1 gamma	Pip5k1c	3.1	1.000	3.1			1.0	NO
Isoform 2 of Epimerase family protein SDR39U1	Sdr39u1	3.0	0.015	3.0	3.9	2.4		
Neurofilament medium polypeptide	Nefm	3.0	0.023	2.8	4.2	2.4	1.0	NO
Guanylate-binding protein 5	Gbp5	3.0	0.019	2.6	2.5	4.1		
Methylated-DNA--protein-cysteine methyltransferase	Mgmt	2.9	0.308	13.9	1.5	1.1	0.9	NO
Keratin, type II cytoskeletal 1	Krt1	2.9	1.000	2.9			1.0	NO
Kallikrein-8	Klk8	2.8	0.408	6.2	1.3		1.2	NO
Protein FAM64A	Fam64a	2.8	0.097	1.9	5.7	2.2		
Intermediate conductance calcium-activated potassium channel protein 4	Kcnn4	2.8	1.000		2.8		1.2	NO
Cystatin-C	Cst3	2.8	0.006	2.7	3.3	2.5	1.2	NO
Protein FAM65B	Fam65b	2.8	0.033	1.9	3.5	3.2		
Isoform 2 of NACHT, LRR and PYD domains-containing protein 6	Nlrp6	2.8	0.074		3.1	2.5	1.3	NO
NEDD4-like E3 ubiquitin-protein ligase WWP1	Wwp1	2.8	0.057		2.5	3.0	0.9	NO
H-2 class II histocompatibility antigen, A beta chain	H2-Ab1	2.8	0.026	3.5	2.0	3.0	0.6	NO
Isoform 2 of Box C/D snoRNA protein 1	Znhit6	2.8	0.380		1.4	5.5		
Isoform 1S of Ral GTPase-activating protein subunit alpha-1	Ralgapa1	2.8	0.037	2.0	2.6	4.0		
Intercellular adhesion molecule 2	Icam2	2.7	0.000	2.6	2.8	2.8	2.2	YES
Phosphoinositide 3-kinase regulatory subunit 5	Pik3r5	2.7	0.058	2.5	3.0	∞	1.1	NO
Isoform 2 of DDB1- and CUL4-associated factor 10	Dcaf10	2.7	0.069		2.4	3.0		
Small integral membrane protein 4	Smim4	2.7	0.312	1.6		4.6		
Probable G-protein coupled receptor 132	Gpr132	2.7	0.180	2.0		3.6	1.1	NO
Neutrophil cytosol factor 1	Ncf1	2.7	0.001	2.5	2.8	2.6	1.1	NO
Metalloendopeptidase OMA1, mitochondrial	Oma1	2.6	1.000			2.6	1.1	NO
Coiled-coil domain-containing protein 96	Ccdc96	2.6	0.087		2.3	3.0	1.0	NO
Tubulin beta-3 chain	Tubb3	2.6	0.462	2.9	0.4	15.9	0.9	NO

Protein	Gene							
Isoform 3 of SH3 domain-containing kinase-binding protein 1	Sh3kbp1	2.6	0.333		1.5	4.6	1.0	NO
O-acetyl-ADP-ribose deacetylase MACROD1	Macrod1	2.6	0.099	3.3	4.0	1.4	1.3	NO
HSPB1-associated protein 1	Hspbap1	2.6	0.032	2.7	3.4	1.9	1.2	NO
Alpha-N-acetylgalactosaminidase	Naga	2.6	0.230	5.4	3.7	0.9	0.7	YES
Repressor of RNA polymerase III transcription MAF1 homolog	Maf1	2.6	0.002	2.5	2.5	2.8	1.3	NO
Eukaryotic translation initiation factor 2 subunit 3, Y-linked	Eif2s3y	2.6	0.158	2.0		3.3	1.1	NO
Constitutive coactivator of PPAR-gamma-like protein 2	Fam120c	2.6	0.011	3.0	2.1	2.7		
Alpha/beta hydrolase domain-containing protein 14B	Abhd14b	2.5	0.287	1.1	9.0	1.6	1.1	NO
Isoform 2 of Protein Wiz	Wiz	2.5	0.474		6.0	1.1	1.1	NO
Caspase-2	Casp2	2.5	0.027	2.0	3.4	2.3	1.5	YES
Hexaprenyldihydroxybenzoate methyltransferase, mitochondrial	Coq3	2.5	0.006	2.2	2.5	2.8	0.9	NO
Histone H2A type 2-B	Hist2h2ab	2.5	0.115	2.4	1.4	4.6		
Isoform 2 of Zinc finger protein 740	Znf740	2.5	0.062		2.3	2.7		
Sideroflexin-3	Sfxn3	2.5	0.036	3.0	2.9	1.7	1.0	NO
Cytochrome c oxidase subunit 2	Mtco2	2.5	0.105	1.8	4.6	1.8		
JmjC domain-containing protein 7	Jmjd7	2.5	0.005	2.8	2.4	2.2		
NAD-dependent protein deacetylase sirtuin-3	Sirt3	2.5	0.065	2.0	4.0	1.9	1.3	YES
NADH dehydrogenase [ubiquinone] 1 alpha subcomplex subunit 13	Ndufa13	2.4	0.229	6.9	1.3	1.7	0.9	NO
Myosin-1	Myh1	2.4	0.233	3.4		1.7	1.0	NO
Tripartite motif-containing protein 35	Trim35	2.4	0.198	1.7	6.1	1.4	1.0	NO
Myotubularin-related protein 14	Mtmr14	2.4	0.097	1.9	4.4	1.8	1.5	YES
Pyrin and HIN domain-containing protein 1	Pyhin1	2.4	0.065	1.5	3.1	3.0	0.7	NO
Isoform 2 of Lactadherin	Mfge8	2.4	0.134	4.5	1.3	2.4	1.3	NO
Isoform 2 of SUN domain-containing protein 2	Sun2	2.4	0.007	2.5	2.1	2.6		
Guanine nucleotide-binding protein G(olf) subunit alpha	Gnal	2.4	0.384		4.4	1.3	1.0	NO
Major facilitator superfamily domain-containing protein 8	Mfsd8	2.4	1.000			2.4	0.9	NO
Carbonic anhydrase 2	Ca2	2.4	0.017	3.0	2.1	2.1		
tRNA methyltransferase 112 homolog	Trmt112	2.4	0.047	3.0	1.6	2.8		

Isoform 2 of Rho guanine nucleotide exchange factor 18	Arhgef18	2.4	0.016	1.9	2.5	2.8	1.0	NO
Vacuolar protein sorting-associated protein 37B	Vps37b	2.4	0.061	3.7	1.9	1.8	1.7	YES
Actin-related protein 2/3 complex subunit 4	Arpc4	2.4	0.097	4.0	2.2	1.5	0.9	NO
Spectrin beta chain, erythrocytic	Sptb	2.3	1.000		2.3			
Neutrophil cytosol factor 2	Ncf2	2.3	0.509	1.0	5.6		0.9	NO
N(4)-(beta-N-acetylglucosaminyl)-L-asparaginase	Aga	2.3	1.000	2.3			1.1	NO
Natural killer cells antigen CD94	Klrd1	2.3	0.184	1.8	3.0		1.3	NO
Isoform 5 of Protein NLRC3	Nlrc3	2.3	1.000		2.3	1/∞	1.2	NO
Sodium/hydrogen exchanger 9	Slc9a9	2.3	1.000		2.3		1.0	NO
Granzyme C	Gzmc	2.3	0.008	2.6	2.4	2.0	0.9	NO
Ubiquitin-like domain-containing CTD phosphatase 1	Ublcp1	2.3	0.041	2.7	1.6	2.8	1.1	NO
Kelch-like protein 11	Klhl11	2.3	0.237	1.7	6.2	1.2	1.0	NO
Putative lipoyltransferase 2, mitochondrial	Lipt2	2.3	1.000	2.3				
Dipeptidyl peptidase 2	Dpp7	2.3	0.056	1.8	1.9	3.5	1.1	NO
NADH dehydrogenase [ubiquinone] 1 beta subcomplex subunit 3	Ndufb3	2.3	0.236	2.0	5.8	1.1	1.0	NO
Protein S100-A1	S100a1	2.3	0.080	3.2	1.4	2.7	1.2	NO
Protein S100-A13	S100a13	2.3	0.095	1.9	4.0	1.6	1.2	NO
T-cell receptor alpha chain C region	Tcra	2.3	0.264	0.9	5.5	2.6	1.2	NO
Transmembrane protein 206	Tmem206	2.3	0.217	1.7	1.2	5.7		
H-2 class II histocompatibility antigen, A-B alpha chain	H2-Aa	2.3	0.148	1.1	3.6	3.0	1.1	NO
GTP-binding protein GEM	Gem	2.3	0.011	2.2	2.7	2.0	1.0	NO
Cryptochrome-1	Cry1	2.3	1.000	2.3			1.2	NO
Nucleoside diphosphate-linked moiety X motif 8, mitochondrial	Nudt8	2.3	0.031	3.1	2.0	2.0	0.9	NO
Maternal embryonic leucine zipper kinase	Melk	2.3	0.191	2.3	4.7	1.1	1.7	YES
Isoform 2 of WD repeat domain phosphoinositide-interacting protein 4	Wdr45	2.3	0.263	3.3	1.6	∞	1.3	NO
WD and tetratricopeptide repeats protein 1	Wdtc1	2.3	0.314	0.8	6.9	2.1	1.1	NO
Protein Jade-2	Phf15	2.3	0.090	1.3	2.9	3.0	1.3	NO
Isoform 2 of Dedicator of cytokinesis protein 1	Dock1	2.3	0.008	2.4	2.4	1.9	1.0	NO

G2/M phase-specific E3 ubiquitin-protein ligase	G2e3	2.3	0.026	2.9	2.2	1.8		
Isoform 2 of GPI ethanolamine phosphate transferase 1	Pign	2.2	0.217		1.7	3.0	1.0	NO
Cyclin-dependent kinases regulatory subunit 1	Cks1b	2.2	0.042	1.9	3.1	1.9	1.6	YES
Intraflagellar transport protein 81 homolog	Ift81	2.2	0.184		2.8	1.8	1.0	NO
T-cell immunoreceptor with Ig and ITIM domains	Tigit	2.2	0.048	1.8	3.2	1.9		
Probable peptide chain release factor C12orf65 homolog, mitochondrial		2.2	1.000			2.2		
tRNA pseudouridine synthase-like 1	Pusl1	2.2	0.003	2.1	2.4	2.2		
DNA-directed DNA/RNA polymerase mu	Polm	2.2	1.000	2.2			1.1	NO
Isoform 2 of Solute carrier family 12 member 6	Slc12a6	2.2	1.000	2.2			1.0	NO
Isoform 2 of Ubinuclein-1	Ubn1	2.2	0.387		3.9	1.3	1.1	NO
Coiled-coil domain-containing protein 82	Ccdc82	2.2	1.000	2.2			1.1	NO
Protein C-ets-1	Ets1	2.2	0.223	2.5	1.0	4.5	1.2	NO
Steryl-sulfatase	Sts	2.2	0.218	2.9		1.7	1.0	NO
Sorting nexin-25	Snx25	2.2	0.062	2.4	2.0		1.0	NO
rRNA methyltransferase 1, mitochondrial	Mrm1	2.2	0.171		2.7	1.8	1.2	NO
Nuclear receptor subfamily 2 group C member 2	Nr2c2	2.2	0.054	1.7	2.0	3.2	1.0	NO
Isoform 3 of LETM1 domain-containing protein 1	Letmd1	2.2	0.098	1.3	3.3	2.4	1.0	NO
Methylglutaconyl-CoA hydratase, mitochondrial	Auh	2.2	0.013	1.8	2.5	2.3	1.1	NO
Heterogeneous nuclear ribonucleoproteins A2/B1	Hnrnpa2b1	2.2	0.120	2.3	3.5	1.3		
Isoform 2 of Poly(U)-specific endoribonuclease	Endou	2.2	0.276	3.1		1.5		
Sodium channel modifier 1	Scnm1	2.2	0.130	1.3	2.0	3.8	1.0	NO
Isoform Cytoplasmic+peroxisomal of Malonyl-CoA decarboxylase, mitochondrial	Mlycd	2.2	0.141	2.9	3.1	1.1	1.1	NO
Isoform 3 of N-acetyltransferase ESCO1	Esco1	2.2	0.561	1.1	0.5	18.9	0.9	NO
Dipeptidyl peptidase 4	Dpp4	2.2	0.352	4.0	4.2	0.6	1.2	NO
Dihydropyrimidinase-related protein 1	Crmp1	2.1	0.002	2.3	2.1	2.1	1.2	NO
NADH dehydrogenase [ubiquinone] 1 beta subcomplex subunit 4	Ndufb4	2.1	0.250	4.4	2.5	0.9	0.9	NO
Isoform Short of Transcription intermediary factor 1-alpha	Trim24	2.1	0.008	2.3	2.3	1.9	1.0	NO

Protein	Gene							
Protein Hikeshi	L7rn6	2.1	0.015	2.6	1.9	2.1		
Zinc finger protein 609	Znf609	2.1	0.140	3.2	2.7	1.1		
NGFI-A-binding protein 1	Nab1	2.1	0.047		2.3	2.0	1.1	NO
Probable histidine--tRNA ligase, mitochondrial	Hars2	2.1	0.270	5.0	2.2	0.9	1.0	NO
Proline dehydrogenase 1, mitochondrial	Prodh	2.1	0.206		2.7	1.7	1.1	NO
Hemogen	Hemgn	2.1	0.054	1.6	2.1	3.0	1.8	YES
DNA fragmentation factor subunit alpha	Dffa	2.1	0.113	1.2	3.2	2.4	0.8	NO
Tumor necrosis factor alpha-induced protein 8-like protein 2	Tnfaip8l2	2.1	0.146	1.4	1.7	4.0	1.0	NO
Insulin receptor substrate 2	Irs2	2.1	1.000	∞		2.1	1.2	NO
Pancreatic progenitor cell differentiation and proliferation factor	Ppdpf	2.1	1.000	2.1				
Enkurin domain-containing protein 1	Enkd1	2.1	0.532	0.9	4.8			
Protein SET	Set	2.1	0.380	0.6	2.4	6.3	1.1	NO
Palmitoyl-protein thioesterase 1	Ppt1	2.1	0.005	2.1	2.3	1.9	1.1	NO
Probable methyltransferase-like protein 15	Mettl15	2.1	0.007	1.9	2.2	2.3		
Cytochrome c oxidase subunit 7A2, mitochondrial	Cox7a2	2.1	0.113	1.4	3.5	2.0	0.9	NO
Isoform Gamma of Receptor-type tyrosine-protein phosphatase R	Ptprr	2.1	1.000	2.1			0.9	NO
Proteolipid protein 2	Plp2	2.1	0.133	3.9	1.7	1.5	1.2	NO
von Willebrand factor A domain-containing protein 5A	Vwa5a	2.1	0.056	2.3	2.8	1.5		
PIH1 domain-containing protein 1	Pih1d1	2.1	0.173	3.4	2.6	1.0	1.1	NO
Voltage-dependent P/Q-type calcium channel subunit alpha-1A	Cacna1a	2.1	0.520	11.0	0.4	2.0	1.0	NO
Vitamin K epoxide reductase complex subunit 1	Vkorc1	2.1	1.000	2.1			1.2	NO
Protein SCO1 homolog, mitochondrial	Sco1	2.1	0.094	2.6	2.7	1.3	1.2	NO
Neudesin	Nenf	2.1	0.141	3.7	1.9	1.3	1.6	YES
Acyl-CoA:lysophosphatidylglycerol acyltransferase 1	Lpgat1	2.1	0.394	3.5		1.2	0.9	NO
Serine/threonine-protein phosphatase 2B catalytic subunit gamma isoform	Ppp3cc	2.1	0.062	1.5	2.9	2.0	1.1	NO
Dolichyl-diphosphooligosaccharide--protein glycosyltransferase subunit STT3A	Stt3a	2.1	0.413	2.5	6.3	0.6	1.0	NO
Lymphocyte activation gene 3 protein	Lag3	2.0	0.012	2.4	1.8	2.0	1.4	NO

Cytochrome c oxidase subunit 6C	Cox6c	2.0	0.104	1.7	3.3	1.5	1.1	NO
Isoform 2 of Ubiquitin carboxyl-terminal hydrolase 37	Usp37	2.0	0.363	0.7	5.5	2.3	1.2	NO
Stathmin	Stmn1	2.0	0.001	2.1	2.0	2.0	2.3	YES
28S ribosomal protein S12, mitochondrial	Mrps12	2.0	0.301	1.1	5.6	1.4	0.8	NO
Cytoplasmic FMR1-interacting protein 1	Cyfip1	2.0	0.251	1.4	4.9	1.2	1.0	NO

Figure S2: Proteins more than 2-fold up-regulated upon mTORC1 inhibition.

All proteins with an average up-regulation of more than 2-fold are shown. Ratios for the individual replicates are given. Proteins found in either Ctrl or rapamycin treated samples were assigned a ratio of ∞ (when found only in control) or $1/\infty$ (when only found in rapamycin treated cells). Ratios from micro array analysis are also given.

protein name	gene name	protein fold change	t-test	ratio Exp1	ratio Exp2	ratio Exp3	transcript fold change	transcript significant
Homeobox protein Nkx-3.2	Nkx3-2	0.1	0.288		0.0	0.2	1.0	NO
Ornithine decarboxylase	Odc1	0.2	0.002	0.2	0.1	0.2	1.0	NO
Interferon gamma	Ifng	0.2	0.003	0.2	0.2	0.2	0.2	YES
Myosin-7B	Myh7b	0.2	0.042	0.3	0.1	0.2	1.0	NO
Metallothionein-1	Mt1	0.2	1.000	0.2			0.9	NO
Acyl-CoA-binding domain-containing protein 6	Acbd6	0.2	0.096	0.1	0.2	0.6	1.0	NO
Rho-related GTP-binding protein Rho6	Rnd1	0.2	0.657	0.0	4.3	3.5	0.9	NO
RING finger and CHY zinc finger domain-containing protein 1	Rchy1	0.2	0.086	0.5	0.1	0.2	0.9	NO
Granzyme G	Gzmg	0.2	1.000		0.2		0.0	YES
Isoform 2 of Cellular nucleic acid-binding protein	Cnbp	0.3	0.049	0.1	0.4	0.3	1.0	NO
Isoform IIa of Prolyl 4-hydroxylase subunit alpha-2	P4ha2	0.3	0.028	0.2	0.3	0.4	0.4	YES
Interferon-related developmental regulator 1	Ifrd1	0.3	0.077		0.2	0.3	0.6	YES
CDGSH iron-sulfur domain-containing protein 3, mitochondrial	Cisd3	0.3	0.273	0.5	0.1	1/∞		
Disintegrin and metalloproteinase domain-containing protein 8	Adam8	0.3	0.005	0.2	0.3	0.2	0.4	YES
Complement component C1q receptor	Cd93	0.3	0.061	0.2	0.2	0.5	0.9	NO
Atlastin-1	Atl1	0.3	0.583	0.0		1.5		
Mitochondrial import inner membrane translocase subunit Tim17-A	Timm17a	0.3	0.043	0.4	0.3	0.2	0.9	NO
Isoform 4 of Cytoplasmic polyadenylation element-binding protein 4	Cpeb4	0.3	0.006	0.3	0.4	0.3	0.6	NO
Protein FAM171A2	Fam171a2	0.3	1.000		0.3			
Sulfatase-modifying factor 2	Sumf2	0.3	0.049	0.4	0.4	0.2	1.0	NO
Cysteine and glycine-rich protein 2	Csrp2	0.3	0.101	0.3	0.4		0.7	NO
RING-box protein 2	Rnf7	0.3	0.280	0.5	0.2	1/∞	1.0	NO
Neuroserpin	Serpini1	0.3	0.298		0.2	0.6	1.1	NO
Heme oxygenase 1	Hmox1	0.3	0.046	0.5	0.2	0.3	0.6	YES
Tumor necrosis factor receptor superfamily member 9	Tnfrsf9	0.3	0.052	0.4	0.2	0.4	0.7	YES
Exonuclease 1	Exo1	0.3	0.393		0.7	0.1	1.1	NO

Lipoma HMGIC fusion partner-like 3 protein	Lhfpl3	0.3	0.254	0.2		0.5	1.0	NO
Cellular nucleic acid-binding protein	Cnbp	0.3	0.040	0.5	0.3	0.2	1.0	NO
Fatty acid desaturase 2	Fads2	0.3	0.018	0.3	0.4	0.2	0.7	NO
Enhancer of filamentation 1	Nedd9	0.3	0.032	0.2	0.3	0.5	0.7	NO
Sorting nexin-32	Snx32	0.3	0.561	0.1	1.3			
Isoform 1B of Cytoplasmic dynein 1 intermediate chain 1	Dync1i1	0.3	1.000	0.3			1.0	NO
Cytochrome b-c1 complex subunit 6, mitochondrial	Uqcrh	0.3	0.141	0.7	0.4	0.1	1.1	NO
Metallothionein-3	Mt3	0.4	0.145	0.6	0.1	0.5	0.9	NO
Creatine kinase B-type	Ckb	0.4	0.002	0.3	0.4	0.4	0.5	YES
Leukocyte elastase inhibitor A	Serpinb1a	0.4	0.003	0.3	0.4	0.3	0.6	NO
FERM domain-containing protein 8	Frmd8	0.4	0.003	0.4	0.4	0.3		
Serine/threonine-protein kinase Chk2	Chek2	0.4	1.000			0.4	1.2	YES
Phosphomevalonate kinase	Pmvk	0.4	0.004	0.4	0.3	0.4	0.6	YES
Asparagine synthetase [glutamine-hydrolyzing]	Asns	0.4	0.035	0.5	0.3	0.4	0.4	YES
Zinc finger protein-like 1	Zfpl1	0.4	0.356	0.6	0.1	1.1	1.0	NO
NADP-dependent malic enzyme	Me1	0.4	0.012	0.4	0.4	0.3		
Phosphoenolpyruvate carboxykinase [GTP], mitochondrial	Pck2	0.4	0.000	0.4	0.4	0.4	0.6	YES
Tubulin beta-6 chain	Tubb6	0.4	0.016	0.4	0.5	0.3	0.7	NO
Cleavage and polyadenylation specificity factor subunit 4	Cpsf4	0.4	0.063	0.4	0.2	0.6	1.1	NO
Amyloid protein-binding protein 2	Appbp2	0.4	1.000	0.4			1.0	NO
Tetraspanin-31	Tspan31	0.4	0.222	0.5		0.3	0.7	NO
Isoform 3 of Tripartite motif-containing protein 16	Trim16	0.4	0.050	0.6	0.3	0.4	0.6	YES
Glycoprotein-N-acetylgalactosamine 3-beta-galactosyltransferase 1	C1galt1	0.4	0.230	0.1	0.6	0.7	1.0	NO
GPI mannosyltransferase 3	Pigb	0.4	0.265	0.2	0.6		1.0	NO
Isoform 3 of Profilin-2	Pfn2	0.4	0.144	0.6	0.2	0.6	0.7	NO
Long-chain-fatty-acid--CoA ligase 3	Acsl3	0.4	0.005	0.4	0.4	0.3	1.0	NO
Lymphocyte antigen 6E	Ly6e	0.4	0.388	2.2	0.2	0.2	1.4	NO
Ras-related protein Rab-3D	Rab3d	0.4	0.137	0.2	0.8	0.4	0.9	NO

Mediator of RNA polymerase II transcription subunit 28	Med28	0.4	0.205	1.1	0.2	0.3	1.0	NO
Stomatin-like protein 1	Stoml1	0.4	1.000	0.4			0.9	NO
KAT8 regulatory NSL complex subunit 1	Kansl1	0.4	0.023	0.5	0.3	0.4		
Isoform 2 of Zinc finger protein 367	Znf367	0.4	0.516		0.2	1.0		
Isoform 2 of Nuclear distribution protein nudE-like 1	Ndel1	0.4	1.000		0.4		0.8	NO
Armadillo repeat-containing X-linked protein 2	Armcx2	0.4	0.236	0.6		0.3	0.6	NO
Ubiquitin-associated protein 1	Ubap1	0.4	0.180	1.0	0.3	0.3	0.9	NO
Mediator of RNA polymerase II transcription subunit 11	Med11	0.4	0.092	0.4	0.2	0.7	1.0	NO
Ras-related protein Rab-28	Rab28	0.4	0.697	2.3	0.1		0.8	NO
MAGUK p55 subfamily member 2	Mpp2	0.4	0.054	0.6	0.3	0.3	1.0	NO
Four and a half LIM domains protein 2	Fhl2	0.4	0.240	0.9	0.1	0.6	0.8	NO
Hydroxymethylglutaryl-CoA synthase, cytoplasmic	Hmgcs1	0.4	0.033	0.4	0.3	0.6	0.6	NO
Dual specificity protein phosphatase 3	Dusp3	0.4	0.011	0.5	0.4	0.4	0.8	NO
Liprin-alpha-2	Ppfia2	0.4	0.090	0.5	0.2	0.6	1.0	NO
Ubiquitin-conjugating enzyme E2 A	Ube2a	0.4	0.025	0.3	0.4	0.5	0.9	NO
Zinc finger CCHC domain-containing protein 10	Zcchc10	0.4	0.167	0.5	1/∞	0.3	0.9	NO
ATP synthase subunit s-like protein	Atp5sl	0.4	0.448		0.2	0.9		
Protein-lysine methyltransferase METTL21D	Mettl21d	0.4	0.228	0.6	0.3	∞		
SUZ domain-containing protein 1	Szrd1	0.4	0.106	0.2	0.5	0.6		
Integrin alpha-V	Itgav	0.4	0.055	0.6	0.4	0.3	1.0	NO
Protein unc-119 homolog A	Unc119	0.4	0.156	0.8	0.5	0.2	0.7	YES
Zinc fingers and homeoboxes protein 2	Zhx2	0.4	0.417	0.1	1.1	0.9	0.9	NO
Eukaryotic translation initiation factor 4H	Eif4h	0.4	0.007	0.4	0.4	0.5	1.0	NO
Mitochondrial uncoupling protein 2	Ucp2	0.4	1.000	0.4			0.9	NO
Isoform 1B of Beta-arrestin-1	Arrb1	0.4	0.110	0.4	0.7	0.2	0.6	NO
Interleukin-10	Il10	0.4	0.304	0.1	0.4	1.3	0.7	NO
Sphingolipid delta(4)-desaturase DES1	Degs1	0.4	0.203	0.3	1.1	0.3	1.0	NO
Protein slowmo homolog 2	Slmo2	0.4	0.169	0.6	0.7	0.2	1.0	NO

E3 ubiquitin-protein ligase TRIM32	Trim32	0.4	0.122	0.2	0.7	0.5	0.9	NO
Protein FAM101B	Fam101b	0.4	1.000	0.4				
BTB/POZ domain-containing adapter for CUL3-mediated RhoA degradation protein 1	Kctd13	0.4	1.000	0.4			1.0	NO
DCN1-like protein 5	Dcun1d5	0.4	0.029	0.4	0.6	0.4	1.0	NO
Transmembrane protein 131	Tmem131	0.4	0.118	0.8	0.3	0.4	0.9	NO
P2Y purinoceptor 14	P2ry14	0.4	0.016	0.5	0.4	0.5	0.8	NO
Isoform 3 of Receptor-type tyrosine-protein phosphatase epsilon	Ptpre	0.4	0.148	0.2	0.8	0.5	0.9	NO
Flavin reductase (NADPH)	Blvrb	0.4	0.113	0.6	0.2	0.6	0.7	YES
Pyrin and HIN domain-containing protein 1-like		0.4	1.000	0.440	0.4			
Isoform 2 of STE20-related kinase adapter protein alpha	Strada	0.4	0.514	0.2		1.0		
PHD finger-like domain-containing protein 5A	Phf5a	0.4	0.193	0.9	0.2	0.4	1.0	NO
NADPH--cytochrome P450 reductase	Por	0.4	0.083	0.4	0.7	0.3	0.9	NO
Polypeptide N-acetylgalactosaminyltransferase 6	Galnt6	0.4	0.128	0.3	0.8	0.5	0.7	NO
Voltage-gated hydrogen channel 1	Hvcn1	0.4	0.103	0.7	0.4	0.3	0.8	NO
G1/S-specific cyclin-D3	Ccnd3	0.4	0.277	1.3	0.3	0.3	1.1	NO
Origin recognition complex subunit 3	Orc3	0.4	1.000	0.4				
Branched-chain-amino-acid aminotransferase, cytosolic	Bcat1	0.4	0.072	0.5	0.6	0.3	0.7	NO
Phosphopantothenate--cysteine ligase	Ppcs	0.4	0.235	1.0	0.2	0.5	0.9	NO
Isoform 2 of Tropomyosin alpha-1 chain	Tpm1	0.4	0.311	0.2	0.5	1.2	1.0	NO
Cytoskeleton-associated protein 4	Ckap4	0.5	0.075	0.7	0.4	0.3	1.0	NO
N(6)-adenine-specific DNA methyltransferase 2	N6amt2	0.5	0.398	0.3	0.2	2.0	1.0	NO
Perforin-1	Prf1	0.5	0.039	0.3	0.6	0.5	0.4	YES
Isoform B of SWI/SNF-related matrix-associated actin-dependent regulator of chromatin subfamily B member 1	Smarcb1	0.5	0.166	0.6	0.2	0.8	1.1	NO
Phosphoinositide 3-kinase adapter protein 1	Pik3ap1	0.5	0.160	0.6	0.2	0.7	0.8	NO
Alpha-1,2-mannosyltransferase ALG9	Alg9	0.5	0.170	0.2	0.7	0.7	1.0	NO
Serine/threonine-protein kinase N2	Pkn2	0.5	0.053	0.5	0.3	0.6	1.0	NO
C-C chemokine receptor type 2	Ccr2	0.5	1.000	0.5			0.9	NO

Protein	Gene								
Epididymis-specific alpha-mannosidase	Man2b2	0.5	0.035	0.4	0.4	0.6	0.9	NO
Kinesin light chain 3	Klc3	0.5	0.161	0.3	0.4	0.9	0.8	NO
Ankyrin repeat domain-containing protein 10	Ankrd10	0.5	0.165	0.3	0.3	1.0	1.1	NO
Procollagen-lysine,2-oxoglutarate 5-dioxygenase 2	Plod2	0.5	0.000	0.5	0.5	0.5	0.7	NO
E3 ubiquitin-protein ligase HECTD1	Hectd1	0.5	0.045	0.7	0.4	0.4	0.8	NO
Interferon-induced protein with tetratricopeptide repeats 1	Ifit1	0.5	1.000	0.5			1.2	NO
Dynactin subunit 6	Dctn6	0.5	0.161	0.2	0.6	0.7	0.9	NO
Sterile alpha motif domain-containing protein 9-like	Samd9l	0.5	0.346	0.3	1.6	0.2	0.7	YES
Phosphatidylinositol 3,4,5-trisphosphate 3-phosphatase and dual-specificity protein phosphatase PTEN	Pten	0.5	0.013	0.5	0.6	0.4	1.1	NO
Adenylate kinase 4, mitochondrial	Ak4	0.5	0.009	0.5	0.4	0.5		
Isoform 2 of CKLF-like MARVEL transmembrane domain-containing protein 7	Cmtm7	0.5	0.202	0.2	1.0	0.4	1.2	NO
Proteasome assembly chaperone 3	Psmg3	0.5	0.270	1.2	0.2	0.4		
SLAM family member 7	Slamf7	0.5	0.054	0.6	0.3	0.5	0.8	YES
CLK4-associating serine/arginine rich protein	Clasrp	0.5	0.130	0.3	0.4	0.8		
Isoform 6 of Runt-related transcription factor 2	Runx2	0.5	0.187		0.4	0.6	0.9	NO
Ceramide synthase 5	Cers5	0.5	0.217	0.3	0.4	1.1		
Retinoblastoma-like protein 2	Rbl2	0.5	0.004	0.5	0.5	0.4	1.0	NO
Cysteine--tRNA ligase, cytoplasmic	Cars	0.5	0.006	0.4	0.4	0.5	0.8	NO
Cathepsin B	Ctsb	0.5	0.066	0.6	0.3	0.6	0.9	NO
60S ribosomal protein L30	Rpl30	0.5	0.165	0.9	0.3	0.4	1.1	NO
Asparagine--tRNA ligase, cytoplasmic	Nars	0.5	0.010	0.5	0.4	0.5	0.6	YES
WD repeat domain-containing protein 83	Wdr83	0.5	0.024	0.4	0.5	0.6		
Nucleobindin-2	Nucb2	0.5	0.073	0.7	0.3	0.5	0.8	NO
Protein phosphatase Slingshot homolog 2	Ssh2	0.5	0.056	0.7	0.4	0.4	1.4	YES
ADP-ribosylation factor GTPase-activating protein 3	Arfgap3	0.5	0.034	0.6	0.5	0.4	0.8	NO
Ubiquitin-conjugating enzyme E2 O	Ube2o	0.5	0.043	0.4	0.6	0.5	1.2	NO
CAS1 domain-containing protein 1	Casd1	0.5	0.347	1.4	0.2	0.4	1.1	NO

Activating signal cointegrator 1 complex subunit 2	Ascc2	0.5	0.259	0.7	0.2	0.8	1.2	NO
Isoform Short of Eukaryotic translation initiation factor 4H	Eif4h	0.5	1.000	0.5			1.0	NO
Actin, cytoplasmic 2	Actg1	0.5	0.164	0.6	0.8	0.3	0.7	YES
Zinc transporter 7	Slc30a7	0.5	0.200	1.0	0.4	0.3	0.9	NO
Glioma pathogenesis-related protein 1	Glipr1	0.5	0.316	0.7	0.3		0.9	NO
Apolipoprotein B receptor	Apobr	0.5	0.019	0.6	0.4	0.5		
Bifunctional 3-phosphoadenosine 5-phosphosulfate synthase 1	Papss1	0.5	0.023	0.5	0.4	0.6	0.7	YES
H-2 class I histocompatibility antigen, Q10 alpha chain	H2-Q10	0.5	1.000			0.5	0.3	YES
Glia-derived nexin	Serpine2	0.5	0.046	0.7	0.5	0.4	0.5	YES
Protein lin-7 homolog B	Lin7b	0.5	1.000	0.5			1.0	NO
Isoform 2 of Poly [ADP-ribose] polymerase 9	Parp9	0.5	0.093	0.8	0.4	0.4	1.1	NO
Solute carrier family 2, facilitated glucose transporter member 1	Slc2a1	0.5	0.191	0.3	0.4	1.0	0.6	YES
Interleukin-12 receptor subunit beta-1	Il12rb1	0.5	0.009	0.5	0.4	0.6	0.7	YES
Isoform 2 of Polypeptide N-acetylgalactosaminyltransferase 2	Galnt2	0.5	0.097	0.6	0.6	0.3	0.8	NO
Succinate dehydrogenase assembly factor 2, mitochondrial	Sdhaf2	0.5	0.086	0.7	0.3	0.5		
Isoform 2 of Chitobiosyldiphosphodolichol beta-mannosyltransferase	Alg1	0.5	0.113	0.4	$1/\infty$	0.6	0.9	NO
Synaptosomal-associated protein 23	Snap23	0.5	0.078	0.5	0.7	0.3	0.8	NO
ADP-ribosylation factor-like protein 6-interacting protein 1	Arl6ip1	0.5	0.047	0.7	0.5	0.4	1.3	NO
Protein Wiz	Wiz	0.5	1.000	0.5		$1/\infty$	1.1	NO
Isoform 2 of Zinc finger MIZ domain-containing protein 1	Zmiz1	0.5	0.111	0.3	0.6	0.7	1.1	NO
Golgi reassembly-stacking protein 2	Gorasp2	0.5	0.006	0.5	0.5	0.5	0.8	NO
Kinesin-like protein KIF13A	Kif13a	0.5	0.189		0.4	0.6	1.0	NO
Isoform 2 of Sequestosome-1	Sqstm1	0.5	0.435	0.9		0.3	0.9	NO
Histone-lysine N-methyltransferase SETDB1	Setdb1	0.5	0.173	1.0	0.3	0.4	1.1	NO

Figure S3: Proteins more than 2-fold down-regulated upon mTORC1 inhibition.
All proteins with an average down-regulation of more than 2-fold are shown. Ratios for the individual replicates are given. Proteins found in either Ctrl or rapamycin treated samples were assigned a ratio of ∞ (when found only in control) or $1/\infty$ (when only found in rapamycin treated cells). Ratios from

micro array analysis are also given.

probe set ID	gene title	gene symbol	fold change
1419480_at	selectin, lymphocyte	Sell	6.5
1419481_at	selectin, lymphocyte	Sell	5.9
1423756_s_at	insulin-like growth factor binding protein 4	Igfbp4	3.3
1429351_at	kelch-like 24 (Drosophila)	Klhl24	3.1
1437405_a_at	insulin-like growth factor binding protein 4	Igfbp4	3.1
1426852_x_at	nephroblastoma overexpressed gene	Nov	2.9
1418240_at	guanylate nucleotide binding protein 2	Gbp2	2.9
1424923_at	serine (or cysteine) peptidase inhibitor, clade A, member 3G	Serpina3g	2.8
1419042_at	interferon inducible GTPase 1	Iigp1	2.8
1435906_x_at	guanylate nucleotide binding protein 2	Gbp2	2.7
1426851_a_at	nephroblastoma overexpressed gene	Nov	2.5
1448113_at	similar to Pr22///similar to Stathmin 1/oncoprotein 18///stathmin 1	LOC100039888///LOC623112///Stmn1	2.5
1419043_a_at	interferon inducible GTPase 1	Iigp1	2.4
1449925_at	chemokine (C-X-C motif) receptor 3	Cxcr3	2.4
1428559_at	follicular lymphoma variant translocation 1	Fvt1	2.3
1428029_a_at	H2A histone family, member V	H2afv	2.3
1448364_at	cyclin G2	Ccng2	2.3
1428224_at	heterogeneous nuclear ribonucleoprotein D-like	Hnrpdl	2.2
1437187_at	E2F transcription factor 7///similar to E2F transcription factor 7	E2f7///LOC639365	2.1
1417804_at	RAS, guanyl releasing protein 2	Rasgrp2	2.1
1422814_at	asp (abnormal spindle)-like, microcephaly associated (Drosophila)	Aspm	2.1
1427161_at	centromere protein F	Cenpf	2.1
1439068_at	type 1 tumor necrosis factor receptor shedding aminopeptidase regulator	Arts1	2.1
1416488_at	cyclin G2	Ccng2	2.1
1420805_at	myosin light chain 2, precursor lymphocyte-specific	Mylc2pl	2.1
1452426_x_at	NA	NA	2.1

1415849_s_at	stathmin 1	Stmn1	2.1
1452389_at	CD antigen 27///similar to Tumor necrosis factor receptor superfamily member 7 precursor (CD27L receptor) (T-cell activation antigen CD27)	Cd27///LOC100048672	2.0
1452073_at	RIKEN cDNA 6720460F02 gene	6720460F02Rik	2.0
1451190_a_at	SH3-binding kinase 1	Sbk1	2.0
1416326_at	cysteine-rich protein 1 (intestinal)	Crip1	2.0
1417971_at	nurim (nuclear envelope membrane protein)	Nrm	2.0
1436515_at	RIKEN cDNA E030004N02 gene	E030004N02Rik	2.0
1455031_at	cell division cycle 2-like 6 (CDK8-like)	Cdc2l6	2.0
1433623_at	zinc finger protein 367	Zfp367	1.9
1449207_a_at	kinesin family member 20A	Kif20a	1.9
1436460_at	cDNA sequence BC030440	BC030440	1.9
1434891_at	prostaglandin F2 receptor negative regulator	Ptgfrn	1.9
1433892_at	sperm associated antigen 5	Spag5	1.9
1418553_at	rho/rac guanine nucleotide exchange factor (GEF) 18	Arhgef18	1.9
1423847_at	non-SMC condensin I complex, subunit D2	Ncapd2	1.9
1424033_at	splicing factor, arginine/serine-rich 7	Sfrs7	1.9
1423909_at	transmembrane protein 176A	Tmem176a	1.9
1416757_at	Zwilch, kinetochore associated, homolog (Drosophila)	Zwilch	1.9
1416746_at	H2A histone family, member X	H2afx	1.9
1456393_at	RIKEN cDNA 2310002J21 gene	2310002J21Rik	1.9
1434997_at	cell division cycle 2-like 6 (CDK8-like)	Cdc2l6	1.9
1423466_at	chemokine (C-C motif) receptor 7	Ccr7	1.9
1453107_s_at	RIKEN cDNA 4933413G19 gene///forkhead box M1///phosphatidylethanolamine binding protein 1	4933413G19Rik///Foxm1///Pebp1	1.9
1422513_at	cyclin F	Ccnf	1.9
1435573_at	OTU domain containing 5	Otud5	1.9
1432478_a_at	IBR domain containing 3	Ibrdc3	1.9
1436036_at	Wolf-Hirschhorn syndrome candidate 1 (human)	Whsc1	1.9

1448466_at	cell division cycle associated 5	Cdca5	1.9
1418199_at	hemogen	Hemgn	1.8
1452377_at	myeloid/lymphoid or mixed-lineage leukemia 1	Mll1	1.8
1430514_a_at	CD99 antigen	Cd99	1.8
1419749_at	tRNA aspartic acid methyltransferase 1	Trdmt1	1.8
1447541_s_at	integrin, alpha E, epithelial-associated	Itgae	1.8
1425436_x_at	killer cell lectin-like receptor subfamily A, member 10///killer cell lectin-like receptor subfamily A, member 9///killer cell lectin-like receptor, subfamily A, member 3	Klra10///Klra3///Klra9	1.8
1437370_at	shugoshin-like 2 (S. pombe)	Sgol2	1.8
1429478_at	RIKEN cDNA 6720463M24 gene	6720463M24Rik	1.8
1421571_a_at	lymphocyte antigen 6 complex, locus C1///lymphocyte antigen 6 complex, locus C2///similar to Lymphocyte antigen 6C precursor (Ly-6C)	LOC100041546///LOC100045833///Ly6c1///Ly6c2	1.8
1447818_x_at	Ras homolog enriched in brain like 1	Rhebl1	1.8
1452712_at	heterogeneous nuclear ribonucleoprotein A3	Hnrpa3	1.8
1455585_at	ring fnger protein 168	Rnf168	1.8
1429095_at	centromere protein P	Cenpp	1.8
1422697_s_at	jumonji, AT rich interactive domain 2	Jarid2	1.8
1428976_at	thymopoietin	Tmpo	1.8
1439695_a_at	M-phase phosphoprotein 1	Mphosph1	1.8
1448878_at	Max dimerization protein 3	Mxd3	1.8
1452209_at	plakophilin 4	Pkp4	1.8
1448591_at	cathepsin S	Ctss	1.8
1455818_at	RIKEN cDNA 4930427A07 gene	4930427A07Rik	1.8
1434561_at	additional sex combs like 1 (Drosophila)	Asxl1	1.8
1417292_at	interferon gamma inducible protein 47	Ifi47	1.8
1427162_a_at	ELK4, member of ETS oncogene family	Elk4	1.8
1435306_a_at	kinesin family member 11	Kif11	1.8
1418264_at	centromere protein K	Cenpk	1.8
1418840_at	programmed cell death 4	Pdcd4	1.8

1460403_at	PC4 and SFRS1 interacting protein 1	Psip1	1.8
1443466_s_at	polymerase (RNA) III (DNA directed) polypeptide B	Polr3b	1.8
1424629_at	breast cancer 1	Brca1	1.8
1416988_at	mutS homolog 2 (E. coli)	Msh2	1.8
1456055_x_at	polymerase (DNA directed), delta 1, catalytic subunit	Pold1	1.8
1451306_at	cell division cycle associated 7 like	Cdca7l	1.7
1453556_x_at	CD99 antigen	Cd99	1.7
1454952_s_at	non-SMC condensin II complex, subunit D3	Ncapd3	1.7
1420081_s_at	DNA segment, Chr 2, ERATO Doi 750, expressed	D2Ertd750e	1.7
1450033_a_at	signal transducer and activator of transcription 1	Stat1	1.7
1419226_at	CD96 antigen	Cd96	1.7
1417445_at	NDC80 homolog, kinetochore complex component (S. cerevisiae)	Ndc80	1.7
1416558_at	maternal embryonic leucine zipper kinase	Melk	1.7
1435000_at	G1 to S phase transition 1	Gspt1	1.7
1428304_at	establishment of cohesion 1 homolog 2 (S. cerevisiae)	Esco2	1.7
1435938_at	cytoskeleton associated protein 2-like	Ckap2l	1.7
1437900_at	RIKEN cDNA 4930523C07 gene	4930523C07Rik	1.7
1460555_at	RIKEN cDNA 6330500D04 gene	6330500D04Rik	1.7
1455990_at	kinesin family member 23	Kif23	1.7
1436199_at	NA	NA	1.7
1451516_at	Ras homolog enriched in brain like 1	Rhebl1	1.7
1456080_a_at	serine incorporator 3	Serinc3	1.7
1420477_at	nucleosome assembly protein 1-like 1	Nap1l1	1.7
1450034_at	signal transducer and activator of transcription 1	Stat1	1.7
1435597_at	ATPase family, AAA domain containing 5	Atad5	1.7
1452912_at	RIKEN cDNA 2600005O03 gene	2600005O03Rik	1.7
1460314_s_at	histone cluster 1, H3a///histone cluster 1, H3b///histone cluster 1, H3c///histone cluster 1, H3d///histone cluster 1, H3e///histone cluster 1, H3f///histone cluster 1, H3g///histone cluster 1, H3h///histone cluster 1, H3i///histone cluster 2, H2aa1///histone cluster 2, H3b///histone cluster 2, H3c1///histone cluster 2, H3c2	Hist1h3a///Hist1h3b///Hist1h3c///Hist1h3d///Hist1h3e///Hist1h3f///Hist1h3g///Hist1h3	1.7

		h///Hist1h3i///Hist2h2aa1///Hist2h3b///Hist2h3c1///Hist2h3c2	
1455790_at	E2F transcription factor 2	E2f2	1.7
1455228_at	Wolf-Hirschhorn syndrome candidate 1 (human)	Whsc1	1.7
1428105_at	TPX2, microtubule-associated protein homolog (Xenopus laevis)	Tpx2	1.7
1416802_a_at	cell division cycle associated 5	Cdca5	1.7
1416155_at	high mobility group box 3	Hmgb3	1.7
1437580_s_at	NIMA (never in mitosis gene a)-related expressed kinase 2	Nek2	1.7
1427233_at	teashirt zinc finger family member 1	Tshz1	1.7
1424380_at	vacuolar protein sorting 37B (yeast)	Vps37b	1.7
1424156_at	retinoblastoma-like 1 (p107)	Rbl1	1.7
1418126_at	chemokine (C-C motif) ligand 5	Ccl5	1.7
1443837_x_at	B-cell leukemia/lymphoma 2	Bcl2	1.7
1433685_a_at	RIKEN cDNA 6430706D22 gene	6430706D22Rik	1.7
1437611_x_at	kinesin family member 2C	Kif2c	1.7
1417299_at	NIMA (never in mitosis gene a)-related expressed kinase 2	Nek2	1.7
1416060_at	TBC1 domain family, member 15	Tbc1d15	1.7
1420915_at	signal transducer and activator of transcription 1	Stat1	1.7
1421963_a_at	cell division cycle 25 homolog B (S. pombe)	Cdc25b	1.7
1453865_a_at	OTU domain containing 5	Otud5	1.7
1439736_at	RIKEN cDNA 5830453J16 gene	5830453J16Rik	1.7
1416958_at	nuclear receptor subfamily 1, group D, member 2	Nr1d2	1.7
1423577_at	ankyrin repeat domain 32	Ankrd32	1.7
1434699_at	RIKEN cDNA 6030408C04 gene	6030408C04Rik	1.7
1456485_at	nuclear protein in the AT region	Npat	1.7
1435005_at	centromere protein E	Cenpe	1.7
1438006_at	RIKEN cDNA 4933439F18 gene	4933439F18Rik	1.7
1451128_s_at	kinesin family member 22	Kif22	1.7

1439269_x_at	minichromosome maintenance deficient 7 (S. cerevisiae)	Mcm7	1.7
1424781_at	receptor accessory protein 3	Reep3	1.7
1448650_a_at	polymerase (DNA directed), epsilon	Pole	1.7
1458589_at	NA	NA	1.7
1427891_at	GTPase, IMAP family member 6	Gimap6	1.7
1415788_at	ubiquitin-like domain containing CTD phosphatase 1	Ublcp1	1.7
1434789_at	DEP domain containing 1B	Depdc1b	1.7
1433862_at	extra spindle poles-like 1 (S. cerevisiae)	Espl1	1.7
1449346_s_at	RIO kinase 1 (yeast)	Riok1	1.7
1434767_at	expressed sequence C79407	C79407	1.7
1448398_s_at	ribosomal protein L22	Rpl22	1.7
1452314_at	kinesin family member 11	Kif11	1.7
1428522_at	transcription termination factor, RNA polymerase II	Ttf2	1.7
1437868_at	cDNA sequence BC023892	BC023892	1.7
1416309_at	nucleolar and spindle associated protein 1	Nusap1	1.7
1440770_at	B-cell leukemia/lymphoma 2	Bcl2	1.7
1416722_at	high mobility group 20A	Hmg20a	1.7
1440825_s_at	coiled-coil domain containing 28A///similar to coiled-coil domain containing 28A	Ccdc28a///LOC100045472	1.7
1421546_a_at	Rac GTPase-activating protein 1	Racgap1	1.7
1428850_x_at	CD99 antigen	Cd99	1.7
1429383_at	casein kinase 1, gamma 3///similar to casein kinase 1, gamma 3	Csnk1g3///LOC100047516	1.7
1424780_a_at	receptor accessory protein 3	Reep3	1.7
1437432_a_at	tripartite motif protein 12	Trim12	1.7
1438676_at	macrophage activation 2 like	Mpa2l	1.7
1442454_at	topoisomerase (DNA) II alpha	Top2a	1.7
1427202_at	RIKEN cDNA 4833442J19 gene	4833442J19Rik	1.7
1420093_s_at	heterogeneous nuclear ribonucleoprotein D-like	Hnrpdl	1.6
1428830_at	ataxia telangiectasia mutated homolog (human)	Atm	1.6

1417166_at	PC4 and SFRS1 interacting protein 1	Psip1	1.6
1452268_at	RIKEN cDNA 2810485I05 gene	2810485I05Rik	1.6
1450710_at	jumonji, AT rich interactive domain 2	Jarid2	1.6
1448627_s_at	PDZ binding kinase	Pbk	1.6
1429252_at	RIKEN cDNA 0610010K14 gene	0610010K14Rik	1.6
1452972_at	tetratricopeptide repeat domain 32	Ttc32	1.6
1450627_at	progressive ankylosis	Ank	1.6
1448187_at	polymerase (DNA directed), delta 1, catalytic subunit	Pold1	1.6
1452681_at	deoxythymidylate kinase	Dtymk	1.6
1460678_at	kelch domain containing 2	Klhdc2	1.6
1423092_at	inner centromere protein	Incenp	1.6
1433893_s_at	sperm associated antigen 5	Spag5	1.6
1434390_at	Heterogeneous nuclear ribonucleoprotein U	Hnrpu	1.6
1434426_at	non-SMC condensin II complex, subunit D3	Ncapd3	1.6
1426810_at	jumonji domain containing 1A	Jmjd1a	1.6
1433543_at	anillin, actin binding protein (scraps homolog, Drosophila)	Anln	1.6
1422527_at	histocompatibility 2, class II, locus DMa	H2-DMa	1.6
1418442_at	exportin 1, CRM1 homolog (yeast)	Xpo1	1.6
1430811_a_at	NUF2, NDC80 kinetochore complex component, homolog (S. cerevisiae)	Nuf2	1.6
1435694_at	Rho GTPase activating protein 26	Arhgap26	1.6
1435753_a_at	nuclear casein kinase and cyclin-dependent kinase substrate 1	Nucks1	1.6
1449171_at	Ttk protein kinase	Ttk	1.6
1434427_a_at	ring finger protein 157	Rnf157	1.6
1434630_at	ankyrin repeat domain 28	Ankrd28	1.6
1433832_at	unc-84 homolog B (C. elegans)	Unc84b	1.6
1447483_s_at	Small nucleolar RNA host gene (non-protein coding) 7	Snhg7	1.6
1456698_s_at	heterogeneous nuclear ribonucleoprotein D-like	Hnrpdl	1.6
1460564_at	suppressor of hairy wing homolog 2 (Drosophila)	Suhw2	1.6

1448441_at	CDC28 protein kinase 1b	Cks1b	1.6
1426834_s_at	RIKEN cDNA D930015E06 gene	D930015E06Rik	1.6
1436318_at	TAR DNA binding protein	Tardbp	1.6
1424208_at	prostaglandin E receptor 4 (subtype EP4)	Ptger4	1.6
1428467_at	TAR DNA binding protein	Tardbp	1.6
1451246_s_at	aurora kinase B	Aurkb	1.6
1416602_a_at	RAD52 homolog (S. cerevisiae)	Rad52	1.6
1452313_at	RIKEN cDNA 5930416I19 gene	5930416I19Rik	1.6
1439040_at	centromere protein E	Cenpe	1.6
1428694_at	RIKEN cDNA 5033413D16 gene	5033413D16Rik	1.6
1435474_at	TAF5 RNA polymerase II, TATA box binding protein (TBP)-associated factor	Taf5	1.6
1450920_at	cyclin B2	Ccnb2	1.6
1424128_x_at	aurora kinase B	Aurkb	1.6
1434691_at	splicing factor, arginine/serine-rich 2, interacting protein	Sfrs2ip	1.6
1419152_at	RIKEN cDNA 2810417H13 gene	2810417H13Rik	1.6
1453226_at	RIKEN cDNA 3000004C01 gene	3000004C01Rik	1.6
1424278_a_at	baculoviral IAP repeat-containing 5	Birc5	1.6
1421073_a_at	prostaglandin E receptor 4 (subtype EP4)	Ptger4	1.6
1418640_at	sirtuin 1 ((silent mating type information regulation 2, homolog) 1 (S. cerevisiae)	Sirt1	1.6
1452534_a_at	high mobility group box 2	Hmgb2	1.6
1451358_a_at	Rac GTPase-activating protein 1	Racgap1	1.6
1459869_x_at	RIKEN cDNA 4930402E16 gene	4930402E16Rik	1.6
1450644_at	zinc finger protein 36, C3H type-like 1	Zfp36l1	1.6
1446085_at	NA	NA	1.6
1436747_at	RIKEN cDNA 1110014K08 gene	1110014K08Rik	1.6
1438096_a_at	deoxythymidylate kinase	Dtymk	1.6
1433640_at	far upstream element (FUSE) binding protein 1	Fubp1	1.6
1433696_at	hematological and neurological expressed 1-like	Hn1l	1.6

1417910_at	cyclin A2	Ccna2	1.6
1449060_at	kinesin family member 2C///similar to Kinesin-like protein KIF2C (Mitotic centromere-associated kinesin) (MCAK)	Kif2c///LOC631653	1.6
1459293_at	NA	NA	1.6
1449699_s_at	RIKEN cDNA C330027C09 gene	C330027C09Rik	1.6
1430574_at	cyclin-dependent kinase inhibitor 3	Cdkn3	1.6
1416901_at	Niemann Pick type C2	Npc2	1.6
1426221_at	loss of heterozygosity, 11, chromosomal region 2, gene A homolog (human)	Loh11cr2a	1.6
1447363_s_at	budding uninhibited by benzimidazoles 1 homolog, beta (S. cerevisiae)	Bub1b	1.6
1416698_a_at	CDC28 protein kinase 1b	Cks1b	1.6
1455345_at	PHD finger protein 15	Phf15	1.6
1452162_at	WD repeat domain 48	Wdr48	1.6
1452592_at	microsomal glutathione S-transferase 2	Mgst2	1.6
1434860_at	NMDA receptor-regulated gene 3	Narg3	1.6
1418004_a_at	transmembrane protein 176B	Tmem176b	1.6
1455103_at	similar to Probable ATP-dependent RNA helicase DDX46 (DEAD box protein 46)	LOC100046698	1.6
1417793_at	interferon inducible GTPase 2	Iigp2	1.6
1415810_at	ubiquitin-like, containing PHD and RING finger domains, 1	Uhrf1	1.6
1429900_at	RIKEN cDNA 5330406M23 gene	5330406M23Rik	1.6
1417586_at	timeless homolog (Drosophila)	Timeless	1.6
1424571_at	similar to Probable ATP-dependent RNA helicase DDX46 (DEAD box protein 46)	LOC100046698	1.6
1417167_at	exosome component 5	Exosc5	1.6
1450677_at	checkpoint kinase 1 homolog (S. pombe)	Chek1	1.6
1422462_at	ubiquitin-conjugating enzyme E2T (putative)	Ube2t	1.6
1443733_x_at	polymerase (DNA-directed), delta 3, accessory subunit	Pold3	1.6
1452232_at	UDP-N-acetyl-alpha-D-galactosamine: polypeptide N-acetylgalactosaminyltransferase 7	Galnt7	1.6
1442083_at	arginine/serine-rich coiled-coil 2	Rsrc2	1.6
1426002_a_at	cell division cycle 7 (S. cerevisiae)	Cdc7	1.6
1447275_at	Bardet-Biedl syndrome 12 (human)	Bbs12	1.6

1429499_at	F-box protein 5	Fbxo5	1.6
1416030_a_at	minichromosome maintenance deficient 7 (S. cerevisiae)	Mcm7	1.6
1435226_at	IBR domain containing 3	Ibrdc3	1.6
1452969_at	ATPase, Ca++ transporting, plasma membrane 1	Atp2b1	1.6
1417926_at	non-SMC condensin II complex, subunit G2	Ncapg2	1.6
1435302_at	TAF4B RNA polymerase II, TATA box binding protein (TBP)-associated factor	Taf4b	1.6
1418851_at	tripartite motif protein 39	Trim39	1.6
1419838_s_at	polo-like kinase 4 (Drosophila)	Plk4	1.6
1425811_a_at	cysteine and glycine-rich protein 1	Csrp1	1.6
1429588_at	RIKEN cDNA 2810474O19 gene	2810474O19Rik	1.6
1460573_at	expressed sequence AI848100	AI848100	1.6
1435397_at	cDNA sequence BC038156	BC038156	1.5
1416299_at	Shc SH2-domain binding protein 1	Shcbp1	1.5
1428280_at	FIP1 like 1 (S. cerevisiae)	Fip1l1	1.5
1436738_at	PIF1 5'-to-3' DNA helicase homolog (S. cerevisiae)	Pif1	1.5
1423440_at	RIKEN cDNA 1110001A07 gene	1110001A07Rik	1.5
1455311_at	DiGeorge syndrome critical region gene 8	Dgcr8	1.5
1437251_at	cell division cycle associated 2	Cdca2	1.5
1448493_at	polyadenylate-binding protein-interacting protein 2	Paip2	1.5
1436427_at	PRP4 pre-mRNA processing factor 4 homolog B (yeast)	Prpf4b	1.5
1416664_at	cell division cycle 20 homolog (S. cerevisiae)	Cdc20	1.5
1426846_at	centromere protein T	Cenpt	1.5
1416031_s_at	minichromosome maintenance deficient 7 (S. cerevisiae)	Mcm7	1.5
1456735_x_at	acid phosphatase-like 2	Acpl2	1.5
1437313_x_at	high mobility group box 2	Hmgb2	1.5
1455173_at	G1 to S phase transition 1	Gspt1	1.5
1432264_x_at	cytochrome c oxidase subunit VIIa polypeptide 2-like	Cox7a2l	1.5
1422698_s_at	jumonji, AT rich interactive domain 2	Jarid2	1.5

1428052_a_at	zinc finger, MYM domain containing 1	Zmym1	1.5
1425495_at	zinc finger protein 62	Zfp62	1.5
1448165_at	caspase 2	Casp2	1.5
1450886_at	germ cell-specific gene 2	Gsg2	1.5
1435952_at	Transcribed locus	NA	1.5
1436161_at	PDS5, regulator of cohesion maintenance, homolog B (S. cerevisiae)	Pds5b	1.5
1428600_at	ninein	Nin	1.5
1434695_at	denticleless homolog (Drosophila)	Dtl	1.5
1424539_at	ubiquitin-like 4	Ubl4	1.5
1438320_s_at	minichromosome maintenance deficient 7 (S. cerevisiae)	Mcm7	1.5
1438852_x_at	minichromosome maintenance deficient 6 (MIS5 homolog, S. pombe) (S. cerevisiae)	Mcm6	1.5
1436707_x_at	non-SMC condensin I complex, subunit H	Ncaph	1.5
1419403_at	cDNA sequence BC017612	BC017612	1.5
1422460_at	MAD2 (mitotic arrest deficient, homolog)-like 1 (yeast)	Mad2l1	1.5
1434911_s_at	Rho GTPase activating protein 19	Arhgap19	1.5
1449523_at	B-cell CLL/lymphoma 7C	Bcl7c	1.5
1426838_at	polymerase (DNA-directed), delta 3, accessory subunit	Pold3	1.5
1460713_at	cDNA sequence BC048355	BC048355	1.5
1452242_at	centrosomal protein 55	Cep55	1.5
1429477_at	non-SMC condensin II complex, subunit H2	Ncaph2	1.5
1448240_at	membrane-bound transcription factor peptidase, site 1	Mbtps1	1.5
1433957_at	RIKEN cDNA C030048B08 gene	C030048B08Rik	1.5
1454967_at	Transcribed locus	NA	1.5
1435773_at	RIKEN cDNA 4930547N16 gene	4930547N16Rik	1.5
1422418_s_at	similar to suppressor of Ty 4 homolog 2///suppressor of Ty 4 homolog 1 (S. cerevisiae)///suppressor of Ty 4 homolog 2 (S. cerevisiae)	LOC100041294///LOC100046679///Supt4h1///Supt4h2	1.5
1454875_a_at	retinoblastoma binding protein 4	Rbbp4	1.5
1418040_at	transmembrane protein 186	Tmem186	1.5

1437911_at	RIKEN cDNA 6330416L07 gene	6330416L07Rik	1.5
1435737_a_at	nuclear distribution gene E homolog 1 (A nidulans)	Nde1	1.5
1418281_at	RAD51 homolog (S. cerevisiae)	Rad51	1.5
1429387_at	GRB2-related adaptor protein	Grap	1.5
1417821_at	DNA segment, Chr 17, human D6S56E 5	D17H6S56E-5	1.5
1455161_at	expressed sequence AI504432	AI504432	1.5
1453307_a_at	anaphase-promoting complex subunit 5	Anapc5	1.5
1452954_at	ubiquitin-conjugating enzyme E2C	Ube2c	1.5
1452540_a_at	H2b histone family, member A///histone cluster 1, H2bc///histone cluster 1, H2be///histone cluster 1, H2bl///histone cluster 1, H2bm///histone cluster 1, H2bp///histone cluster 2, H2bb///histone pseudogene///similar to Hist1h2bj protein	Hist1h2bc///Hist1h2be///Hist1h2bl///Hist1h2bm///Hist1h2bp///Hist2h2bb///LOC100046213///LOC665622///RP23-38E20.1	1.5
1433973_at	selenophosphate synthetase 1	Sephs1	1.5
1453018_at	nuclear VCP-like	Nvl	1.5
1447877_x_at	DNA methyltransferase (cytosine-5) 1	Dnmt1	1.5
1429390_at	acid phosphatase-like 2	Acpl2	1.5

Figure S4: Transcripts up-regulated upon rapamycin treatment.

All transcripts with a statistically significant up-regulation of more than 1.5 are shown.

probe set ID	gene title	gene symbol	fold change
1420344_x_at	granzyme D	Gzmd	0.1
1420343_at	granzyme D	Gzmd	0.1
1450171_x_at	granzyme E	Gzme	0.1
1418679_at	granzyme F	Gzmf	0.1
1425947_at	interferon gamma	Ifng	0.2
1452794_x_at	Speer1-like///predicted gene, EG545728///predicted gene, EG623898///predicted gene, EG667901///similar to EG545728 protein///spermatogenesis associated glutamate (E)-rich protein 1, pseudogene 1	EG545728///EG623898///EG667901///LOC545732///LOC623998///LOC667974///LOC668008///LOC668017///Speer1-ps1	0.2
1437171_x_at	gelsolin	Gsn	0.3
1427347_s_at	tubulin, beta 2a	Tubb2a	0.3
1424268_at	spermine oxidase	Smox	0.3
1415964_at	stearoyl-Coenzyme A desaturase 1	Scd1	0.3
1456312_x_at	gelsolin	Gsn	0.3
1425145_at	interleukin 1 receptor-like 1	Il1rl1	0.3
1416645_a_at	alpha fetoprotein	Afp	0.3
1448213_at	annexin A1	Anxa1	0.3
1451584_at	hepatitis A virus cellular receptor 2	Havcr2	0.4
1455898_x_at	solute carrier family 2 (facilitated glucose transporter), member 3	Slc2a3	0.4
1415965_at	stearoyl-Coenzyme A desaturase 1	Scd1	0.4
1451862_a_at	perforin 1 (pore forming protein)	Prf1	0.4
1419030_at	ERO1-like (S. cerevisiae)	Ero1l	0.4
1437052_s_at	solute carrier family 2 (facilitated glucose transporter), member 3	Slc2a3	0.4
1441917_s_at	transmembrane protein 40	Tmem40	0.4
1416871_at	a disintegrin and metallopeptidase domain 8	Adam8	0.4
1421578_at	chemokine (C-C motif) ligand 4	Ccl4	0.4

1433988_s_at	RIKEN cDNA C230098O21 gene	C230098O21Rik	0.4
1448318_at	adipose differentiation related protein	Adfp	0.4
1419029_at	ERO1-like (S. cerevisiae)	Ero1l	0.4
1449254_at	secreted phosphoprotein 1	Spp1	0.4
1421031_a_at	RIKEN cDNA 2310016C08 gene	2310016C08Rik	0.4
1438385_s_at	glutamic pyruvate transaminase (alanine aminotransferase) 2	Gpt2	0.4
1451828_a_at	acyl-CoA synthetase long-chain family member 4	Acsl4	0.4
1425615_a_at	phosphoenolpyruvate carboxykinase 2 (mitochondrial)	Pck2	0.4
1415995_at	caspase 6	Casp6	0.4
1415673_at	phosphoserine phosphatase	Psph	0.4
1423306_at	RIKEN cDNA 2010002N04 gene	2010002N04Rik	0.4
1451095_at	asparagine synthetase	Asns	0.4
1456225_x_at	tribbles homolog 3 (Drosophila)	Trib3	0.4
1422804_at	serine (or cysteine) peptidase inhibitor, clade B, member 6b	Serpinb6b	0.4
1424140_at	galactose-4-epimerase, UDP	Gale	0.4
1426065_a_at	tribbles homolog 3 (Drosophila)	Trib3	0.4
1436212_at	transmembrane protein 71	Tmem71	0.4
1418649_at	EGL nine homolog 3 (C. elegans)	Egln3	0.4
1421732_at	glutamine repeat protein 1	Glrp1	0.4
1416168_at	serine (or cysteine) peptidase inhibitor, clade F, member 1	Serpinf1	0.4
1424356_a_at	meteorin, glial cell differentiation regulator-like	Metrnl	0.4
1437247_at	fos-like antigen 2///similar to fos-like antigen 2	Fosl2///LOC634417	0.4
1433966_x_at	asparagine synthetase	Asns	0.4
1426808_at	lectin, galactose binding, soluble 3	Lgals3	0.5
1451461_a_at	aldolase 3, C isoform	Aldoc	0.5
1454731_at	myosin X	Myo10	0.5
1452714_at	tetratricopeptide repeat, ankyrin repeat and coiled-coil containing 1	Tanc1	0.5
1455106_a_at	creatine kinase, brain	Ckb	0.5

1428444_at	ankyrin repeat and SOCS box-containing protein 2	Asb2	0.5
1416431_at	tubulin, beta 6	Tubb6	0.5
AFFX-MURINE_b1_at	NA	NA	0.5
1428306_at	DNA-damage-inducible transcript 4	Ddit4	0.5
1426471_at	zinc finger protein 52	Zfp52	0.5
1417335_at	sulfotransferase family, cytosolic, 2B, member 1	Sult2b1	0.5
1426972_at	SEC24 related gene family, member D (S. cerevisiae)	Sec24d	0.5
1448175_at	EH-domain containing 1	Ehd1	0.5
1449324_at	ERO1-like (S. cerevisiae)	Ero1l	0.5
1450650_at	myosin X	Myo10	0.5
1434976_x_at	eukaryotic translation initiation factor 4E binding protein 1	Eif4ebp1	0.5
1416666_at	serine (or cysteine) peptidase inhibitor, clade E, member 2	Serpine2	0.5
1417562_at	eukaryotic translation initiation factor 4E binding protein 1	Eif4ebp1	0.5
1453313_at	sestrin 3	Sesn3	0.5
1429475_at	RIKEN cDNA 2810457I06 gene///similar to RIKEN cDNA 2810457I06	2810457I06Rik///LOC677224	0.5
1422601_at	serine (or cysteine) peptidase inhibitor, clade B, member 9	Serpinb9	0.5
1435137_s_at	RIKEN cDNA 1200015M12 gene///RIKEN cDNA 1200016E24 gene///RIKEN cDNA A130040M12 gene///RIKEN cDNA E430024C06 gene	1200015M12Rik///1200016E24Rik///A130040M12Rik///E430024C06Rik	0.5
1423176_at	transducer of ErbB-2.1	Tob1	0.5
1416303_at	LPS-induced TN factor	Litaf	0.5
1447800_x_at	NA	NA	0.5
1455679_at	oligonucleotide/oligosaccharide-binding fold containing 2A	Obfc2a	0.5
1417772_at	glyoxylate reductase/hydroxypyruvate reductase	Grhpr	0.5
1459903_at	sema domain, immunoglobulin domain (Ig), and GPI membrane anchor, (semaphorin) 7A	Sema7a	0.5
1427932_s_at	RIKEN cDNA 1200003I10 gene///RIKEN cDNA 1200015M12 gene///RIKEN cDNA 1200016E24 gene///RIKEN cDNA A130040M12 gene///RIKEN cDNA E430024C06 gene///similar to gag protein	1200003I10Rik///1200015M12Rik///1200016E24Rik///A130040M12Rik///E430024C	0.5

		06Rik///LOC100039464	
1453021_at	syntaxin binding protein 5 (tomosyn)	Stxbp5	0.5
1434140_at	mcf.2 transforming sequence-like	Mcf2l	0.5
1416503_at	latexin	Lxn	0.5
1422537_a_at	inhibitor of DNA binding 2	Id2	0.5
1418350_at	heparin-binding EGF-like growth factor	Hbegf	0.5
1440298_at	similar to trem-like transcript 2///triggering receptor expressed on myeloid cells-like 2	LOC100047904///Treml2	0.5
1422470_at	BCL2/adenovirus E1B interacting protein 1, NIP3	Bnip3	0.5
1450698_at	dual specificity phosphatase 2	Dusp2	0.5
1449085_at	PHD finger protein 10	Phf10	0.5
1434895_s_at	protein phosphatase 1, regulatory (inhibitor) subunit 13B	Ppp1r13b	0.5
1423918_at	rhomboid domain containing 1	Rhbdd1	0.5
1453238_s_at	RIKEN cDNA 3930401B19 gene///RIKEN cDNA A130040M12 gene///RIKEN cDNA E430024C06 gene///similar to gag protein	3930401B19Rik///A130040M12Rik///E430024C06Rik///LOC100039378///LOC100039583///LOC100041150///LOC100041274///LOC100041962///LOC100043154///LOC100043406///LOC100048290	0.5
1449007_at	B-cell translocation gene 3///predicted gene, EG654432///similar to BTG3	Btg3///EG654432///LOC100048453	0.5
1449221_a_at	ribosome binding protein 1	Rrbp1	0.5
1421679_a_at	cyclin-dependent kinase inhibitor 1A (P21)	Cdkn1a	0.5
1437356_at	Epstein-Barr virus induced gene 2	Ebi2	0.5
1450871_a_at	branched chain aminotransferase 1, cytosolic	Bcat1	0.6
1423543_at	SWA-70 protein	Swap70	0.6
1426724_at	calponin 3, acidic///similar to calponin 3, acidic	Cnn3///LOC100047856	0.6
1433446_at	3-hydroxy-3-methylglutaryl-Coenzyme A synthase 1///similar to Hmgcs1 protein	Hmgcs1///LOC100040592	0.6
1422433_s_at	isocitrate dehydrogenase 1 (NADP+), soluble	Idh1	0.6

1436836_x_at	calponin 3, acidic///similar to calponin 3, acidic	Cnn3///LOC100047856	0.6
1436590_at	protein phosphatase 1, regulatory (inhibitor) subunit 3B	Ppp1r3b	0.6
1418295_s_at	diacylglycerol O-acyltransferase 1	Dgat1	0.6
1433443_a_at	3-hydroxy-3-methylglutaryl-Coenzyme A synthase 1///similar to Hmgcs1 protein	Hmgcs1///LOC100040592	0.6
1415780_a_at	armadillo repeat containing, X-linked 2	Armcx2	0.6
1419647_a_at	immediate early response 3	Ier3	0.6
1438439_at	G protein-coupled receptor 171	Gpr171	0.6
1434301_at	RIKEN cDNA D330050I23 gene	D330050I23Rik	0.6
1428587_at	transmembrane protein 41B	Tmem41b	0.6
1416687_at	procollagen lysine, 2-oxoglutarate 5-dioxygenase 2	Plod2	0.6
1424704_at	runt related transcription factor 2	Runx2	0.6
1428909_at	RIKEN cDNA A130040M12 gene	A130040M12Rik	0.6
1426721_s_at	TCDD-inducible poly(ADP-ribose) polymerase	Tiparp	0.6
1452058_a_at	ring finger protein 11	Rnf11	0.6
1433445_x_at	3-hydroxy-3-methylglutaryl-Coenzyme A synthase 1///similar to Hmgcs1 protein	Hmgcs1///LOC100040592	0.6
1438391_x_at	hydroxysteroid (17-beta) dehydrogenase 10	Hsd17b10	0.6
1435176_a_at	inhibitor of DNA binding 2	Id2	0.6
1435264_at	elastin microfibril interfacer 2	Emilin2	0.6
1435630_s_at	acetyl-Coenzyme A acetyltransferase 2	Acat2	0.6
1426123_a_at	ribosome binding protein 1	Rrbp1	0.6
1435913_at	beta-1,4-N-acetyl-galactosaminyl transferase 4	B4galnt4	0.6
1417697_at	sterol O-acyltransferase 1	Soat1	0.6
1426600_at	solute carrier family 2 (facilitated glucose transporter), member 1	Slc2a1	0.6
1422544_at	myosin X	Myo10	0.6
1418737_at	nudix (nucleoside diphosphate linked moiety X)-type motif 2	Nudt2	0.6
1448118_a_at	cathepsin D	Ctsd	0.6
1451020_at	glycogen synthase kinase 3 beta	Gsk3b	0.6
1417303_at	mevalonate (diphospho) decarboxylase	Mvd	0.6

1424638_at	cyclin-dependent kinase inhibitor 1A (P21)	Cdkn1a	0.6
1420353_at	lymphotoxin A	Lta	0.6
1451776_s_at	homeobox only domain	Hod	0.6
1433804_at	Janus kinase 1	Jak1	0.6
1416011_x_at	EH-domain containing 1	Ehd1	0.6
1438180_x_at	HCLS1 associated X-1///silica-induced gene 111	Hax1///Silg111	0.6
1418437_a_at	MAX-like protein X	Mlx	0.6
1452394_at	cysteinyl-tRNA synthetase	Cars	0.6
1449056_at	RIKEN cDNA E330009J07 gene	E330009J07Rik	0.6
1449037_at	cAMP responsive element modulator	Crem	0.6
1418436_at	syntaxin 7	Stx7	0.6
1448663_s_at	mevalonate (diphospho) decarboxylase	Mvd	0.6
1416010_a_at	EH-domain containing 1	Ehd1	0.6
1456204_at	small nucleolar RNA host gene (non-protein coding) 8	Snhg8	0.6
1436842_at	RIKEN cDNA B230380D07 gene	B230380D07Rik	0.6
1417696_at	sterol O-acyltransferase 1	Soat1	0.6
1449437_at	DNA segment, Chr 6, Wayne State University 163, expressed	D6Wsu163e	0.6
1449170_at	piwi-like homolog 2 (Drosophila)	Piwil2	0.6
1448286_at	hydroxysteroid (17-beta) dehydrogenase 10	Hsd17b10	0.6
1427893_a_at	phosphomevalonate kinase	Pmvk	0.6
1428666_at	asparaginyl-tRNA synthetase	Nars	0.6
1450241_a_at	ecotropic viral integration site 2a	Evi2a	0.6
1444088_at	NA	NA	0.6
1449303_at	sestrin 3	Sesn3	0.6
1428662_a_at	homeobox only domain	Hod	0.6
1433444_at	3-hydroxy-3-methylglutaryl-Coenzyme A synthase 1///similar to Hmgcs1 protein	Hmgcs1///LOC100040592	0.6
1426187_a_at	HCLS1 associated X-1	Hax1	0.6
1419091_a_at	annexin A2	Anxa2	0.6

1427918_a_at	ras homolog gene family, member Q	Rhoq	0.6
1416067_at	interferon-related developmental regulator 1	Ifrd1	0.6
1449118_at	dihydrolipoamide branched chain transacylase E2	Dbt	0.6
1434773_a_at	solute carrier family 2 (facilitated glucose transporter), member 1	Slc2a1	0.6
1434225_at	SWA-70 protein	Swap70	0.6
1452717_at	solute carrier family 25 (mitochondrial carrier, phosphate carrier), member 24	Slc25a24	0.6
1448135_at	activating transcription factor 4	Atf4	0.6
1423602_at	Tnf receptor-associated factor 1	Traf1	0.6
1428365_a_at	lon peptidase 1, mitochondrial	Lonp1	0.6
1422612_at	hexokinase 2///hypothetical protein LOC100043412///hypothetical protein LOC100047934	Hk2///LOC100043412///LOC100047934	0.6
1434642_at	hydroxysteroid (17-beta) dehydrogenase 11	Hsd17b11	0.6
1426530_a_at	kelch-like 5 (Drosophila)	Klhl5	0.6
1424981_at	neurolysin (metallopeptidase M3 family)	Nln	0.6
1423947_at	RIKEN cDNA 1110008P14 gene	1110008P14Rik	0.6
1452784_at	integrin alpha V	Itgav	0.6
1420618_at	cytoplasmic polyadenylation element binding protein 4	Cpeb4	0.6
1460362_at	RIKEN cDNA 2410001C21 gene	2410001C21Rik	0.6
1418319_at	RIKEN cDNA 1810047C23 gene	1810047C23Rik	0.6
1456739_x_at	armadillo repeat containing, X-linked 2	Armcx2	0.6
1426599_a_at	solute carrier family 2 (facilitated glucose transporter), member 1	Slc2a1	0.6
1417406_at	SERTA domain containing 1	Sertad1	0.6
1420614_at	dynein light chain Tctex-type 3	Dynlt3	0.6
1423082_at	Der1-like domain family, member 1	Derl1	0.6
1438957_x_at	CDP-diacylglycerol synthase (phosphatidate cytidylyltransferase) 2	Cds2	0.6
1450646_at	cytochrome P450, family 51	Cyp51	0.6
1419550_a_at	serine/threonine kinase 39, STE20/SPS1 homolog (yeast)	Stk39	0.6
1420502_at	spermidine/spermine N1-acetyl transferase 1	Sat1	0.6

1460469_at	tumor necrosis factor receptor superfamily, member 9	Tnfrsf9	0.6
1434399_at	UDP-N-acetyl-alpha-D-galactosamine:polypeptide N-acetylgalactosaminyltransferase 6///similar to UDP-N-acetyl-alpha-D-galactosamine:polypeptide N-acetylgalactosaminyltransferase 6	Galnt6///LOC100047499	0.6
1453181_x_at	phospholipid scramblase 1	Plscr1	0.6
1453127_at	protein phosphatase 1J	Ppm1j	0.6
1424465_at	coiled-coil domain containing 58	Ccdc58	0.6
1416041_at	serum/glucocorticoid regulated kinase	Sgk	0.6
1426397_at	transforming growth factor, beta receptor II	Tgfbr2	0.6
1428615_at	purinergic receptor P2Y, G-protein coupled, 5	P2ry5	0.6
1448704_s_at	histocompatibility 47	H47	0.6
1456046_at	CD93 antigen	Cd93	0.6
1450634_at	ATPase, H+ transporting, lysosomal V1 subunit A	Atp6v1a	0.6
1453851_a_at	growth arrest and DNA-damage-inducible 45 gamma	Gadd45g	0.6
1418831_at	plakophilin 3	Pkp3	0.6
1420407_at	leukotriene B4 receptor 1	Ltb4r1	0.6
1435342_at	potassium inwardly-rectifying channel, subfamily K, member 6	Kcnk6	0.6
1452095_a_at	histocompatibility 47	H47	0.6
1437199_at	dual specificity phosphatase 5	Dusp5	0.6
1421457_a_at	SAM domain, SH3 domain and nuclear localization signals, 1	Samsn1	0.6
1417695_a_at	sterol O-acyltransferase 1	Soat1	0.6
1449078_at	ST3 beta-galactoside alpha-2,3-sialyltransferase 6	St3gal6	0.6
1434657_at	Expressed sequence AI314027	AI314027	0.6
1435735_x_at	histocompatibility 47	H47	0.6
1438992_x_at	activating transcription factor 4	Atf4	0.6
1418932_at	nuclear factor, interleukin 3, regulated///similar to NFIL3/E4BP4 transcription factor	LOC100046232///Nfil3	0.6
1417481_at	receptor (calcitonin) activity modifying protein 1	Ramp1	0.6
1416381_a_at	peroxiredoxin 5	Prdx5	0.6
1452866_at	asparaginyl-tRNA synthetase	Nars	0.6

1430029_a_at	tetraspanin 31	Tspan31	0.6
1455105_at	protein tyrosine phosphatase, non-receptor type 12	Ptpn12	0.6
1428154_s_at	phosphatidic acid phosphatase type 2 domain containing 1	Ppapdc1	0.6
1420394_s_at	glycoprotein 49 A///leukocyte immunoglobulin-like receptor, subfamily B, member 4	Gp49a///Lilrb4	0.6
1438511_a_at	RIKEN cDNA 1190002H23 gene	1190002H23Rik	0.6
1429335_at	small nuclear RNA activating complex, polypeptide 1	Snapc1	0.6
1416367_at	RIKEN cDNA 1110001J03 gene	1110001J03Rik	0.6
1435017_at	melanoma nuclear protein 13	Mel13	0.7
1435031_at	transmembrane protein 120A	Tmem120a	0.7
1451442_at	coiled-coil domain containing 104	Ccdc104	0.7
1435640_x_at	RIKEN cDNA A130040M12 gene	A130040M12Rik	0.7
1421947_at	guanine nucleotide binding protein (G protein), gamma 12	Gng12	0.7
1455104_at	MAX dimerization protein 1	Mxd1	0.7
1421624_a_at	enabled homolog (Drosophila)	Enah	0.7
1421302_a_at	guanine nucleotide binding protein, alpha 15	Gna15	0.7
1426257_a_at	seryl-aminoacyl-tRNA synthetase	Sars	0.7
1415890_at	3'-phosphoadenosine 5'-phosphosulfate synthase 1	Papss1	0.7
1460603_at	sterile alpha motif domain containing 9-like	Samd9l	0.7
1420013_s_at	lanosterol synthase	Lss	0.7
1416610_a_at	chloride channel 3	Clcn3	0.7
1416921_x_at	aldolase 1, A isoform	Aldoa	0.7
1433531_at	acyl-CoA synthetase long-chain family member 4	Acsl4	0.7
1424342_at	forty-two-three domain containing 1	Fyttd1	0.7
1448304_a_at	RAB6, member RAS oncogene family	Rab6	0.7
1426554_a_at	phosphoglycerate mutase 1	Pgam1	0.7
1433604_x_at	aldolase 1, A isoform	Aldoa	0.7
1434799_x_at	aldolase 1, A isoform	Aldoa	0.7
1460521_a_at	oligonucleotide/oligosaccharide-binding fold containing 2A	Obfc2a	0.7

1451074_at	ring finger protein 13	Rnf13	0.7
1418911_s_at	acyl-CoA synthetase long-chain family member 4	Acsl4	0.7
1418326_at	similar to solute carrier family 7 (cationic amino acid transporter, y+ system), member 5///solute carrier family 7 (cationic amino acid transporter, y+ system), member 5	LOC100047619///Slc7a5	0.7
1416556_at	tetraspanin 31	Tspan31	0.7
1452000_s_at	seryl-aminoacyl-tRNA synthetase	Sars	0.7
1425515_at	phosphatidylinositol 3-kinase, regulatory subunit, polypeptide 1 (p85 alpha)	Pik3r1	0.7
1438682_at	phosphatidylinositol 3-kinase, regulatory subunit, polypeptide 1 (p85 alpha)	Pik3r1	0.7
1416069_at	phosphofructokinase, platelet	Pfkp	0.7
1424697_at	DTW domain containing 1	Dtwd1	0.7
1428975_at	sushi domain containing 3	Susd3	0.7

Figure S5: Transcripts down-regulated upon rapamycin treatment.
All transcripts with a statistically significant down-regulation of more than 1.5 are shown.